



U.S. Department
of Transportation

**Federal Railroad
Administration**

Analytical Descriptions of Track Geometry Variations

PB85-151355/AS

Office of Research and
Development
Washington DC 20590

Volume II - Appendices

A. Hamid
K. Rasmussen
M. Baluja
T-L. Yang

ENSCO, Inc.
Transportation Technology Engineering Division
5400 Port Royal Road
Springfield VA 22151

DOT/FRA/ORD-83/03.2

December 1983

This document is available to the
Public through the National
Technical Information Service,
Springfield, Virginia 22161.

This document is disseminated under the sponsorship of the Department of Transportation in the interest of information exchange. The United States Government assumes no liability for its contents or use thereof.

The contents of this report reflect the view of ENSCO, Inc. who is responsible for the facts and the accuracy of the data presented herein. The contents do not necessarily reflect the official view or policy of the Department of Transportation. This report does not constitute a standard, specification, or regulation.

| | | | | | |
|---|--|--|--|--|-----------|
| 1. Report No. DOT/FRA/ORD-83/03.2 | | 2. Government Accession No. | | 3. Recipient's Catalog No. | |
| 4. Title and Subtitle ANALYTICAL DESCRIPTIONS OF TRACK GEOMETRY VARIATIONS VOLUME II - APPENDICES | | 5. Report Date December 1983 | | 6. Performing Organization Code 1444-105-08 | |
| | | 8. Performing Organization Report No. DOT-FR-82-03 | | 10. Work Unit No. (TRAIS) | |
| 7. Author(s) A. Hamid, K. Rasmussen, M. Baluja & T-L. Yang | | 9. Performing Organization Name and Address ENSCO, INC TRANSPORTATION TECHNOLOGY ENGINEERING DIVISION 5400 Port Royal Road Springfield, VA 22151 | | 11. Contract or Grant No. DTER53-80-C-00002 | |
| 12. Sponsoring Agency Name and Address DEPARTMENT OF TRANSPORTATION FEDERAL RAILROAD ADMINISTRATION 400 Seventh St., S.W. Washington, DC 20590 | | 13. Type of Report and Period Covered FINAL REPORT MAY 1976-JULY 1981 | | 14. Sponsoring Agency Code | |
| | | 15. Supplementary Notes Volume I contains the main text. | | | |
| 16. Abstract <p>Analyses of recorded track geometry measurements were conducted to develop analytical representations of track geometry variations that exist on the U.S. railroad track. These analytical representations include: 1) continuous stationary random variations described by power spectral density functions with a normalized frequency characteristic and a roughness amplitude; 2) randomly modulated periodic effects associated with rail length which are described by joint amplitude statistics and a shape function; and 3) isolated events described by a shape function, amplitude and characteristic length. The parameters of these representations are obtained as a function of current FRA track classes for gage, surface, crosslevel and alignment.</p> <p>Analyses are also presented to establish the relationships and statistical correlations between the track geometry variables. The effects of curvature and superelevation on gage, alignment and surface variations are also discussed.</p> <p>The results of the work presented here are expected to be applied to vehicle track interaction simulation studies related to rail car safety, performance and lading damage. A current application being conducted under concurrent efforts is the development of performance based limits on permissible track geometry variations that can be directly related to the railroad operational safety.</p> <p>These volumes contains more data and analysis to support the results given in Volume I. It is divided into appendices A through F.</p> | | | | | |
| 17. Key Words Track Geometry Track Irregularities Analytical Descriptions Track Geometry Models | | | 18. Distribution Statement This document is available to the public through the National Technical Information Service, Springfield, VA 22161 | | |
| 19. Security Classif. (of this report) Unclassified | | 20. Security Classif. (of this page) Unclassified | | 21. No. of Pages 274 | 22. Price |

PREFACE

Analytical descriptions of track geometry variations are essential for various design and simulation studies intended to improve the performance, reliability and safety of the rail transportation system. Accordingly, this report gives the analytical descriptions of geometric variations of the United States track in a form suitable for these studies.

The work described in this report was conducted under the track characterization program. This program was directed by the Transportation Systems Center (TSC) in support of the Improved Track Structures Research Program of the Federal Railroad Administration's (FRA) Office of Rail Safety Research. These efforts were carried out under contracts DOT-TSC-1211; DOT-TSC-1631; DOT-FR-64113, Task 462; and DTFR53-80-C-00002, Task 105.

The authors wish to acknowledge the contribution of Dr Herbert Weinstock of TSC in the technical direction of the program. The authors also wish to thank Messrs. W. B. O'Sullivan and R. Krick of FRA for their support and comments.

Appreciation is also expressed to ENSCO co-workers Messrs. E. Cunney, E. Howerter, K. Kesler and Drs. M. Kenworthy and R. Owings for a thorough review which greatly improved the quality of this report. The efforts of Mrs. C. McAlee in typing, editing and assembly of this report are greatly appreciated.

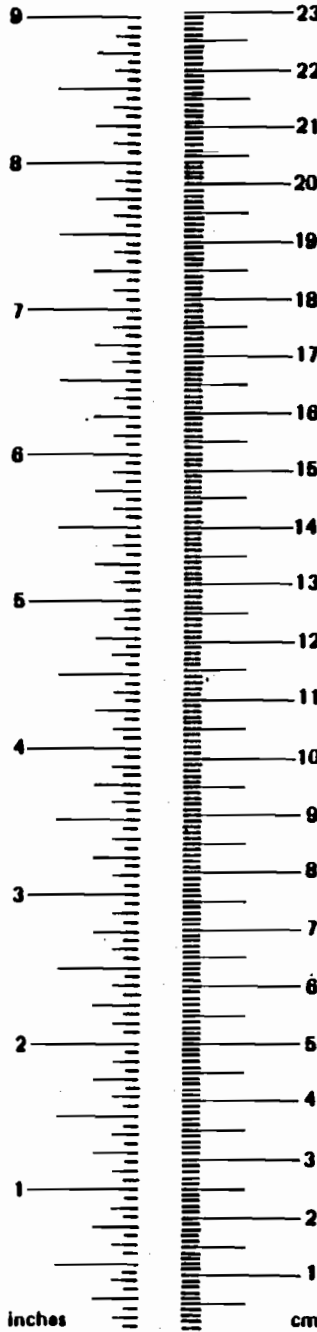
METRIC CONVERSION FACTORS

Approximate Conversions to Metric Measures

| Symbol | When You Know | Multiply by | To Find | Symbol |
|----------------------------|------------------------|----------------------------|---------------------|-----------------|
| LENGTH | | | | |
| in | inches | 2.5 | centimeters | cm |
| ft | feet | 30 | centimeters | cm |
| yd | yards | 0.9 | meters | m |
| mi | miles | 1.6 | kilometers | km |
| AREA | | | | |
| in ² | square inches | 6.5 | square centimeters | cm ² |
| ft ² | square feet | 0.09 | square meters | m ² |
| yd ² | square yards | 0.8 | square meters | m ² |
| mi ² | square miles | 2.6 | square kilometers | km ² |
| | acres | 0.4 | hectares | ha |
| MASS (weight) | | | | |
| oz | ounces | 28 | grams | g |
| lb | pounds | 0.45 | kilograms | kg |
| | short tons (2000 lb) | 0.9 | tonnes | t |
| VOLUME | | | | |
| tsp | teaspoons | 5 | milliliters | ml |
| Tbsp | tablespoons | 15 | milliliters | ml |
| fl oz | fluid ounces | 30 | milliliters | ml |
| c | cups | 0.24 | liters | l |
| pt | pints | 0.47 | liters | l |
| qt | quarts | 0.95 | liters | l |
| gal | gallons | 3.8 | liters | l |
| ft ³ | cubic feet | 0.03 | cubic meters | m ³ |
| yd ³ | cubic yards | 0.76 | cubic meters | m ³ |
| TEMPERATURE (exact) | | | | |
| °F | Fahrenheit temperature | 5/9 (after subtracting 32) | Celsius temperature | °C |

Approximate Conversions from Metric Measures

| Symbol | When You Know | Multiply by | To Find | Symbol |
|----------------------------|-----------------------------------|-------------------|------------------------|-----------------|
| LENGTH | | | | |
| mm | millimeters | 0.04 | inches | in |
| cm | centimeters | 0.4 | inches | in |
| m | meters | 3.3 | feet | ft |
| m | meters | 1.1 | yards | yd |
| km | kilometers | 0.6 | miles | mi |
| AREA | | | | |
| cm ² | square centimeters | 0.16 | square inches | in ² |
| m ² | square meters | 1.2 | square yards | yd ² |
| km ² | square kilometers | 0.4 | square miles | mi ² |
| ha | hectares (10,000 m ²) | 2.5 | acres | |
| MASS (weight) | | | | |
| g | grams | 0.035 | ounces | oz |
| kg | kilograms | 2.2 | pounds | lb |
| t | tonnes (1000 kg) | 1.1 | short tons | |
| VOLUME | | | | |
| ml | milliliters | 0.03 | fluid ounces | fl oz |
| l | liters | 2.1 | pints | pt |
| l | liters | 1.06 | quarts | qt |
| l | liters | 0.26 | gallons | gal |
| m ³ | cubic meters | 36 | cubic feet | ft ³ |
| m ³ | cubic meters | 1.3 | cubic yards | yd ³ |
| TEMPERATURE (exact) | | | | |
| °C | Celsius temperature | 9/5 (then add 32) | Fahrenheit temperature | °F |



^a 1 in. = 2.54 cm (exactly). For other exact conversions and more detail tables see NBS Misc. Publ. 286. Units of Weight and Measures. Price \$2.25 SD Catalog No. C13 10 286.

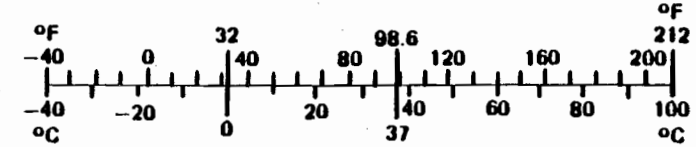


TABLE FOR METRIC CONVERSION OF PSD LEVELS

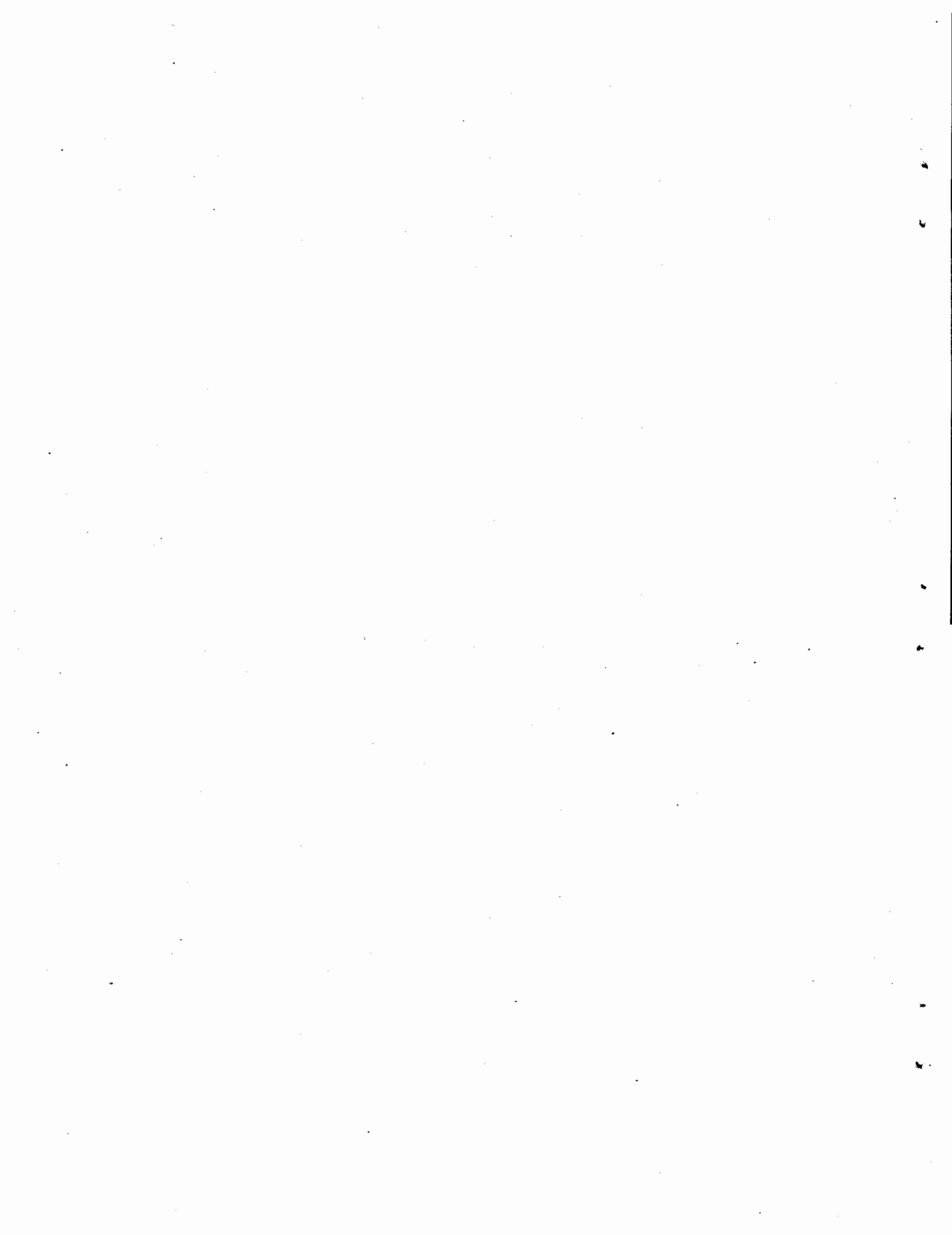
| <u>Given:</u> | To find: | |
|-------------------------|-------------------------|-------------------------|
| | in ² /cy/ft | cm ² /cy/m |
| | <u>Multiply by:</u> | |
| ft ² /cy/ft | 144. | 2.83 × 10 ² |
| in ² /cy/ft | 1.00 | 1.97 |
| in ² /cy/in | 8.33 × 10 ⁻² | 0.164 |
| ft ² /rad/ft | 9.05 × 10 ² | 1.78 × 10 ³ |
| in ² /rad/ft | 6.28 | 12.4 |
| in ² /rad/in | 0.524 | 1.03 |
| m ² /cy/m | 5.09 × 10 ³ | 1.00 × 10 ⁴ |
| cm ² /cy/m | 0.509 | 1.00 |
| cm ² /cy/cm | 5.09 × 10 ⁻³ | 1.00 × 10 ⁻² |
| m ² /rad/m | 3.20 × 10 ⁴ | 6.28 × 10 ⁴ |
| cm ² /rad/m | 3.20 | 6.28 |
| cm ² /rad/cm | 3.20 × 10 ⁻² | 6.28 × 10 ⁻² |

TABLE FOR METRIC CONVERSION OF SPATIAL FREQUENCY

| <u>Given:</u> | To find: | |
|---------------|-------------------------|-------------------------|
| | cy/ft | cy/m |
| | <u>Multiply by:</u> | |
| cy/ft | 1.00 | 3.28 |
| cy/in | 12.0 | 39.4 |
| rad/ft | 0.159 | 4.85 × 10 ⁻² |
| rad/in | 1.91 | 4.04 × 10 ⁻³ |
| cy/m | 0.305 | 1.00 |
| cy/cm | 30.5 | 1.00 × 10 ² |
| rad/m | 4.85 × 10 ⁻² | 0.159 |
| rad/cm | 4.85 | 15.9 |

TABLE FOR METRIC CONVERSION OF
ROUGHNESS PARAMETER UNITS

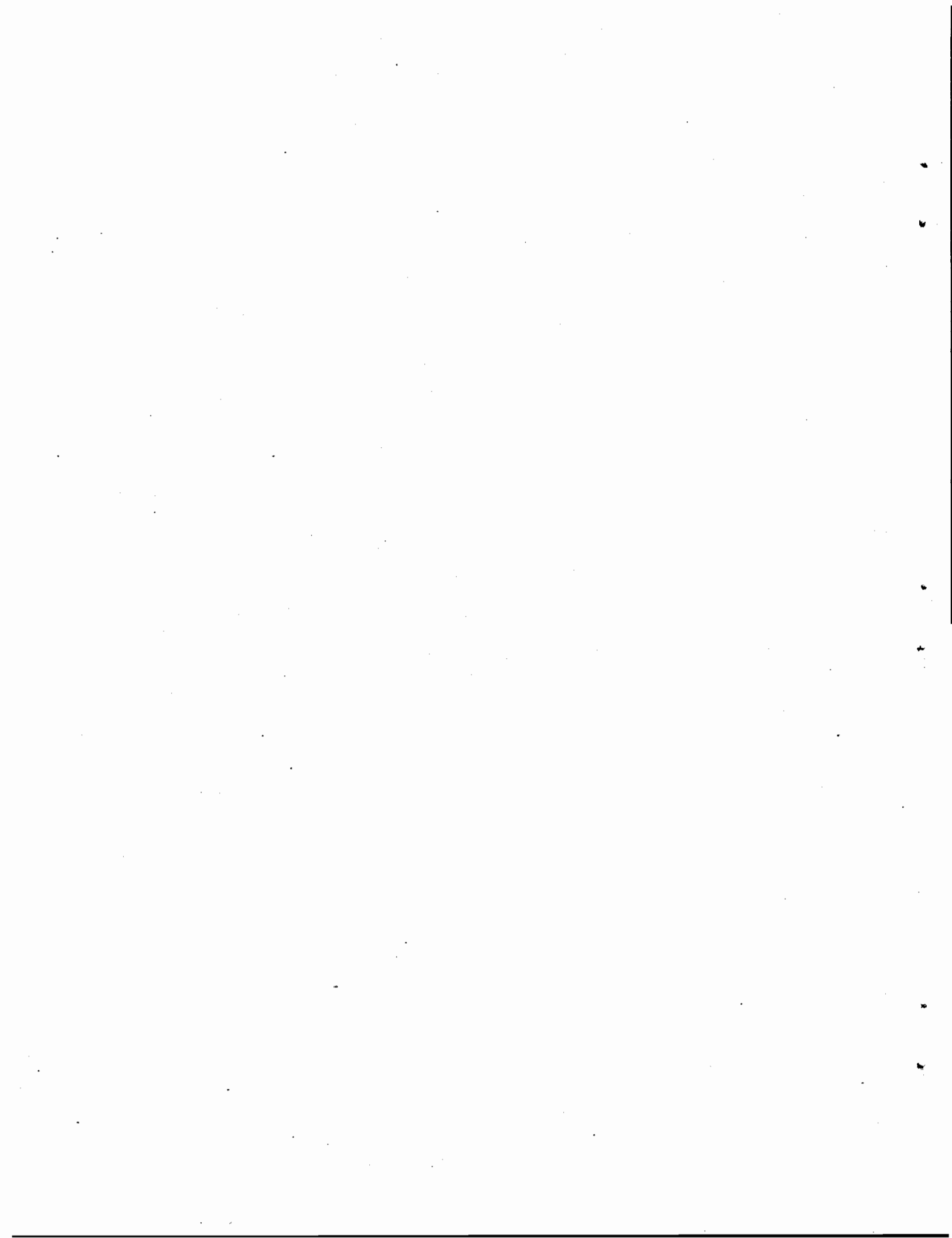
| <u>Given:</u> | To find: | |
|-------------------------|-------------------------|-------------------------|
| | in ² -cy/ft | cm ² -cy/m |
| | Multiply by: | |
| ft ² -cy/ft | 144. | 3.05 × 10 ⁻³ |
| in ² -cy/ft | 1.00 | 21.2 |
| in ² -cy/in | 12.0 | 254. |
| ft ² -rad/ft | 22.9 | 485. |
| in ² -rad/ft | 0.159 | 3.37 |
| in ² -rad/in | 1.91 | 40.4 |
| m ² -cy/m | 472. | 1.00 × 10 ⁴ |
| cm ² -cy/m | 4.72 × 10 ⁻² | 1.00 |
| cm ² -cy/cm | 4.72 | 100. |
| m ² -rad/m | 75.2 | 1.59 × 10 ³ |
| cm ² -rad/m | 7.52 × 10 ⁻³ | 0.159 |
| cm ² -rad/cm | 0.752 | 15.9 |



VOLUME II

TABLE OF CONTENTS

| <u>SECTION</u> | <u>TITLE</u> | <u>PAGE</u> |
|----------------|---|-------------|
| APPENDIX A | Data Base | A-1 |
| APPENDIX B | Power Spectral Densities (PSD's) | B-1 |
| APPENDIX C | Examples of Isolated Track Geometry Variations | C-1 |
| APPENDIX D | Frequency Domain Analysis | D-1 |
| APPENDIX E | Cross Spectral Density, Coherence and Transfer Function Plots | E-1 |
| APPENDIX F | RMS Variations of Gauge and Alignment | F-1 |



APPENDIX A
DATA BASE

A.1 TYPICAL TRACK GEOMETRY VARIATIONS

A data base was established consisting of 29 zones of track to characterize the typical track geometry variations. These zones reflect various types of operating conditions and maintenance practices of different railroads. Typically, the zones vary in length from one to ten miles. In all, this data base consists of approximately 150 miles of track.

Of the 29 zones, 10 represent historical data, 14 were processed under this research effort, and 5 were processed under a companion effort.*

Over the years, a small number of PSD's have been gathered from track geometry data. These were assembled and graphically summarized and used as a baseline for further PSD processing. A brief summary of this PSD data including the methods used to measure the track geometry, general geographical location of the surveys, track classes involved, and other pertinent information is provided in Table A-1.

The earlier PSD's are rather restricted with respect to frequency and dynamic range. Furthermore, some trends present in them may have resulted from processing errors. Therefore, new zones of track geometry were processed using the best available tools for generating PSD's. An overview of these data sources is provided in Table A-2. These data were collected by FRA track geometry cars and a Track Survey Device (TSD). TSD collected data has a low noise floor. Main features of these data are given in Table A-3. Typical PSD's and tabulation of parameters are given in Appendix B.

* Corbin, J., "Correlation of Statistical Representations of Track Geometry with Physical Appearance," Final Report, FRA-ORD-79-35, June 1975.

TABLE A-1
SYNOPSIS OF OLDER PSD DATA SELECTED FOR ANALYSIS

| | British Rail | ENSCO 1971 | ENSCO 1973 | SNCF |
|-----------------------------------|--------------------------------|---------------------|--|--------------|
| Mean Profile | Manual Survey | - | - | Mauzin Chord |
| Individual Rail Profile | - | 14.5' MCO | 14.5' MCO | - |
| Mean Alignment | Manual Survey | - | - | Mauzin Chord |
| Individual Rail Alignment | - | 14.5' MCO | - | - |
| Crosslevel | Manual Survey | Self-Erecting Gyro | - | - |
| Gage | - | Capacitive | Capacitive | - |
| Broken Down by Track Class | Class 4 & Better Main Line CWR | Class 5,4,3, | Class Super 6,5,4,3,2 | Not Known |
| Territory Covered | Great Britian | Northeast (NE) Area | New Construction NE Area, Chicago Pittsburgh,Florida | France |
| Number of PSD Diagrams | 3 | 12 | 10 | 2 |
| Number of PSD's per Range Diagram | 12 | 3 (average) | 3 (average) | 2 |
| Typical Length of Data/PSD | Unknown | 3 mi. (average) | 3 mi. (average) | 1-2 km |
| Resolution of Peaks | Unknown | 0.05 Decade | 0.05 Decade | Unknown |

TABLE A-2
SYNOPSIS OF PSD'S DATA GENERATED UNDER THIS PROGRAM

| | Track Geometry Cars 1977 | Track Survey Device, Data from TG-69 (1973) |
|-----------------------------------|----------------------------------|--|
| Mean Profile | T-3 Profilometers | Laser Tracker + Corrections |
| Individual Rail Profile | T-3 Profilometer | Laser Tracker + Crosslevel + Measurement Frame Dimensions |
| Mean Alignment | N/A | Laser Tracker + Corrections |
| Individual Rail Alignment | N/A | Laser Tracker + Gage + Crosslevel + Measurement Frame Dimensions |
| Crosslevel | Compensated Accelerometer System | Electronic Pendulum (Low Speed) |
| Gage | N/A | Hydraulically Loaded Wheels |
| Track Class | Class 6 thru Class 3 | Class 6 thru Class 1 |
| Territory Covered | Northeastern Area U.S. (NEA) | Area of Pueblo, Colorado |
| Resolution of Peaks | 8.0×10^{-4} cy/ft | 1.0×10^{-3} cy/ft |
| No. of Diagrams | 2 | 8 |
| Number of PSD's Per Range Diagram | 4 | 5 |
| Typical Length of Data/PSD | 5 mi. to 25 mi. | 700 ft. to 7000 ft. |

TABLE A-3
SUMMARY OF CHARACTERISTICS OF TG-69 ZONES

| <u>Zone</u> | <u>Speed Class by Geometry</u> | <u>Rail Weight, Mfr. & Year</u> | <u>Joints</u> | <u>Rail Length, Stagger</u> | <u>Tie Centers & Cond.</u> | <u>Ballast Depth & Shoulders</u> | <u>Zone Length, Application & History</u> |
|-------------|--------------------------------|---|---------------|-----------------------------|--------------------------------|--------------------------------------|---|
| 1 | 6++ | 136 RE CC CF&I 1973 | B6 | 39', 50% | 19 1/2" | S2, 22", 12" C | 1.70 mi, Nh |
| 2 | 6 | 100 RE CC CF&I 1972 | B6 | 39', 50% | 23" | Gr, 17", 21" C | 0.40 mi, U2 |
| 3 | 6+ | 119 CC CF&I 1970 | W | 39', 18% | 24" | Gr, 15", 12" P | 0.36 mi, Nh |
| 4 | 6+ | 119 CC CF&I 1971 | W | 39', 36% | 24" | Gr, 15", 21" C | 0.59 mi, U2 |
| 5 | 6 | 119 CC CF&I 1971 | W | 39', 50% | 19 1/2" | Gr, 18", 10" C | 0.63 mi, Mh |
| 6 | 4 | 112 RE OH COL. 1941 | B4 LBFR | 39', 50%T | 23" CR | Gr, 6", N MW | 0.30 mi, Ah |
| 7 | 4 | 112 RE OH COL. 1943 | B4 LMB | 36', 50% 39', 50% | 20" BC | S2, 10", N MSW | 0.57 mi, TMh |
| 8 | 3 | 115 RE CC CF&I 1951 | B4 LMB | 38', 45% | 21 1/2" CR | S2, N, N MSW | 0.13 mi, Mh |
| 9 | 2 | 90 OH COL. 1912-29 85 CF&I 1905-08 85 ILL.STEEL 1904-06 85 CAMBRIA 1896-1903 | B4 LM | 33', V% | 20" M | S2, 8", 6" L | 0.64 mi, TS2 |
| 10 | 1 | 75 ILL.STEEL 1896-99 | B4 LMBRX | 28', 50% | 20" | N, N", N" MCS | 0.63 mi, S2 |

Legend

| <u>Joints</u> | <u>Rail Lengths</u> | <u>Ballast</u> | <u>Applications & History</u> |
|-----------------------------------|------------------------|----------------------|-----------------------------------|
| W Welded | T Typical | Gr Granite | N New |
| B4 Jointed, 4-hole | V Variable | S2 Slag | U Slightly used |
| B6 Jointed, 6-hole | | N Nondescript/None | M Main |
| L Loose Bolts | <u>Ties</u> | M Fouled with Mud | A Yard Approach |
| M Missing Bolts | B Battered | S Fouled with Sand | B Branch |
| B Battered Joints | R Rotten | P Polymer Stabilized | S Siding |
| R Broken Rails | C Crushed | W Asperities Worn | Y Yard |
| J Broken Joint Bus | M Missing | C Compacted | h Heavy |
| F Joint Bars applied at Rail Flaw | | L Loose | l Light |
| | <u>Rail Weight</u> | | T Taken out of service |
| | CC Control Cooling | | |
| | RE Rail Dimension Code | | |
| | OH Open Hearth | | |

A.2 NEW DATA BASE

New data as collected by the FRA T-6 vehicle during 1980 and 1981 were available during the latter phases of this project. These data included an improved representation of alignment generated from the inertial alignometer. Therefore, these data were used to develop the analytical descriptions of isolated track geometry variations and to develop the relationships between track geometry parameters.

A synopsis of this data is given in Tables A-4 through A-6. The characteristics used to classify track are FRA Track Class, rail type, and track curvature. For the purpose of this study, allowable speeds for passenger trains is used as the criteria to determine track class. The categories of rail type used to further classify the track are bolted rail and welded rail. Tangent track is defined as a section of track having no curvature greater than 2 degrees, and curved track is a section of track that contains one or more curves greater than 2 degrees.

TABLE A-4
DESCRIPTION OF DATA BASE

| <u>SECTION ID - NO</u> | <u>LENGTH (miles)</u> | <u>POSTED SPEED (mph)</u> | <u>BOLTED OR WELDED</u> | <u>CURVED OR TANGENT</u> |
|----------------------------|---------------------------|-------------------------------|-----------------------------|------------------------------|
| 1-1 | 5 | 10 | B | C |
| 102 | 5 | 35 | B | T |
| 2-1 | 4 | 25 | B | C |
| 2-2 | 10 | 25 | B | C |
| 2-3 | 5 | 25 | B | C |
| 2-4 | 10 | 25 | B | C |
| 2-5 | 3.2 | 25 | W | C |
| 3-1 | 28 | 45 | B&W | C |
| 4-1 | 9 | 10 | W | C |
| 4-2 | 10 | 79 | W | T |
| 4-3 | 5 | 65 | B | C |
| 4-4 | 8 | 79 | B | C |
| 5-1 | 10 | 70 | W | T |
| 5-2 | 5 | 70 | B | C |
| 5-3 | 10 | 70 | B | T |
| 5-4 | 10 | 70 | W | T |
| 5-5 | 5 | 90 | W | T |
| 5-6 | 4.5 | 90 | W | T |
| 5-7 | 5 | 79 | B | T |
| 6-1 | 17 | 105 | W | T |
| 6-2 | 21 | 110 | W | T |
| 6-3 | 22 | 100 | W | T |

TABLE A-5
COMPRESSED DATA TAPE
COMPOSITION

| <u>Compiled Tape Number</u> | <u>Track Class</u> | <u>ID No.</u> | <u>Beginning Record Number</u> | <u>Ending Record Number</u> | <u>No. of Records</u> |
|-------------------------------------|------------------------|---------------|--|-------------------------------------|---------------------------|
| TRN-1 | 1 | 1-1 | 1 | 330 | 330 |
| | | 1-2 | 331 | 660 | 330 |
| TRN-2 | 2 | 2-1 | 531 | 854 | 324 |
| | | 2-2 | 1 | 530 | 530 |
| | | 2-3 | 855 | 1120 | 266 |
| | | 2-4 | 1121 | 1650 | 530 |
| | | 2-5 | 1651 | 1811 | 161 |
| TRN-3 (New) | 3 | 3-1 | 1 | 1551 | 1551 |
| TRN-4 | 4 | 4-1 | 1 | 539 | 539 |
| | | 4-2 | 964 | 1493 | 530 |
| | | 4-3 | 1494 | 1758 | 265 |
| | | 4-4 | 540 | 963 | 424 |
| TRN-5 | 5 | 5-1 | 1 | 529 | 529 |
| | | 5-2 | 530 | 793 | 264 |
| | | 5-3 | 1323 | 1850 | 528 |
| | | 5-4 | 794 | 1322 | 529 |
| | | 5-5 | 1851 | 2130 | 280 |
| | | 5-6 | 2131 | 2396 | 266 |
| | | 5-7 | 2397 | 2661 | 265 |
| TRN-6-1 | 6 | 6-1 | 1 | 1021 | 1021 |
| TRN-6-2 | | 6-2 | 1 | 1199 | 1199 |
| TRN-6-3 | | 6-3 | 1 | 1251 | 1251 |

TABLE A-6
PROCESSED DATA TAPES

| <u>Compiled Tape Number</u> | <u>Processed Tape Number</u> | <u>ID No. on Processed Tapes (in order)</u> | <u>No. of Records on Processed Tapes</u> |
|-------------------------------------|--------------------------------------|---|--|
| TRN-1 | TRNP-1 | 1-1 1-2 | 660 |
| TRN-2 | TRNP-2 | 2-2 2-1 203 | 1120 |
| TRN-2 | TRNP-2 | 2-4 2-5 | 691 |
| TRN-3 | TRAMP 296W* TRAMP 296B | 3-1 3-2 | 1548 |
| TRN-4 | TRNP-4 Vol 1 | 4-1 4-4 4-2 | 1104 |
| TRN-4 | TRNP-4 | 4-2 4-3 | 985 |
| TRN-5 | TRNP-5 | 5-1 5-2 5-4 | 1322 |
| TRN-5 | TRNP-5 | 5-3 5-5 5-6 5-7 | 2661 |
| TRN-6-1 | TRAMP 1114 | 6-1 | 1021 |
| TRN-6-2 | TRAMP 1115 | 6-2 | 1199 |
| TRN-6-3 | TRAMP 1116 | 6-3 | 1251 |

*Tape TRAMP 296W contains all welded sections.
Tape TRAMP 296B contains all bolted sections.

APPENDIX B
POWER SPECTRAL DENSITIES (PSD'S)

This appendix contains the PSD's of typical variations generated under this project and a tabulation of parameters of these PSD's. These PSD's satisfy the objective that they improve upon the reliability and the wavelength range of the older PSD's. Some descriptions of data used for these PSD's are contained in Appendix A.

This appendix also outlines the method for extraction of parameters of PSD models given in Section 2, of Volume I.

B.1 TYPICAL PSD'S

Figures B-1 and B-2 show the PSD's generated using the data collected by T-3 from the United States Northeastern Area (NEA). The bandwidth for these PSD's is 8.0×10^{-4} cy/ft. Figures B-3 through B-10 contain the PSD's generated from the data collected by the TSD. The bandwidth for these PSD's is 1.0×10^{-3} cy/ft.

B.2 PARAMETER EXTRACTION

Figure B-11 is an example of an empirical PSD used to characterize the typical track geometry variations. PSD levels are plotted as a function of spatial frequency in log-log format. This is particularly useful for studying power law relationships. The ordinate covers a dynamic range of 10^{-4} to 10^4 in²/cy/ft and abscissa covers a frequency range of 0.001 to 1.0 cycle/ft corresponding a wavelength range of 1000 to 1-foot.

In Figure B-11, a symbol, x, indicates the PSD level at a particular frequency. Where more than one linear PSD value falls in a logarithmic frequency band, they are stacked and the

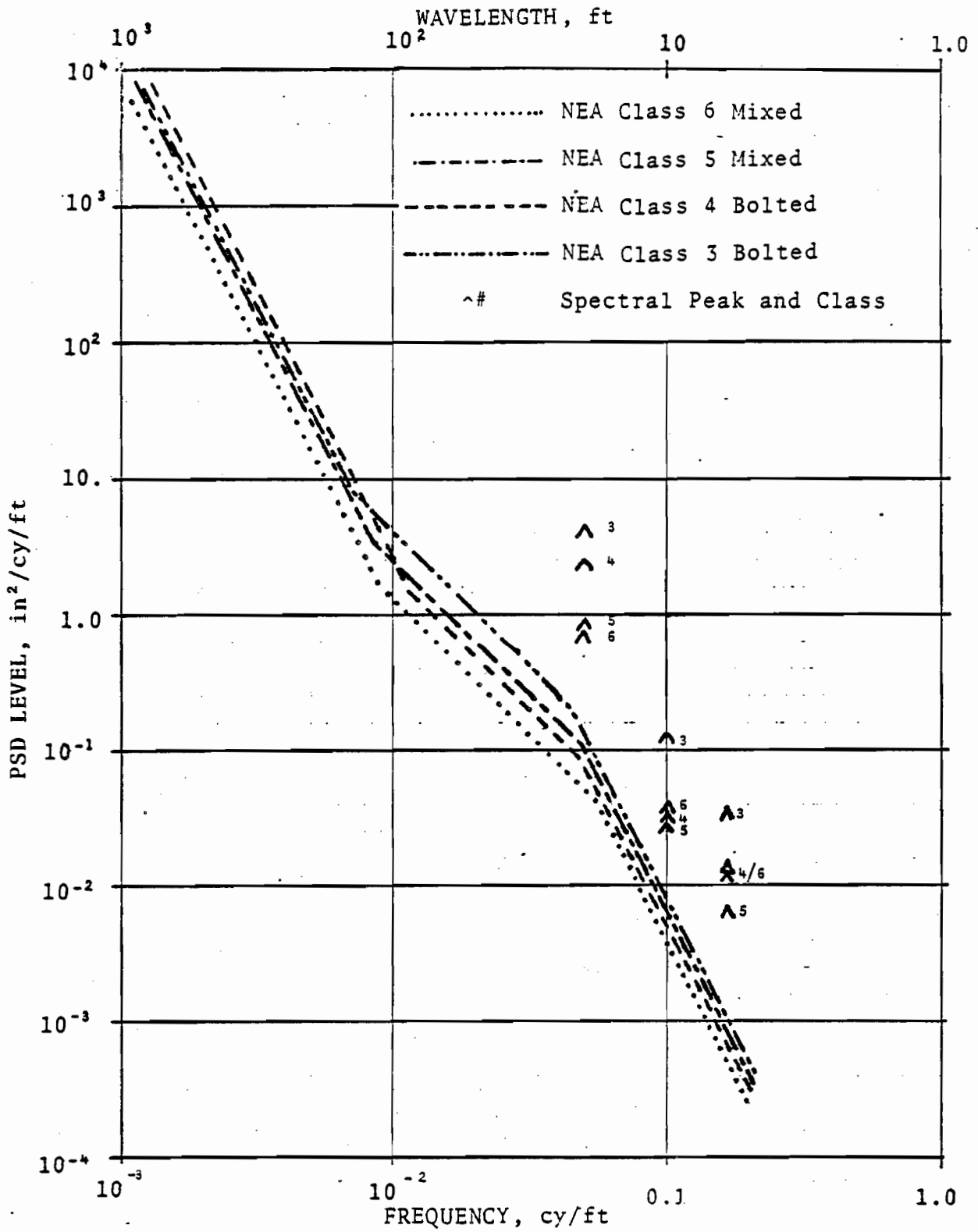


Figure B-1. Mean Profile, NEA, Various Classes

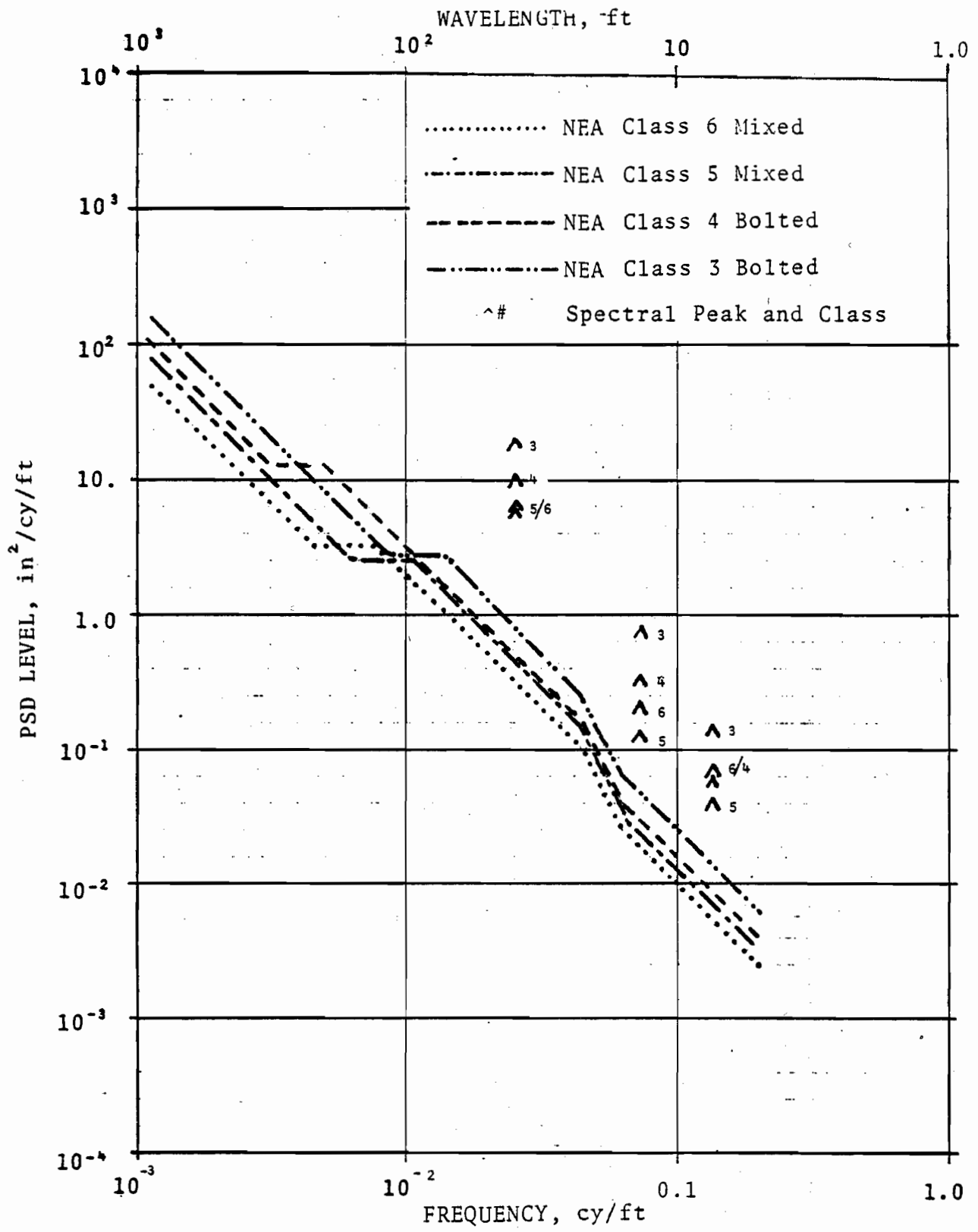


Figure B-2. Crosslevel, NEA, Various Classes

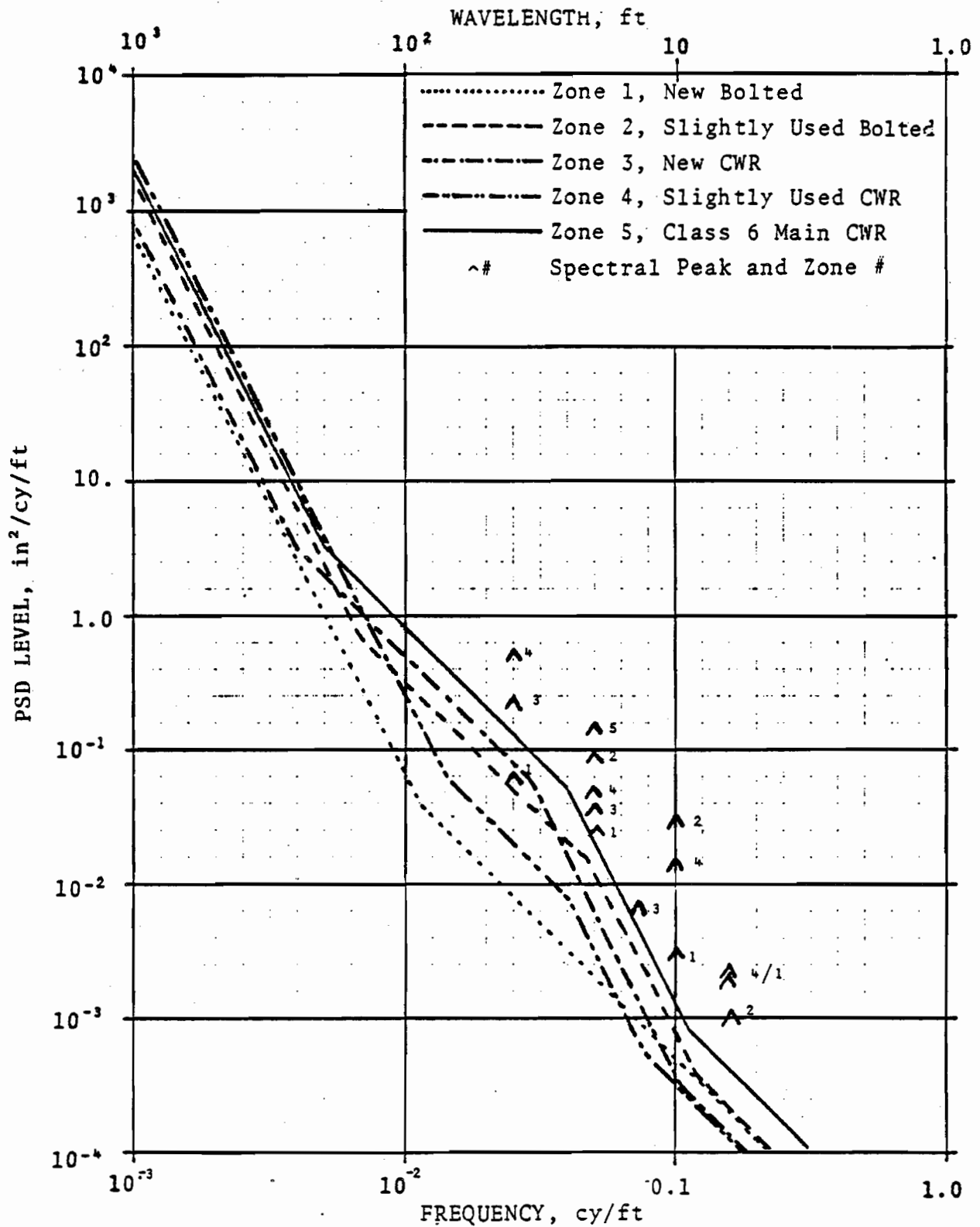


Figure B-3. Mean Profile, Class 6 and Better (TG-69)

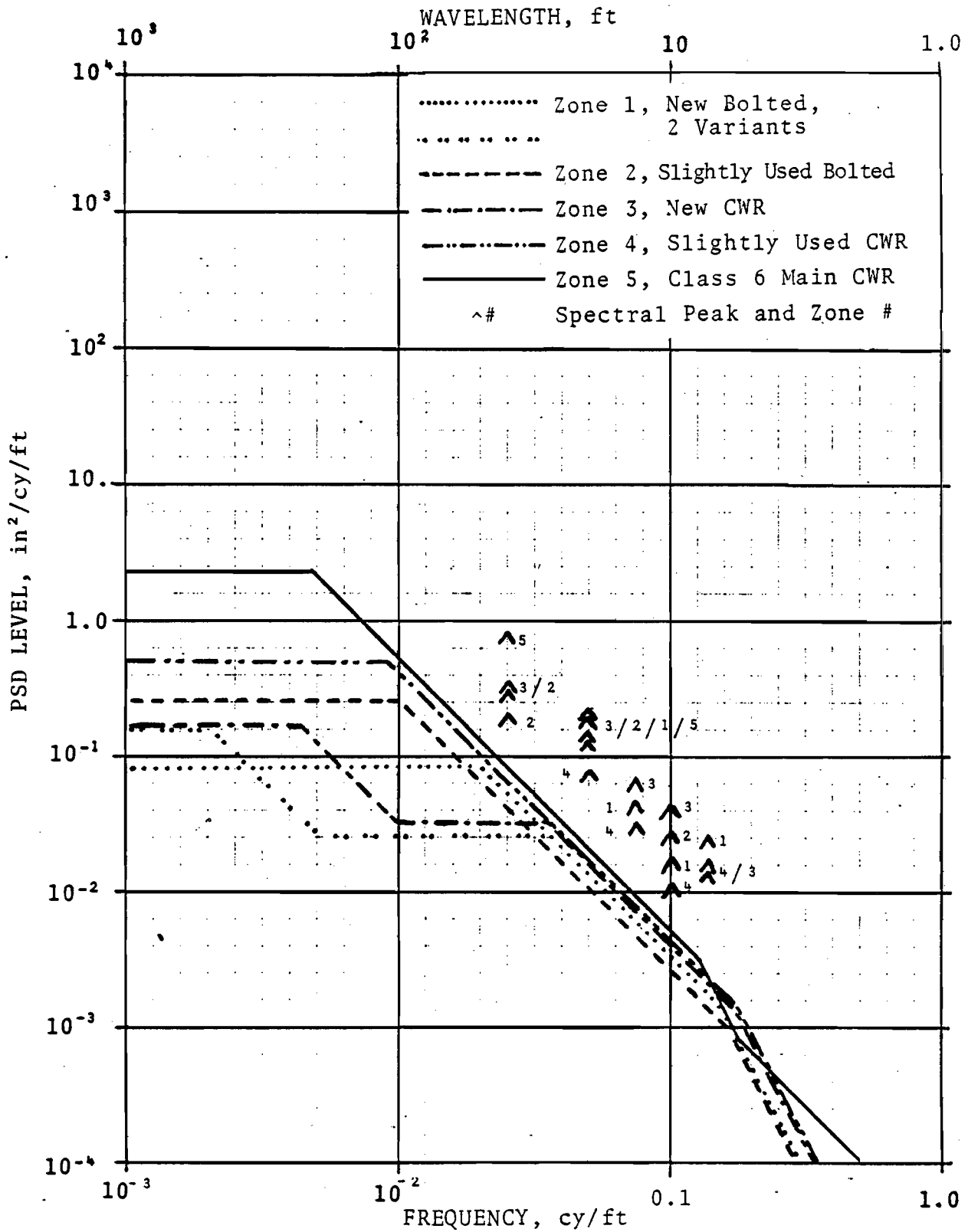


Figure B-4. Crosslevel Class 6 and Better (TG-69)

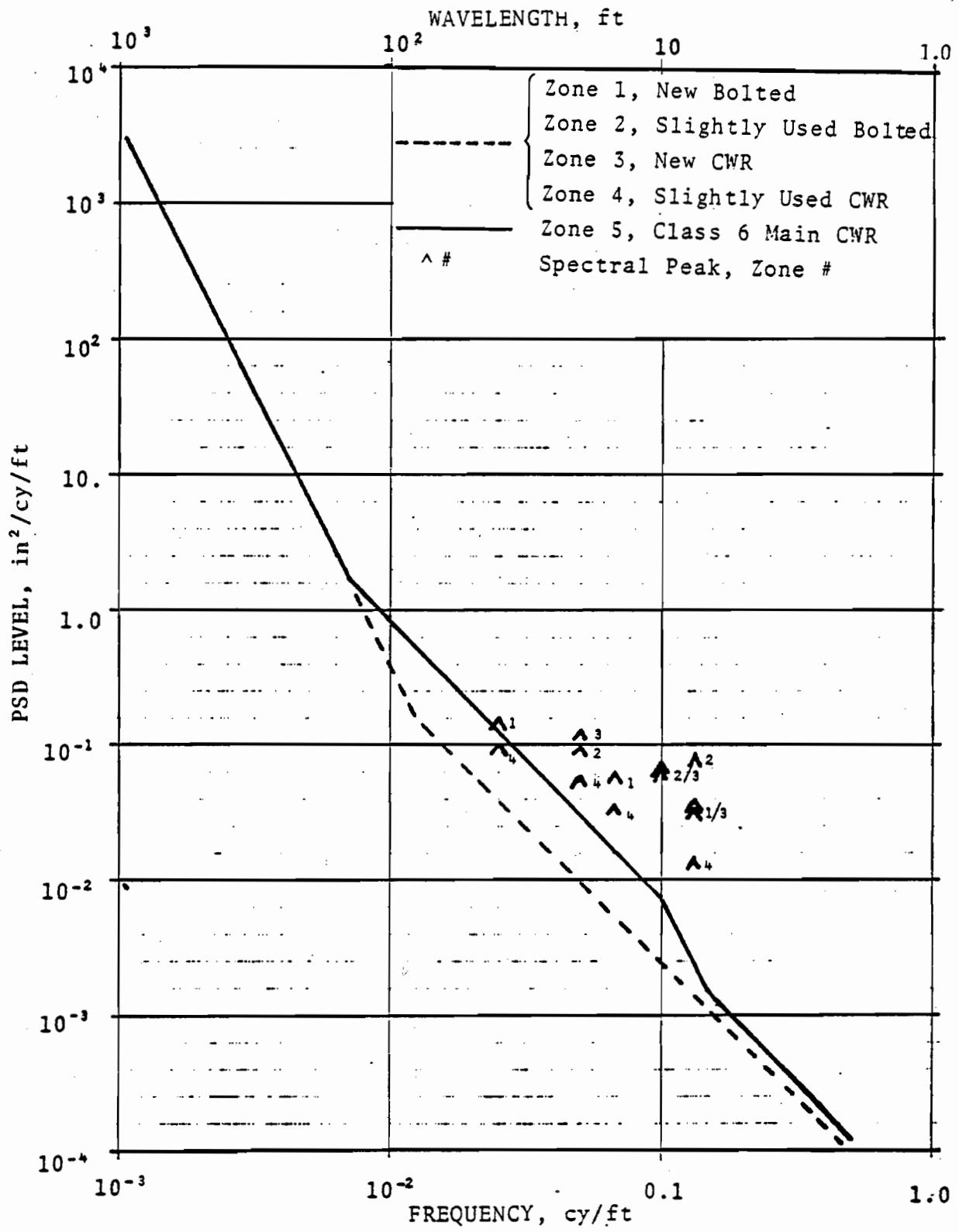


Figure B-5. Mean Alignment, Class 6 and Better (TG-69)

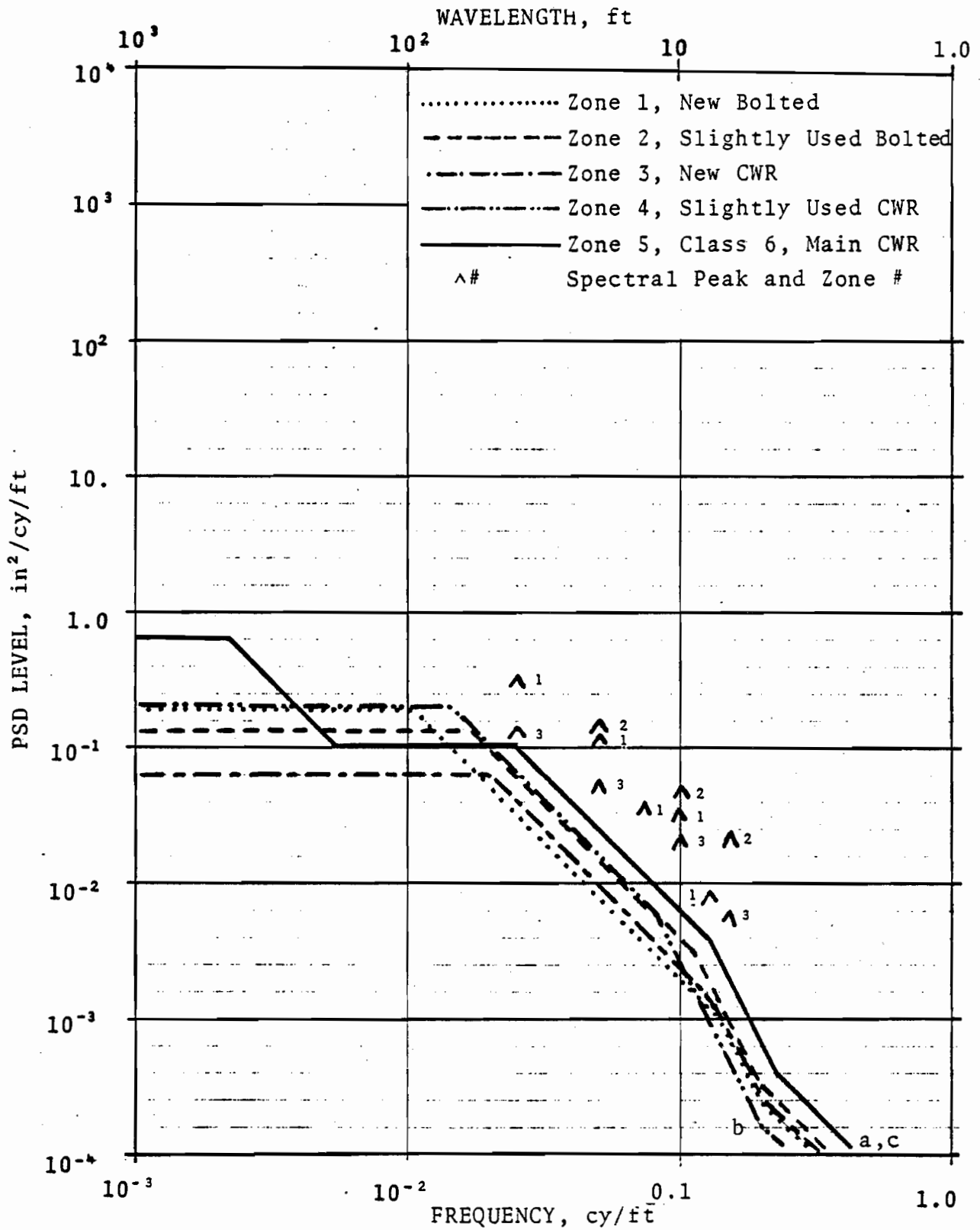


Figure B-6. Gage, Class 6 and Better (TG-69)

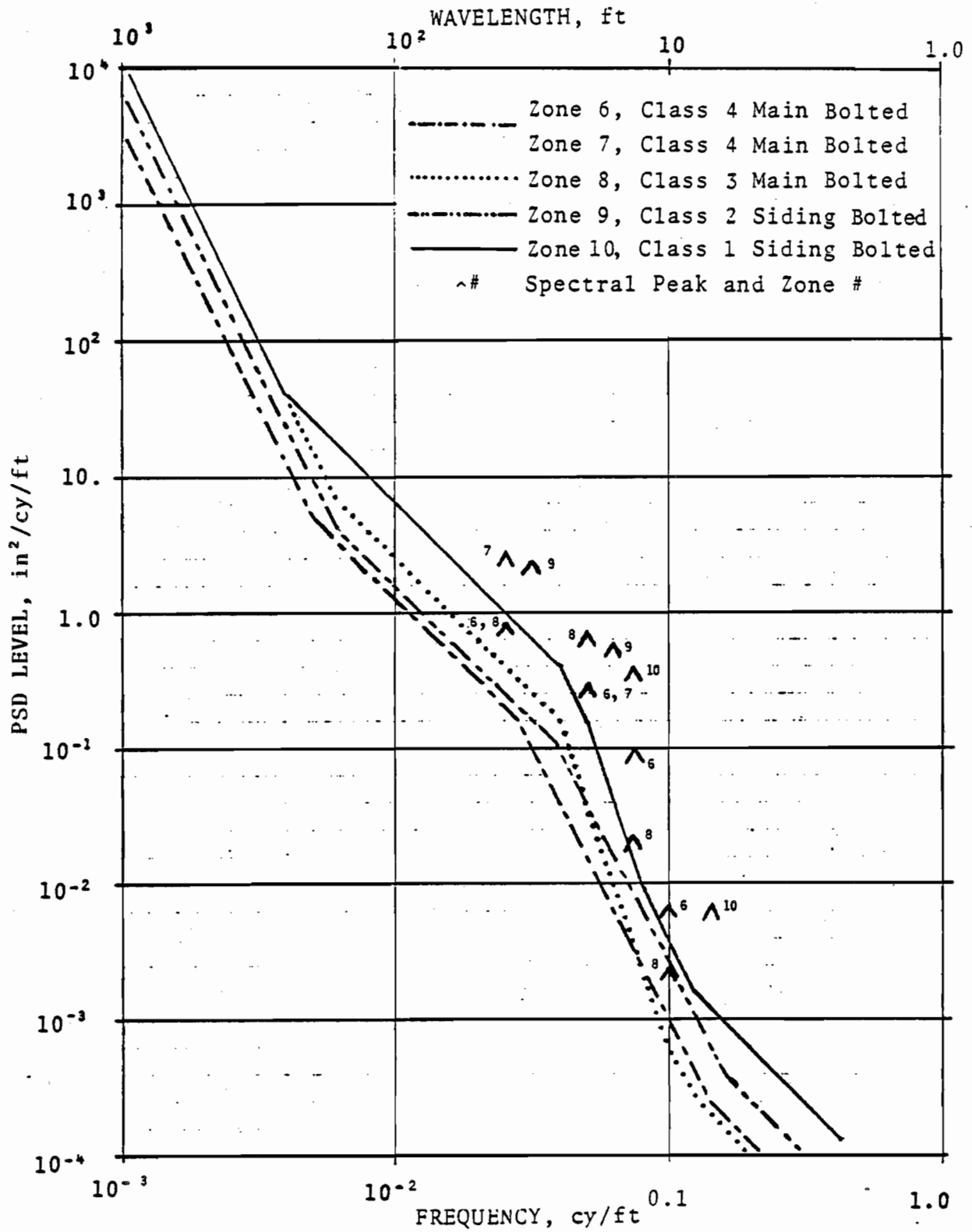


Figure B-7. Mean Profile, Various Bolted (TG-69)

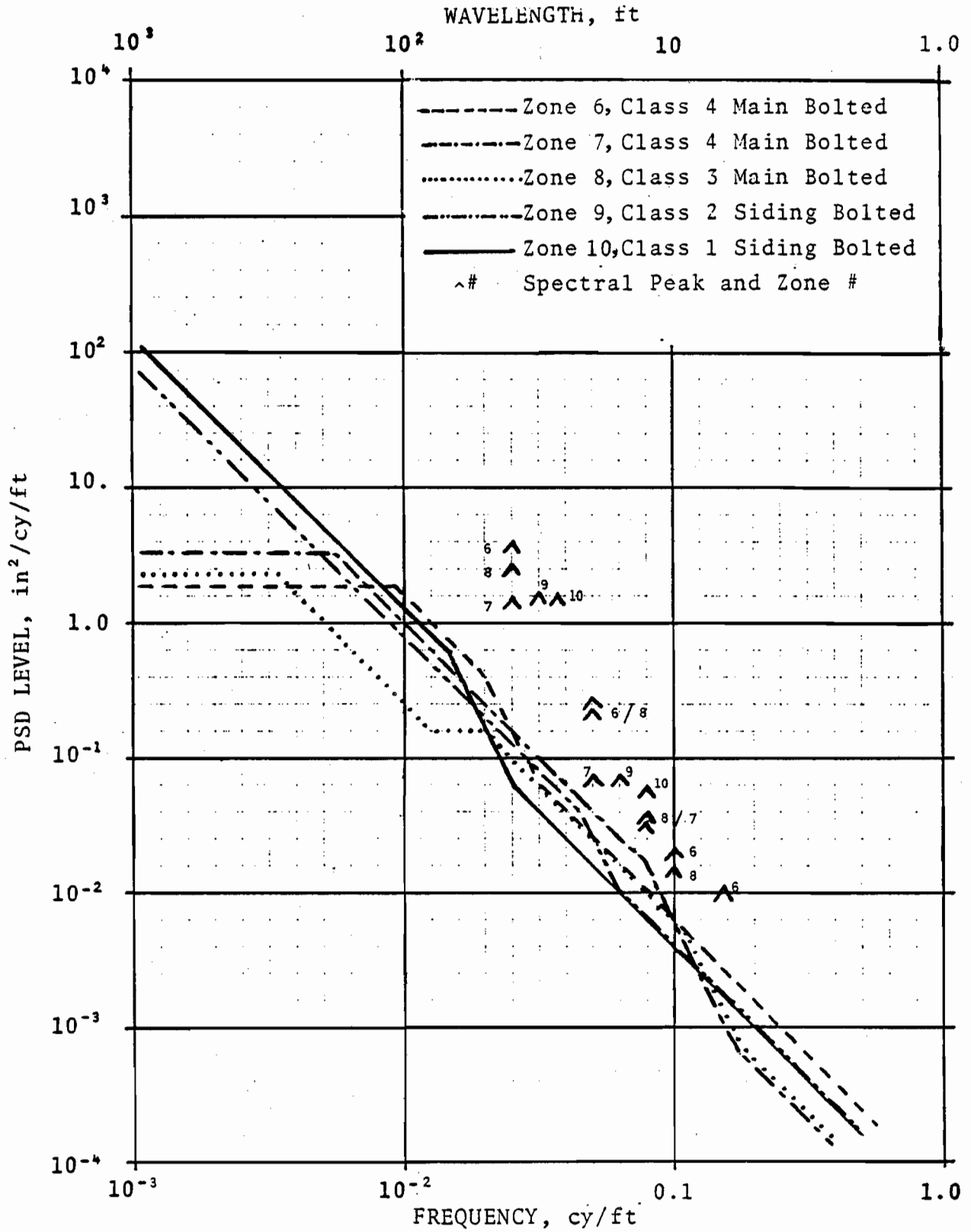


Figure B-8. Crosslevel, Various Bolted (TG-69)

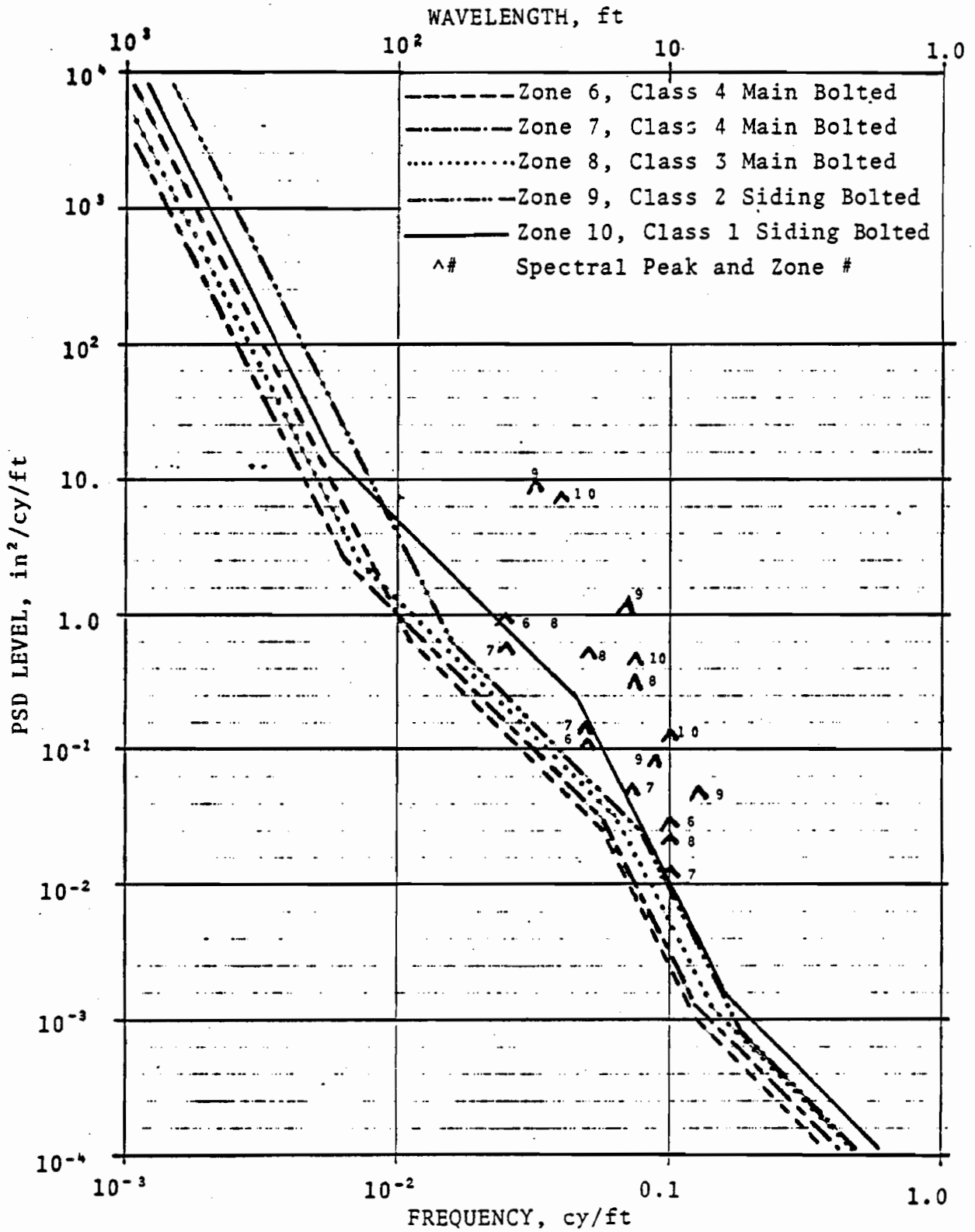


Figure B-9. Mean Alignment, Various Bolted (TG-69)

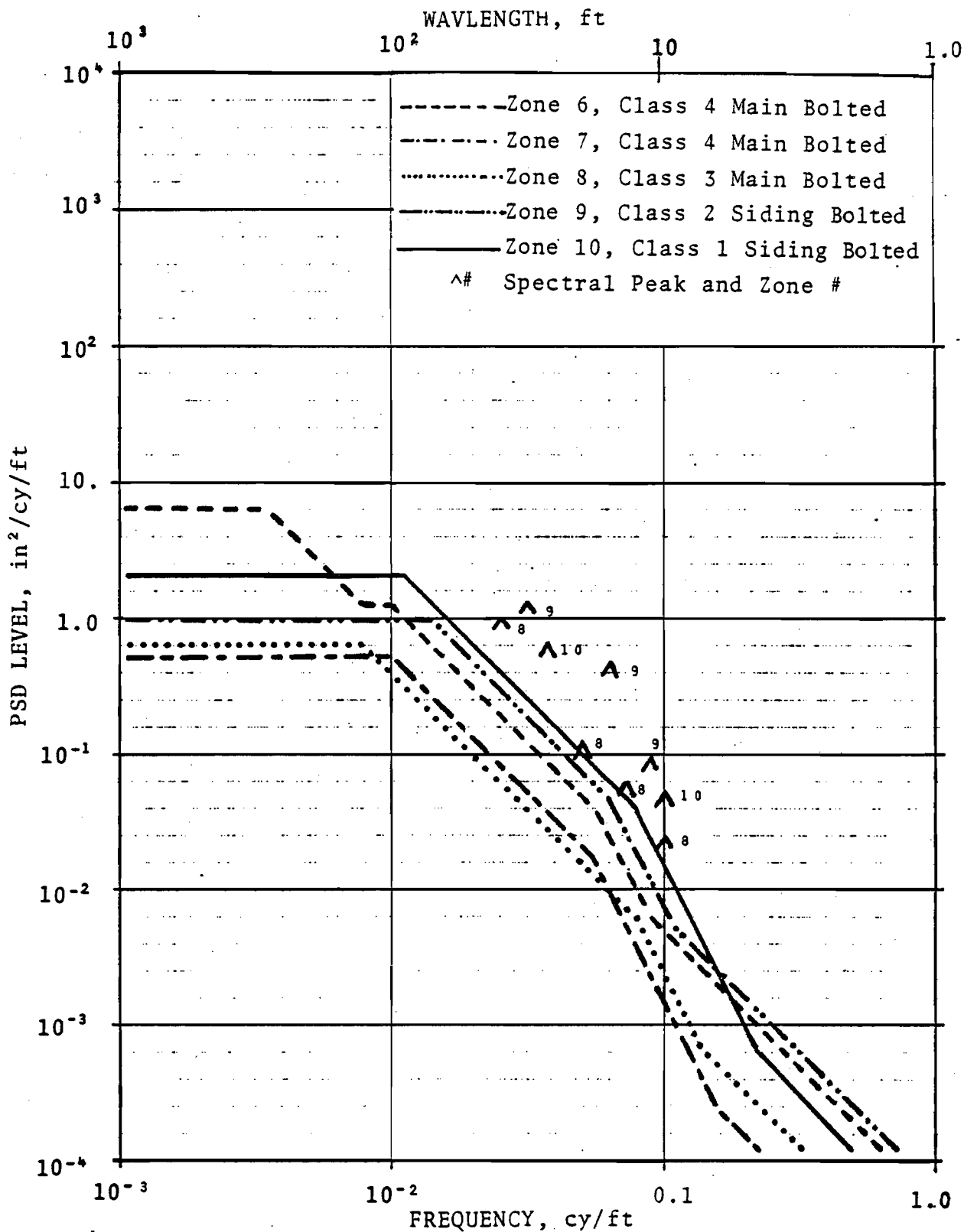


Figure B-10. Gage, Various Bolted (TG-69)

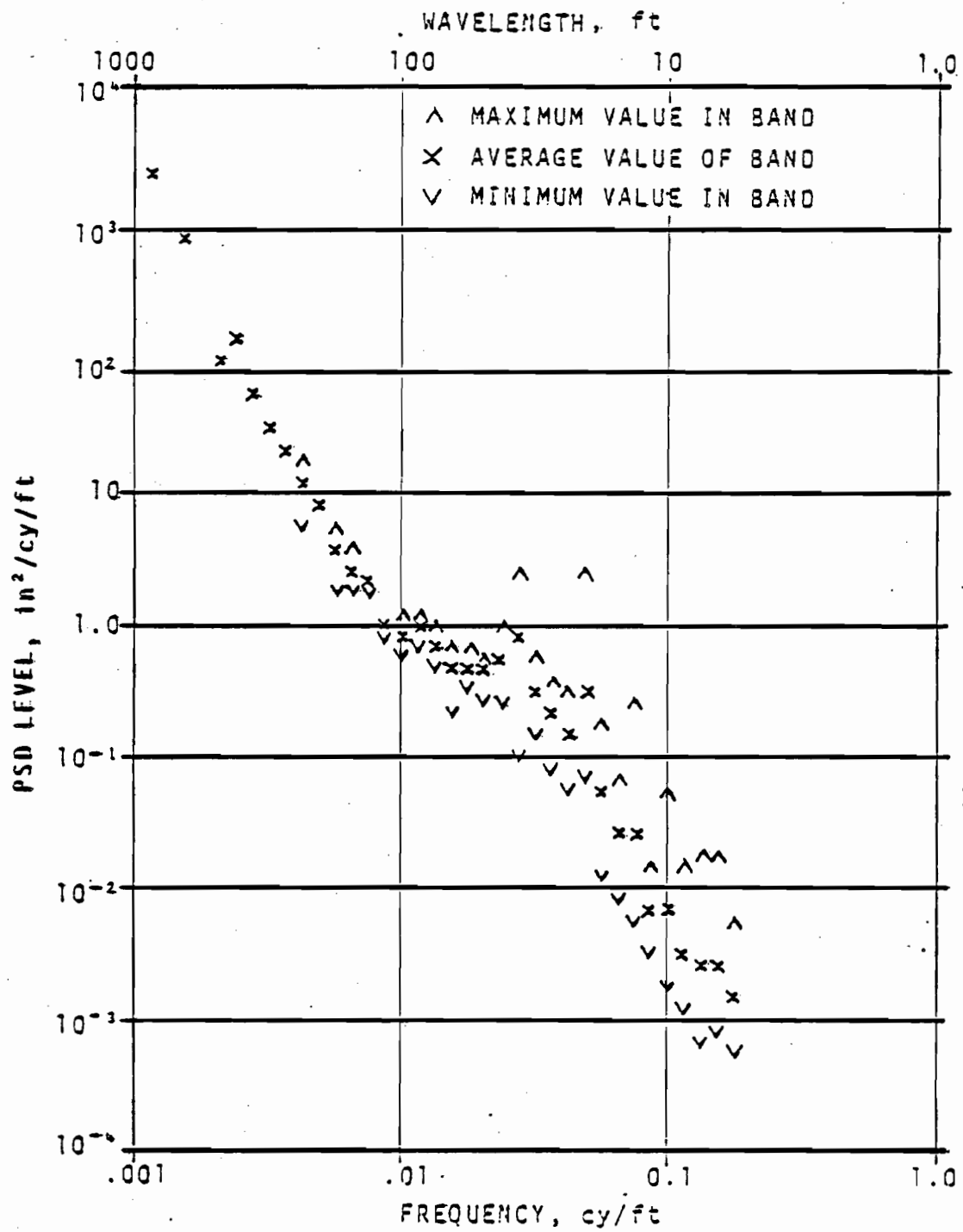


Figure B-11. Example Log-Log Format PSD, Right Profile

maximum/minimum levels are indicated by a \wedge / \vee , respectively. In this way, spectral variations and distinct peak/null frequencies can be noted.

The first step of the parameter extraction consists of eliminating superfluous data from the log-log PSD. Thus an x is retained if it corresponds to a good continuum value, and a \wedge is retained at frequencies corresponding to the rail length periodicity and its harmonics. Application of this procedure results in a PSD graph such as shown in Figure B-12 where the raw data of Figure B-11 has been used.

Next the continuum is fit using the profile -4, -2, -4 power law. This procedure is shown in Figure B-12.

As discussed in Section 2.2.2, PSD models for profile and alignment are of the form:

$$S_1(\phi) = \frac{A_1 \phi_{14}^2 (\phi^2 + \phi_{13}^2)}{\phi^4 (\phi^2 + \phi_{14}^2)} \quad (1)$$

where

$S_1(\phi)$ = power spectral density

A_1 = roughness constant

ϕ_{13}, ϕ_{14} = break frequencies.

The values of parameters of the model given by Equation 1, i.e., $A_1, \phi_{13}, \phi_{14}$ are estimated as follows:

ϕ_{13} = frequency where the spectrum changes from the first -4 to -2 power law

ϕ_{14} = frequency where the spectrum changes from -2 to the second -4 power law

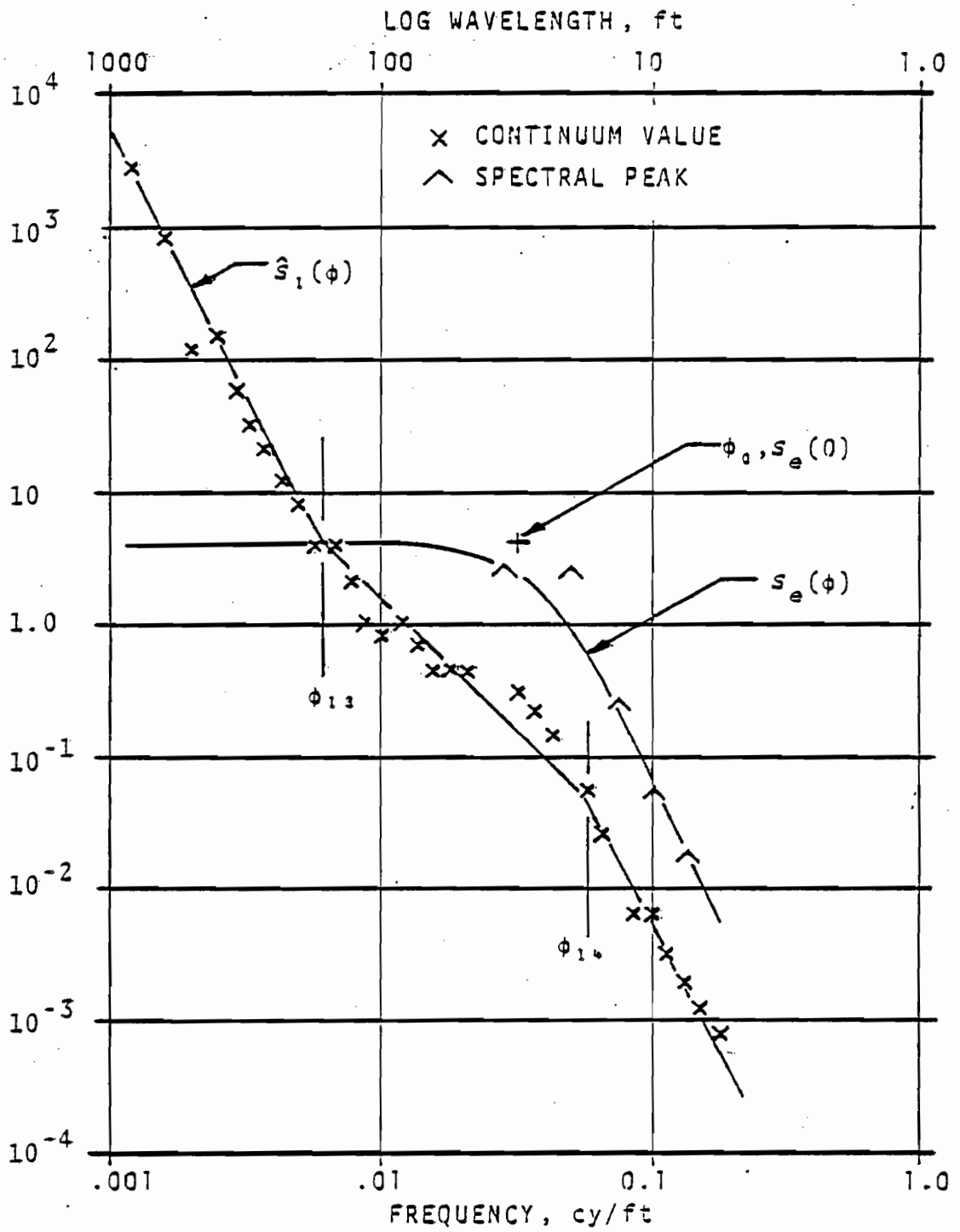


Figure B-12. Procedure for Parameter Determination from PSD Data

and A_1 = PSD level where the -2 power law spectrum intersects the abscissa at a frequency of 1 cycle/foot.

The pertinent parameters extracted from Figure B-12 are as follows:

$$A_1 = 1.6 \times 10^{-4} \text{ in}^2\text{-cy/ft}$$

$$\phi_{13} = 6.3 \times 10^{-3} \text{ cy/ft}$$

$$\phi_{14} = 5.6 \times 10^{-2} \text{ cy/ft}$$

Spectral peaks can be used to estimate the mean joint amplitude, C , and decay rate, k . It can be shown* that the peaks are bounded by an envelope, $S_e(\phi)$ of the form

$$S_e(\phi) = \frac{8}{B} \left(\frac{\bar{C}}{Lk} \right)^2 \left[1 + (2) \phi/k \right]^2^{-2} \quad (2)$$

where B is the resolving bandwidth of the PSD and L is the rail length.

When converted to log-log form, $S_e(\phi)$ is characterized by two straight line asymptotes; one having a constant level as it approaches zero frequency, and the other having ϕ^{-4} characteristic as frequency approaches infinity.

Constants that can be used to characterize the joint are prescribed by the intersection of the two asymptotes. This

* Corbin, J. C., "Statistical Representations of Track Geometry", Volume I, II, Report Nos. FRA/ORD-80/22.1 and FRA/ORD-80/22.2, National Technical Information Service, Springfield, Virginia, March 1980.

intersection defines a frequency on the abscissa, ϕ_0 , that is related to the decay rate by:

$$k = 2 \pi \phi_0. \quad (3)$$

The PSD ordinate at zero frequency, $S_e(0)$, gives the average joint amplitude:

$$C = \pm Lk \left(\frac{BS_e(0)}{8} \right)^{1/2} = \pm L\phi_0 \left(\frac{BS_e(0)}{2} \right)^{1/2} \quad (4)$$

The sign uncertainty is a consequence of the loss in phase information in PSD processing.

The fitting of the $S_e(\phi)$ to the spectral peaks is shown in Figure B-12. The values of different parameters are:

$$\phi_0 = 3.2 \times 10^{-2} \text{ cy/ft}$$

$$S_e(\phi_0) = 4.0 \text{ in}^2/\text{cy/ft}$$

$$k = 0.20 \text{ ft}^{-1}$$

and $\tau = 0.11 \text{ in.}$

The resolving bandwidth of the PSD processor in this case was $4.1 \times 10^{-4} \text{ cy/ft.}$

B.3 EXTREMELY LONG AND SHORT WAVELENGTHS

Routine PSD processing from track geometry data cover a wavelength range of 2 to 1000 feet. The determination of the railway track behavior beyond this range requires the use of data other than the usual track geometry measurements.

To characterize extremely short wavelength behavior, some data already exists in the literature in the form of 13 octave RMS levels*. These were converted to PSD's and the results are contained in Section 2.3, of Volume I.

Survey data from railroad track charts were used to estimate the extremely long wavelength (ELW) behavior of profile, and alignment. In the theoretical analysis of ELW profile let y_n be the height in inches at the distance location, x_n , measured in feet. If the slope is uniform between x_n and x_{n+1} , then the contribution to the Fourier transform of slope (slope spectrum) between x_n and x_{n+1} is given by:

$$U_n(\phi) = M_n e^{-i2\phi X_n} \frac{\sin(\pi\phi L_n)}{\pi\phi}, \quad (5)$$

where

$U_n(\phi)$ = complex spectrum due to slope segment,

X_n = mean location of segment (ft),
 $= (x_{n+1} + x_n)/2$

L_n = length of segment (ft),
 $= x_{n+1} - x_n$,

and M_n = slope of segment (in/ft),
 $= (y_{n+1} - y_n)/L_n$.

Note that the term in the brackets is the Fourier transform of a rectangular pulse of duration L_n and centered symmetrically about the origin. The exponential pre-multiplier is a phase shifter that moves the pulse away from the origin.

* Remington, P.J., et al, "Wheel/Rail Noise and Vibration", final Report (2 Volumes), UMTA-MA-06-0025-75-10 and UMTA-MA-06-0025-11, May 1975.

A length of track, L , is a linear combination of such track segments. The total spectrum due to N such segments is given by:

$$U(\phi) = \sum_{n=1}^{N+1} U_n(\phi) , \quad (6)$$

where $U_{N+1}(\phi)$ is a spectrum detrending term. It is generated as above with:

$$x_{N+1} = (x_{N+1} + x_1)/2,$$

$$L_{N+1} = x_{N+1} - x_1 \equiv L,$$

$$M_{N+1} = (h_{N+1} - h_1)/L.$$

The ELW profile PSD, $S_3(\phi)$, is then obtained by computing:

$$S_3(\phi) = \frac{1}{4 \phi^2 L} U(\phi) U^*(\phi) , \quad (7)$$

In the theoretical analysis of ELW curvature, let Ω_n be the curvature of the n^{th} segment, expressed in (degrees/100 ft). Let x_n be the location of the curve mid-point and I_n be the included angle of the curve. The the Fourier transform of a curvature segment is given by:

$$V_n(\phi) = \ell e^{-i \phi x_n} \Omega_n \frac{\sin(\phi L_n)}{\phi} , \quad (8)$$

where $V_n(\phi)$ = complex spectrum due to n^{th} segment,

L_n = length of segment = 100 (I_n/Ω_n) feet,

and ℓ = conversion constant

$$= \frac{\pi}{1500} \frac{\text{in/ft}}{\text{Degrees/100 ft}}$$

The total curvature spectrum due to N segments is given by:

$$V(\phi) = \sum_{n=1}^{N+1} v_n(\phi) , \quad (9)$$

where $V_{N+1}(\phi)$ is a spectrum detrending term. It is generated as above with:

$$C_{N+1} = - \sum_{n=1}^N I_n/L ,$$

and $x_{N+1} = 1/2L$.

The ELW alignment PSD, $S_Y(\phi)$, is obtained by computing:

$$S_Y(\phi) = \frac{1}{16 \cdot 4 \cdot 4 \cdot L} V(\phi)V^*(\phi) , \quad (10)$$

where the frequency correction for double integration is included.

Results for ELW profile and alignment are given in Section 2.3 of volume I.

B.4 TABULATION OF PARAMETERS

The amplitudes and break frequencies of the continuum portion of the spectra shown in Figure B-1 through B-10 were evaluated. These are summarized in Tables B-1 for surface variables, and B-2

for line variables. The standard deviations of the MCO's constructed on the continuum portion of these spectra are listed in the first part of Table B-3.

Also recognizable in the PSD's of Figure B-1 through B-10 are the line spectral components that are associated with the periodic process. The characteristics of this process were evaluated by applying the procedure described in Section 2.2.4, Volume I, to individual rail profile and alignment PSD's (not shown). The mean joint amplitude, \bar{C} and the decay rate, k , were obtained and these are listed in Table B-3.

TABLE B-1
CONTINUUM PARAMETERS FOR SURFACE GEOMETRY.

| Zone Designator | Geometry Class | Profile | | | | Crosslevel | | | | | | |
|-----------------|----------------|--------------------------------------|--------------------------------------|--------------------------------------|---|--------------------------------------|--------------------------------------|--------------------------------------|--------------------------------------|--------------------------------------|---|------|
| | | ϕ_{13} , cy/ft $\times 10^{-3}$ | ϕ_{14} , cy/ft $\times 10^{-3}$ | ϕ_{15} , cy/ft $\times 10^{-2}$ | A_1 , in ² -cy/ft $\times 10^{-4}$ | ϕ_{h1} , cy/ft $\times 10^{-3}$ | ϕ_{h2} , cy/ft $\times 10^{-3}$ | ϕ_{h3} , cy/ft $\times 10^{-3}$ | ϕ_{h4} , cy/ft $\times 10^{-2}$ | ϕ_{h5} , cy/ft $\times 10^{-2}$ | A_h , in ² -cy/ft $\times 10^{-4}$ | |
| NEC | 6 | 8.9 | 5.6 | U | 1.3 | T | 4.5 | 7.1 | 4.5 | 6.3 | 2.0 | |
| NEC | 5 | 7.9 | 5.0 | U | 2.0 | T | 6.3 | 11.2 | 4.5 | 7.1 | 3.2 | |
| NEC | 4 | 11.2 | 5.0 | U | 2.5 | T | 3.2 | 5.0 | 4.5 | 6.3 | 3.2 | |
| NEC | 3 | 7.1 | 4.5 | U | 4.0 | T | 8.9 | 14.1 | 4.5 | 6.3 | 5.0 | |
| TG-69 Zone # | 1 | 6++ | 11.2 | A | A | 0.05 | { A 2.0 | A 5.0 | { 20.0 35.5 | 15.8 | U | 0.25 |
| | 2 | 6 | 7.1 | 5.0 | 12.6 | 0.32 | A | A | 10.0 | 17.8 | U | 0.32 |
| | 3 | 6+ | 4.0 | 2.8 | 10.0 | 0.50 | 4.5 | 10.0 | 35.5 | 17.8 | U | 0.40 |
| | 4 | 6+ | 14.1 | 4.0 | 7.9 | 0.13 | A | A | 8.9 | 17.8 | U | 0.40 |
| | 5 | 6 | 5.0 | 4.0 | 11.2 | 0.79 | A | A | 5.0 | 12.6 | 17.8 | 0.50 |
| TG-69 Zone # | 6 | 4 | 5.0 | 2.8 | 14.1 | 1.3 | A | A | 8.9 | 2.0 | 3.2 | 1.6 |
| | 7 | 4 | 5.0 | 2.8 | 14.1 | 1.3 | A | A | 5.6 | 7.9 | 17.8 | 1.0 |
| | 8 | 3 | 6.3 | 4.0† | 12.6 | 2.5 | 3.5 | 12.6 | 20.0 | 10.0 | 17.8 | 0.63 |
| | 9 | 2 | 6.3 | 4.0 | 15.8 | 1.6 | T | A | A | 4.5 | 6.3 | 0.8 |
| | 10 | 1 | 4.0 | 4.0† | 12.6 | 6.3 | T | A | A | 1.4 | 2.5 | 1.3 |

NOTES:

A - Degenerate case - set both frequencies to arbitrary but equal values.

T - Frequency below PSD range, set to 10^{-3} cy/ft.

U - Frequency above folding, set to 0.5 cy/ft.

† - Best fit value - spectrum does not obey usual model.

TABLE B-2
CONTINUUM PARAMETERS FOR LINE GEOMETRY

| Zone Designator | Geometry Speed/Class | Alignment | | | | Gage | | | | | | |
|-----------------|----------------------|--------------------------------------|--------------------------------------|--------------------------------------|---|--------------------------------------|--------------------------------------|--------------------------------------|--------------------------------------|--------------------------------------|---|------|
| | | ϕ_{53} , cy/ft $\times 10^{-3}$ | ϕ_{54} , cy/ft $\times 10^{-2}$ | ϕ_{55} , cy/ft $\times 10^{-1}$ | A_5 in ² -cy/ft $\times 10^{-4}$ | ϕ_{81} , cy/ft $\times 10^{-3}$ | ϕ_{82} , cy/ft $\times 10^{-3}$ | ϕ_{83} , cy/ft $\times 10^{-2}$ | ϕ_{84} , cy/ft $\times 10^{-2}$ | ϕ_{85} , cy/ft $\times 10^{-1}$ | A_8 in ² -cy/ft $\times 10^{-4}$ | |
| 69-GT | 1 | 6++ | 12.6 | A | A | 0.25 | A | A | 1.0 | 14.1 | 2.0 | 0.20 |
| | 2 | 6 | 12.6 | A | A | 0.25 | A | A | 1.8 | 11.2 | 2.0 | 0.40 |
| | 3 | 6+ | 12.6 | A | A | 0.25 | A | A | 2.0 | 12.6 | 2.0 | 0.25 |
| | 4 | 6+ | 12.6 | A | A | 0.25 | A | A | 1.4 | 7.9 | 2.0 | 0.40 |
| | 5 | 6 | 7.1 | 10.0 | 1.4 | 0.63 | 2.2 | 5.6 | 2.5 | 12.6 | 3.2 | 0.63 |
| 69-GT | 6 | 4 | 11.2 | 5.6 | 1.3 | 0.8 | 3.5 | 7.9 | 1.0 | 5.6 | 1.1 | 1.26 |
| | 7 | 4 | 6.3 | 5.6 | 1.3 | 1.0 | A | A | 1.0 | 5.6 | 0.9 | 0.50 |
| | 8 | 3 | 7.1 | 6.3 | 1.4 | 1.3 | A | A | 0.8 | 7.9 | 1.4 | 0.40 |
| | 9 | 2 | 15.8 | 7.9 | 1.8 | 1.6 | A | A | 1.4 | 6.3 | 1.1 | 2.00 |
| | 10 | 1 | 5.6 | 4.5 | 1.6 | 5.0 | A | A | 1.1 | 7.9 | 2.2 | 2.50 |

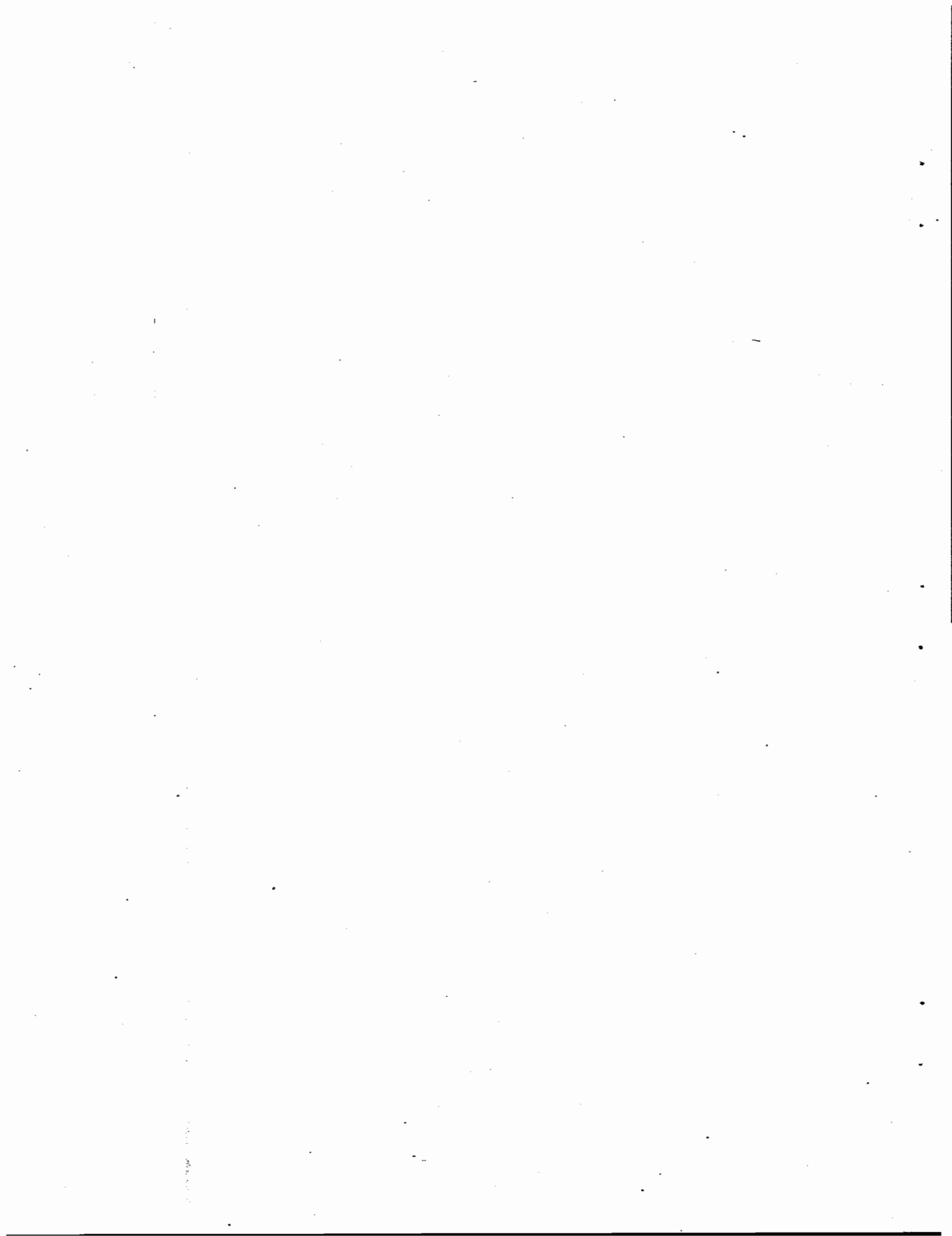
NOTES:

A - Degenerate case - set both frequencies to equal arbitrary values.

TABLE B-3
 CHARACTERIZATION OF PERIODIC PROCESS AND 62-FOOT
 MCO OF CONTINUUM PORTION OF SPECTRA

| | | | 62 ft MCO, Continuum | | | Periodic Process | | | | | | |
|-----------------|----------------|------------------|-------------------------|------------------------------|--------------------------------|--------------------------------|-----------------------------------|--------------|---------------------------------|-----------------------------------|--------------|------|
| | | | | | | Profile | | | Alignment | | | |
| Zone Designator | Geometry Class | Rail Length (ft) | Joint Stagger % | Profile, Standard Error (in) | Alignment, Standard Error (in) | Joint Amplitude \bar{C} (in) | Decay Rate, k (ft ⁻¹) | 62' MCO (in) | Joint Amplitude, \bar{C} (in) | Decay Rate, k (ft ⁻¹) | 62' MCO (in) | |
| NEC | 6 | 39 | 50 | 0.27 | N | 0.19 | 0.20 | 0.15 | N | N | N | |
| NEC | 5 | 39 | 50 | 0.32 | N | 0.19 | 0.14 | 0.13 | N | N | N | |
| NEC | 4 | 39 | 50 | 0.43 | N | 0.18 | 0.16 | 0.13 | N | N | N | |
| NEC | 3 | 39 | 50 | 0.42 | N | 0.27 | 0.22 | 0.22 | N | N | N | |
| # Zone 69-G-L | 1 | 6++ | 39 | 50 | 0.06 | 0.15 | 0.06 | 0.25 | 0.05 | 0.09 | 0.40 | 0.09 |
| | 2 | 6 | 39 | 50 | 0.08 | 0.15 | 0.10 | 0.40 | 0.10 | 0.17 | 0.71 | 0.17 |
| | 3 | 6+ | 39 | 18 | 0.12 | 0.15 | 0.09 | 0.40 | 0.09 | 0.16 | 0.89 | 0.16 |
| | 4 | 6+ | 39 | 36 | 0.11 | 0.15 | 0.07 | 0.35 | 0.07 | 0.08 | 0.45 | 0.08 |
| | 5 | 6 | 39 | 50 | 0.16 | 0.17 | 0.10 | 0.22 | 0.08 | 0.13 | 0.40 | 0.13 |
| # Zone 69-G-L | 6 | 4 | 39 | 50 | 0.20 | 0.24 | 0.18 | 0.18 | 0.13 | 0.15 | 0.16 | 0.11 |
| | 7 | 4 | {36 39} | 50 | 0.20 | 0.20 | 0.23 | 0.10 | 0.08 | 0.11 | 0.28 | 0.09 |
| | 8 | 3 | 38 | 45 | 0.31 | 0.24 | 0.26 | 0.13 | 0.16 | 0.19 | 0.22 | 0.15 |
| | 9 | 2 | 33 | Var. | 0.25 | 0.44 | 0.21 | 0.13 | 0.05 | 0.27 | 0.18 | 0.08 |
| | 10 | 1 | 28 | 50% | 0.44 | 0.43 | 0.15 | 0.16 | 0.06 | 0.17 | 0.25 | 0.13 |

N - Data not available.



APPENDIX C
EXAMPLES OF ISOLATED TRACK GEOMETRY VARIATIONS

This appendix gives examples of selected isolated track geometry variations. These are given as single events, periodic signatures and combined variations. Table C-1 gives an index to the Figures.

The alignment and profile traces are given in the space curve form. The space curve is a pseudo reconstruction of track as a curve in space without the effect of local terrain or curvature. Gage is plotted from a base line of 57.0 inches. Crosslevel is given both as measured crosslevel and crosslevel deviations from uniformity. The crosslevel deviations are calculated by high-pass filtering the measured crosslevel.

TABLE C-1

INDEX TO FIGURES

SINGLE EVENT SIGNATURES

| | | |
|----------------------------------|---|---------------|
| Figures C.1.a.1 through C.1.a.9 | - | Cusp |
| Figures C.1.b.1 through C.1.b.9 | - | Bump |
| Figures C.1.c.1 through C.1.c.12 | - | Jog |
| Figures C.1.d.1 through C.1.d.15 | - | Plateau |
| Figures C.1.e.1 through C.1.e.3 | - | Trough |
| Figures C.1.f.1 through c.1.f.9 | - | Miscellaneous |

PERIODIC VARIATIONS

| | | |
|----------------------------------|---|------------------------|
| Figures C.2.a.1 through C.2.a.11 | - | Cusp |
| Figures C.2.b.1 through C.2.b.9 | - | Sinusoid |
| Figures C.2.c.1 through C.2.c.6 | - | Periodic with Decay |

COMBINED VARIATIONS

| | | |
|---------------------------------|---|---------------------|
| Figures C.3.a.1 through C.3.a.7 | - | Isolated Signatures |
| Figures C.3.b.1 through C.3.b.9 | - | Periodic Signatures |
| Figures C.3.c.1 through C.3.c.2 | - | Miscellaneous |

C.1 SINGLE EVENT SIGNATURES

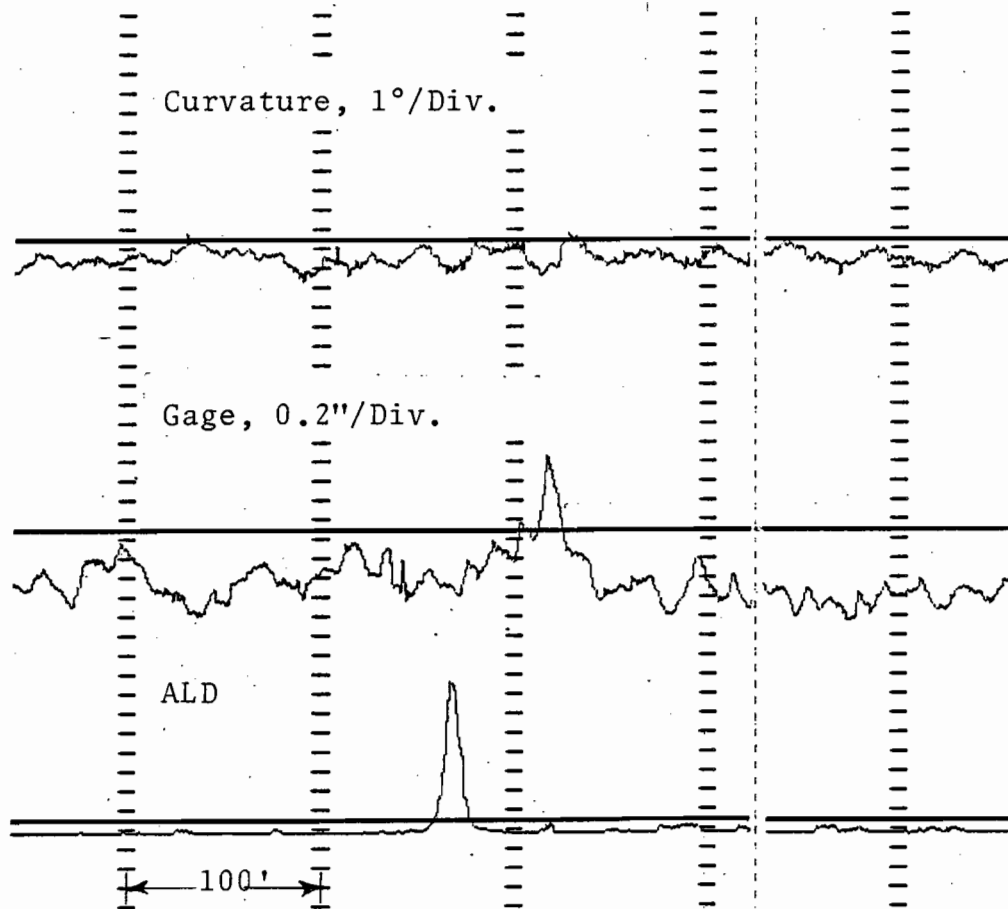


Figure C.1.a.1. Gage Cusp Near a Track Appliance
(Class 2, Curve).

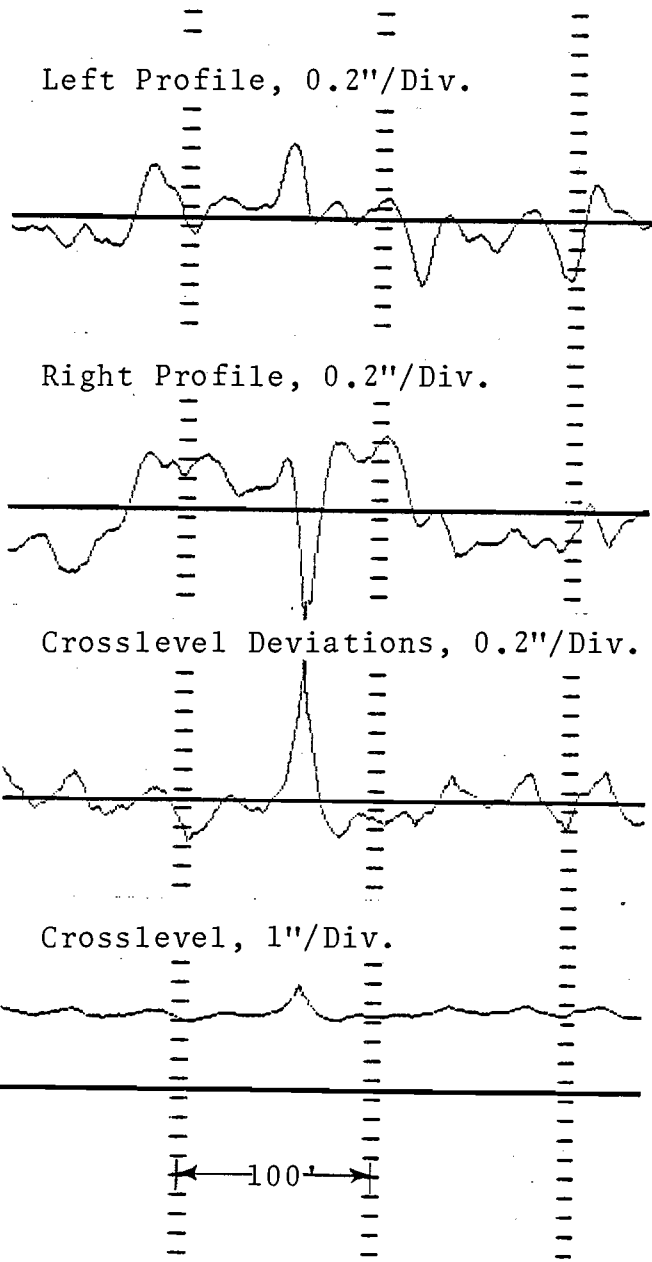


Figure C.1.a.2. Profile and Crosslevel Cusp Due to Low Joint on the Low Rail (Class 3, Bolted, Curve).

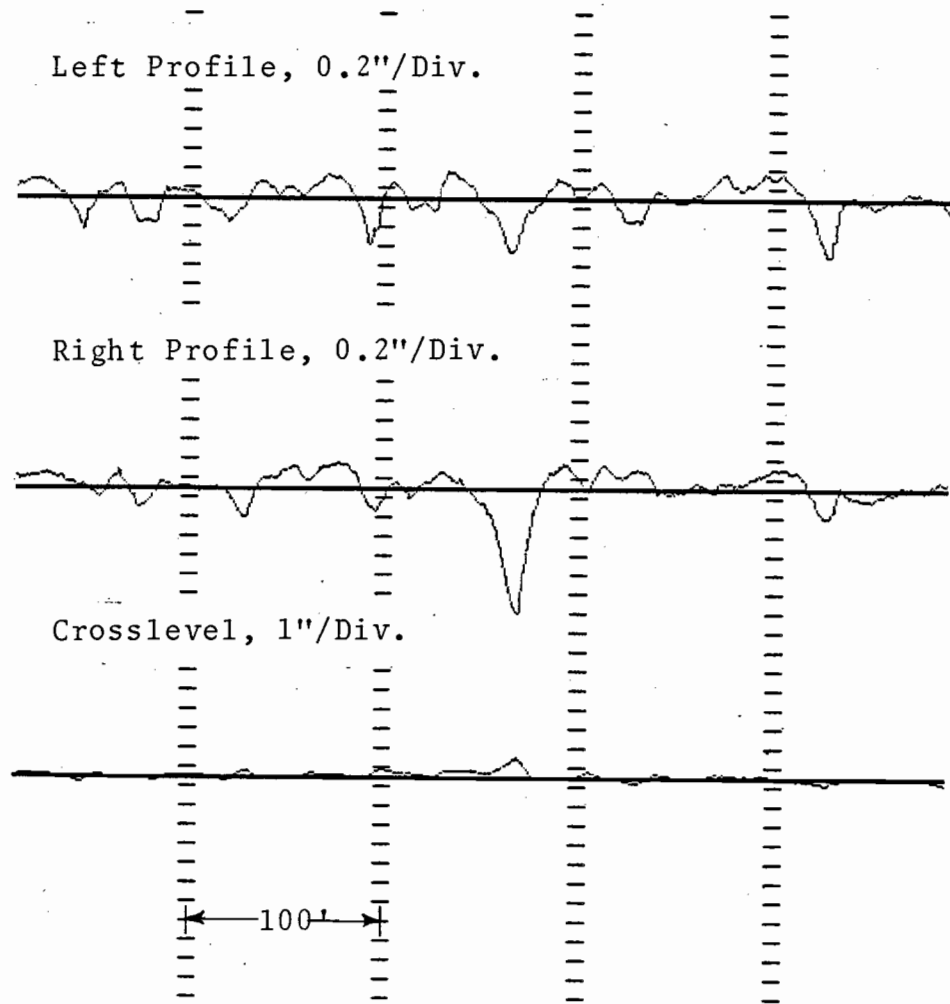
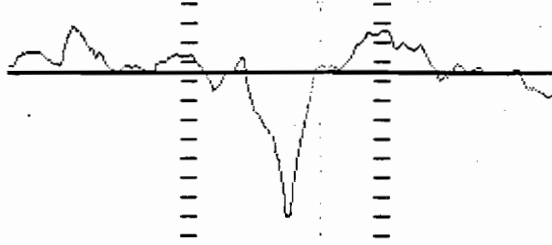


Figure C.1.a.3. Profile and Crosslevel Cusp
(Class 4, Tangent).

Crosslevel Deviations, 0.2"/Div.



Crosslevel, 1"/Div.

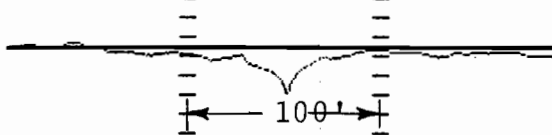
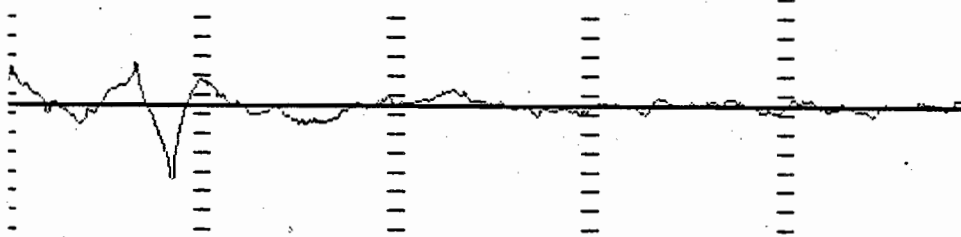
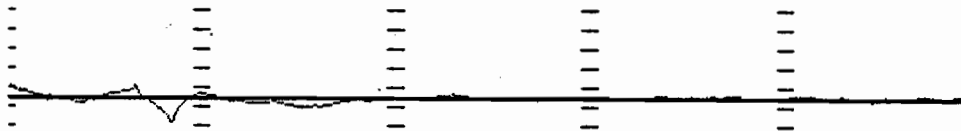


Figure C.1.a.4. Crosslevel Cusp (Class 3, Bolted, Tangent).

Crosslevel Deviations, 0.3"/Div.



Crosslevel, 1"/Div.



ALD



Figure C.1.a.5. Crosslevel and Profile Cusps at a Switch (Class 6, Tangent).

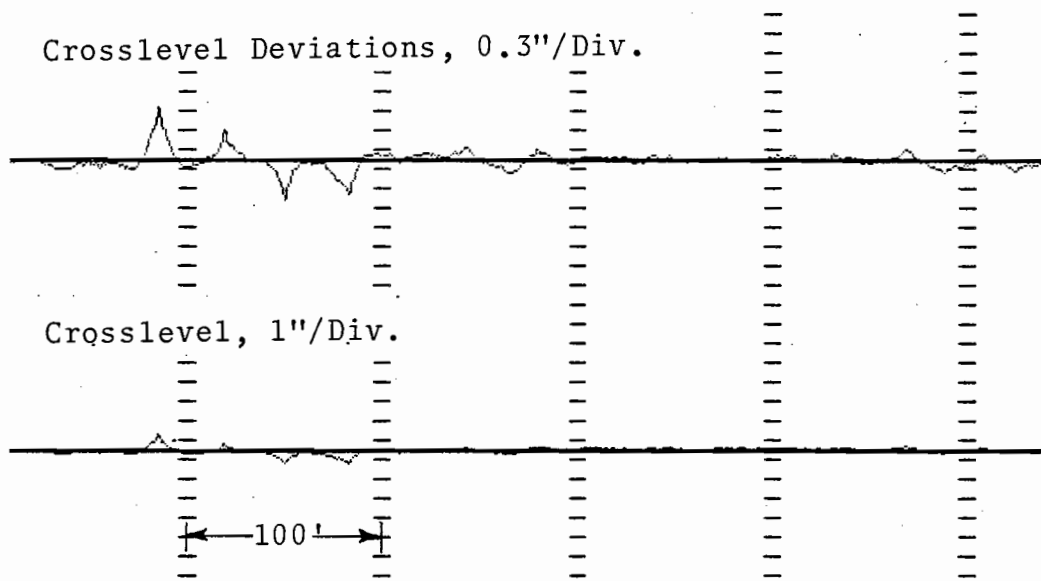


Figure C.1.a.6. Crosslevel and Profile Cusps Due to Staggered, Jointed, Buffer Rails (Class 6, Tangent).

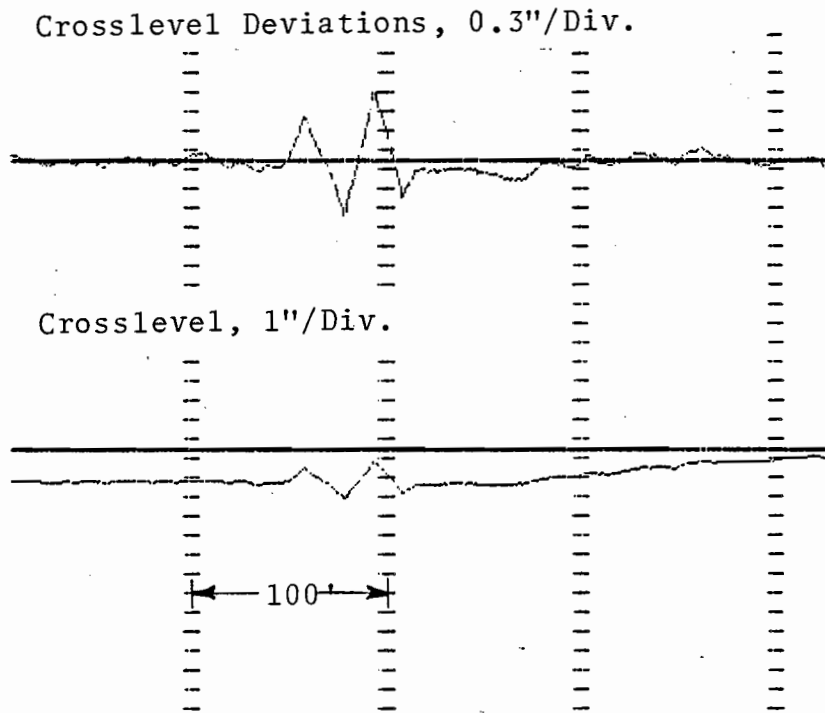


Figure C.1.a.7. Profile Bumps and Crosslevel Cusps Due to Staggered Bolted Buffer Rails in CWR (Class 6, Curve).

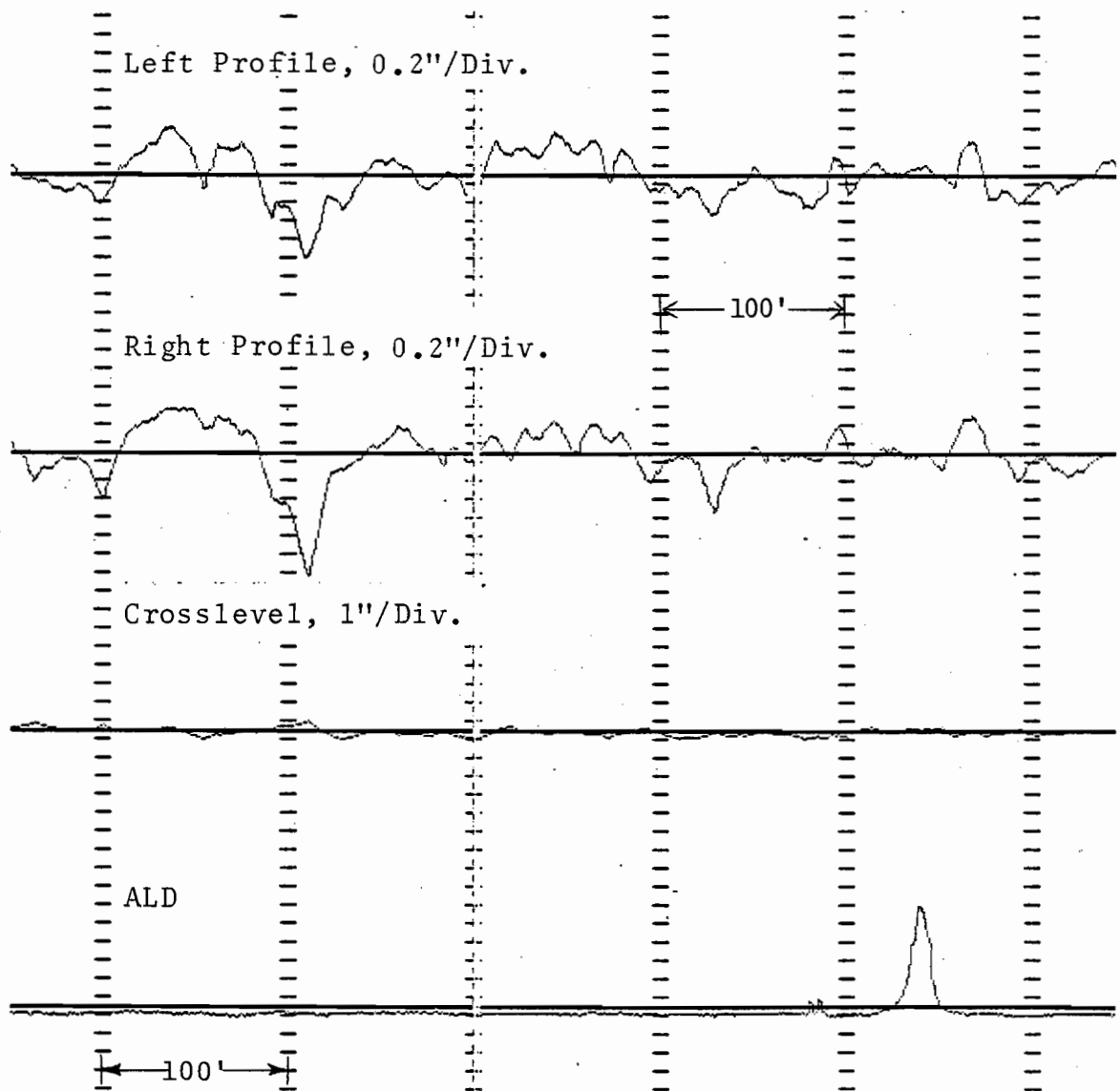


Figure C.1.a.8. Profile Cusp at a Switch (Class 4, Tangent).

C-10

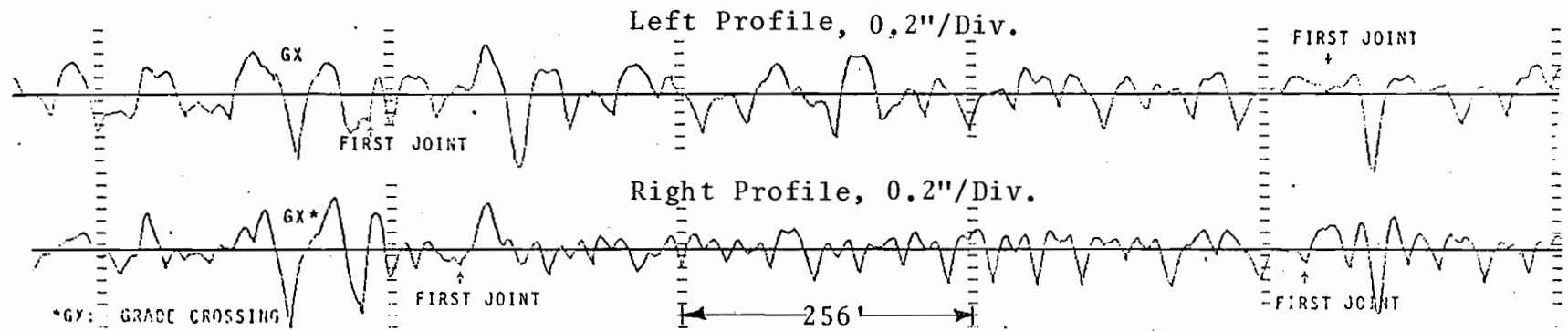


Figure C.1.a.9. Cusps in Mean Profile at a Grade Crossing (Class 3, Bolted).

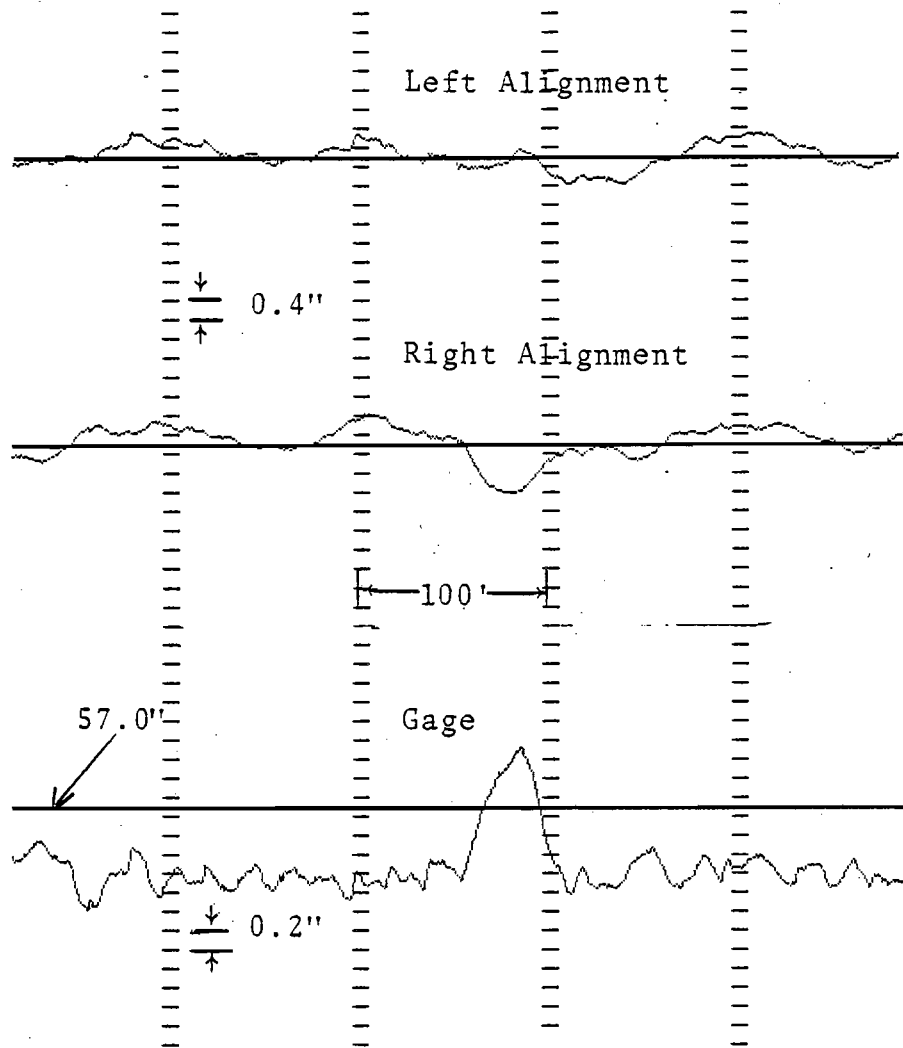


Figure C.1.b.1. A Bump in Gage.

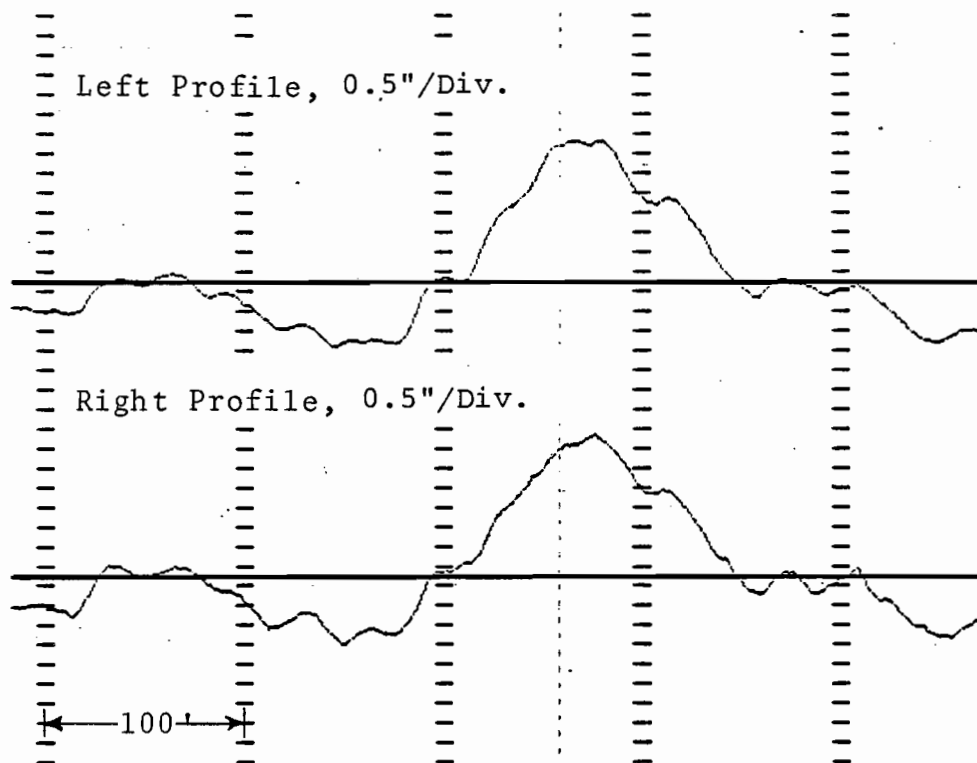


Figure C.1.b.2. Profile Bump in Both Rails at Transition of Reverse Curve Class 1).

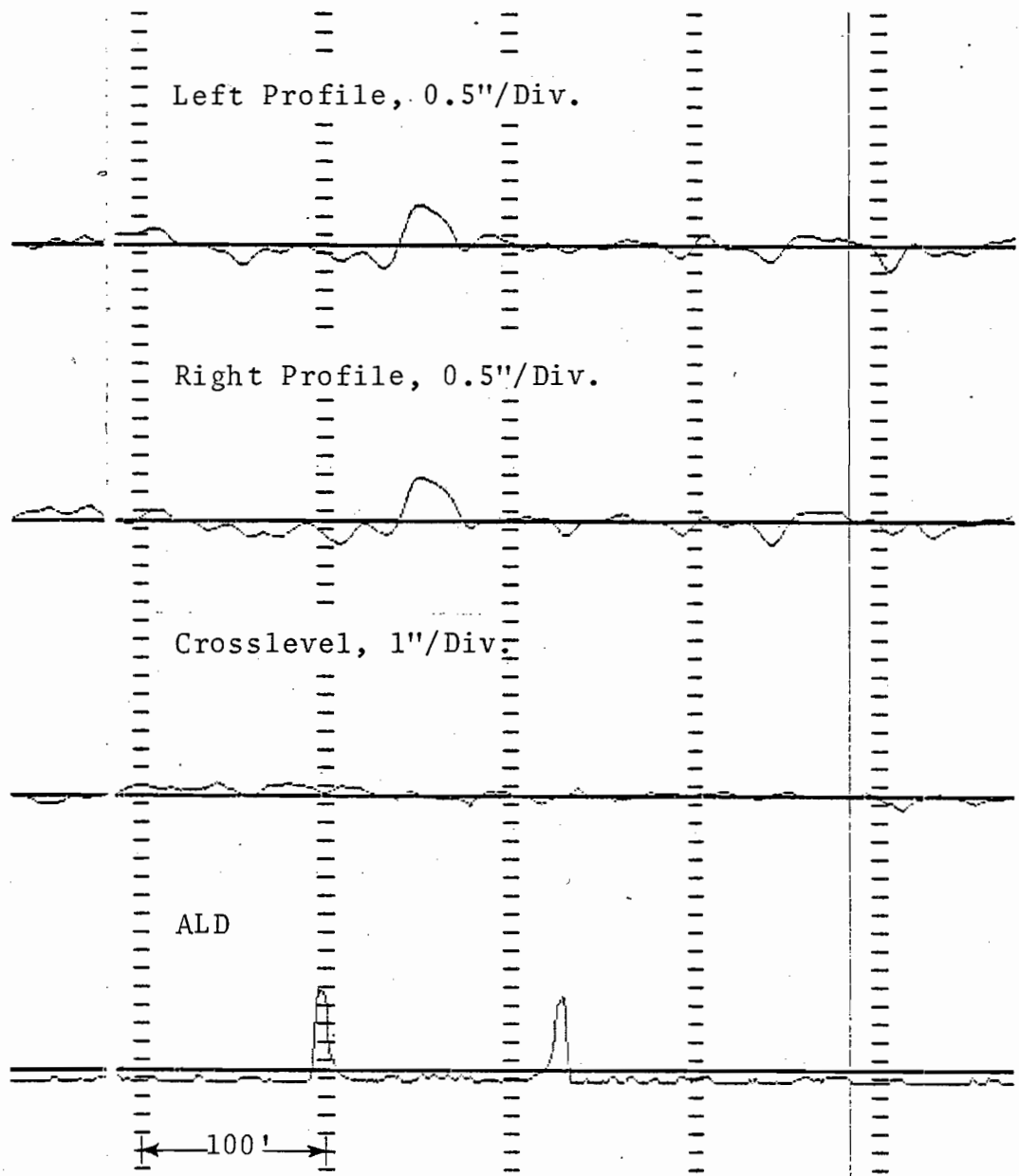


Figure C.1.b.3. Signature of Profile Bump on a Bridge (Class 2, Tangent).

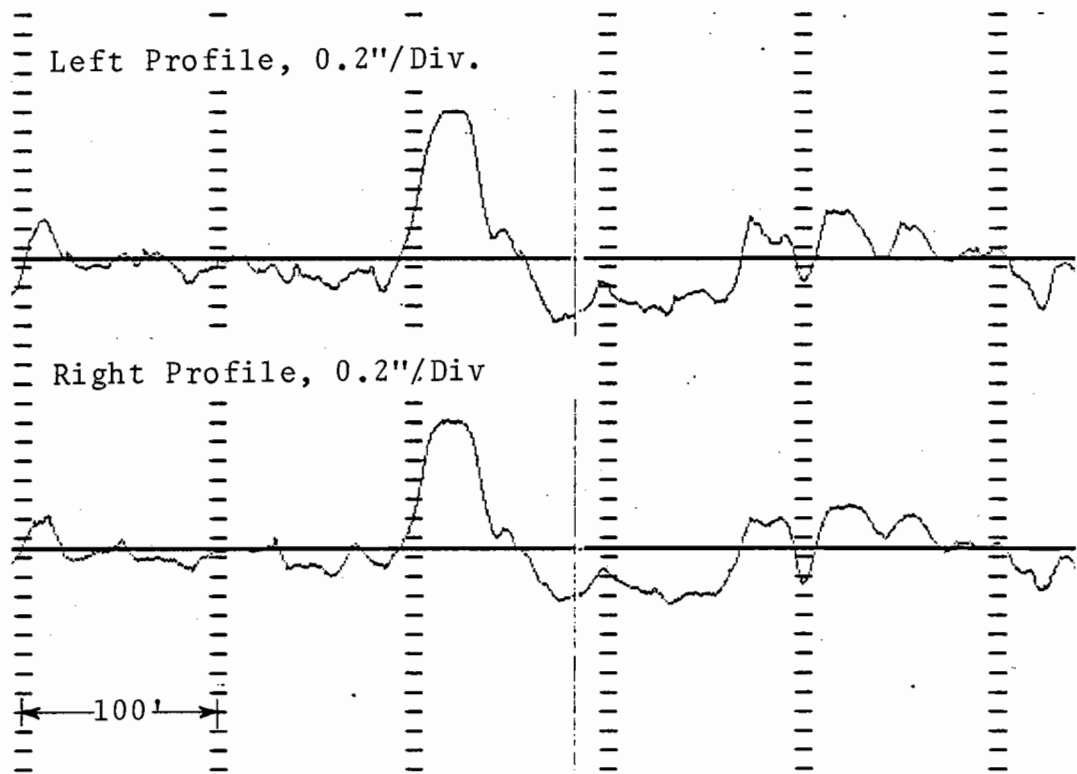


Figure C.1.b.4. Profile Bump (Class 2, Tangent).

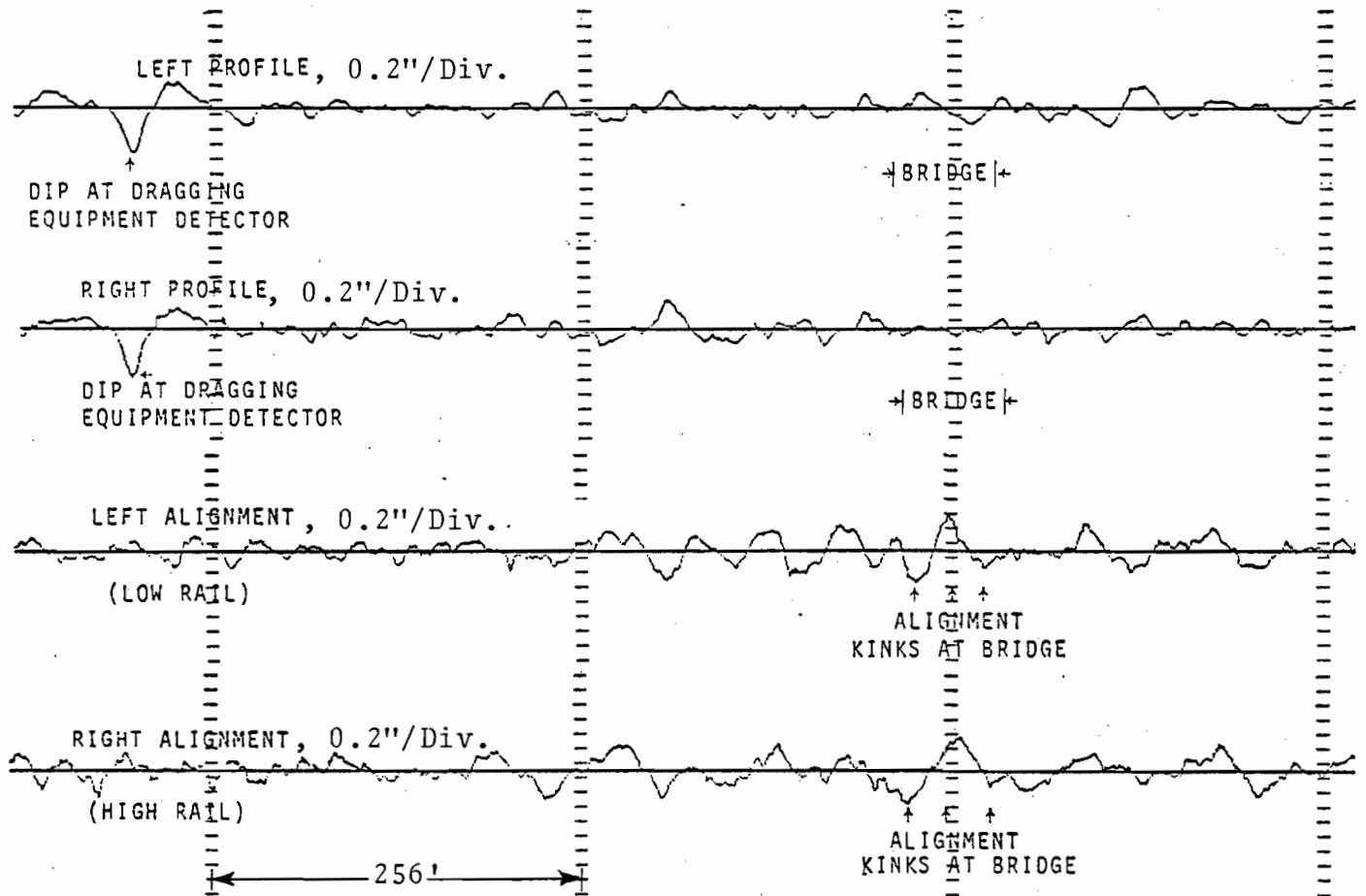


Figure C.1.b.5. Bump in Mean Profile at a Dragging Equipment Detector and a Jog in Mean Alignment at a Bridge (Class 4, CWR).

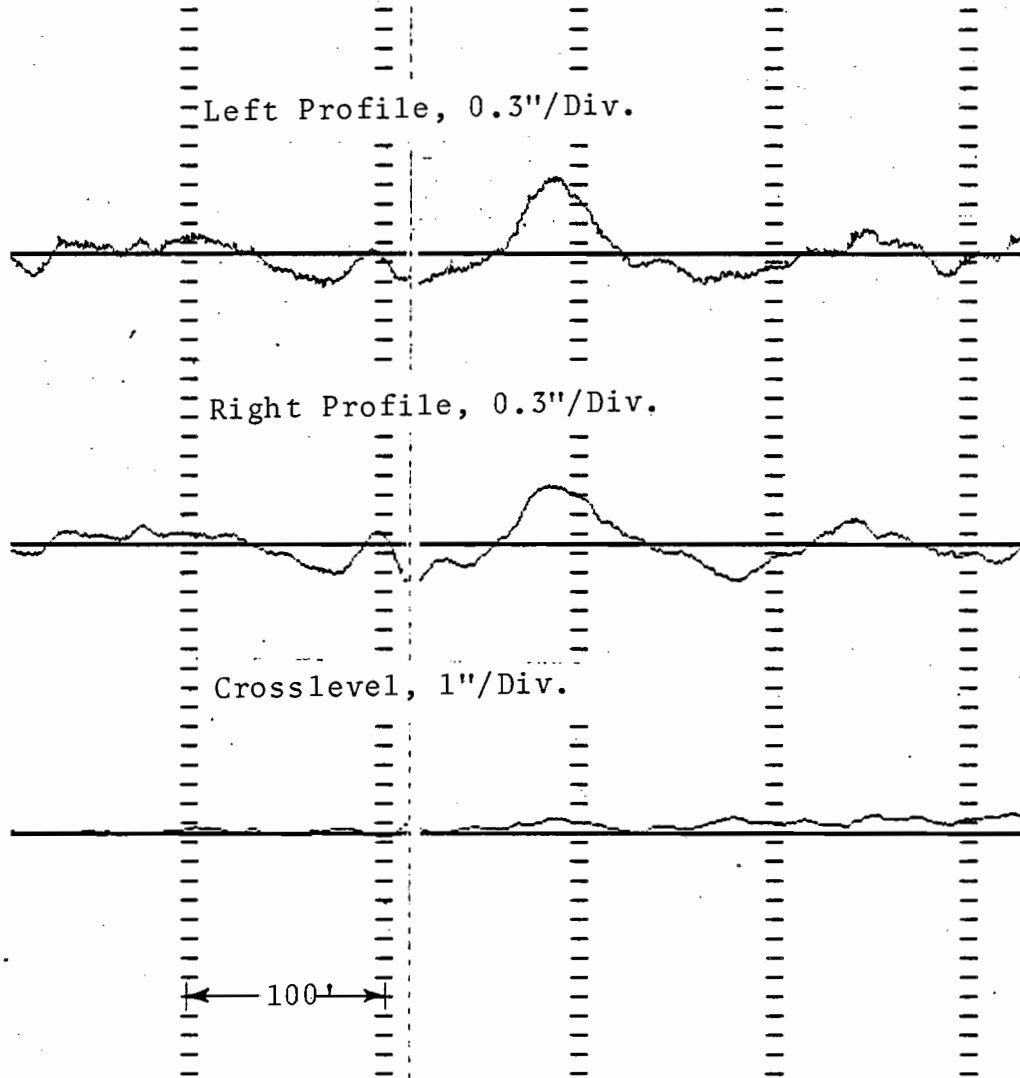
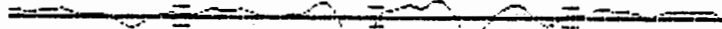


Figure C.1.b.6. Profile Bump on a Bridge (Class 5, Tangent CWR).

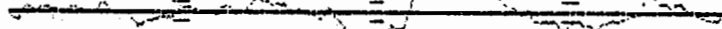
Left Profile, 0.4"/Div.



Right Profile, 0.4"/Div.



Crosslevel Deviations, 1"/Div.



Crosslevel, 1"/Div.



← 100' →

Figure C.1.b.7. Profile Bumps and Crosslevel Cusps
(Class 6, Tangent).

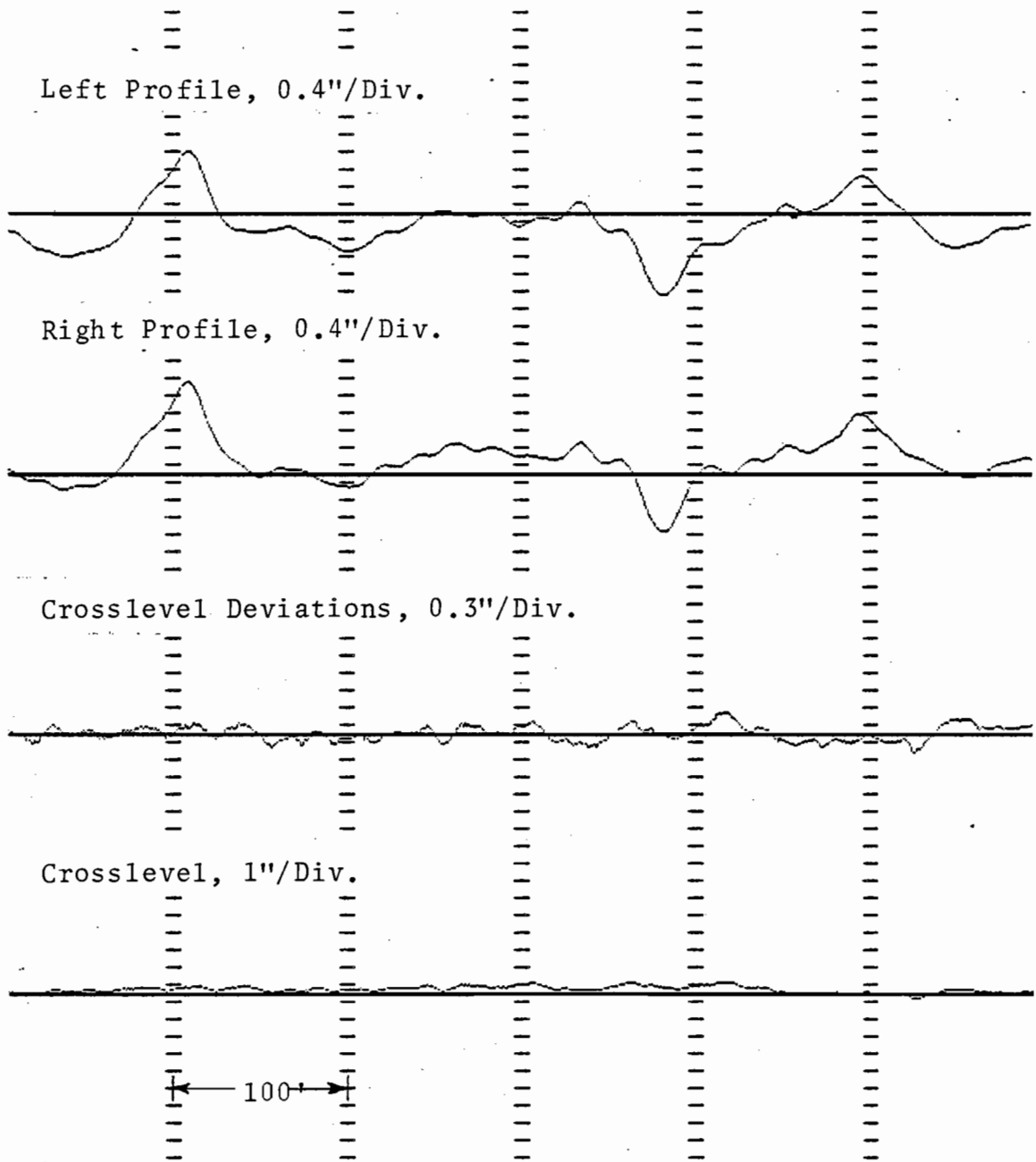


Figure C.1.b.8. Profile Bumps Near a Tunnel (Class 6, Tangent).

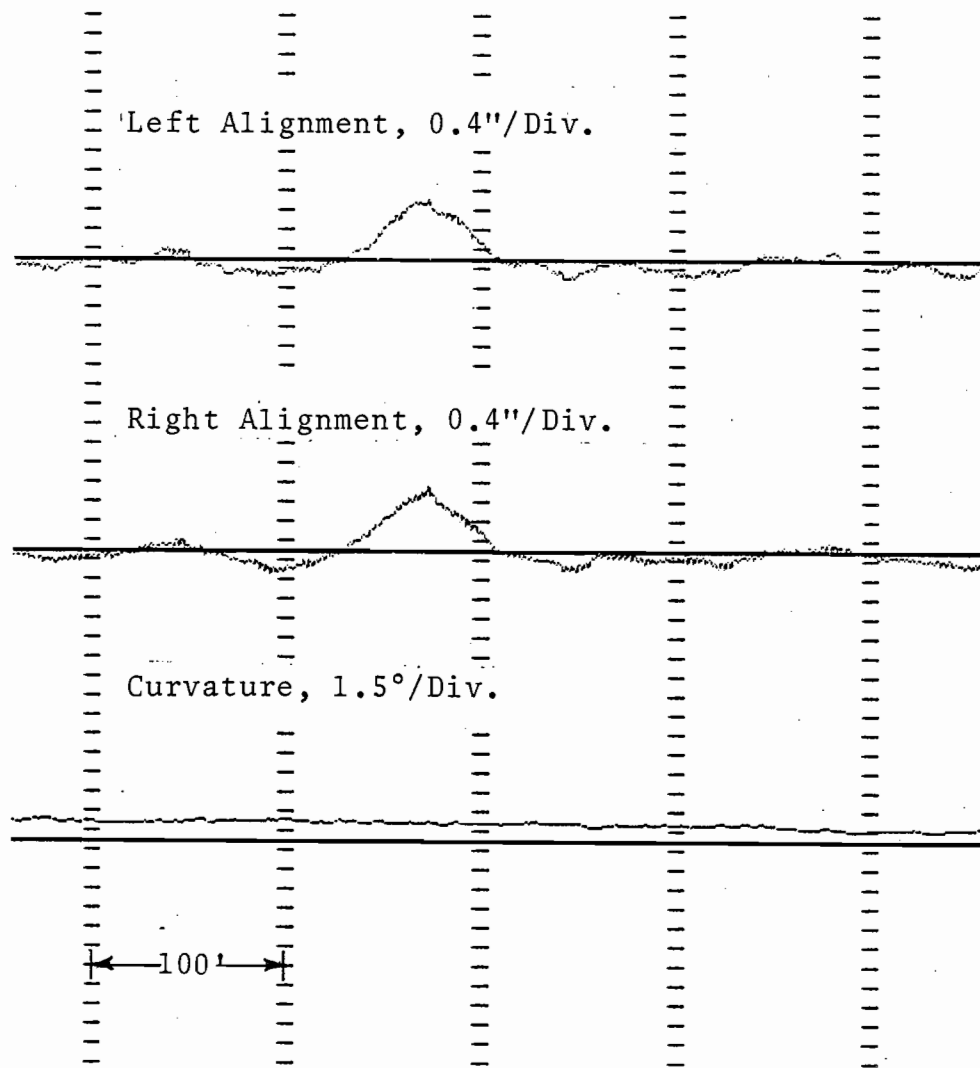


Figure C.1.b.9. Mean Alignment Bump (Class 6, Curve).

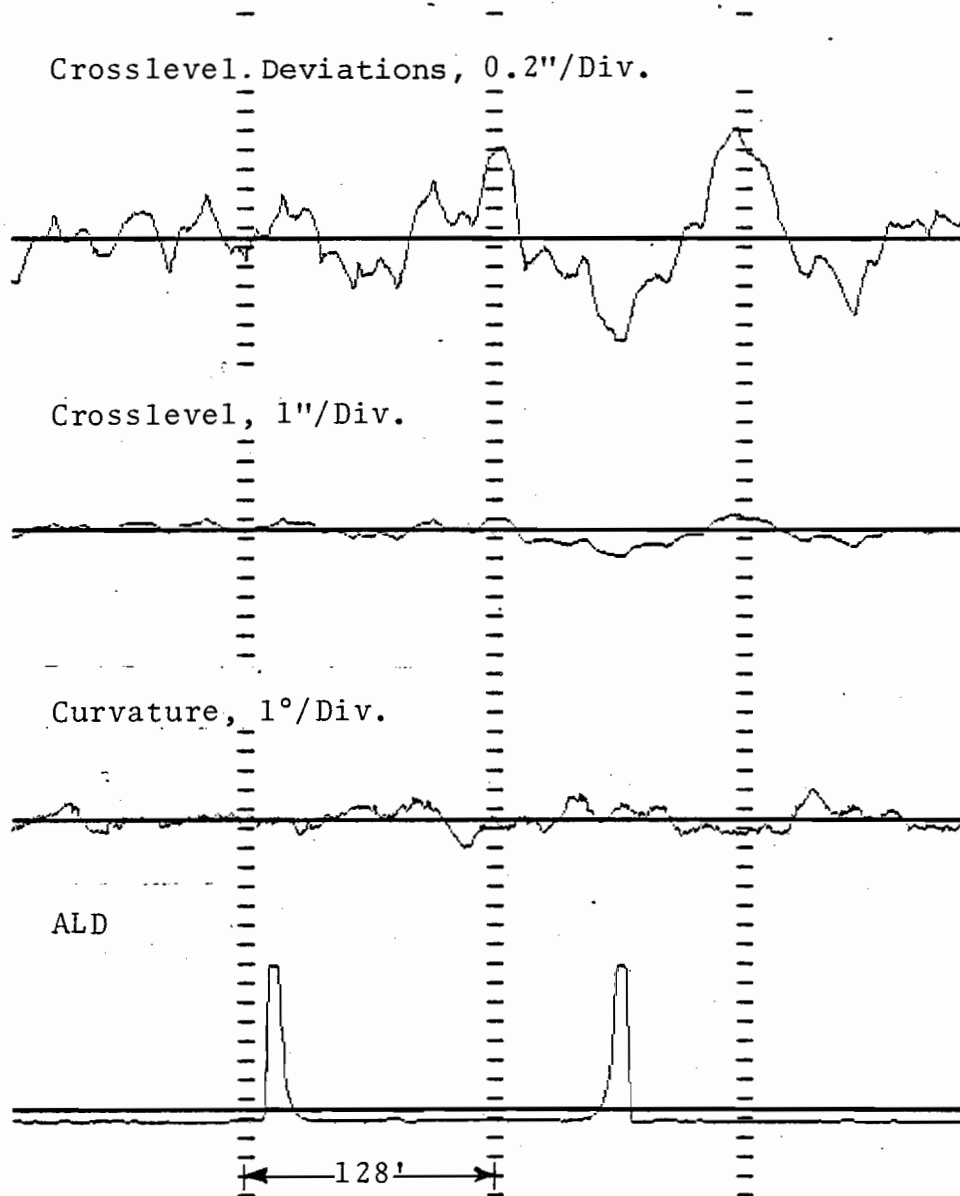
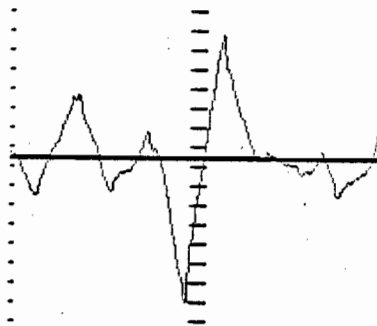


Figure C.1.c.1. Long Wavelength (100') Crosslevel Jog at a Bridge (Class 2, Tangent, Bolted).

Crosslevel Deviations, 0.2"/Div.



Crosslevel, 1"/Div.

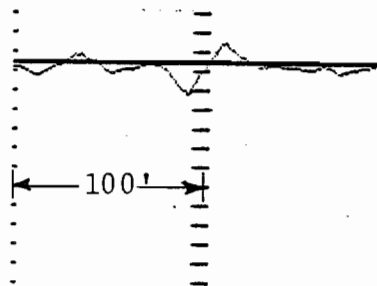


Figure C.1.c.2. Jog in Crosslevel (Class 3, Bolted, Tangent).

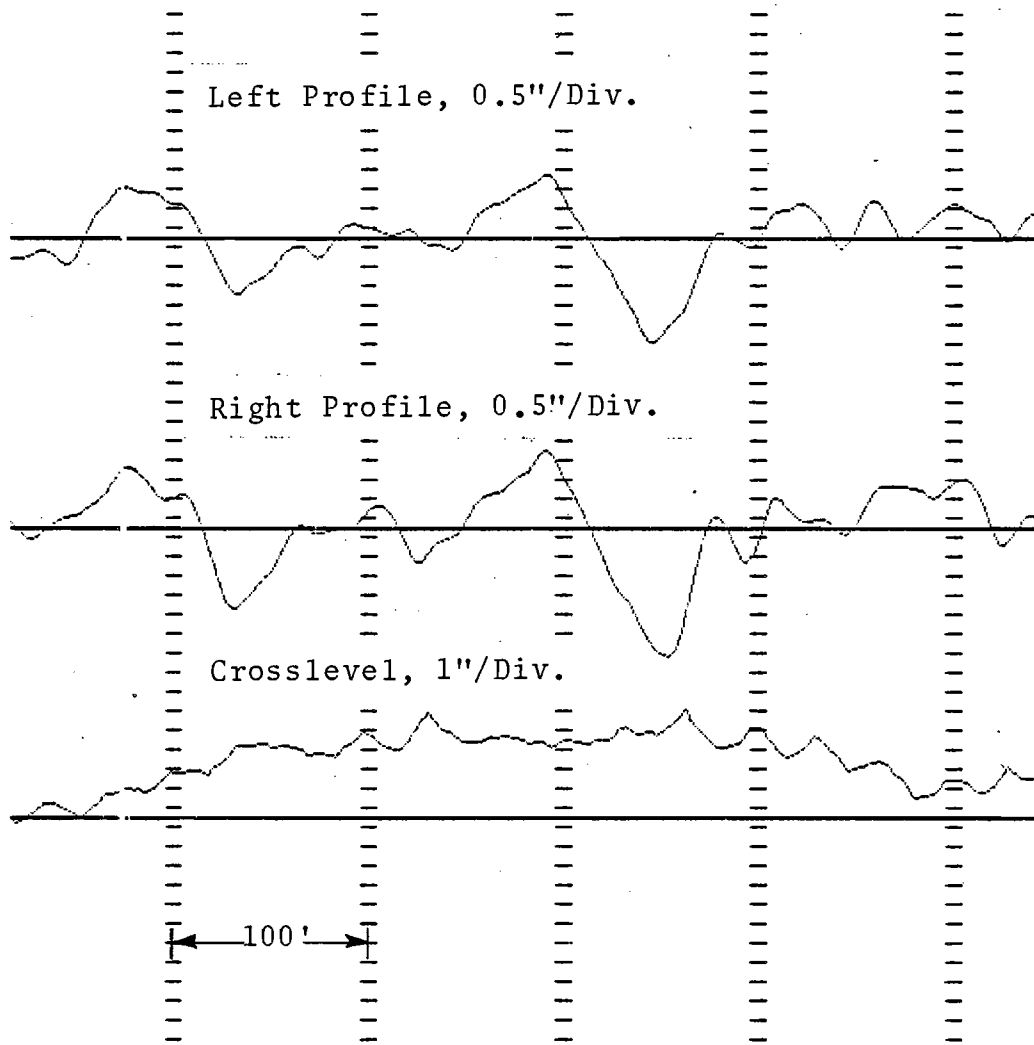


Figure C.1.c.3. Profile Jog on Both Rails (Class 1, Curve).

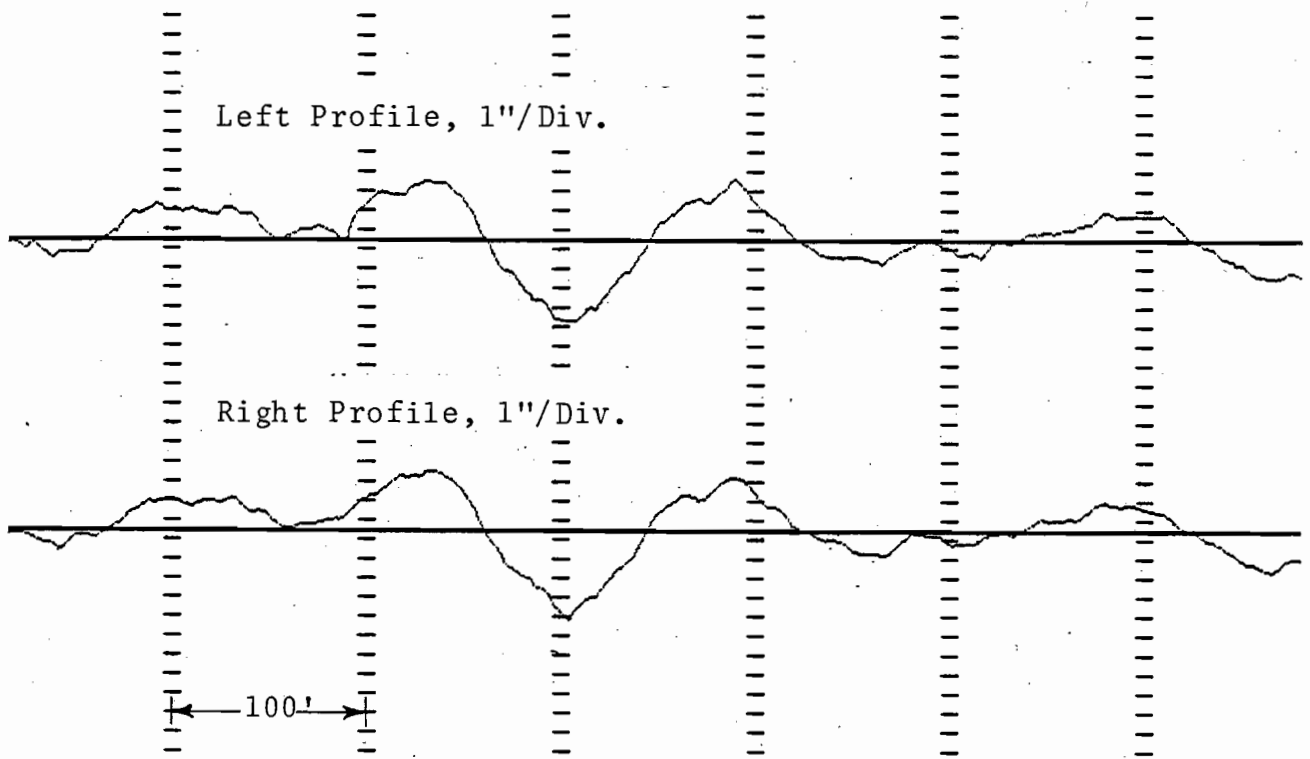


Figure C.1.c.4. Profile Jog on Both Rails (Class 1, Curve).

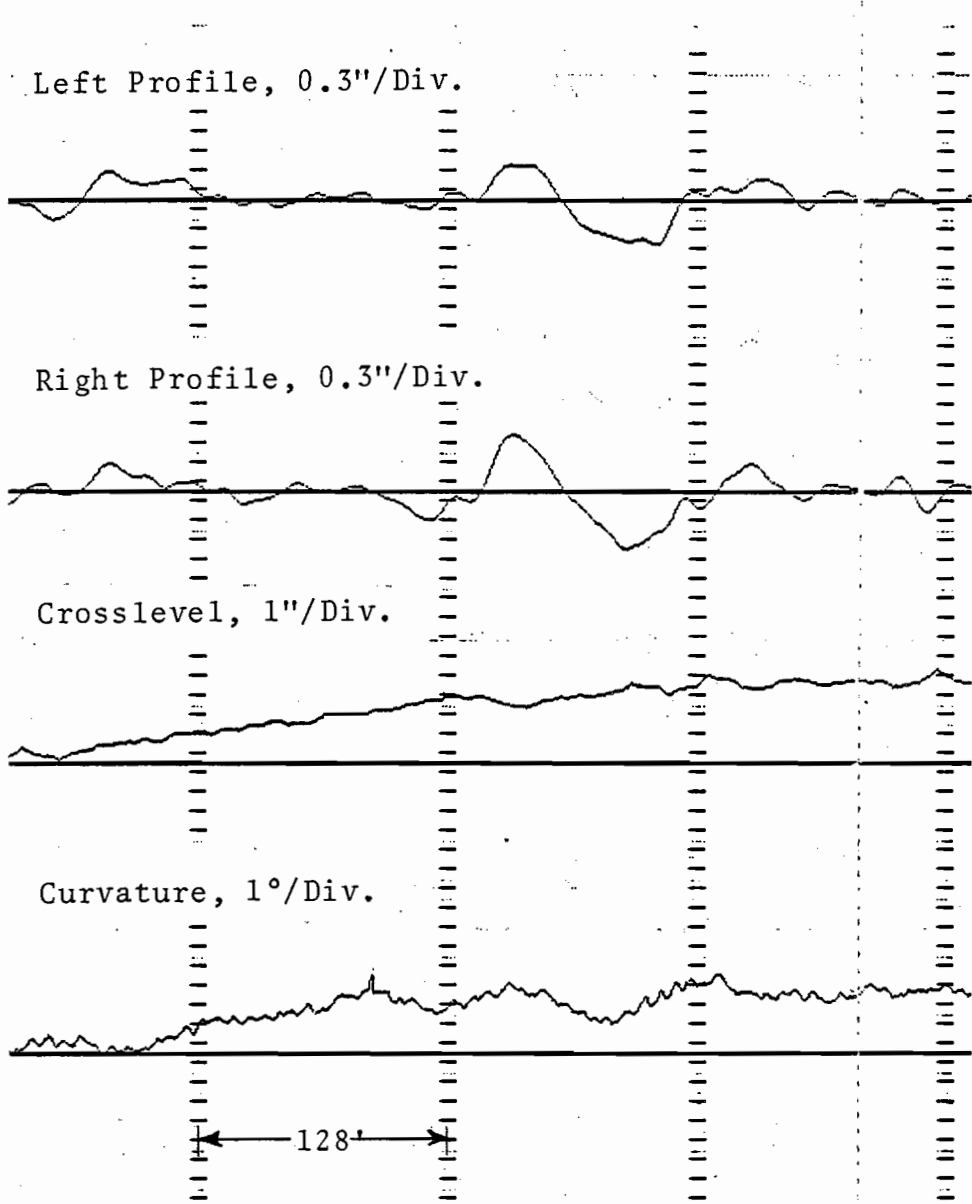


Figure C.1.c.5. Profile Jog (Class 3, Bolted, Spiral).

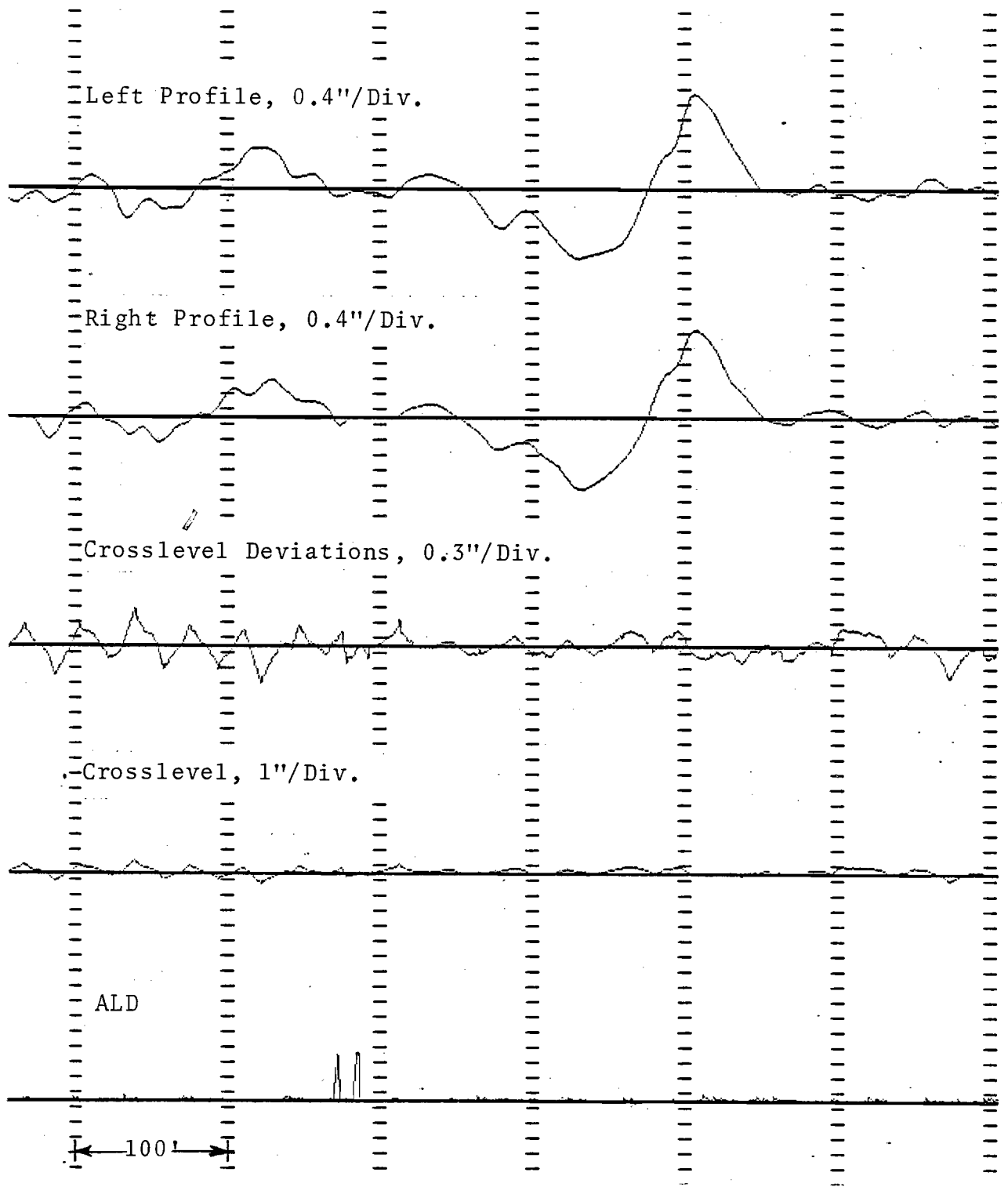


Figure C.1.c.6. Profile Jog at Interlocking (Class 4, Tangent).

C-26

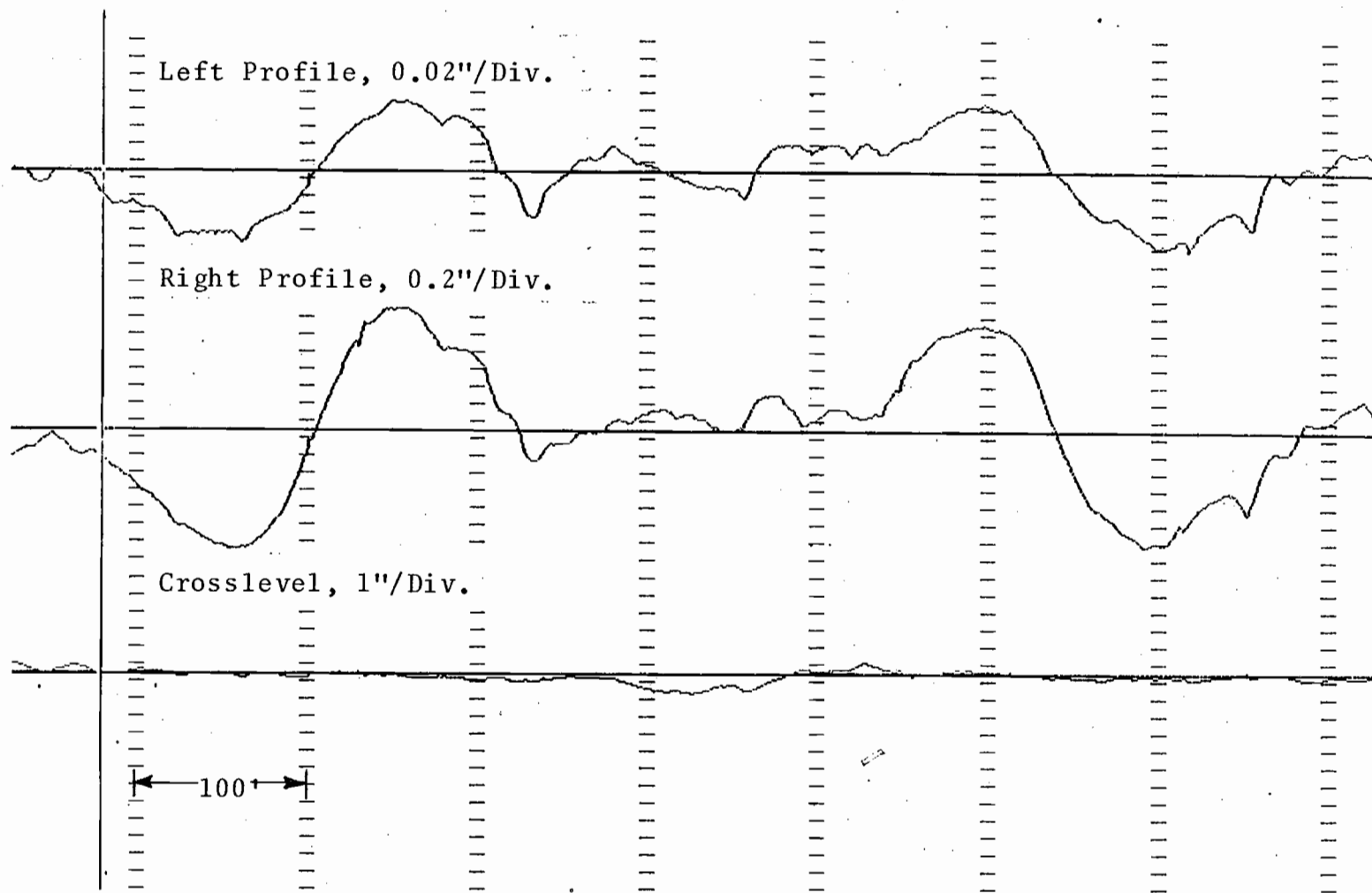


Fig. C.l.c.7. Two Profile Jogs Due to Special Track Works (Class 5, Bolted, Tangent).

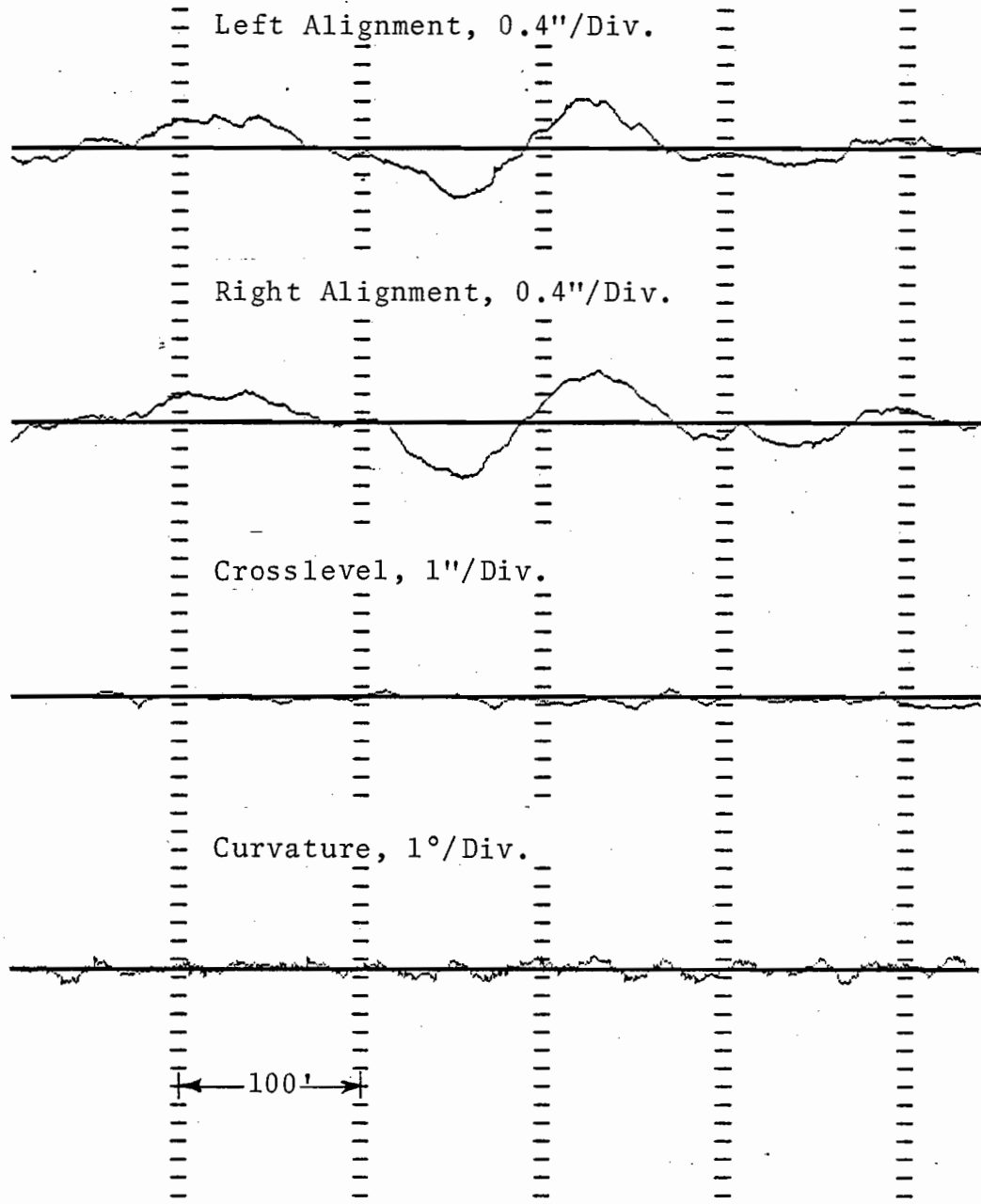


Figure C.1.c.8. Alignment Jog (180') on Both Rails (Class 2, Tangent).

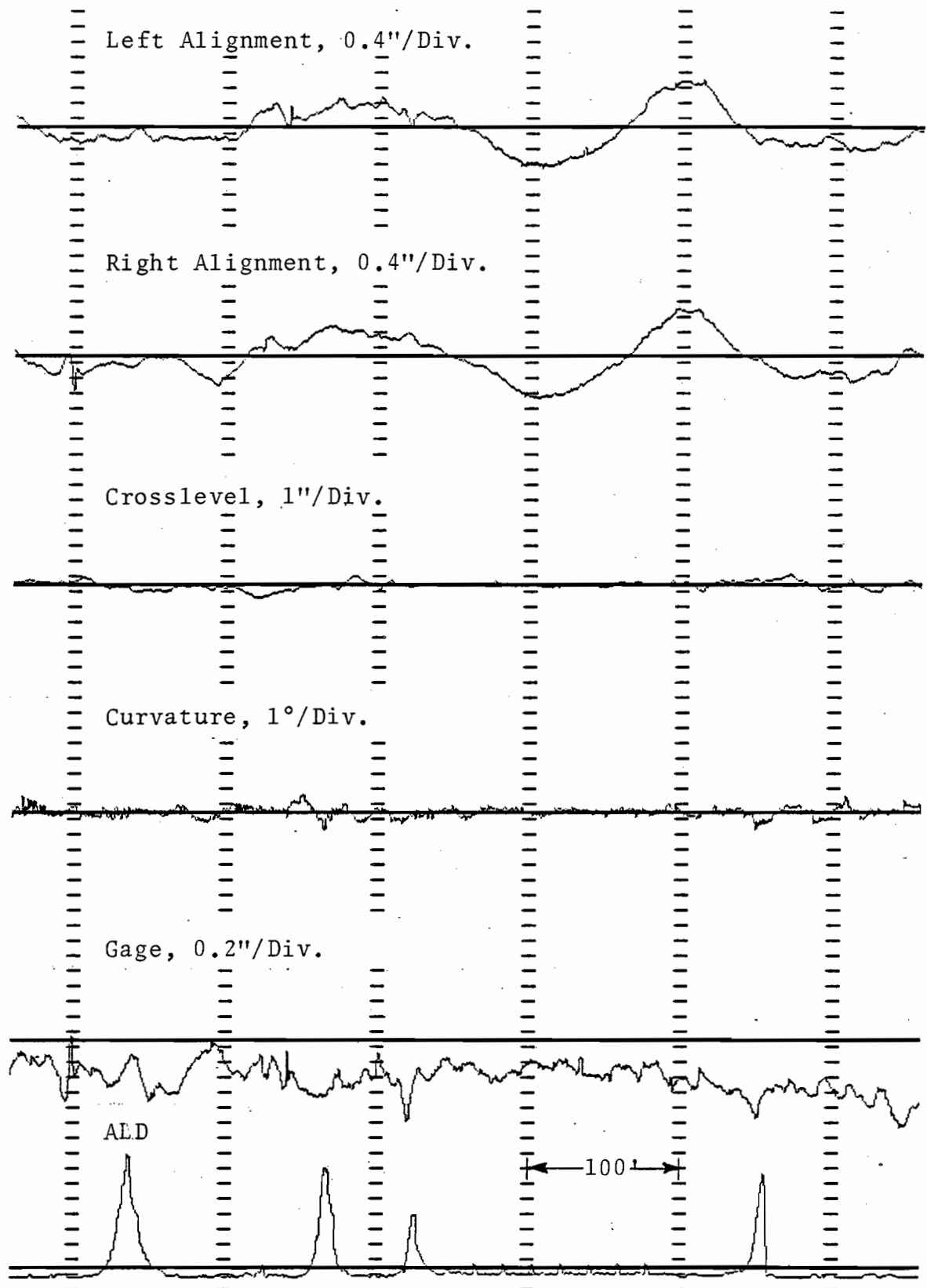


Figure C.1.c.9. Alignment Jog (120') Near a Switch and a Bridge (Class 2, Tangent).

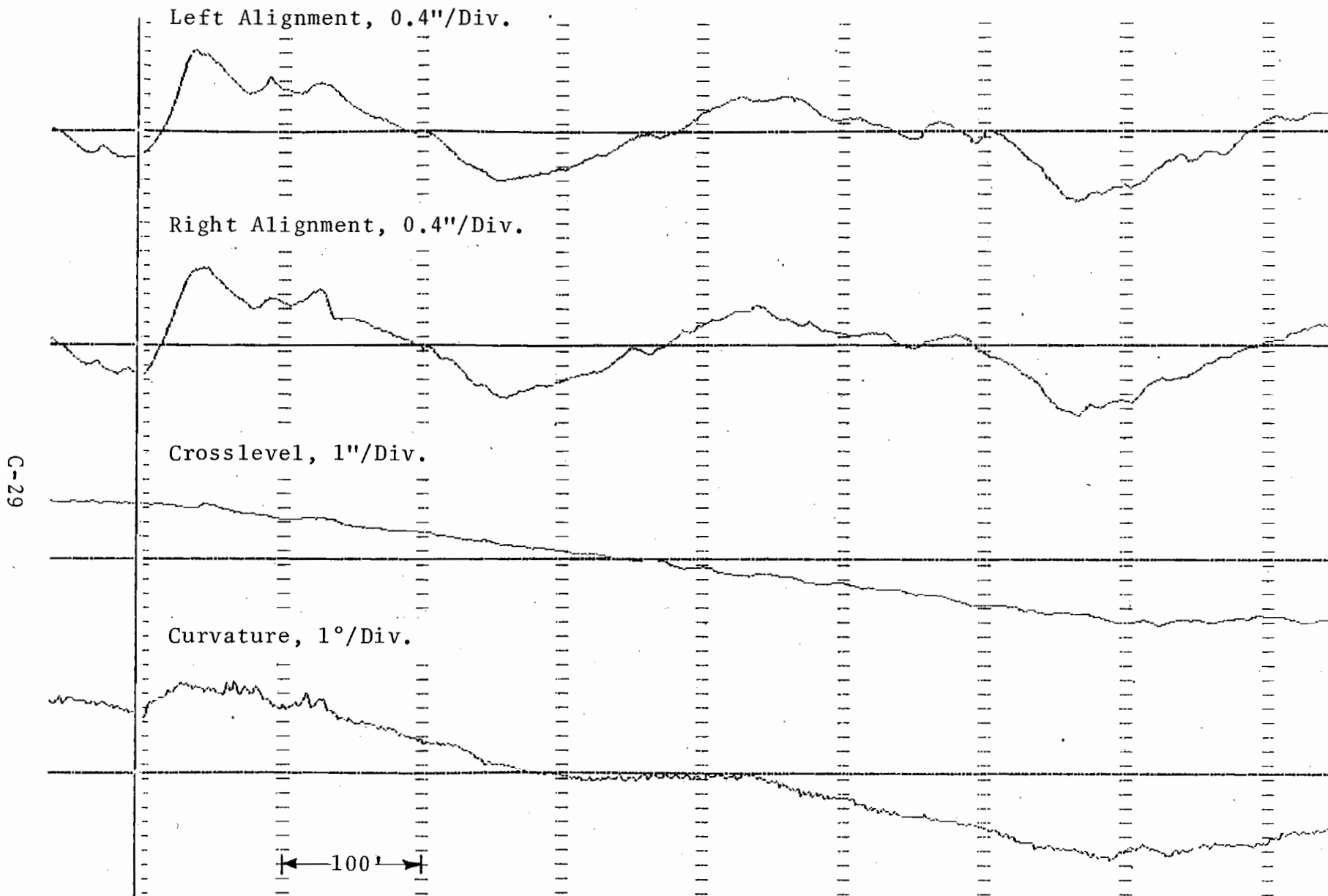


Figure C.1.c.10. Alignment Jogs at Transition of Reverse Curves (Class 3, Reverse Curve).

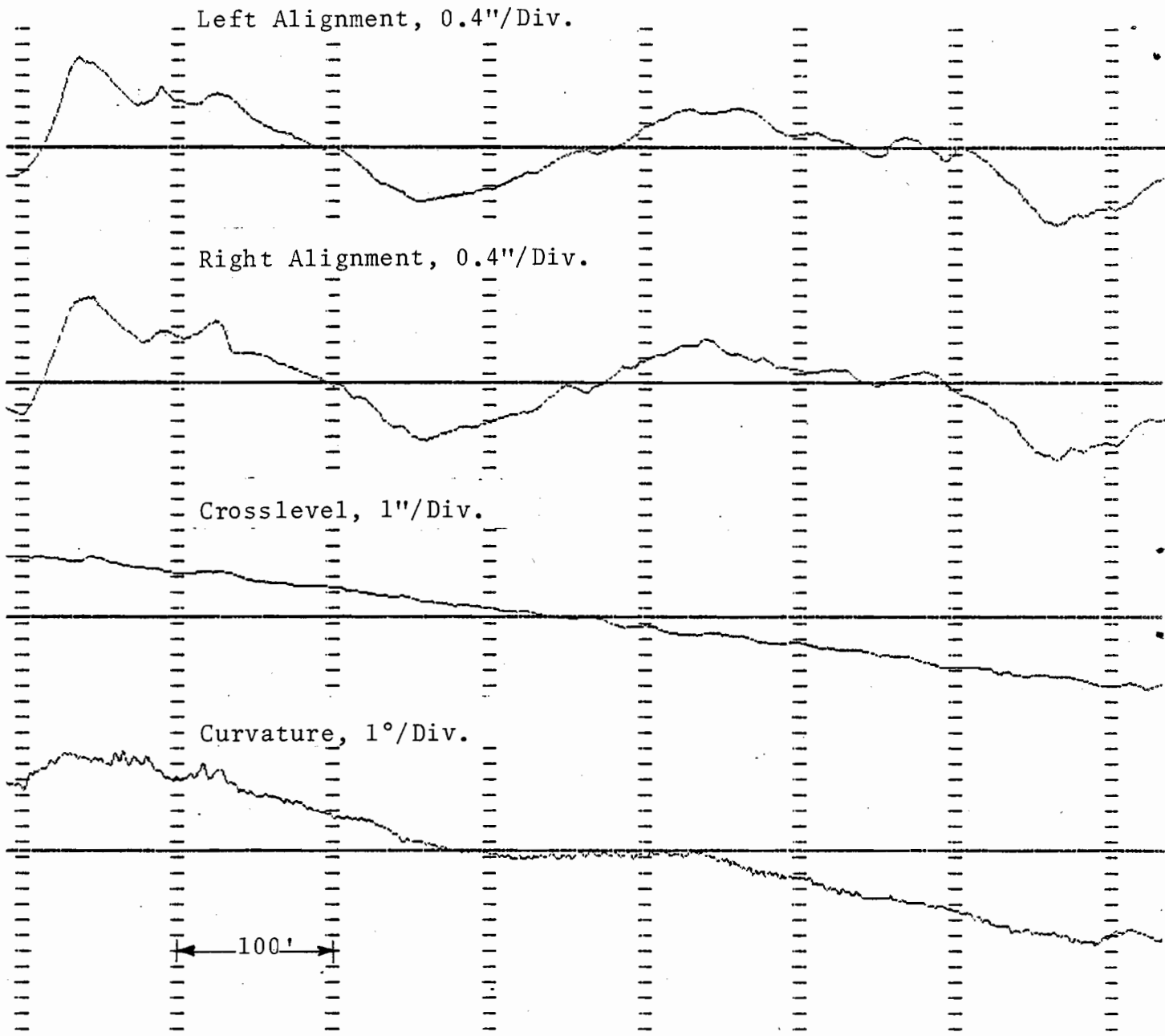


Figure C.1.c.11. Long Wavelength Jog (400') in Alignment at Junction of Reverse Curve (Class 3, Spiral).

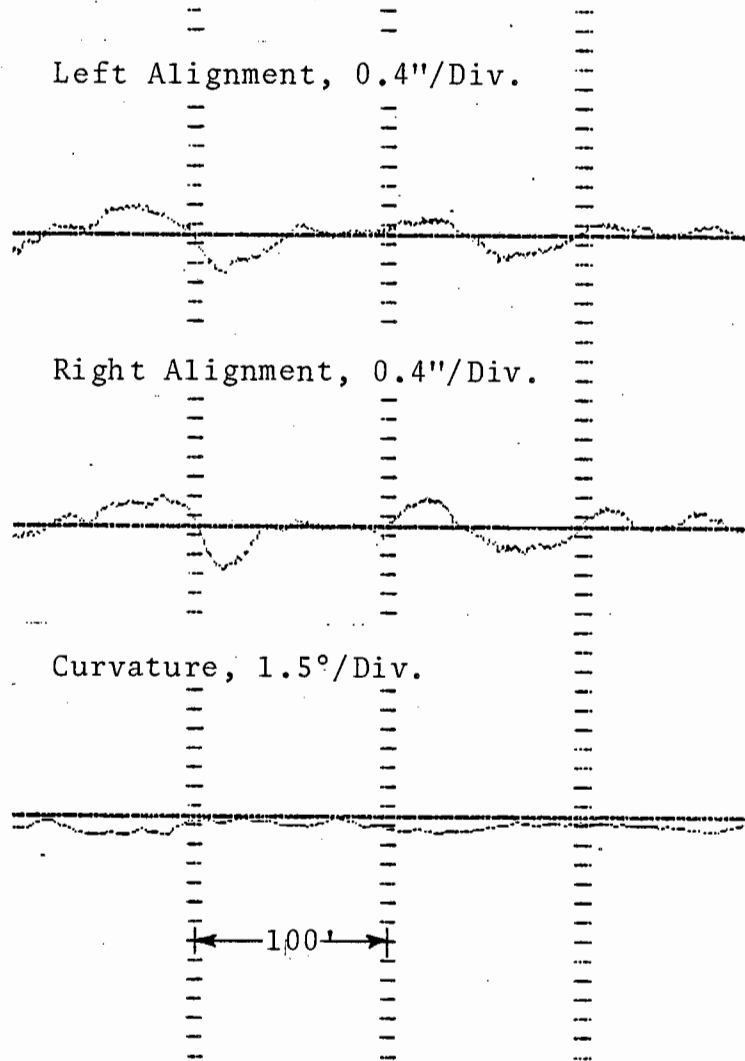


Figure C.1.c.12. Alignment Jog and Trough (Class 6, Curve).

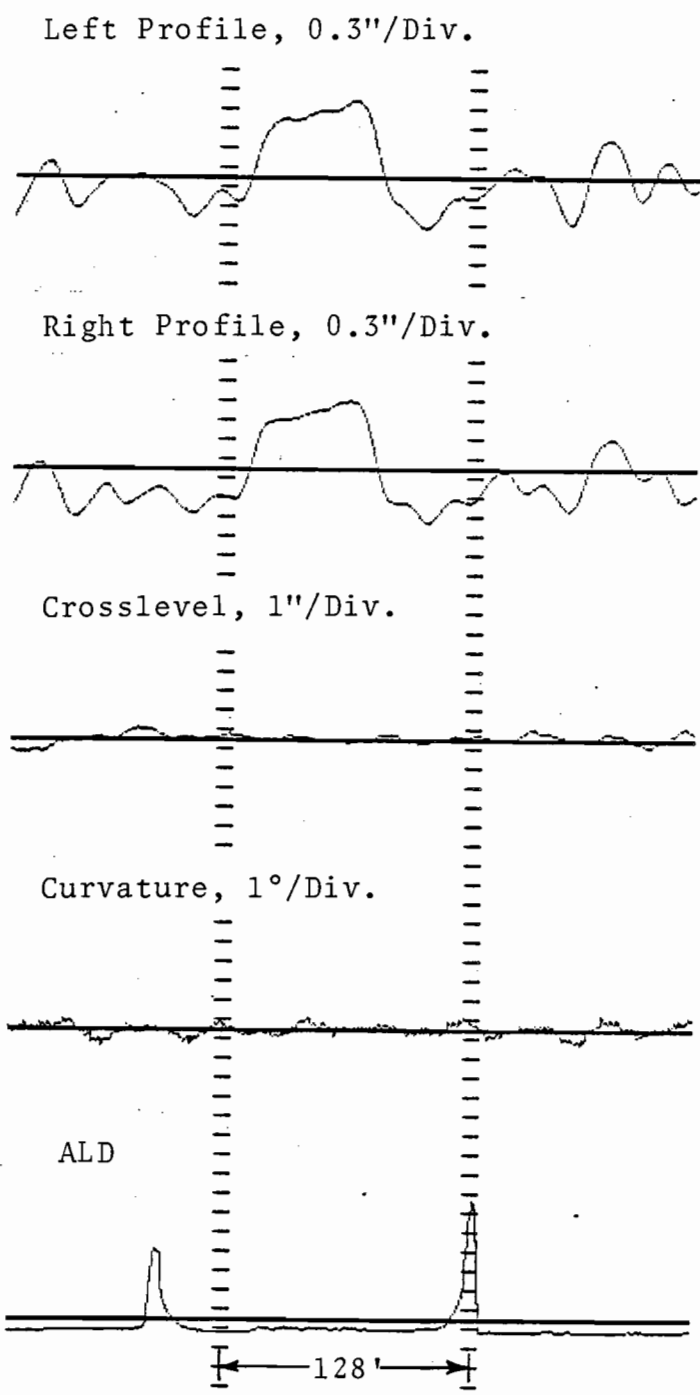


Figure C.1.d.1. Profile Plateau at a Bridge (Class 2, Tangent).

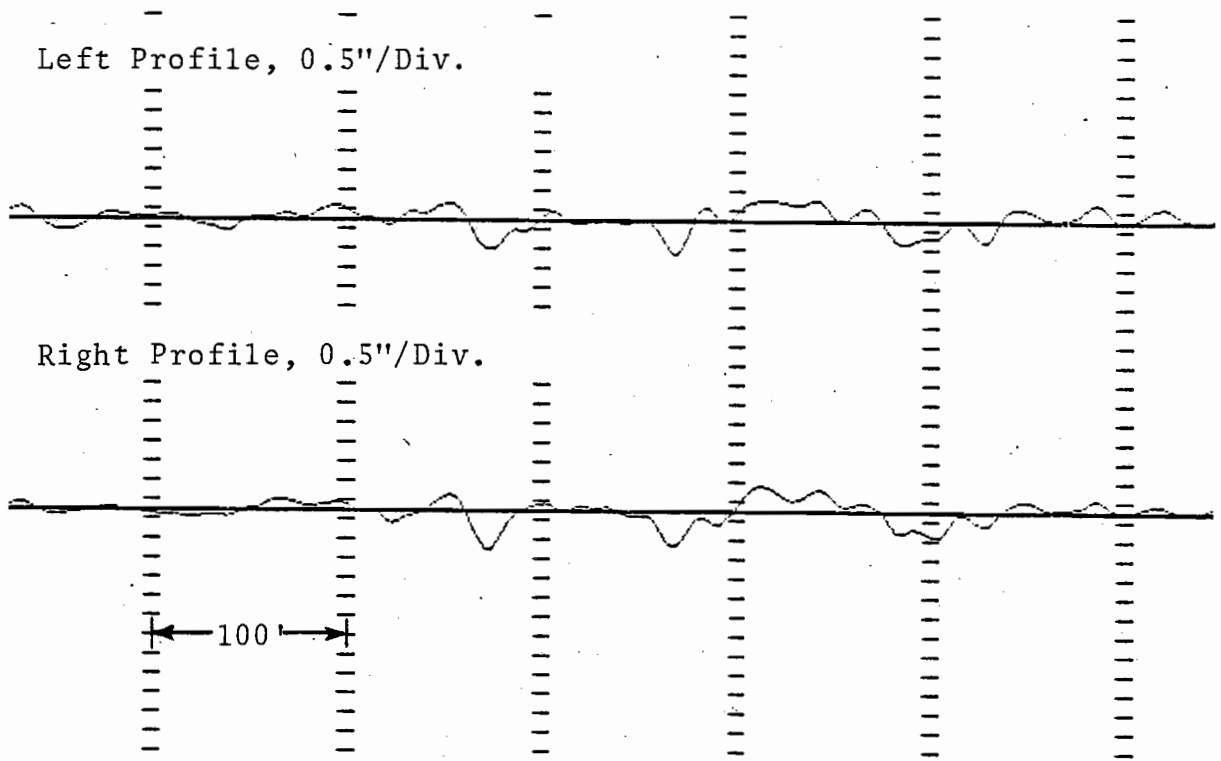


Figure C.1.d.2. Signature of Farm Crossing in Profile
(Class 2, Tangent).

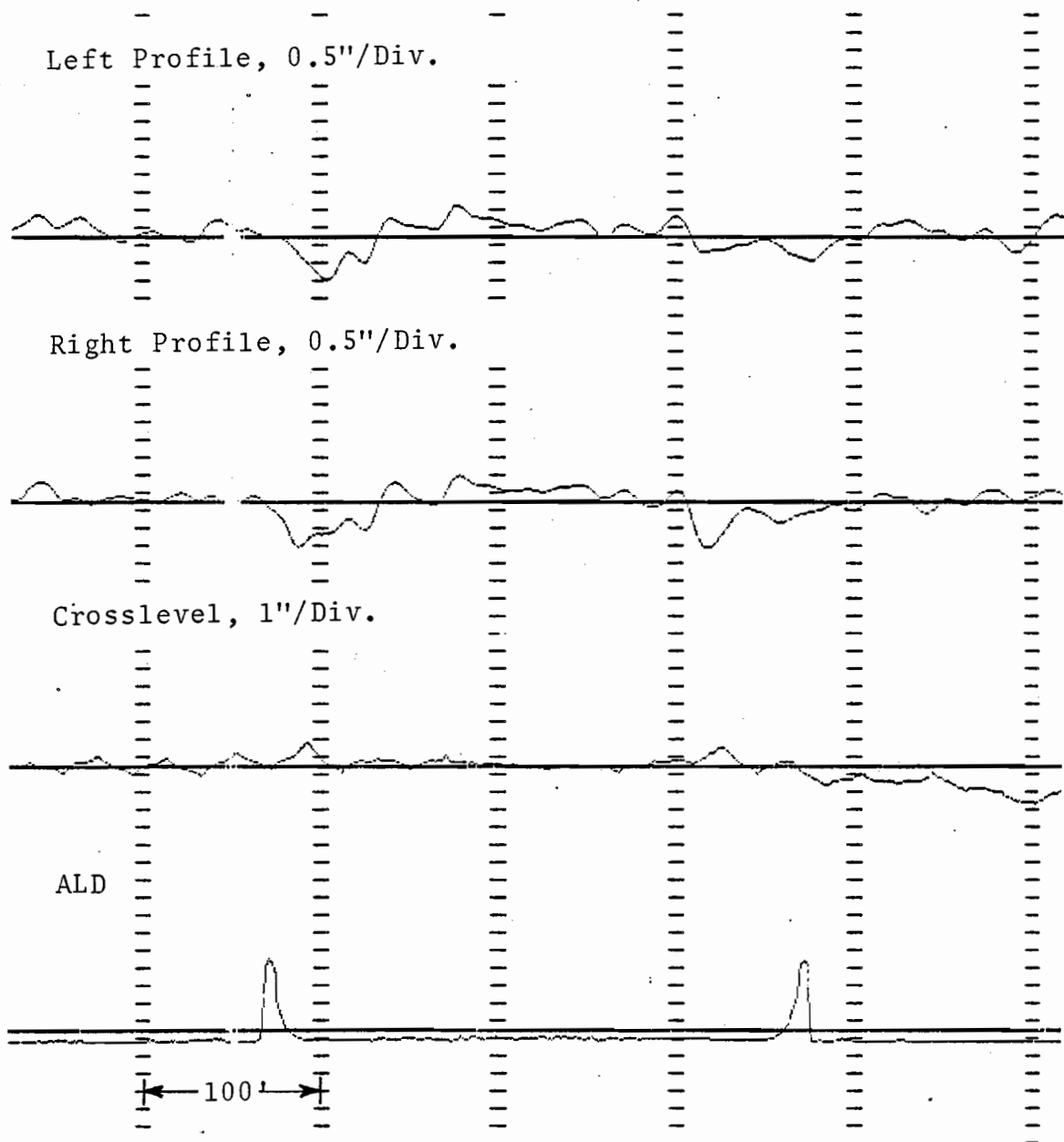


Figure C.1.d.3. Profile Signature of Soft Spots on Either End of a Bridge (Class 2, Tangent).

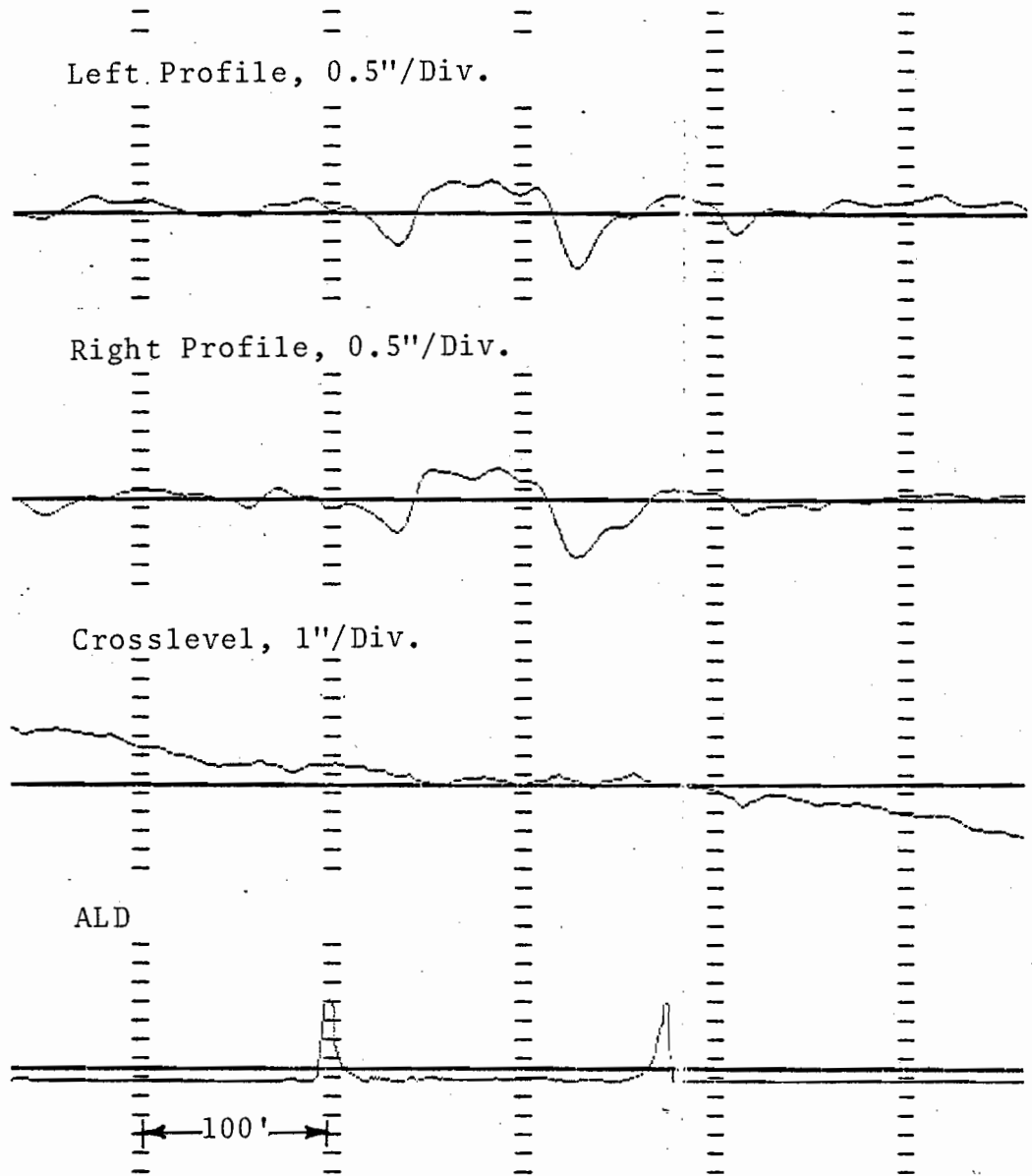


Figure C.1.d.4. Profile Plateau at a Bridge at Reverse Curve (Class 2, Tangent).

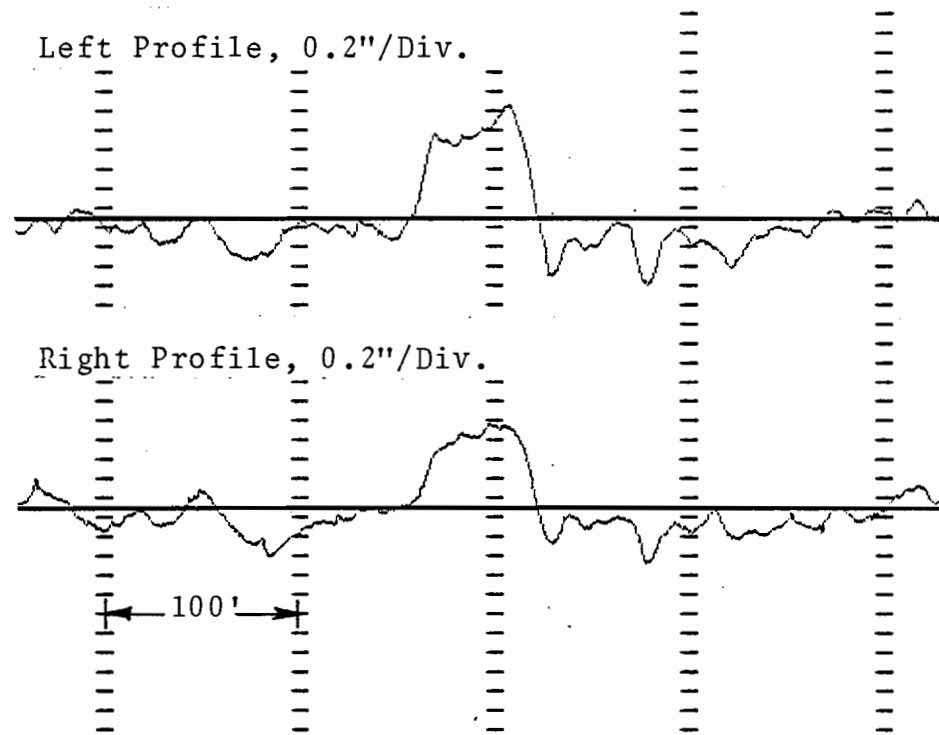


Figure C.1.d.5. Example of Profile Plateau (Class 2, Tangent).

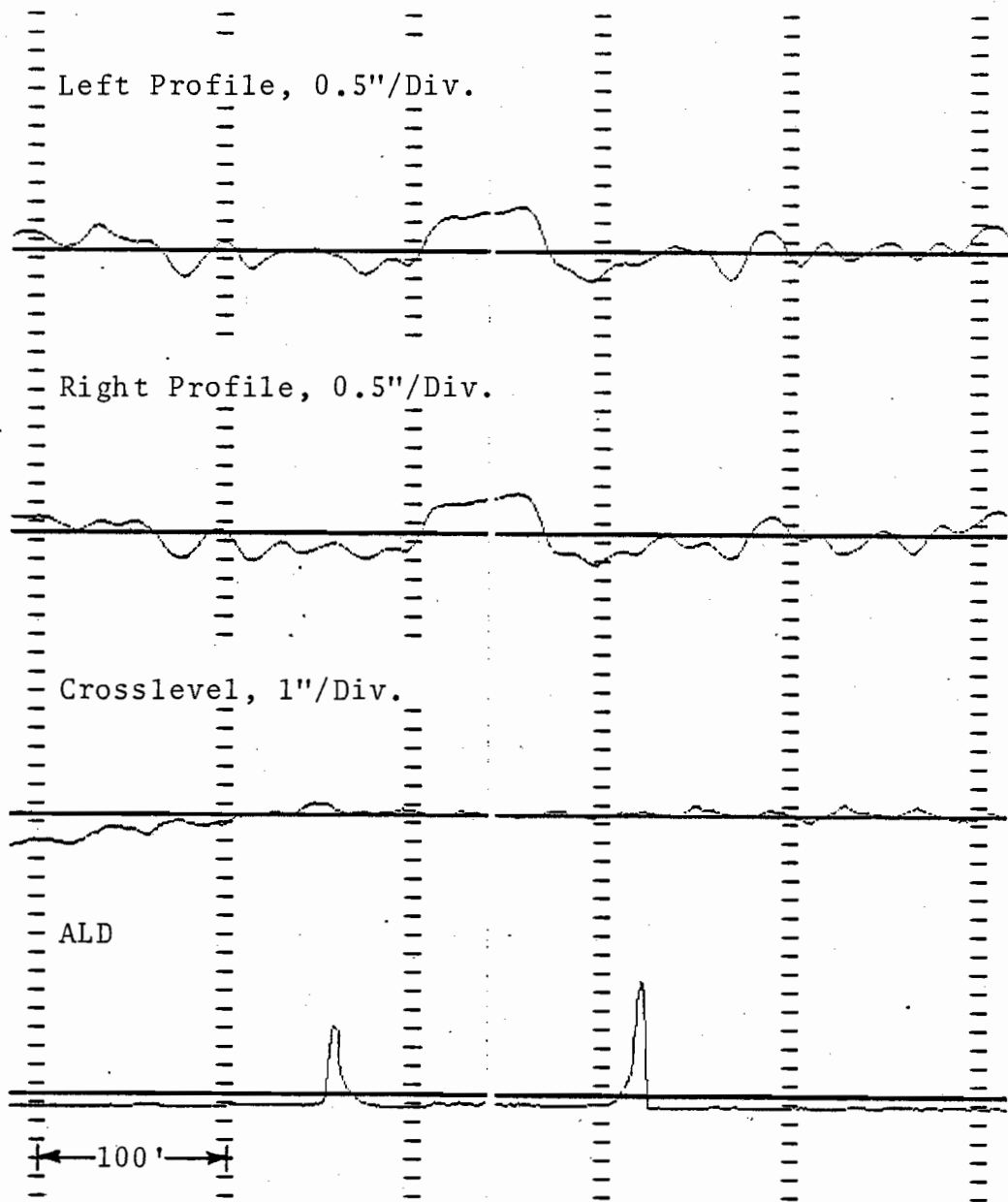


Figure C.1.d.6. Profile Plateau Signature at a Bridge (Class 2, Tangent).

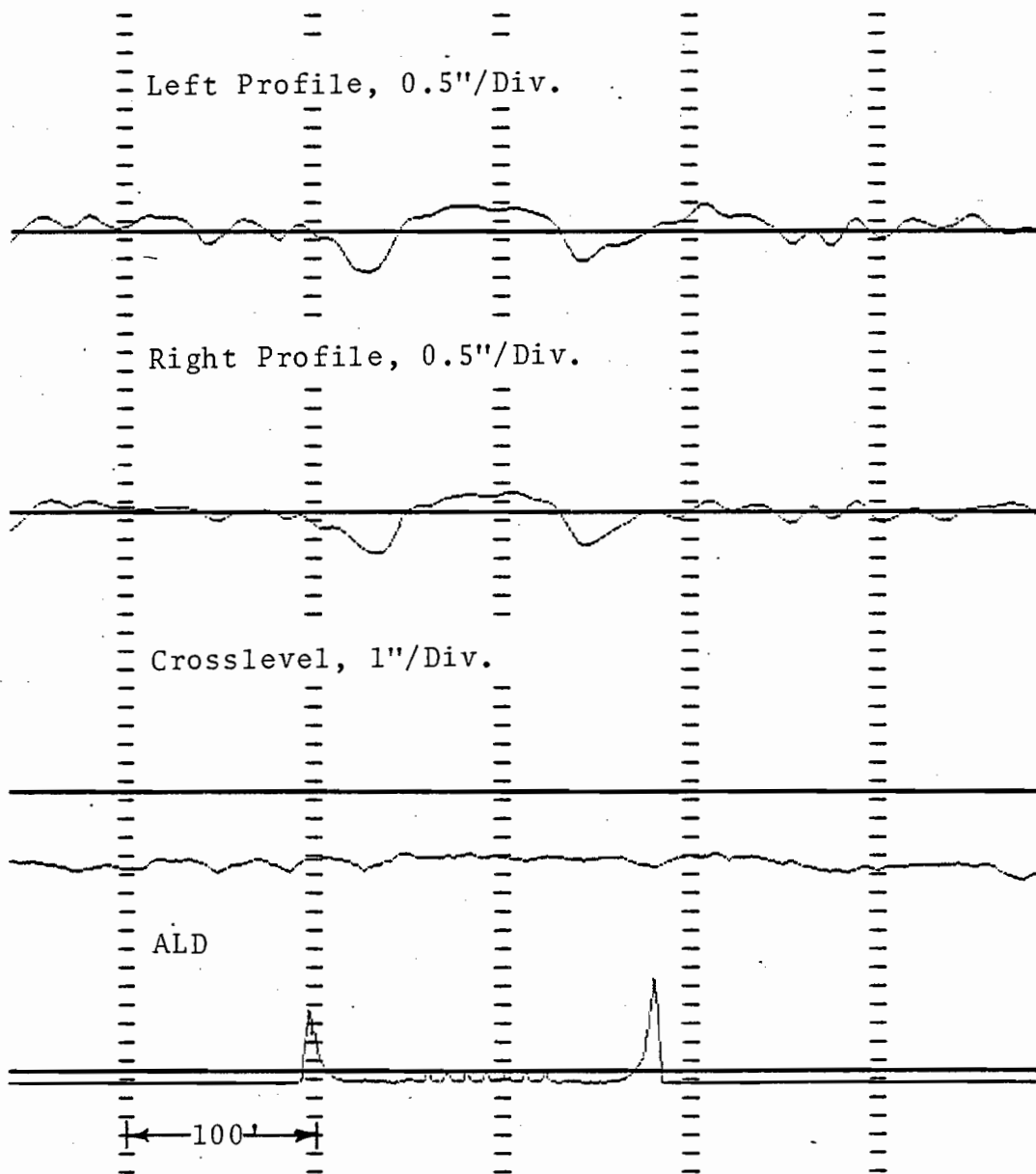


Figure C.1.d.7. Profile Plateau Signature at a Bridge on a Curve (Class 2, Curve).

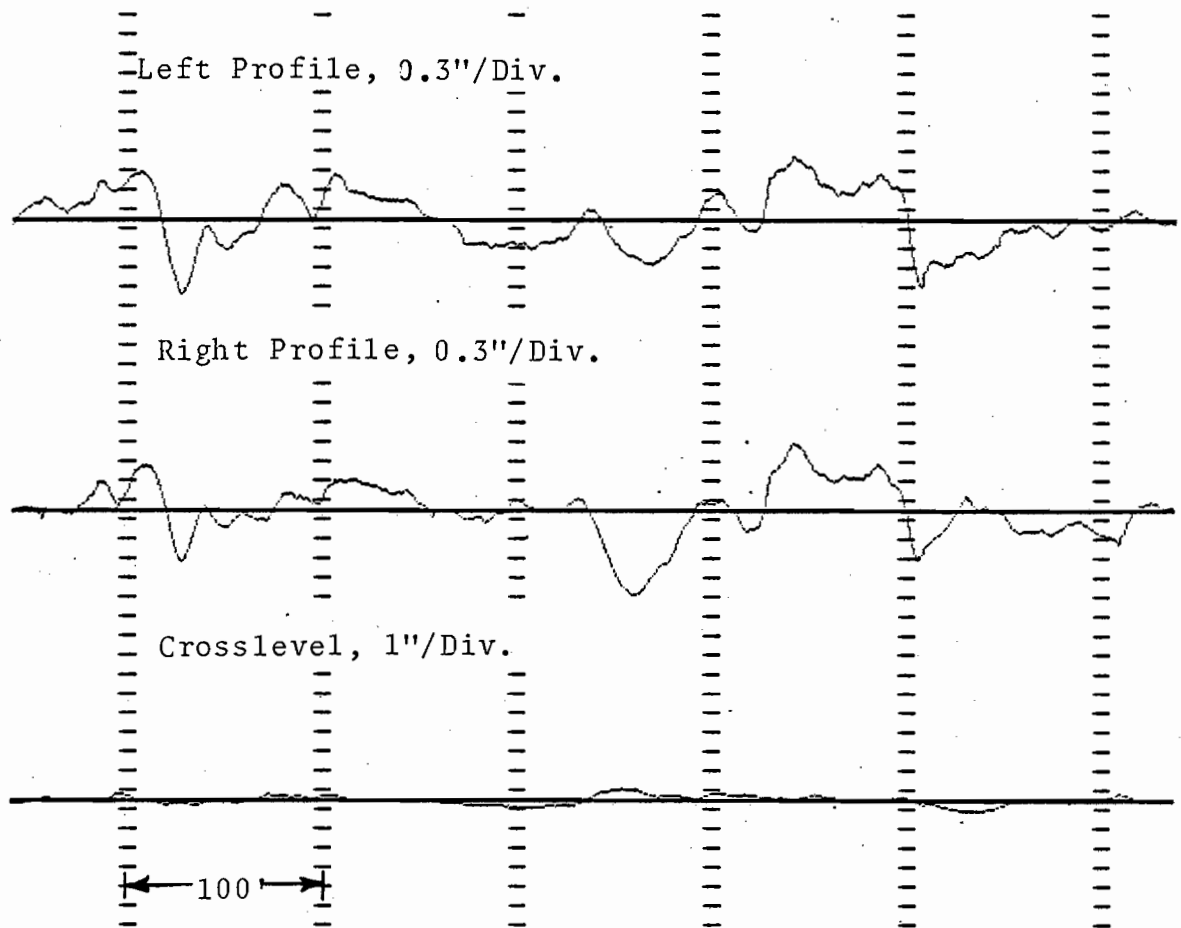


Figure C.1.d.8. Profile Signature of Two Consecutive Concrete Slab Ballast Deck Bridges (Class 4, Tangent).

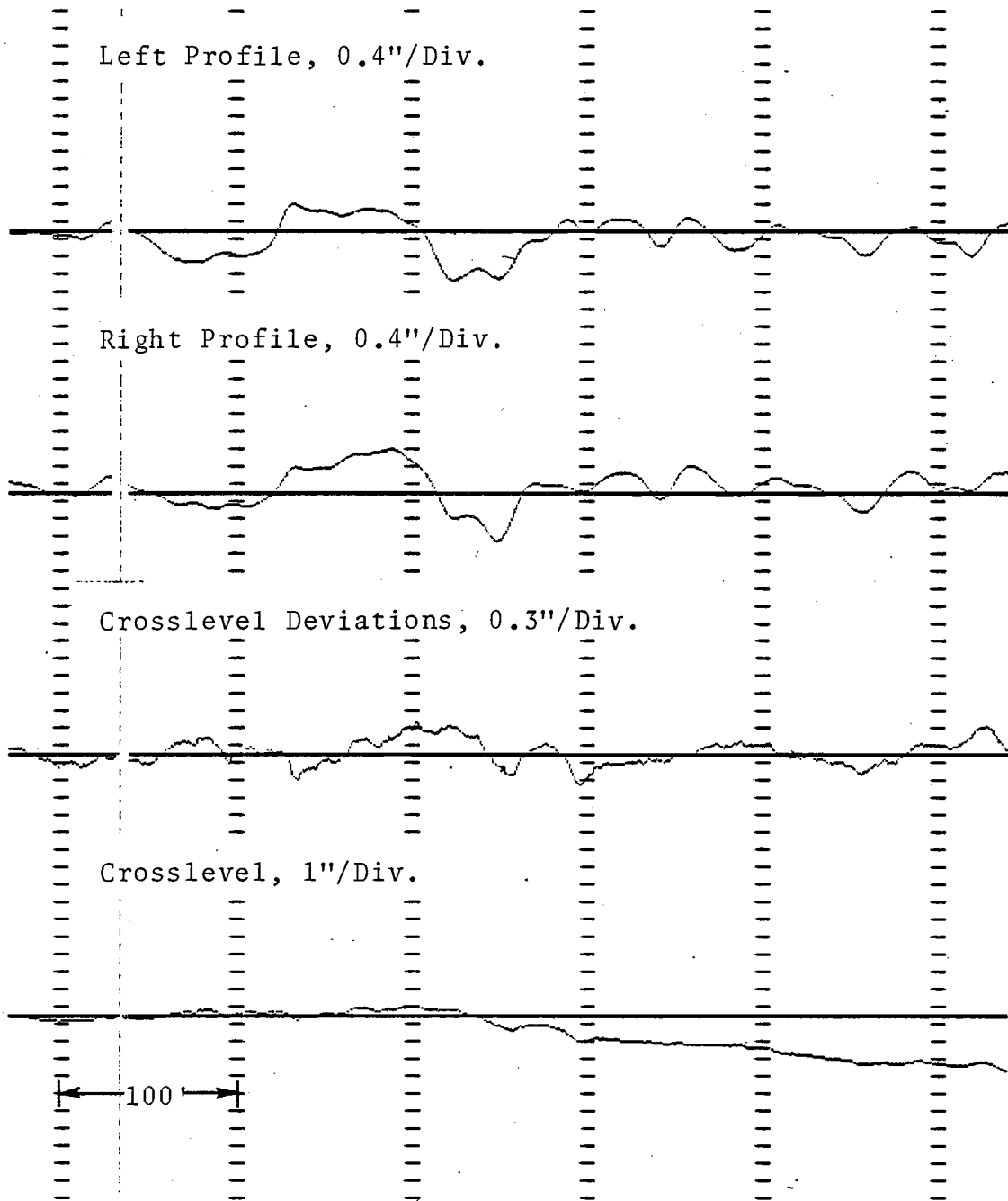


Figure C.1.d.9. Profile Plateau (Class 4, Spiral Entry).

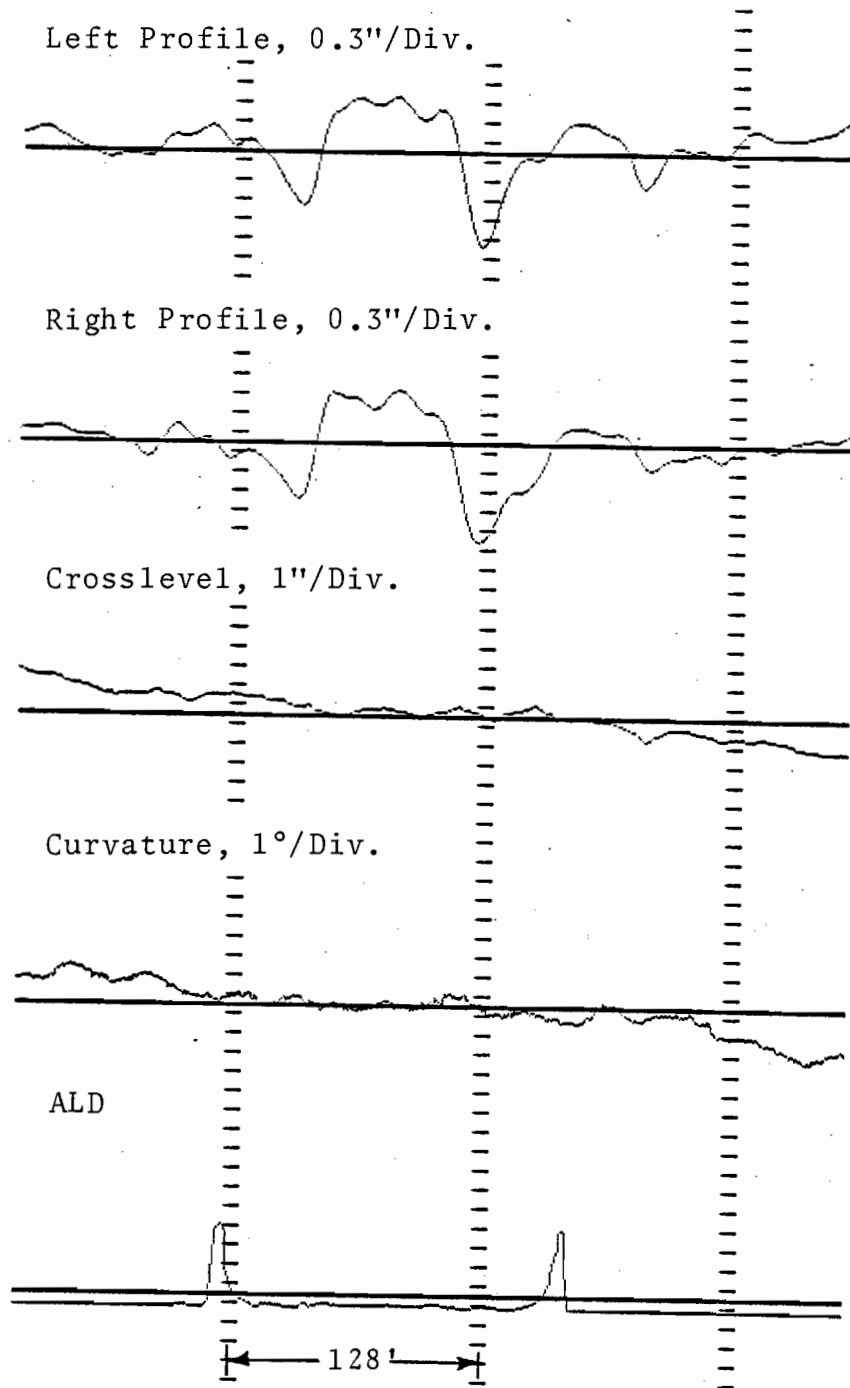


Figure C.1.d.10. Profile Plateau at a Bridge (Class 2, Tangent Between Reverse Curves).

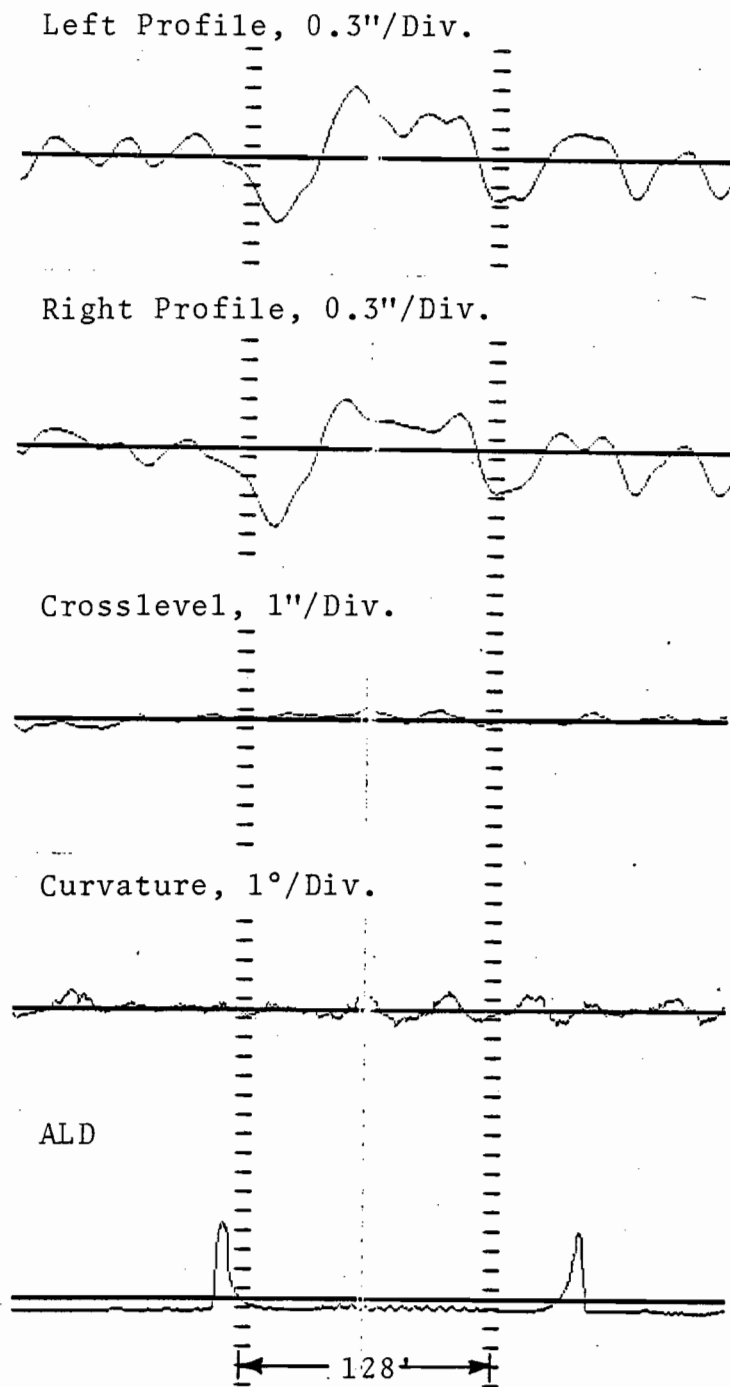


Figure C.1.d.11. Profile Plateau at a Bridge (Class 2, Tangent).

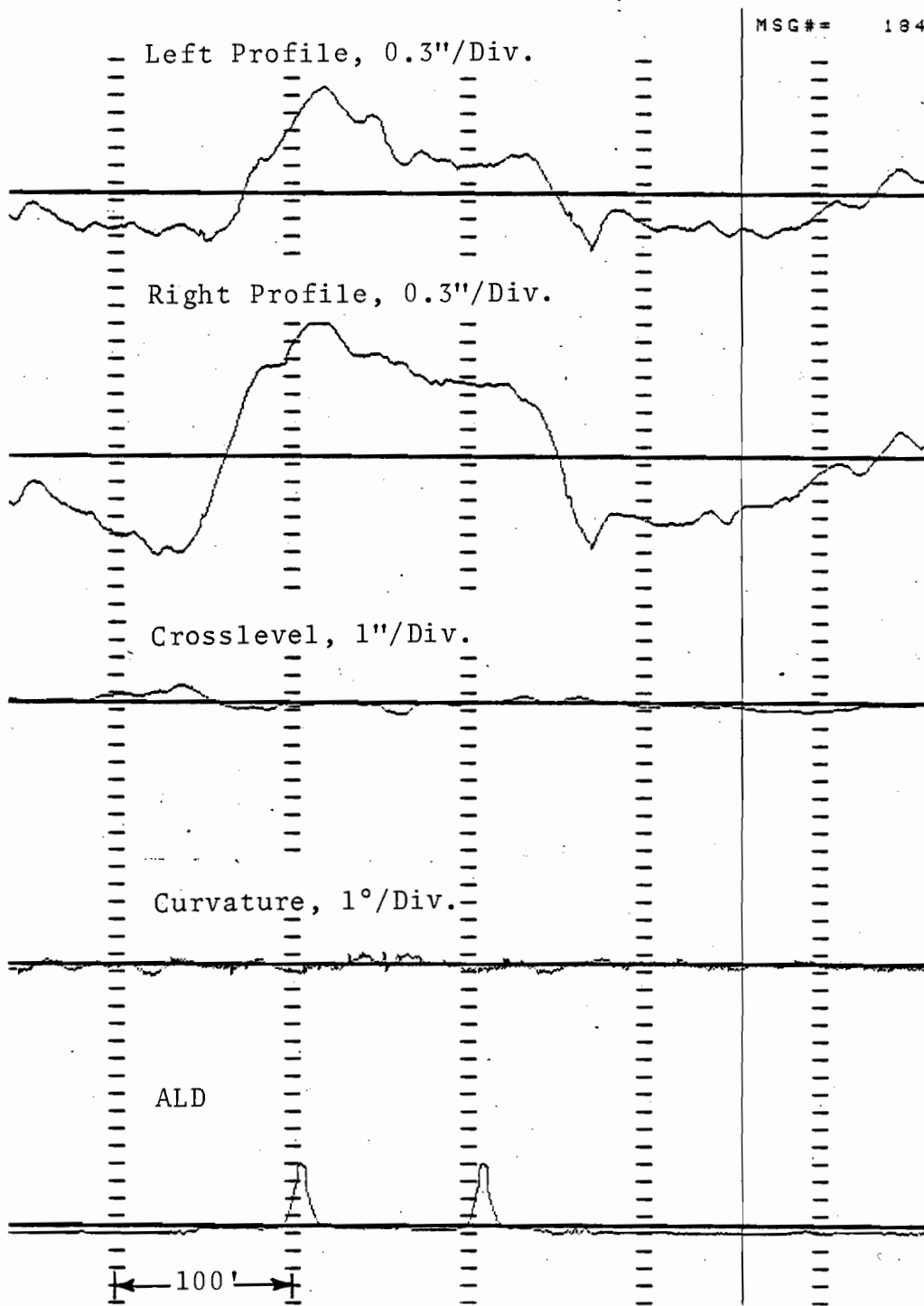


Figure C.1.d.12. Profile Plateau at a Bridge (Class 5, Bolted, Tangent).

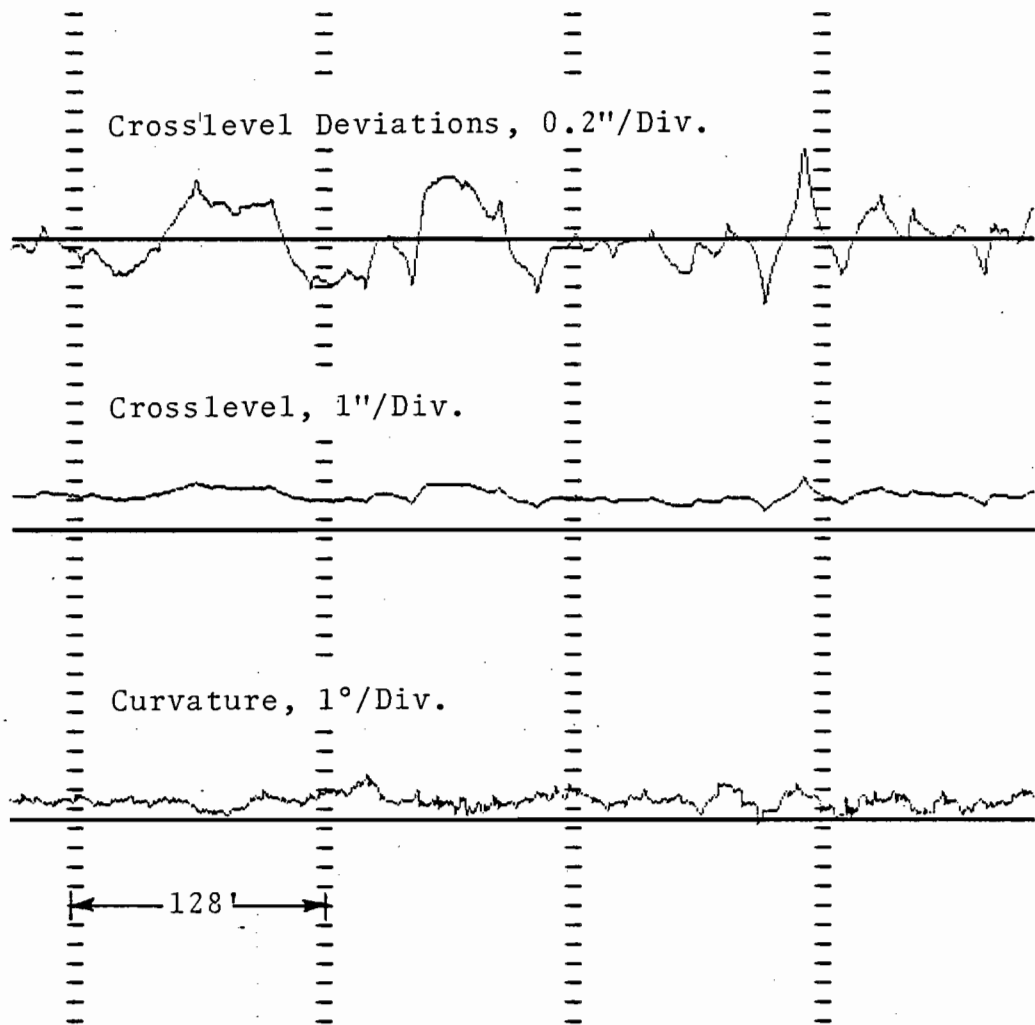
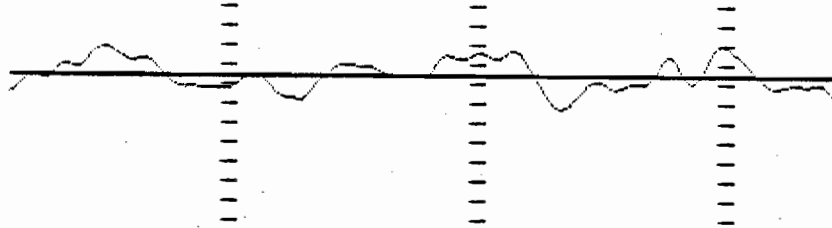


Figure C.l.d.13. Plateaus and Cusps in Crosslevel (Class 2, Curve, Bolted).

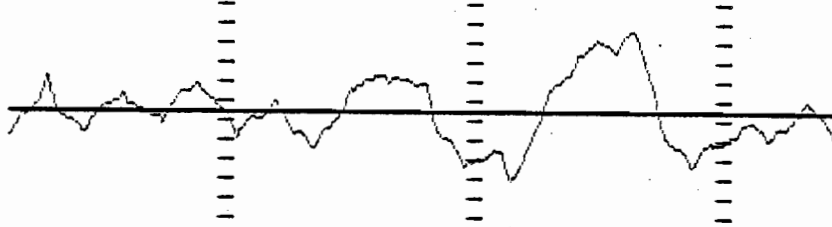
Left Profile, 0.3"/Div.



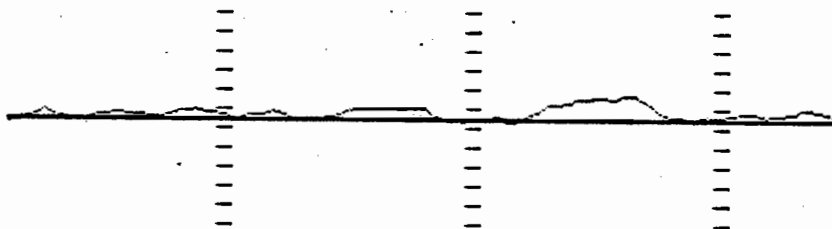
Right Profile, 0.3"/Div.



Crosslevel Deviations, 0.2"/Div.



Crosslevel, 1"/Div.



Curvature, 1°/Div.



128'

Figure C.1.d.14. Plateau in Profile and Crosslevel (Class 2, Tangent, Bolted).

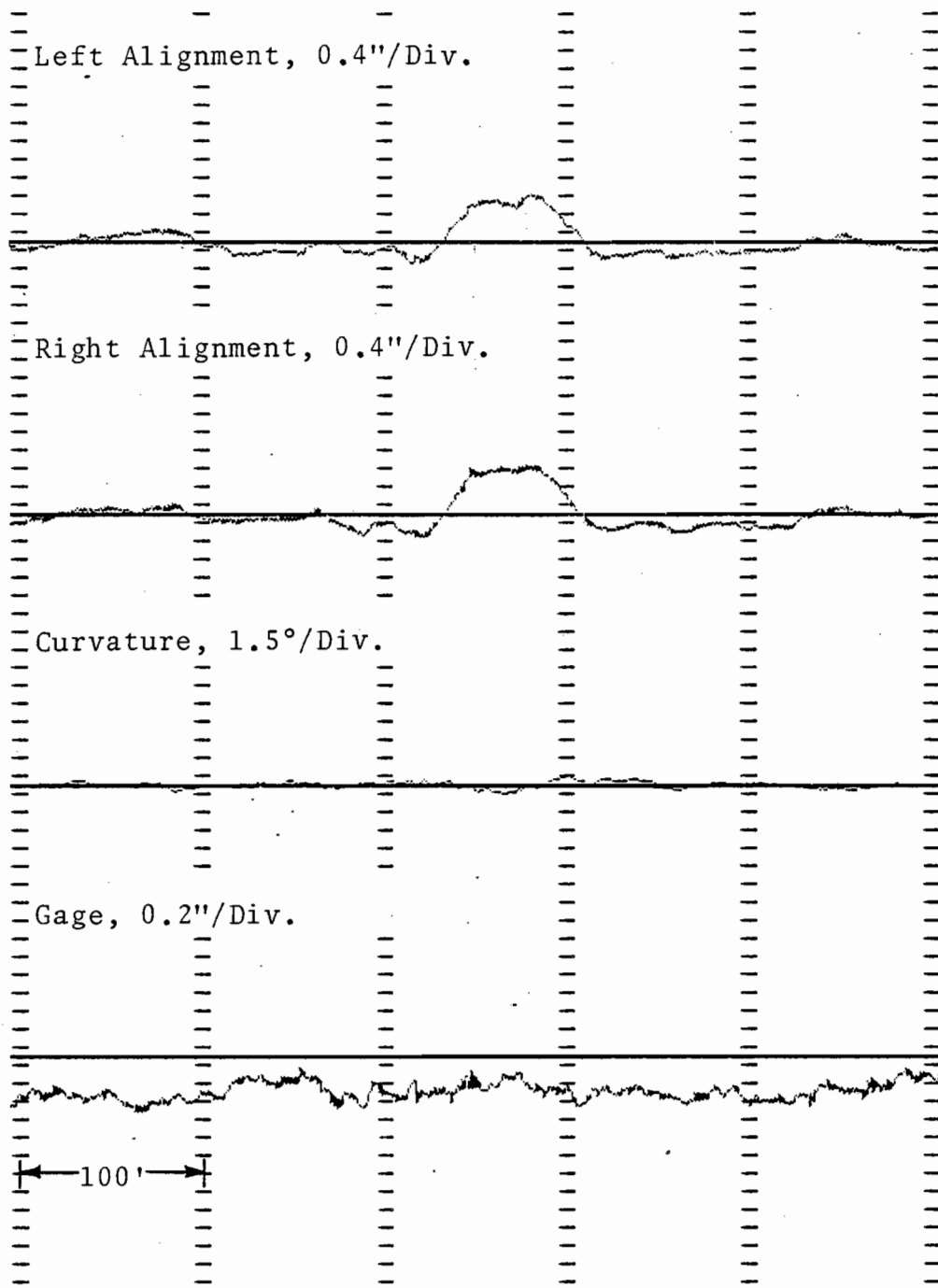


Figure C.1.d.15. Plateau in Alignment (Class 5, Tangent).

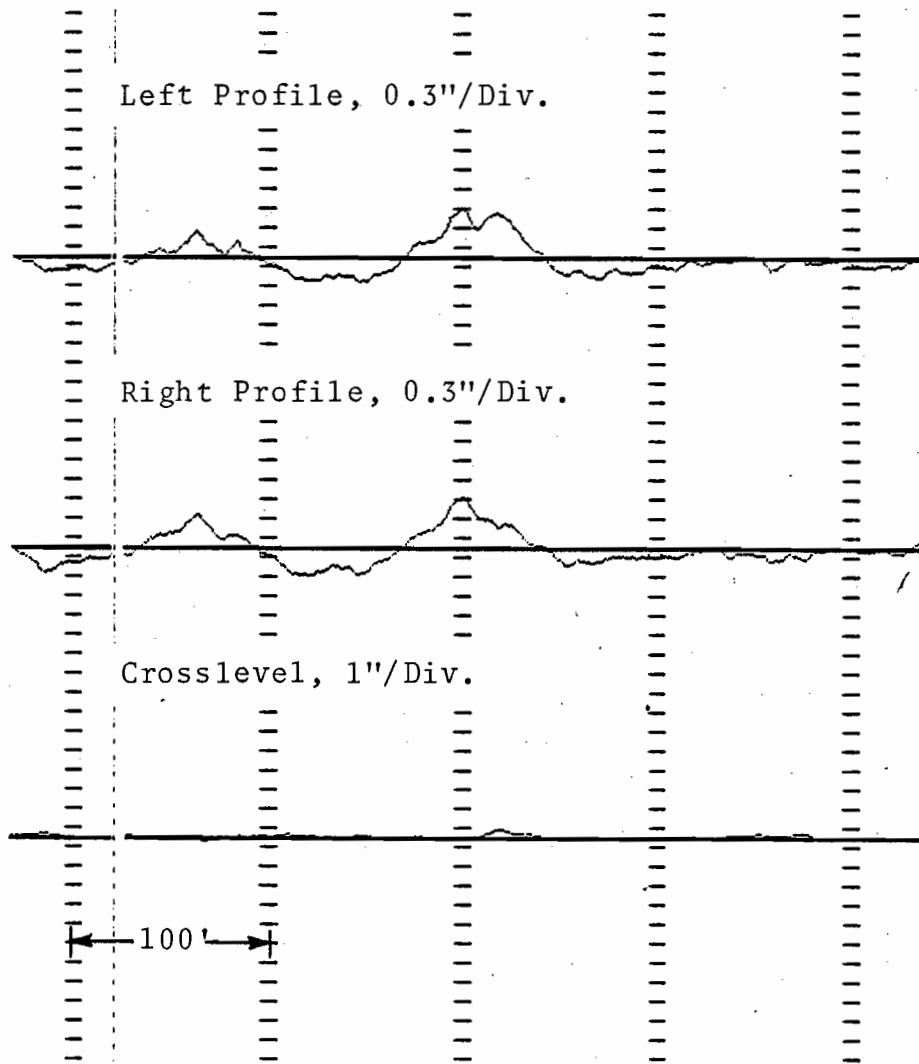


Figure C.1.e.1. Profile Trough Signature on a Bridge (Class 5, Tangent).

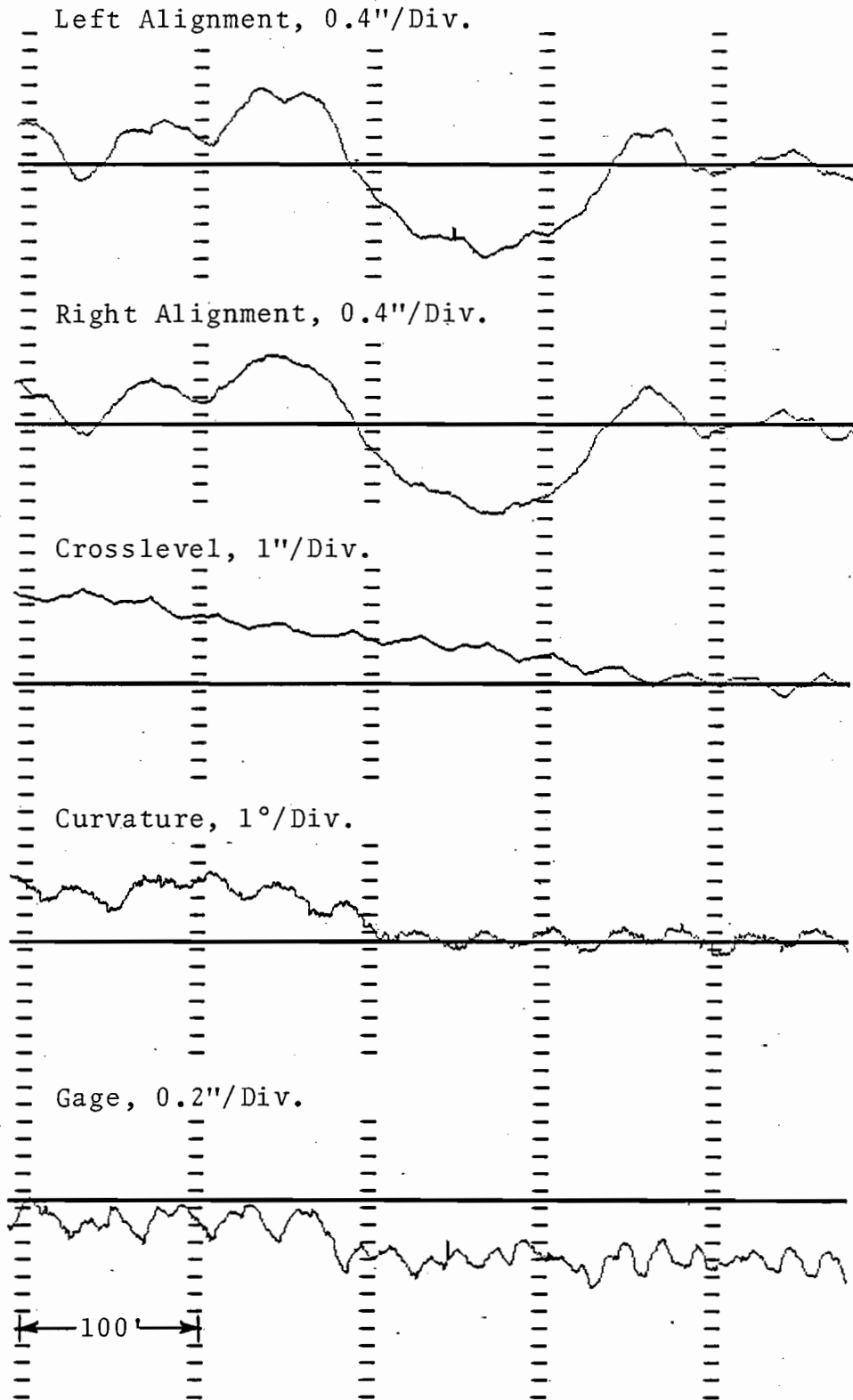


Figure C.1.e.2. Alignment Trough, Note also Change in Gage (Class 2, Spiral).

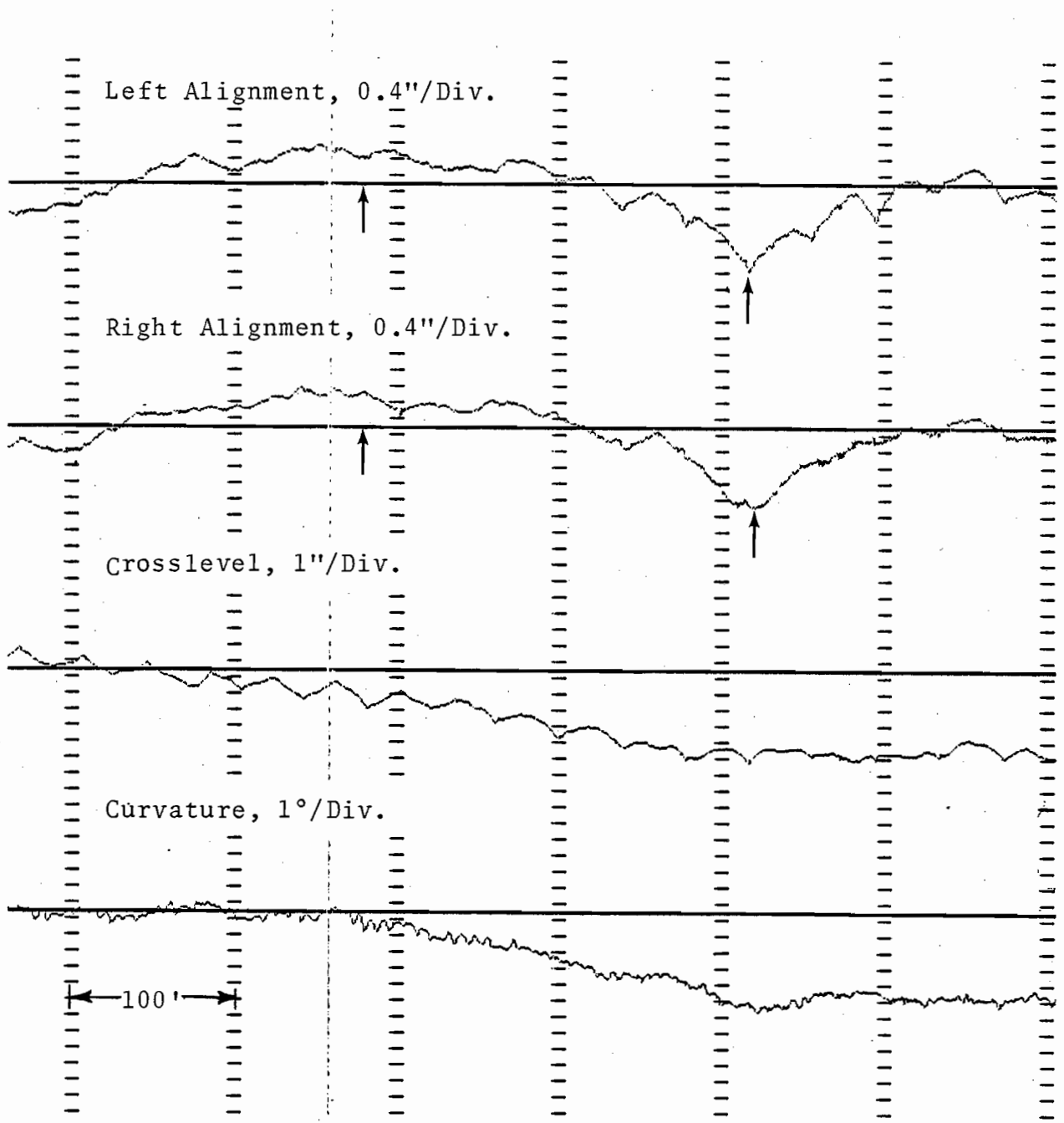


Figure C.1.e.3. A Long Trough (400') and a Bump (120') in Alignment (Class 3, Spiral).

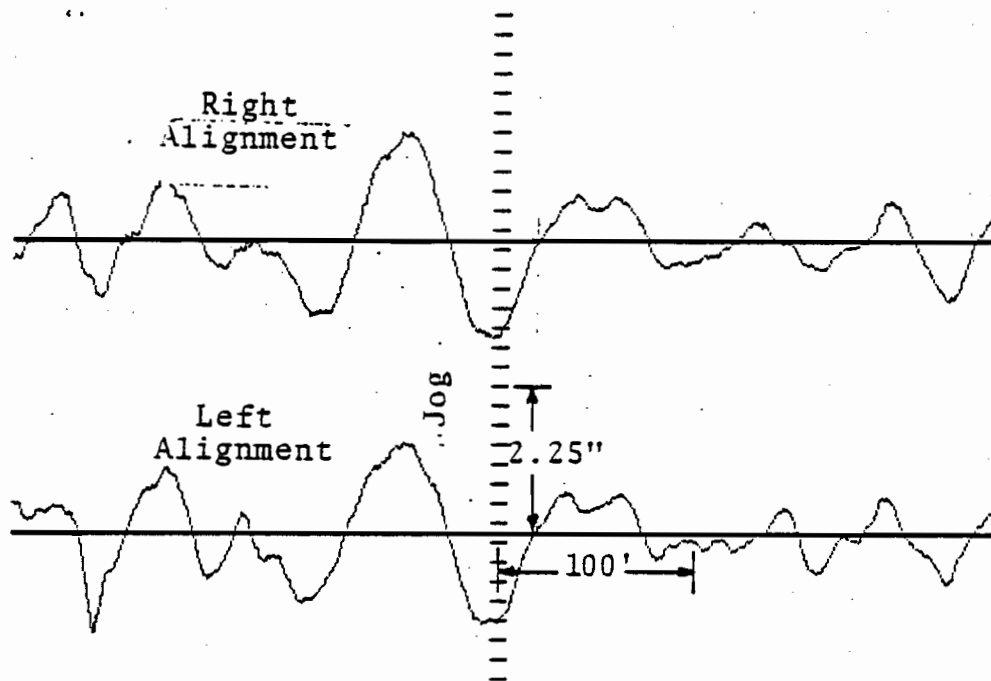


Figure C.1.f.1. A Sinusoid in Alignment.

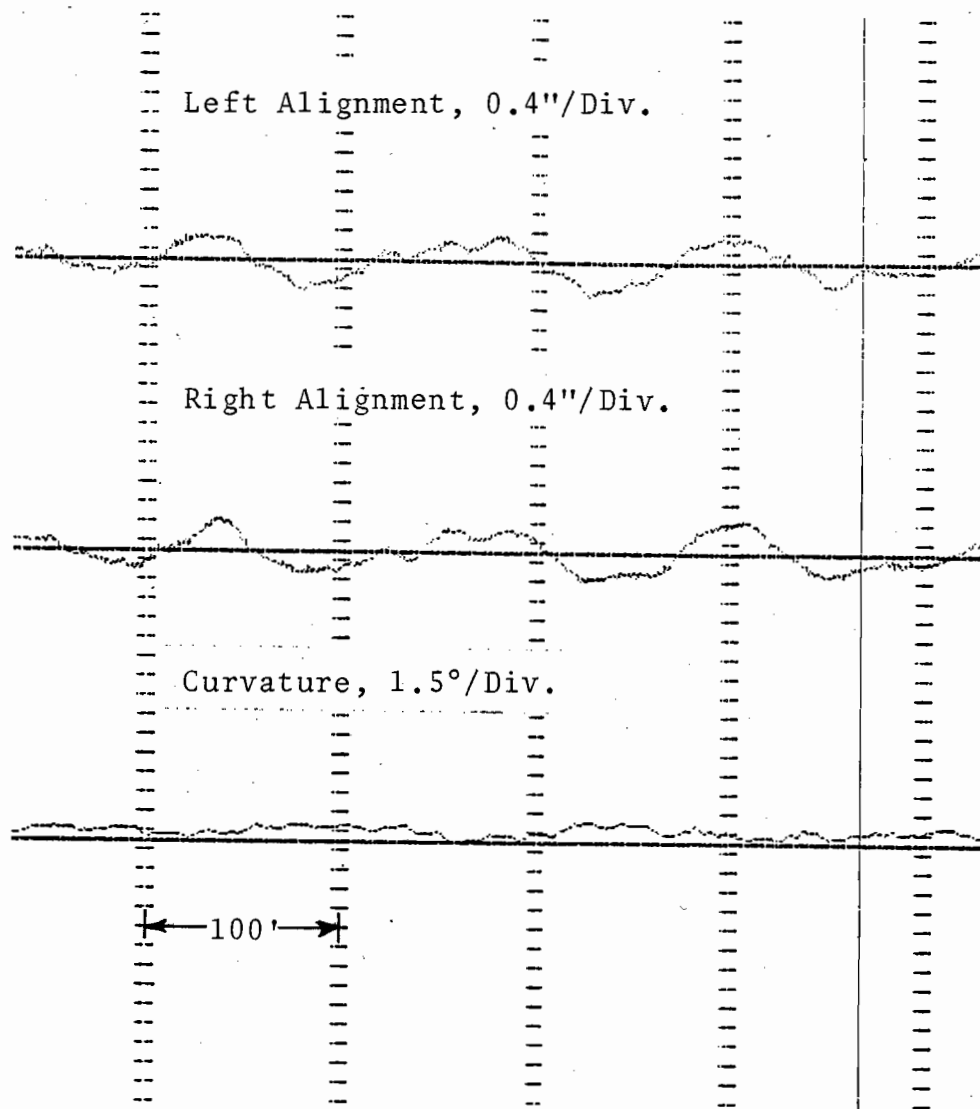


Figure C.1.f.2. Sinusoidal Alignment (Class 6, Curve, CWR).

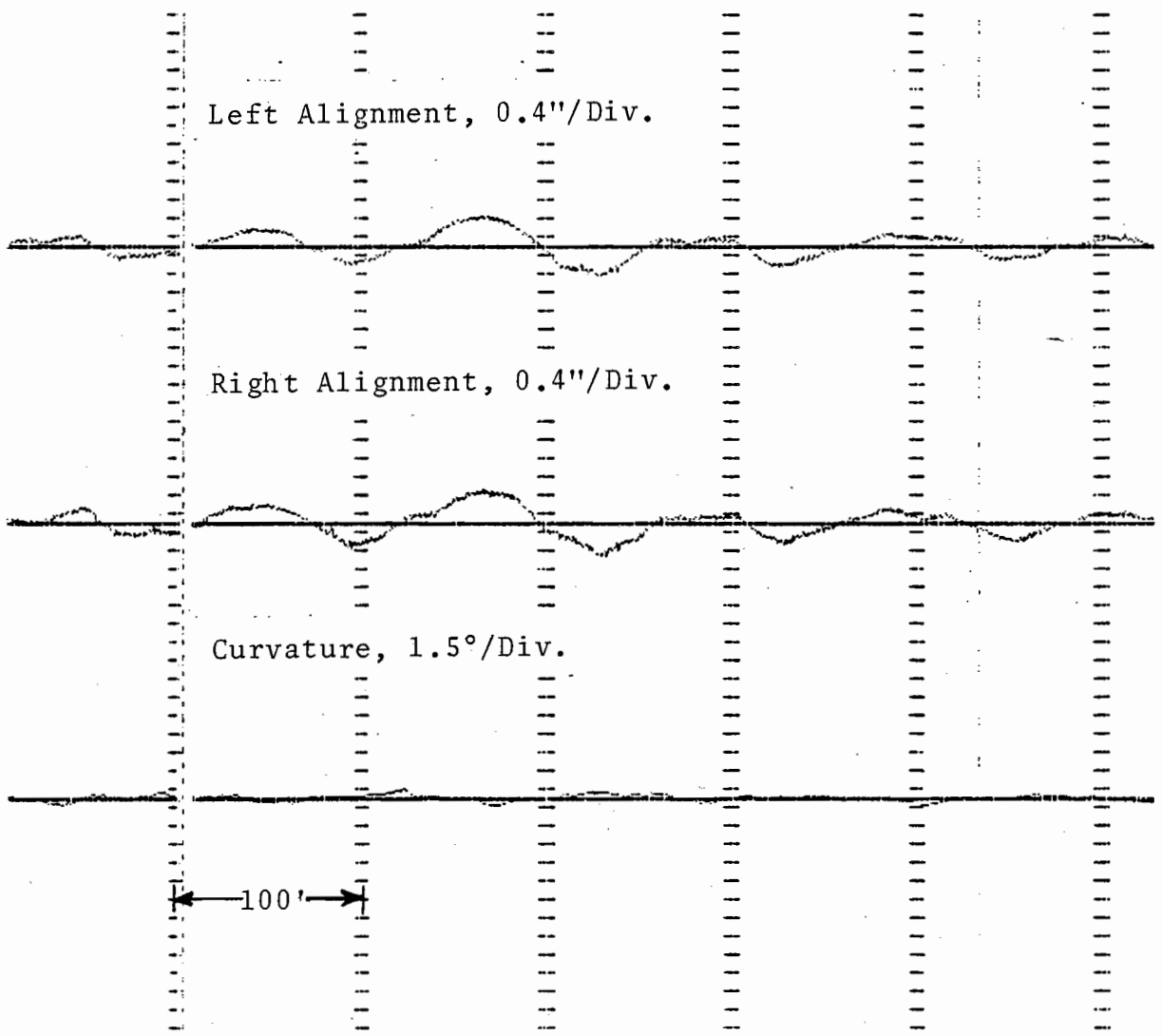


Figure C.1.f.3. Sinusoidal Alignment with Decay on Both Ends (Class 6, Tangent).

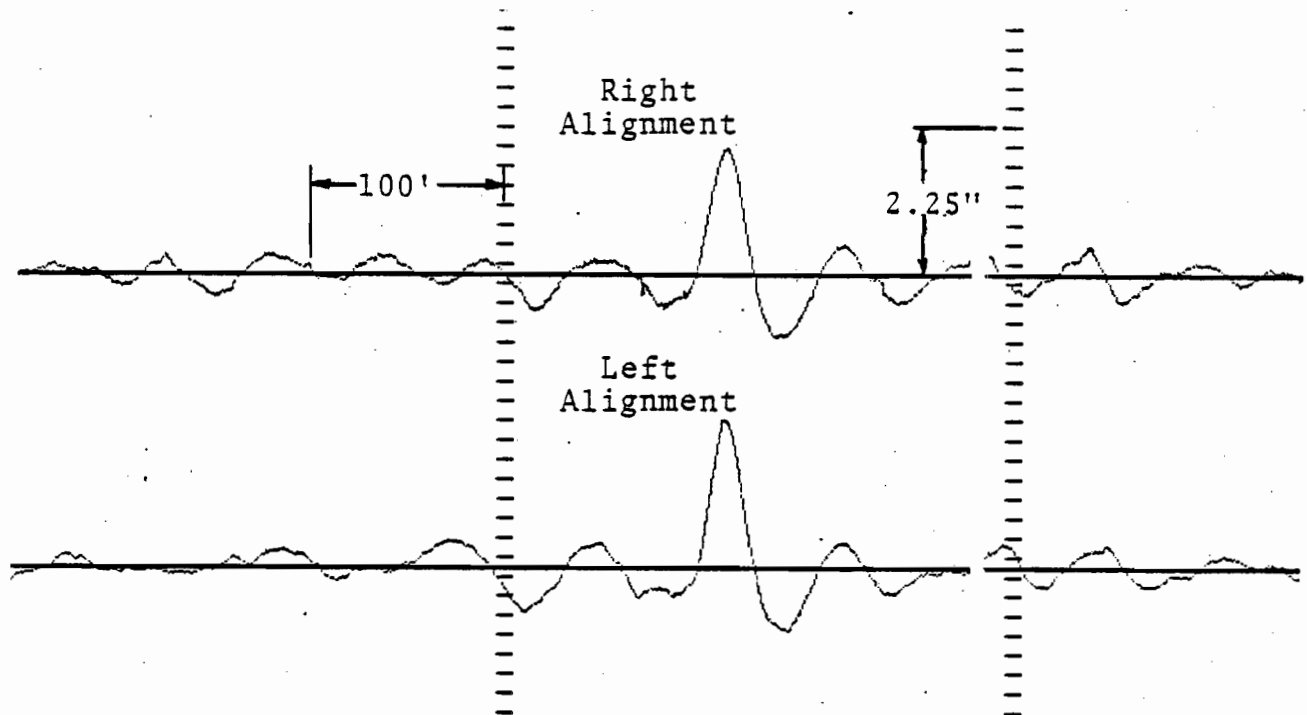


Figure C.1.f.4. A Damped Sinusoid in Alignment (Class 3).

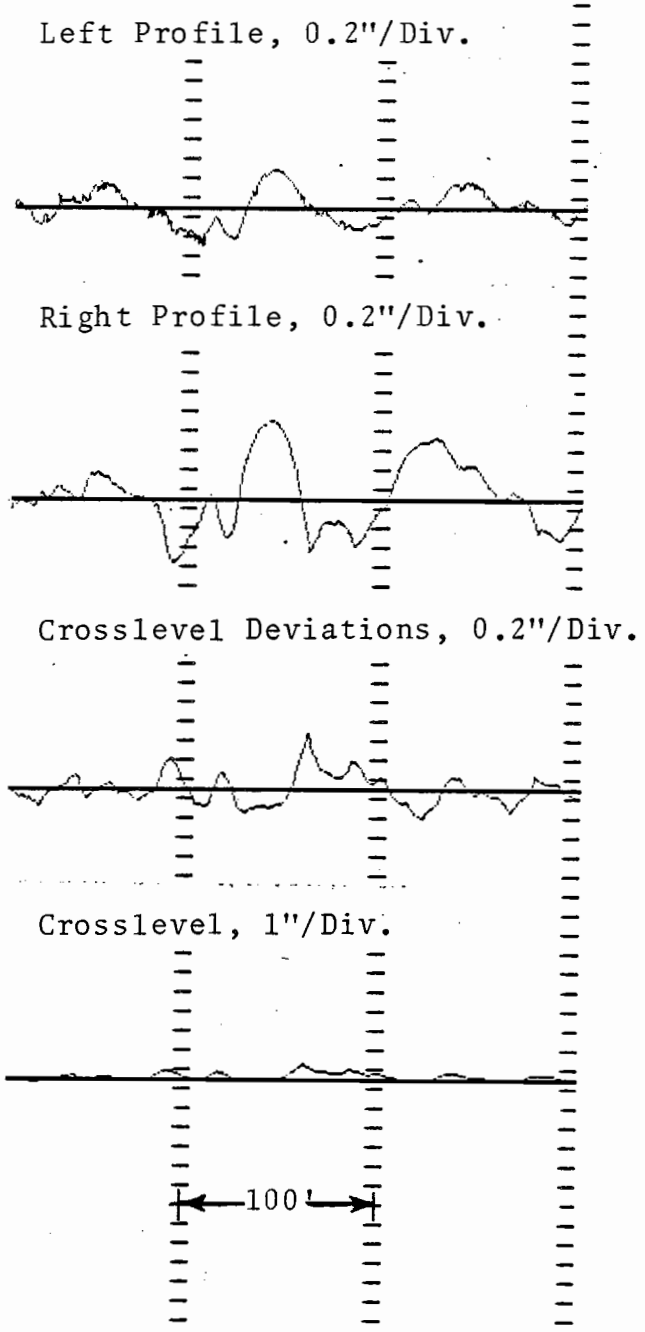


Figure C.1.f.5. Sin x/x Signature in Profile (Class 3, Bolted, Tangent).

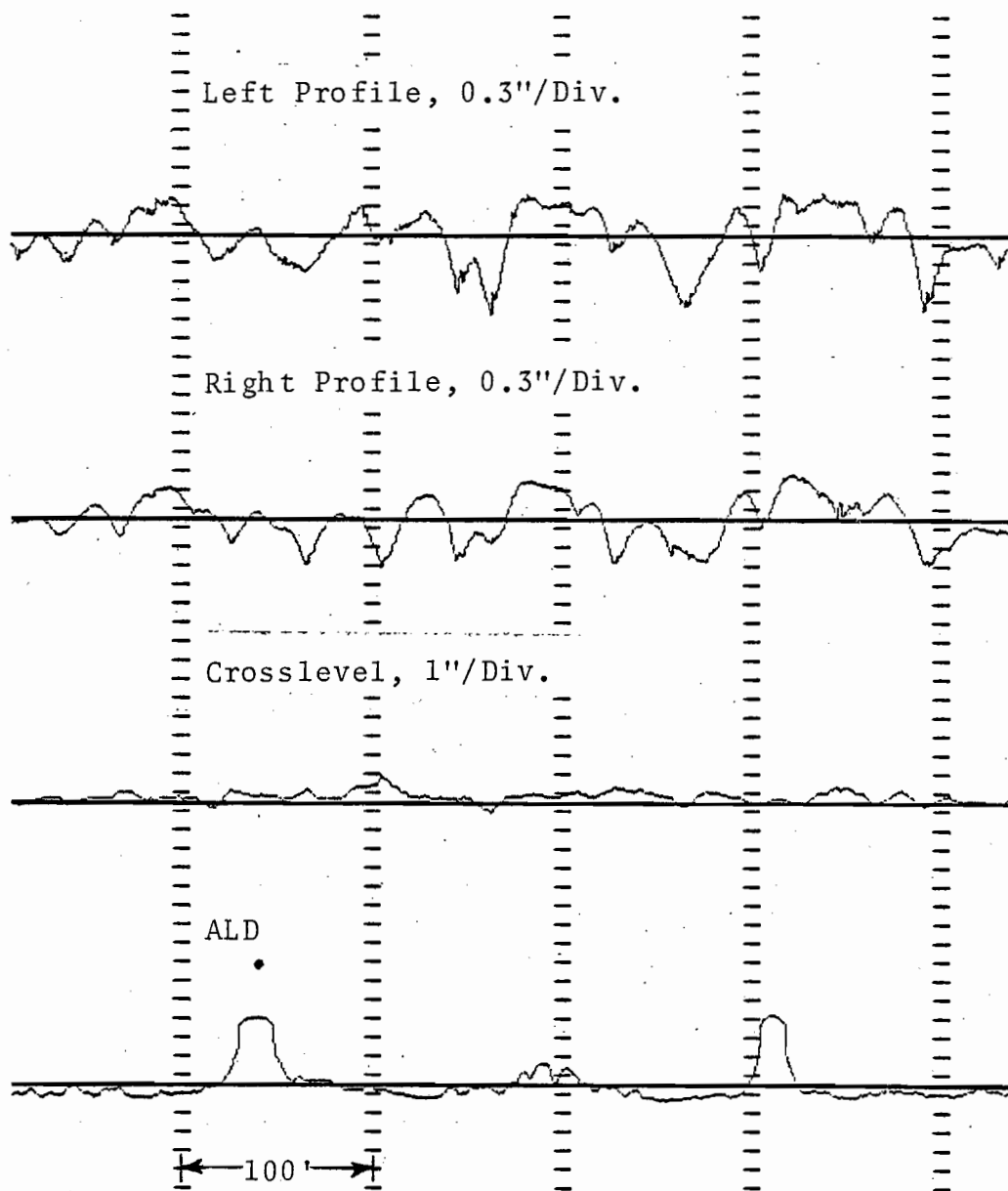


Figure C.1.f.6. Profile Signatures at a Road Crossing
(Class 5, Tangent, Bolted)

C-56

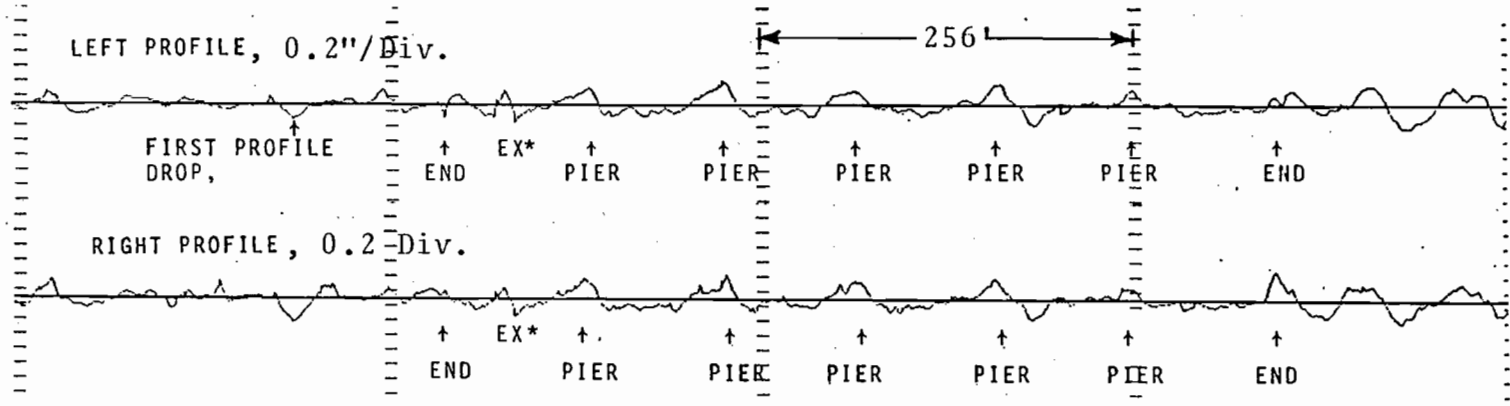


Figure C.1.f.7. Profile Signatures at a Bridge (Class 4, CWR).

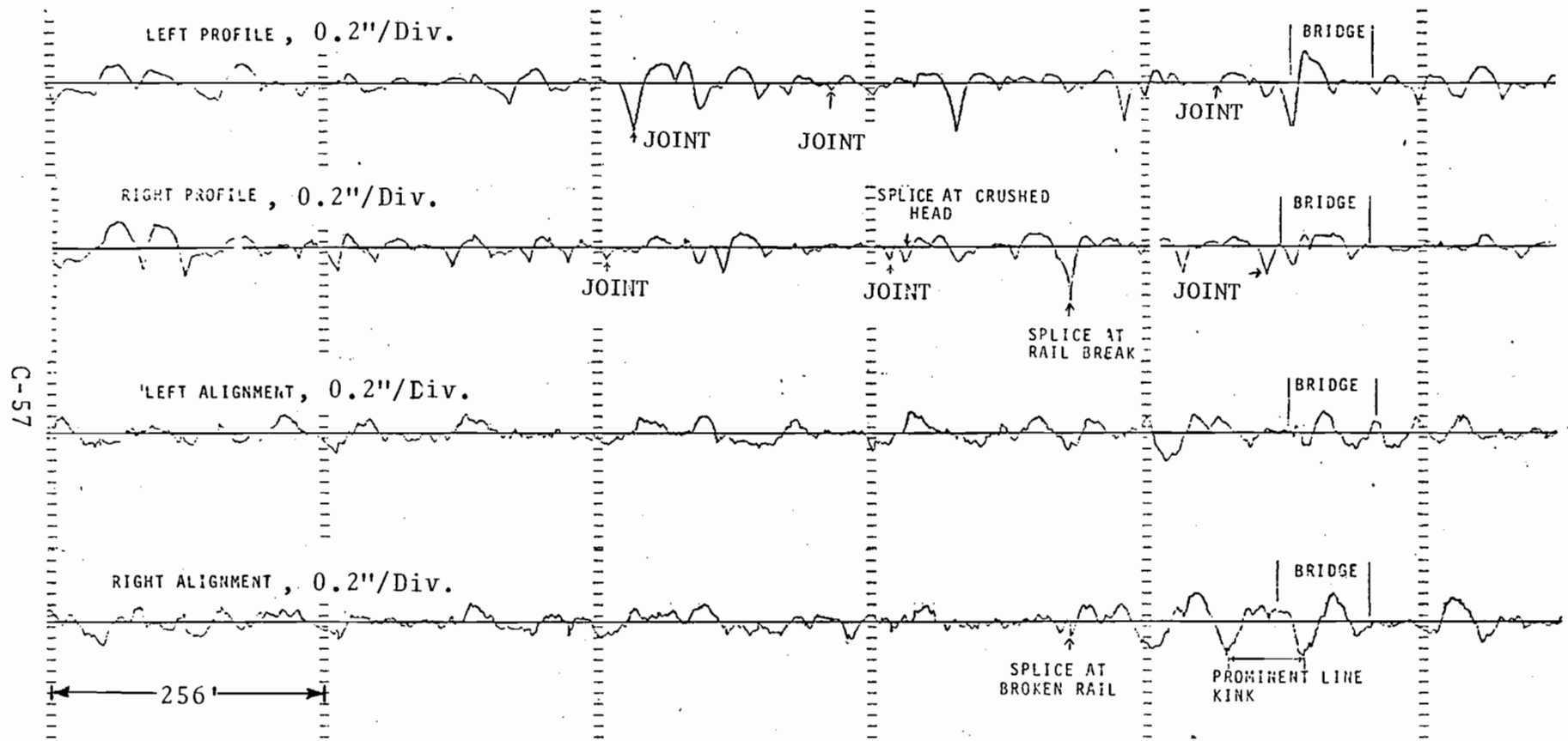


Figure C.1.f.8. Cusps in Single Rail Profile and a Jog in Single Rail Alignment (Class 3, Bolted).

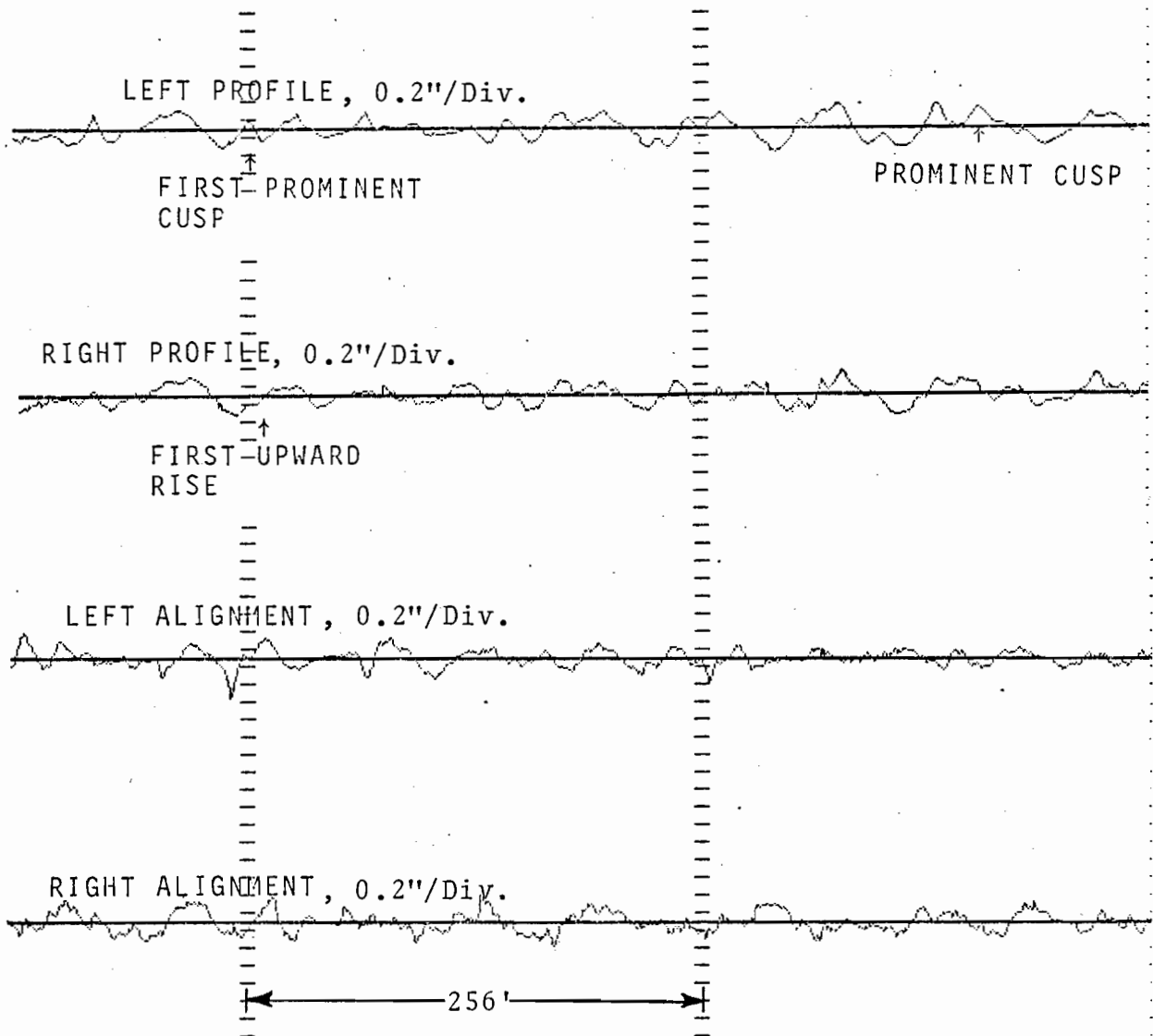


Figure C.I.f.9. Positive Cusps in Profile and Alignment Cusps Towards Track Center Line at Welds (Class 4 CWR).

C.2 PERIODIC VARIATIONS

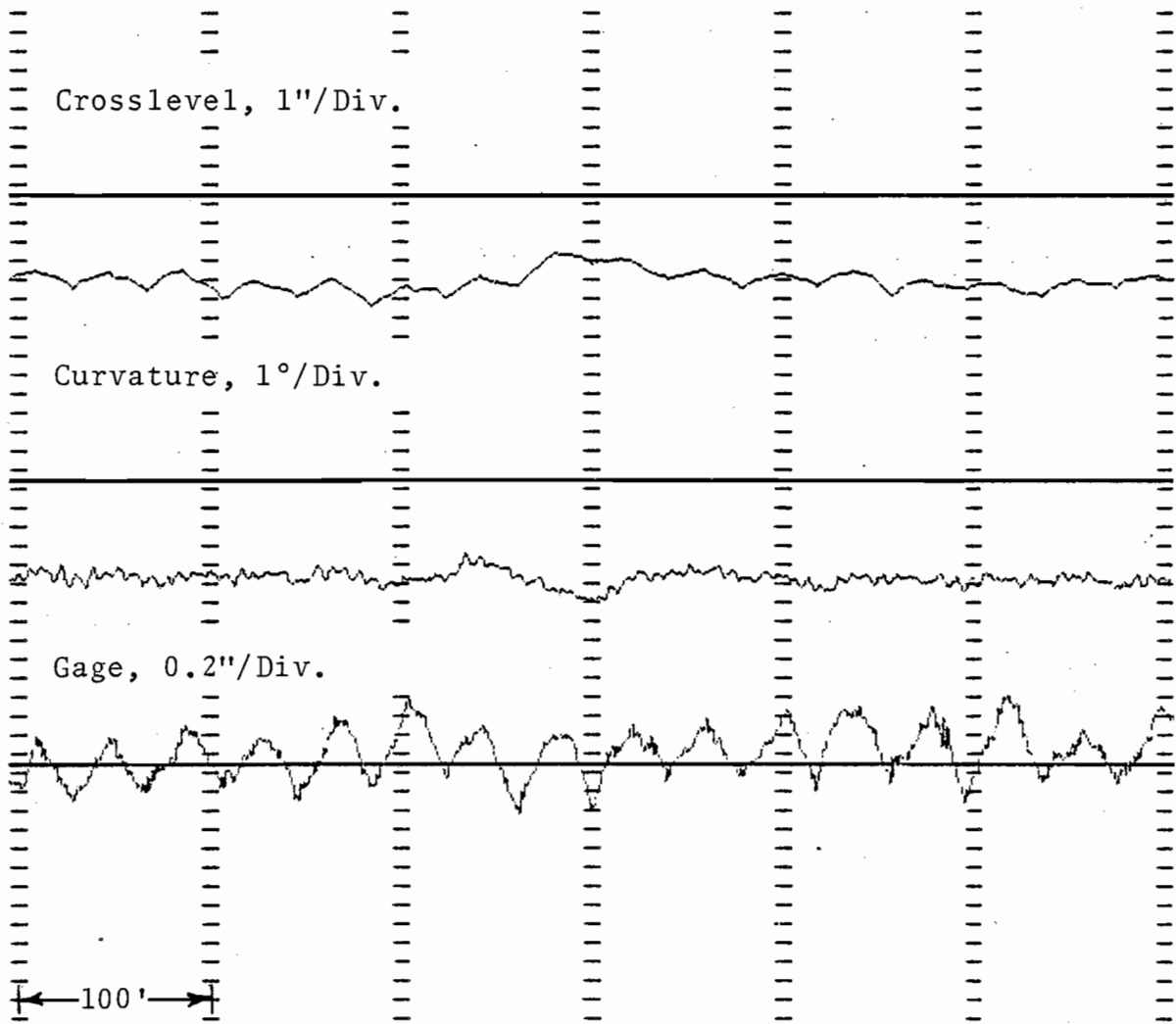


Figure C.2.a.1. Periodic (Sawtooth) Gage (Class 3, Curve).

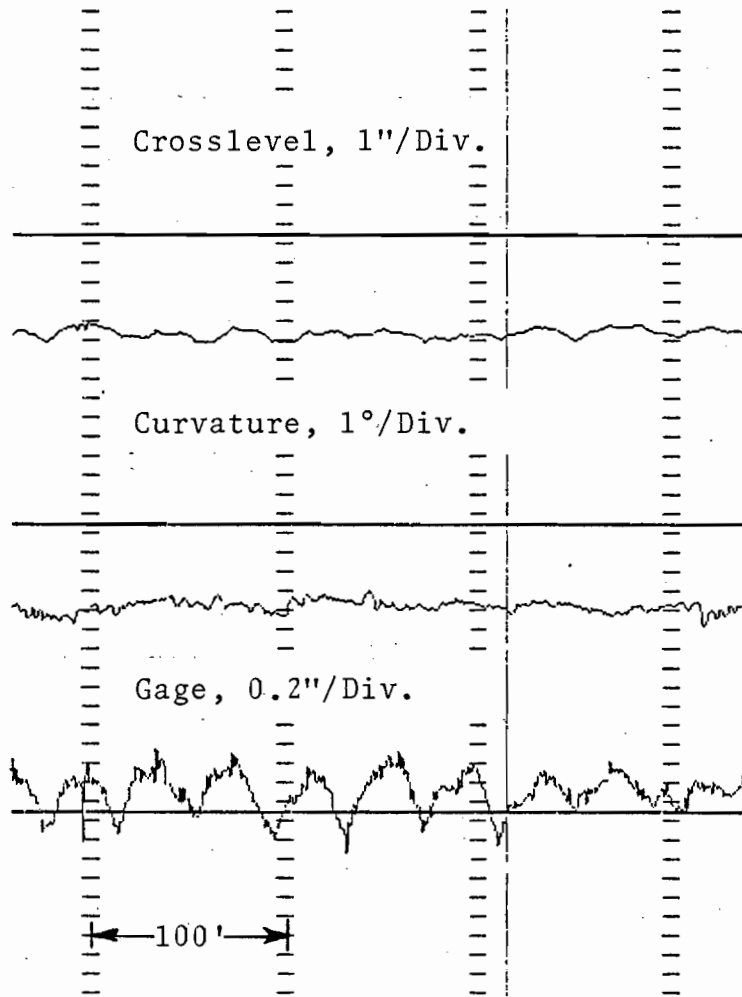


Figure C.2.a.2. Periodic Gage Cusps, Narrow at Joints on Low Rail (Class 3, Curve).

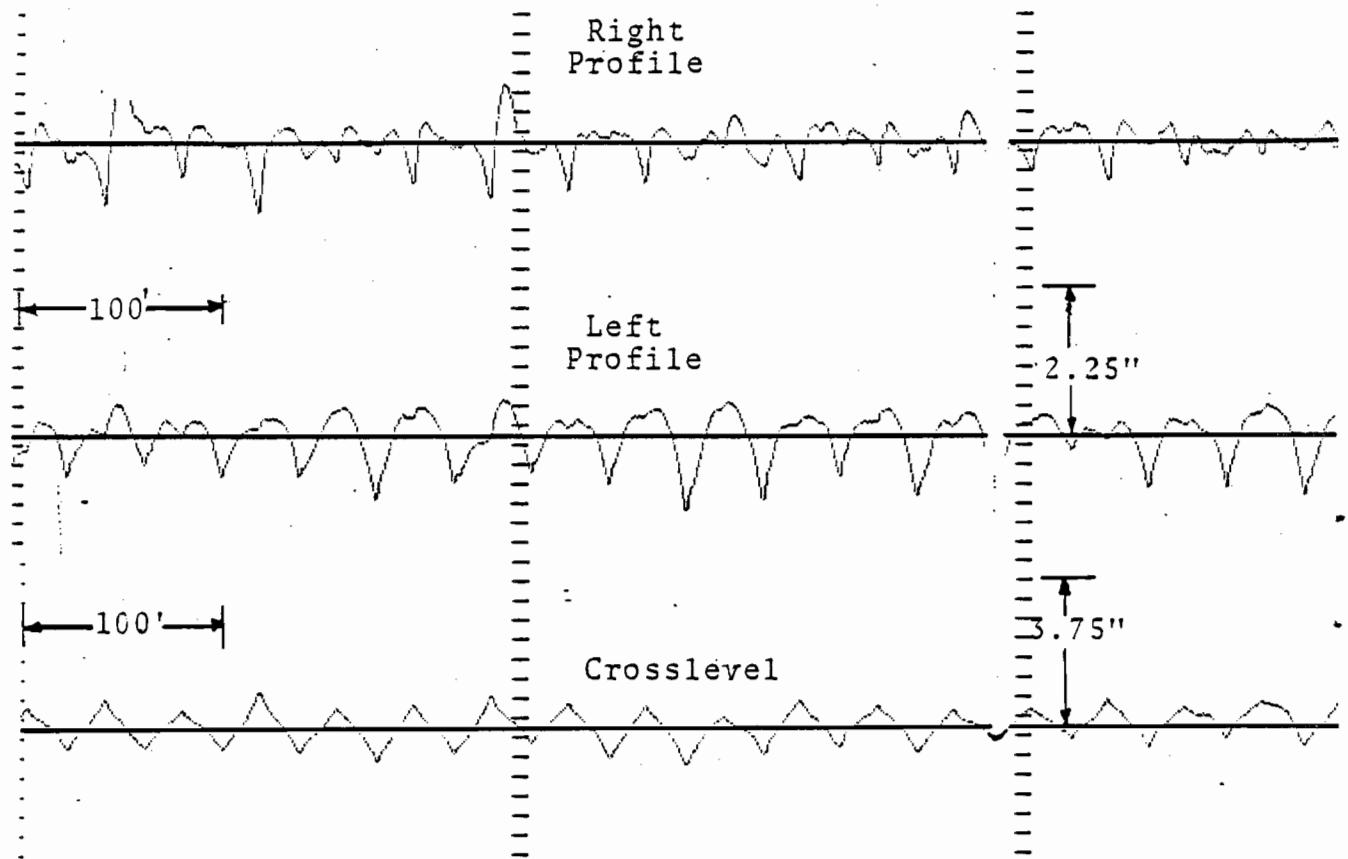


Figure C.2.a.3. Periodic Crosslevel and Profile (Class 3, Bolted).

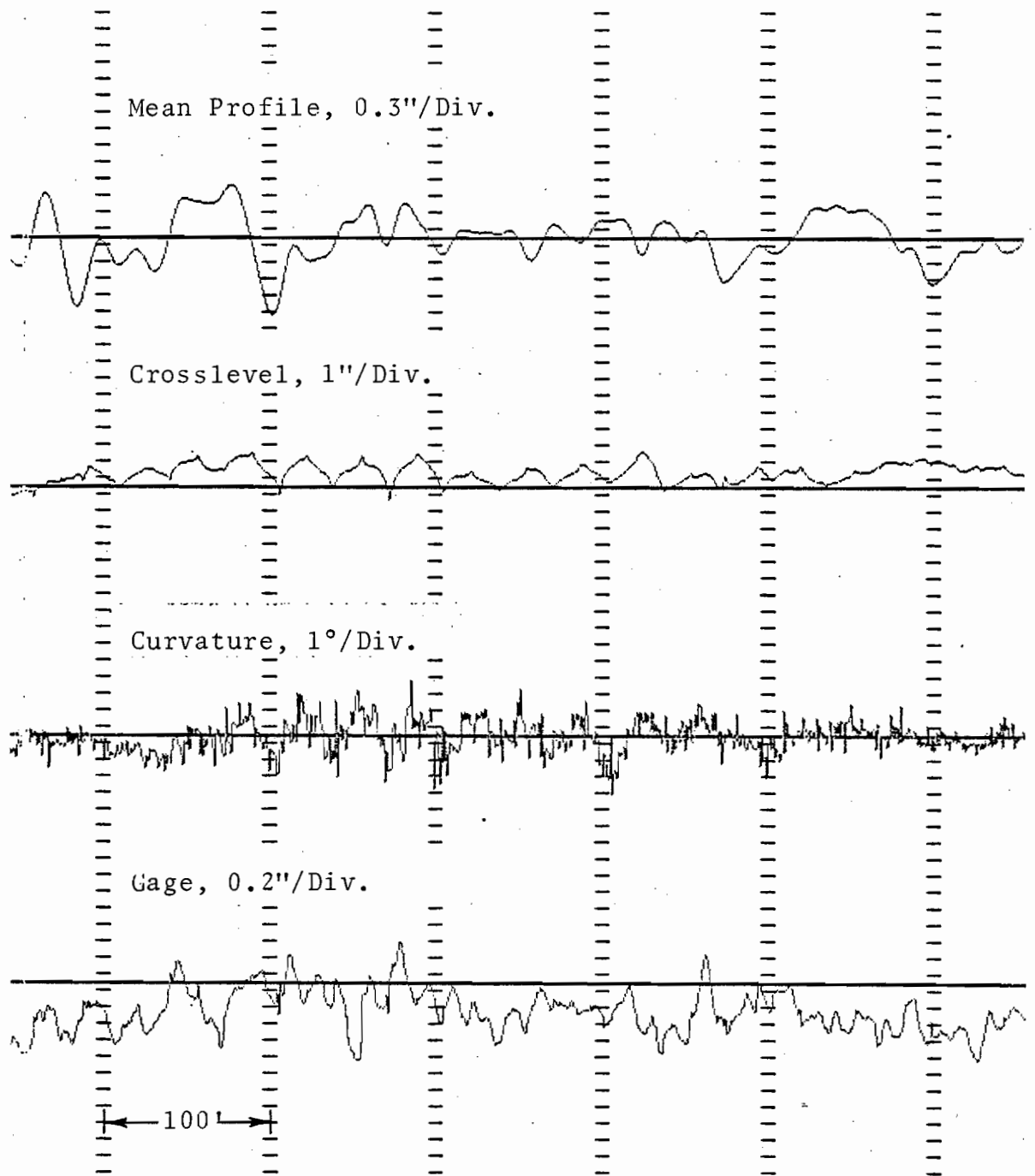


Figure C.2.a.4. Periodic Crosslevel Caused by Badly Deteriorated Joints on Both Rails (Class 1, Tangent).

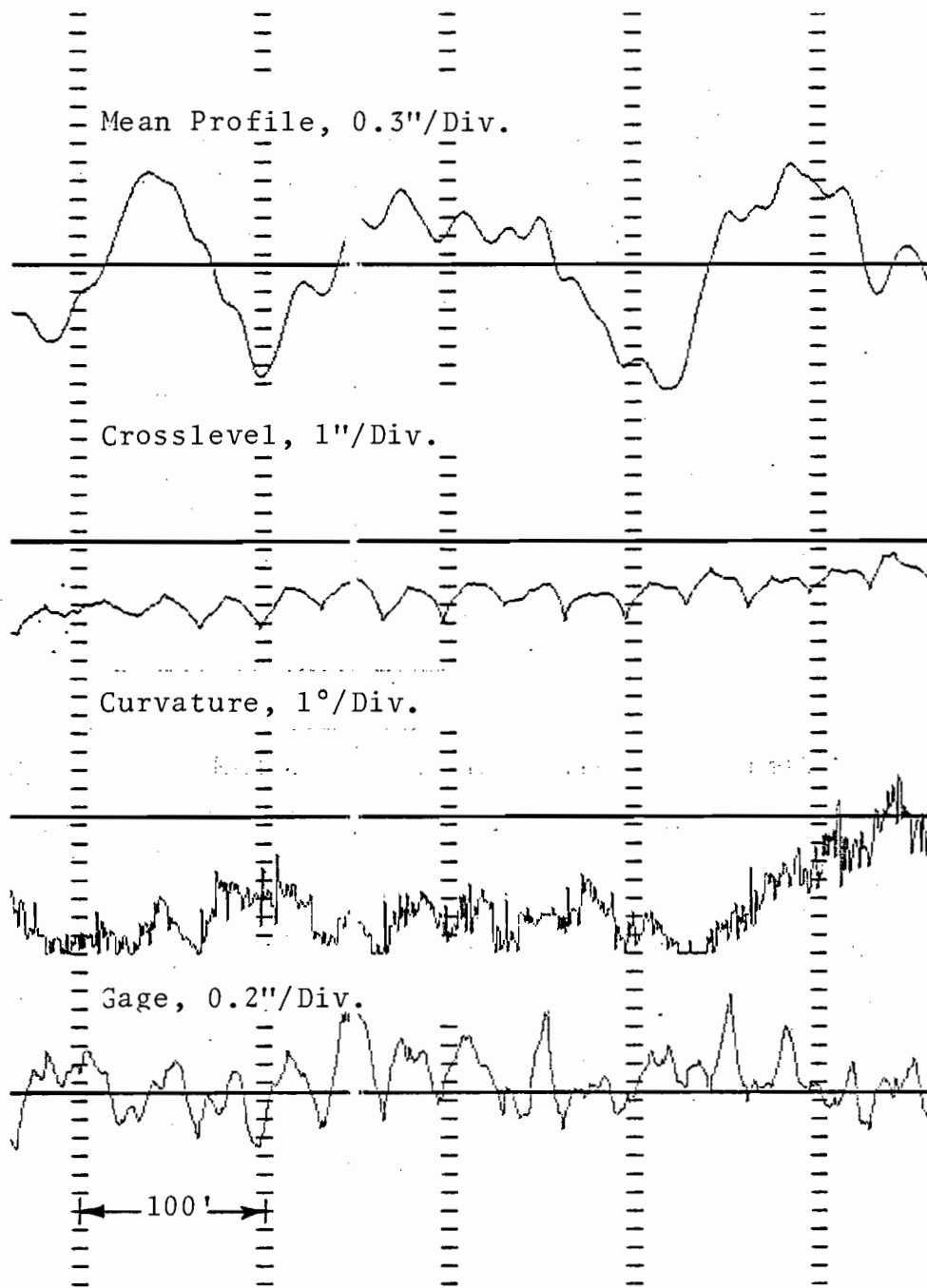


Figure C.2.a.5. Periodic Crosslevel Due to Badly Deteriorated Joints on the Low Rail (Class 1, Curve).

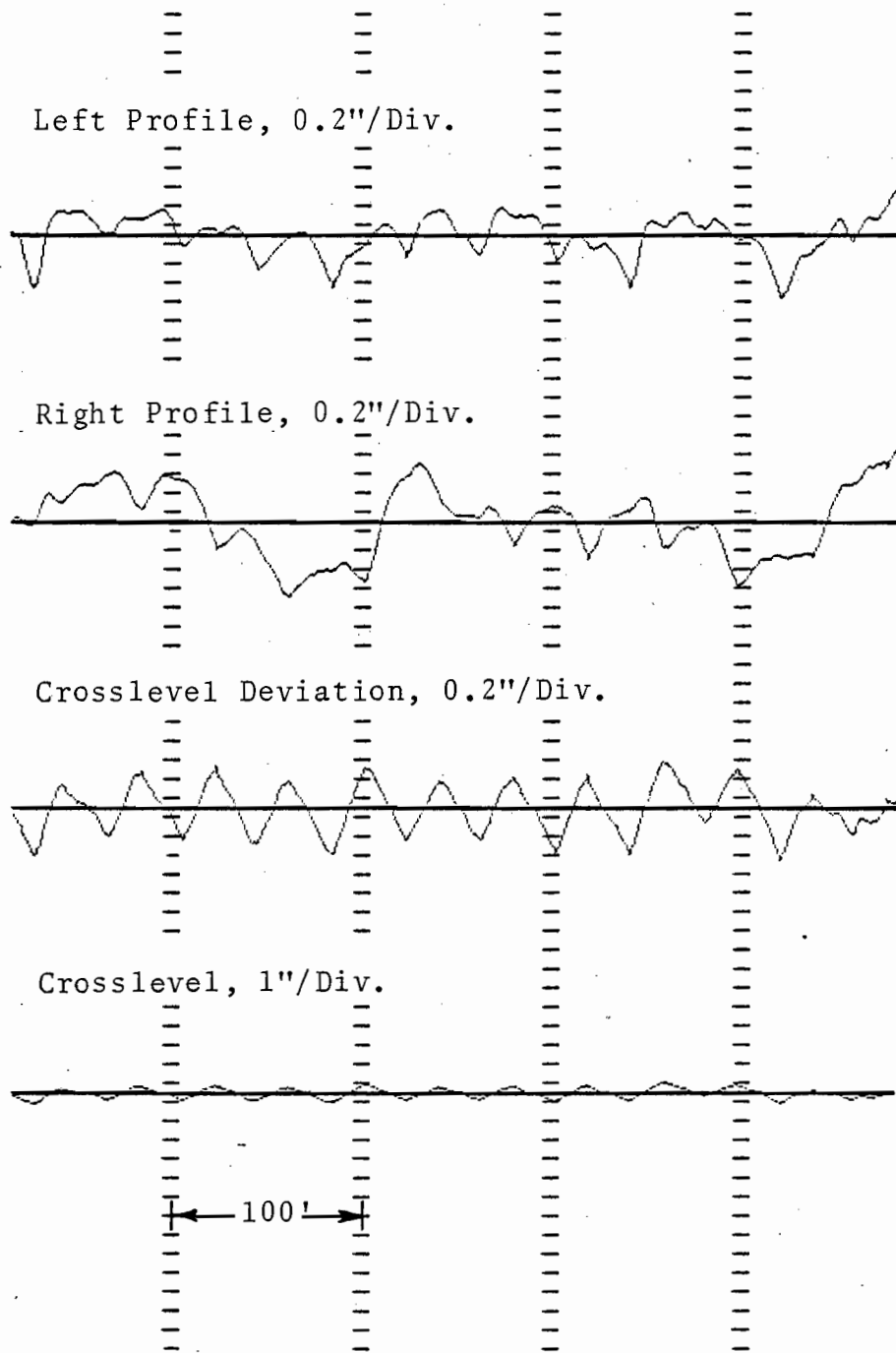


Figure C.2.a.6. Periodic Crosslevel (Class 3, Tangent).

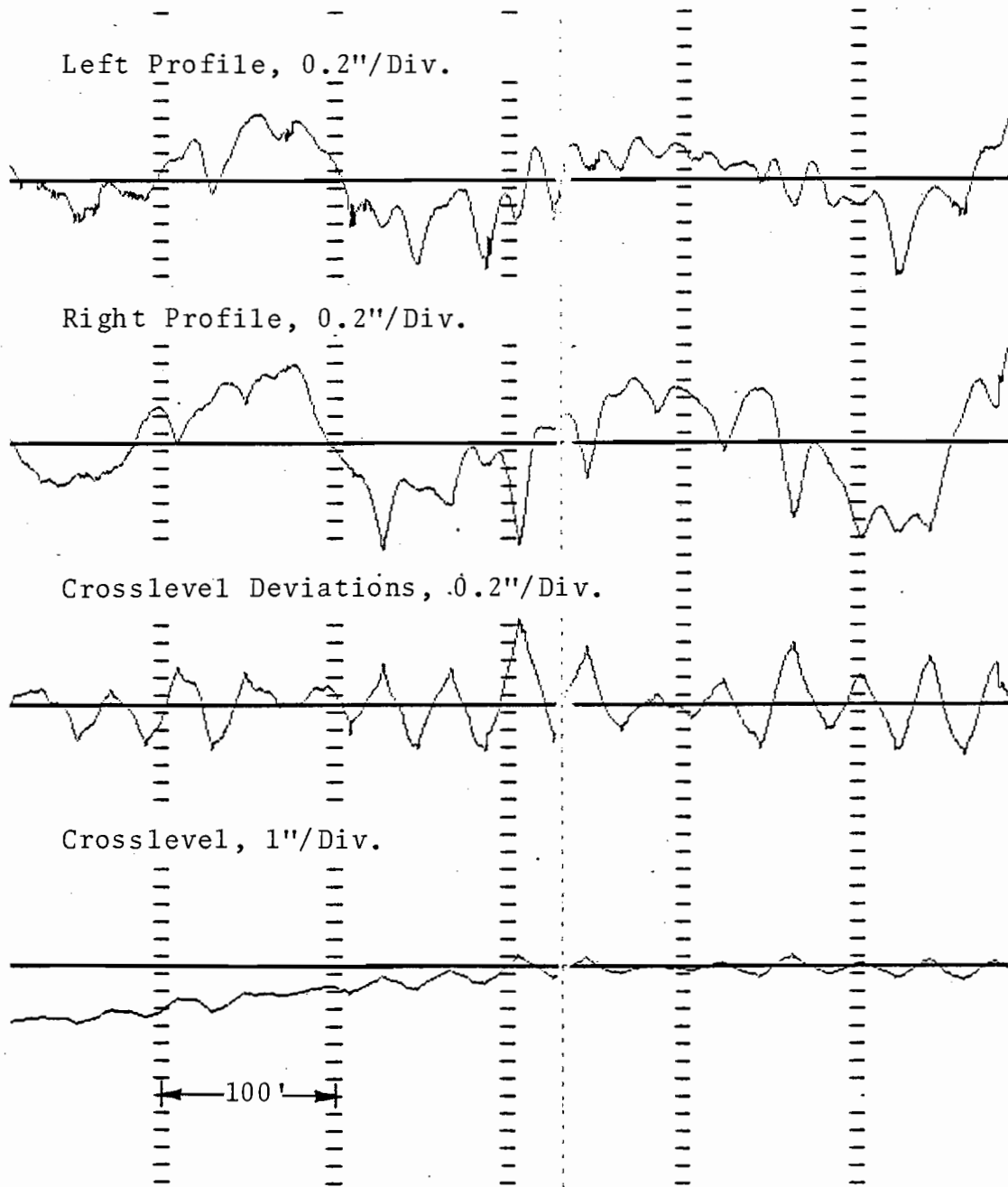


Figure C.2.a.7. Periodic Crosslevel (Class 3, Bolted, Spiral and Tangent).

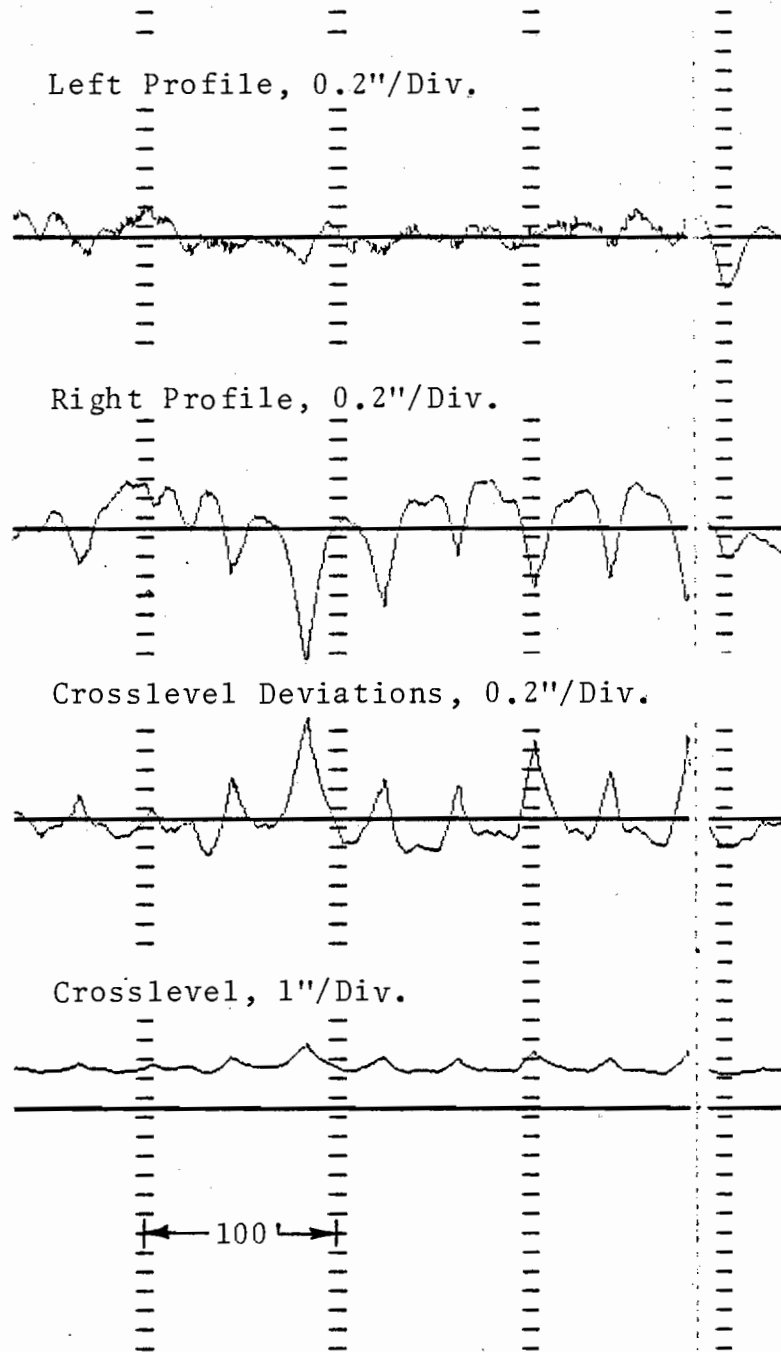
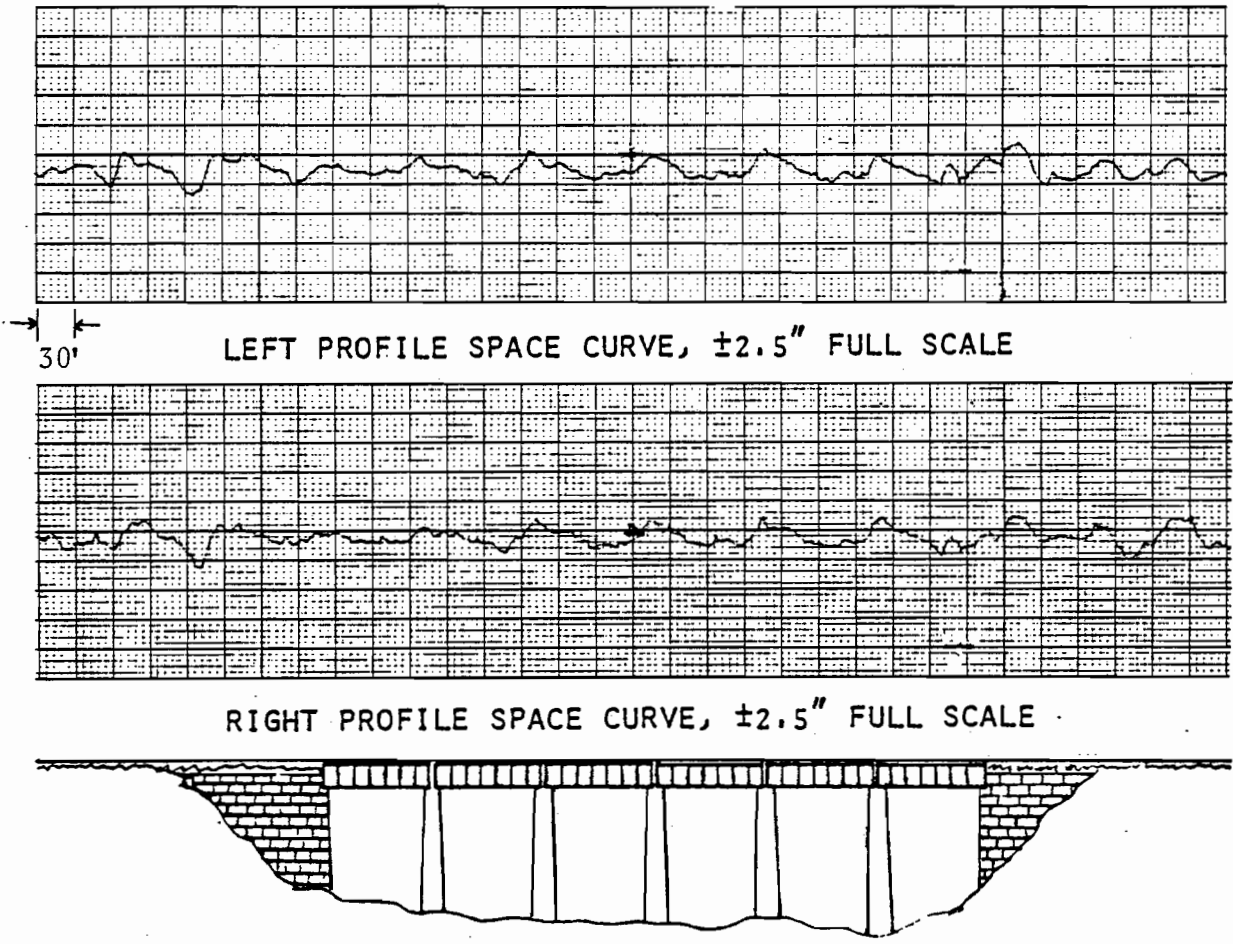


Figure C.2.a.8. Periodic Cuspy Profile and Crosslevel Due to Low Joints in the Low Rail (Class 3, Bolted, Curve).



SIDE VIEW MULTIPLE SPAN DECK GIRDER BRIDGE

Figure C.2.a.9. Periodic Profile on a Bridge.

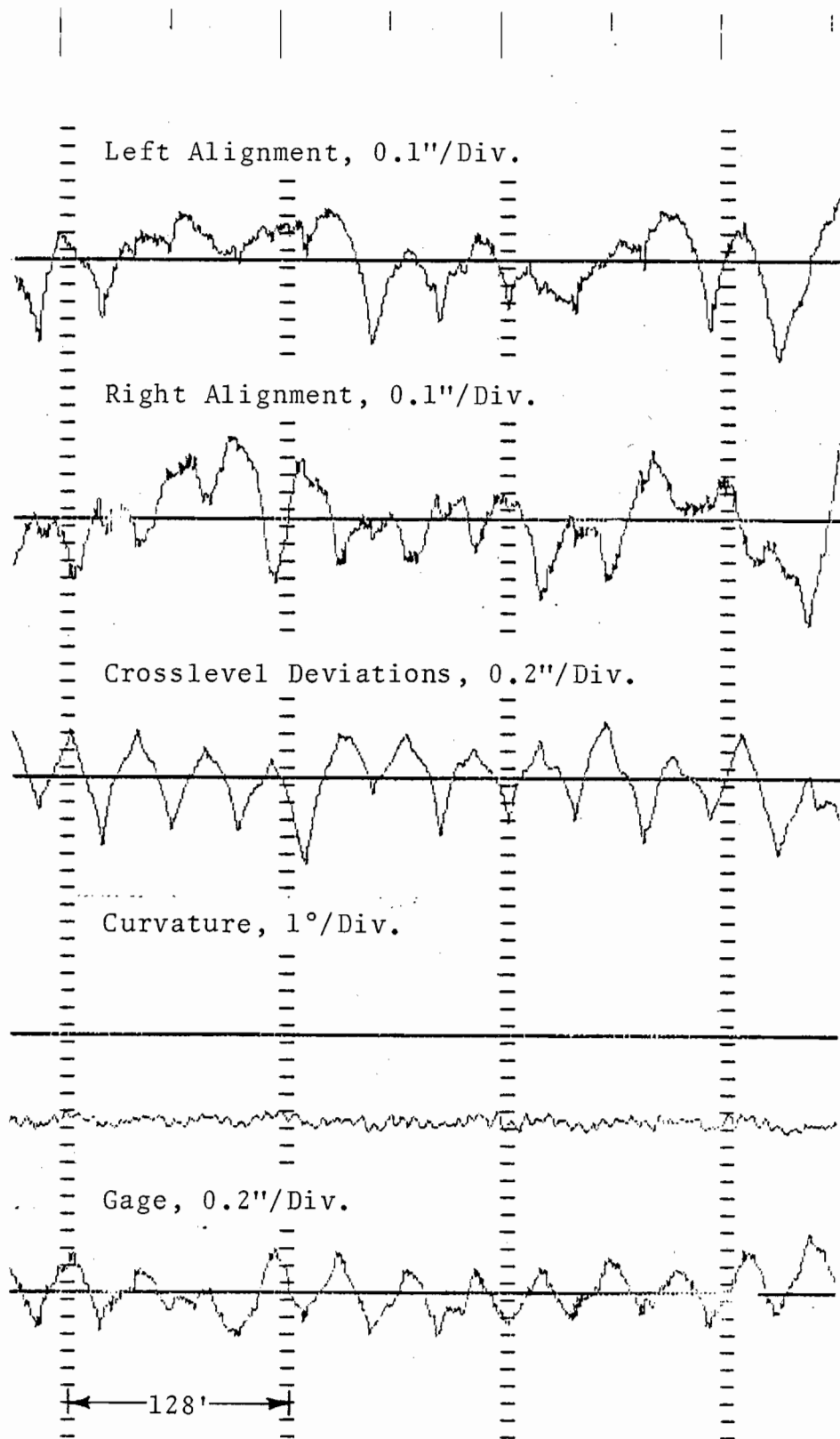


Figure C.2.a.10. Combined Periodic Gage and Alignment (Class 3, Curve).

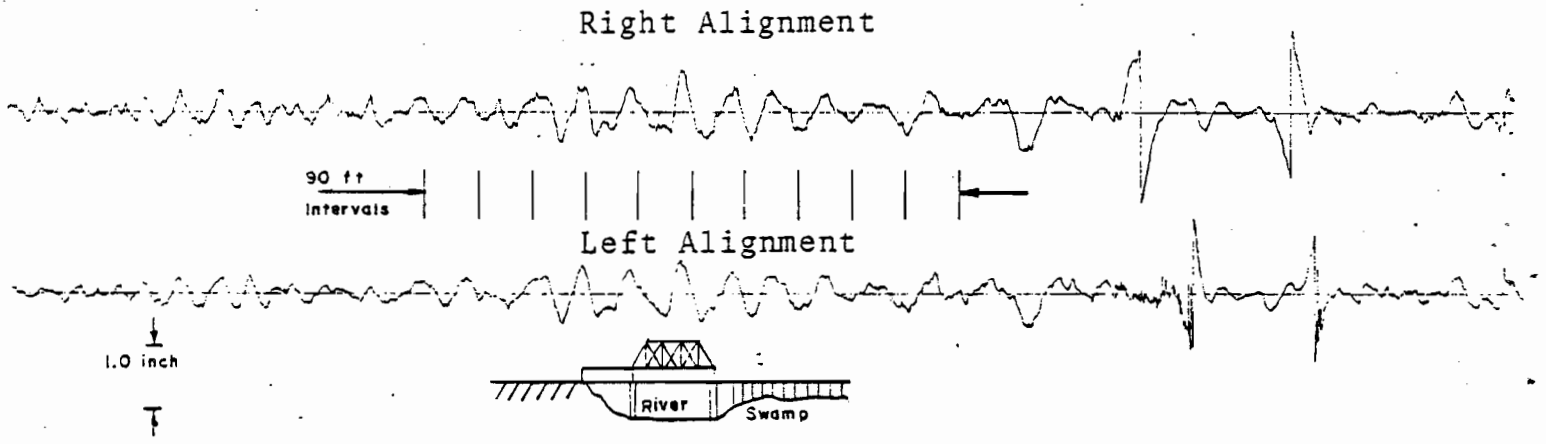


Figure C.2.a.11. Periodic Alignment Bumps on a Bridge.

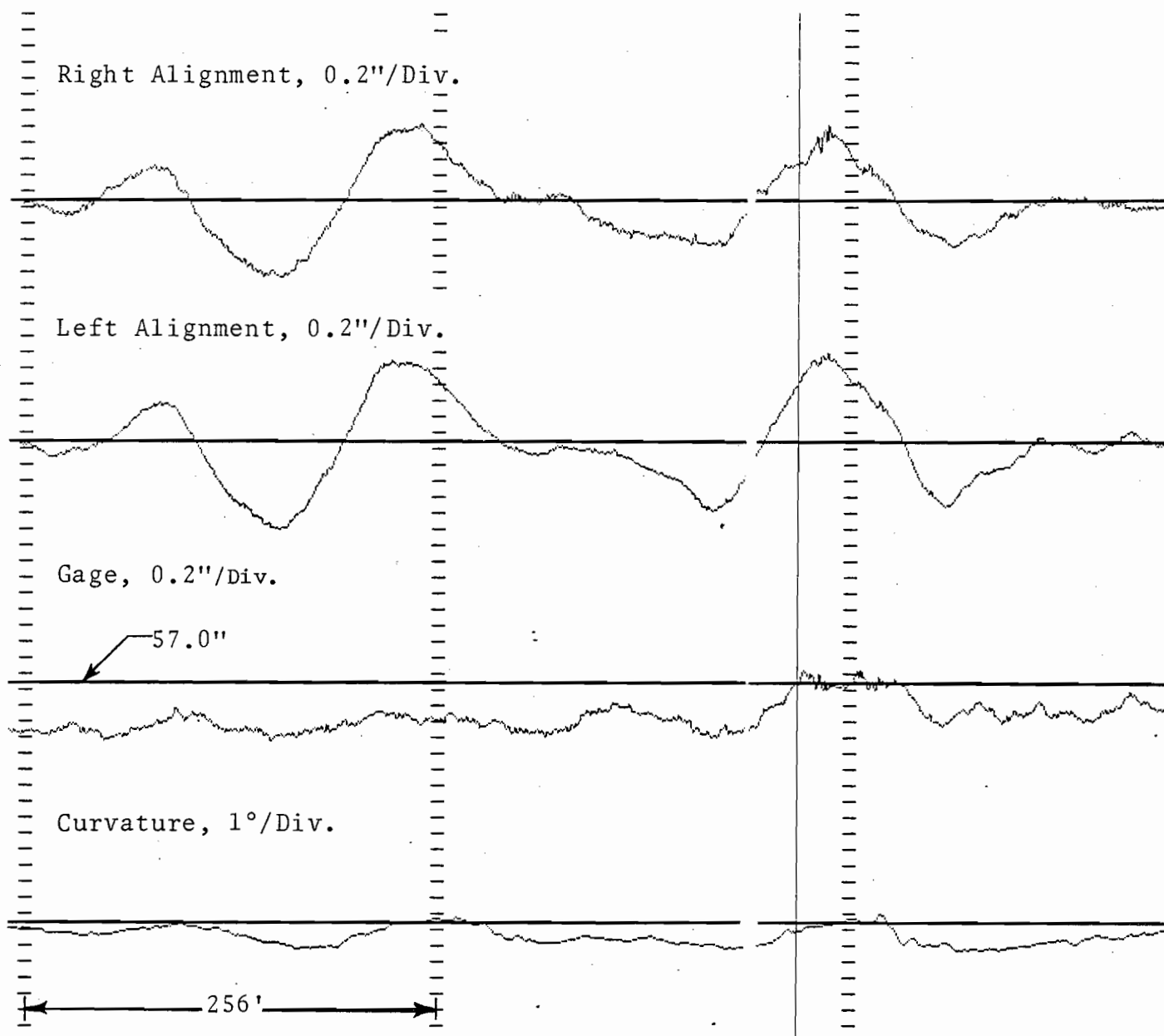


Figure C.2.b.1. Series of Jogs in Mean Alignment (Class 6).

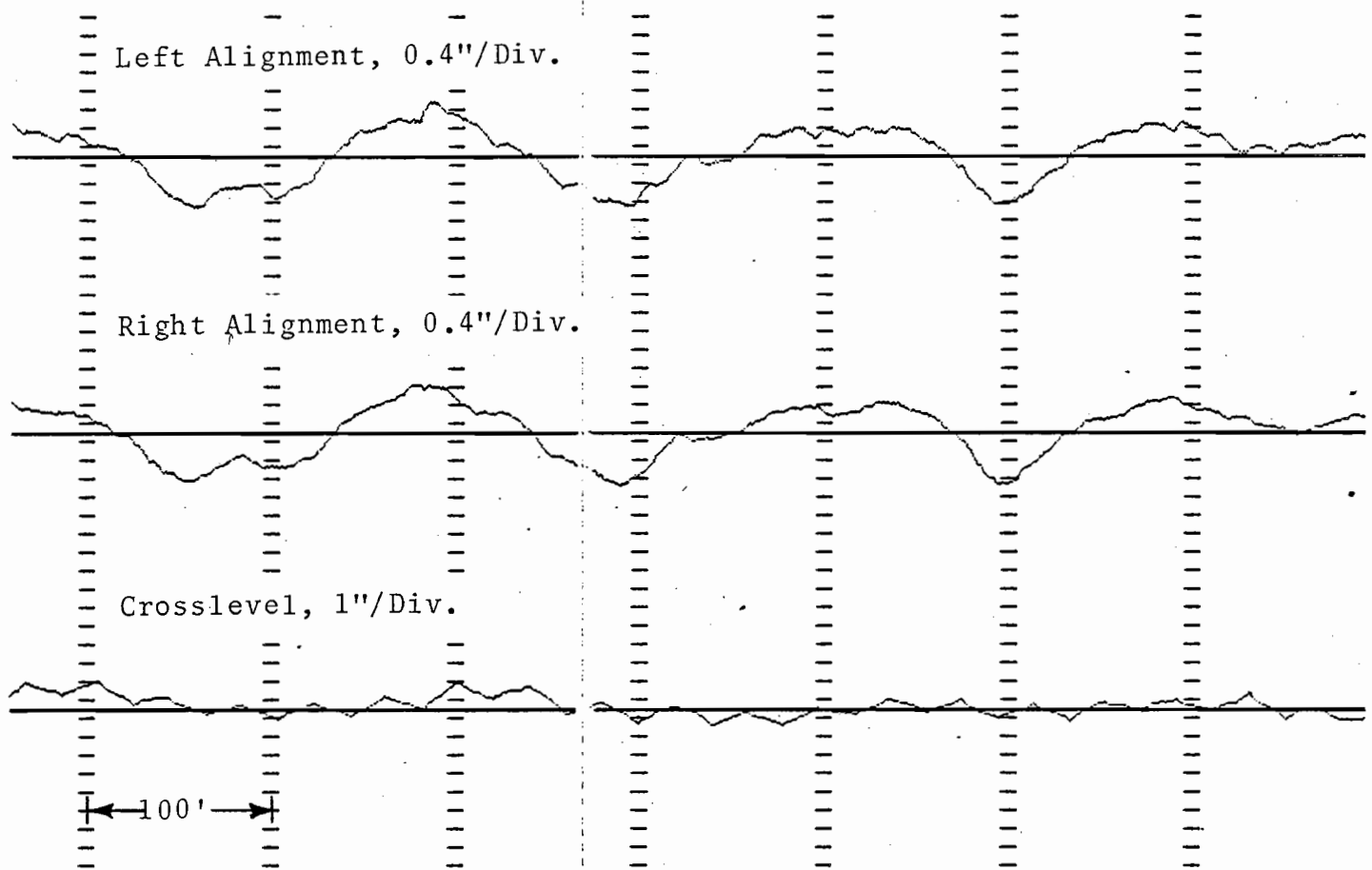


Figure C.2.b.2. Long Wavelength (200') Periodic Alignment
(Class 2, Tangent).

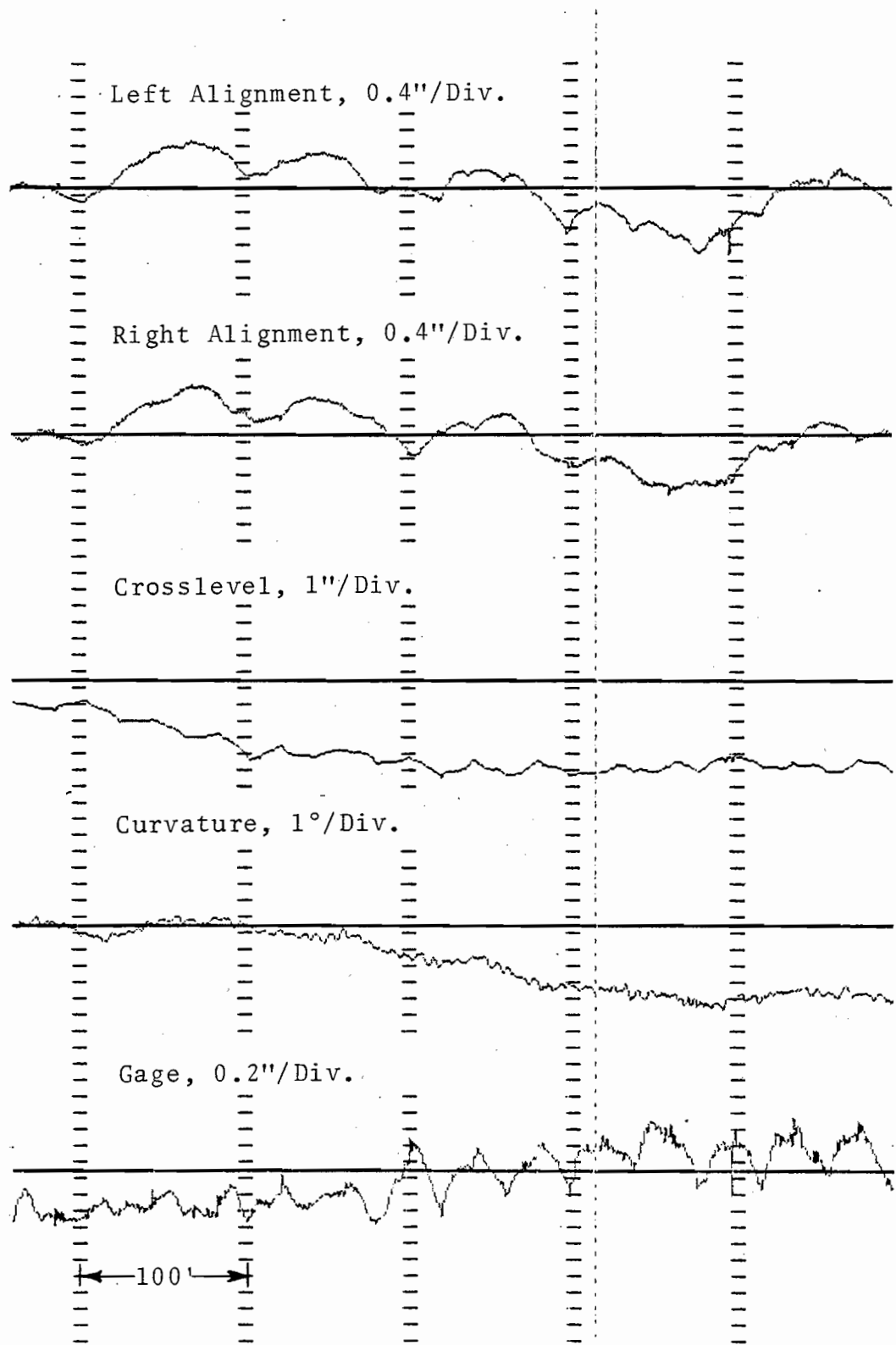


Figure C.2.b.3. Medium Wavelength (80') Periodic Alignment in a Spiral (Class 3, Spiral).

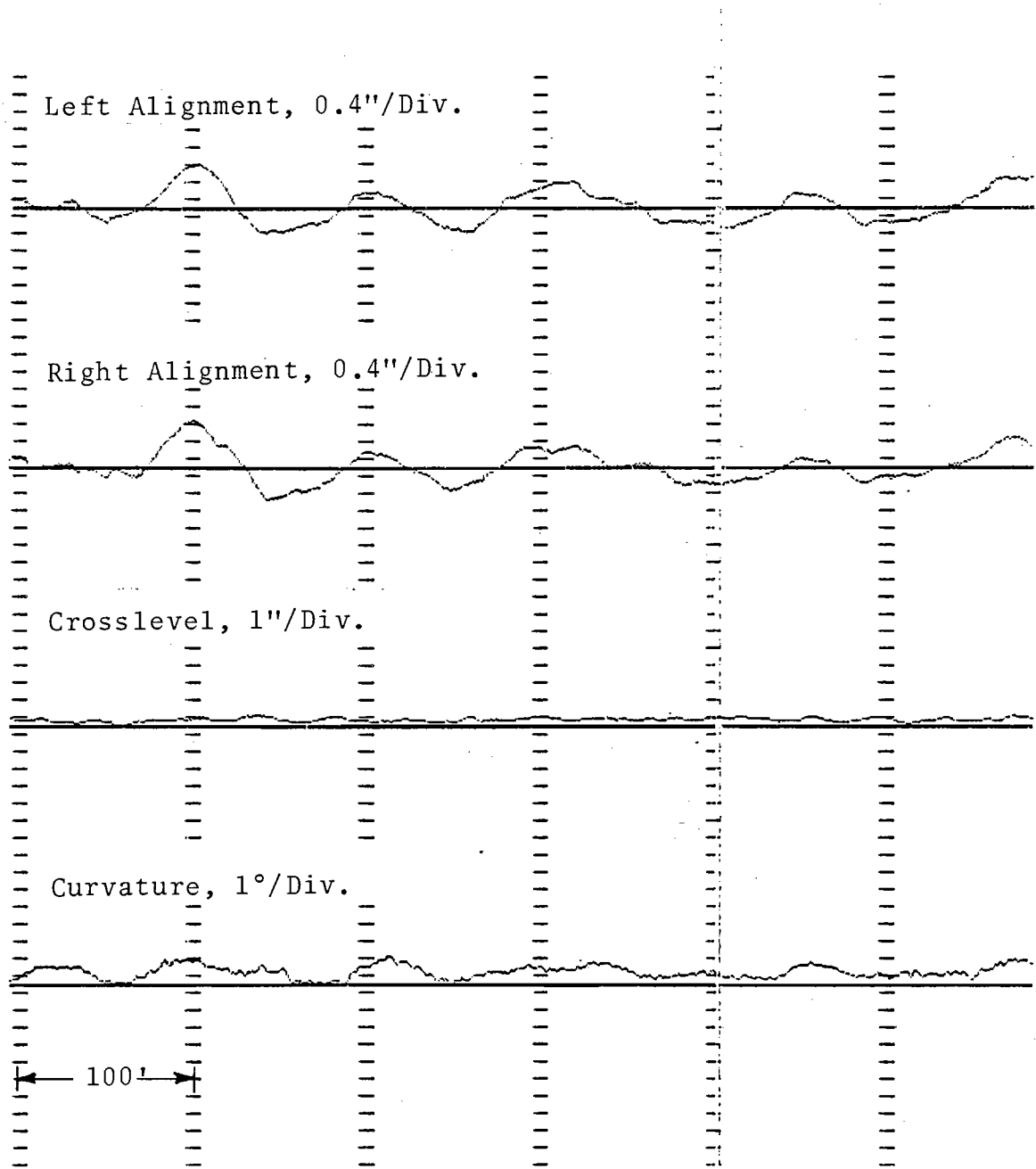


Figure C.2.b.4. Medium Wavelength (100') Alignment Sinusoids in a Shallow Curve (Class 3, Curve).

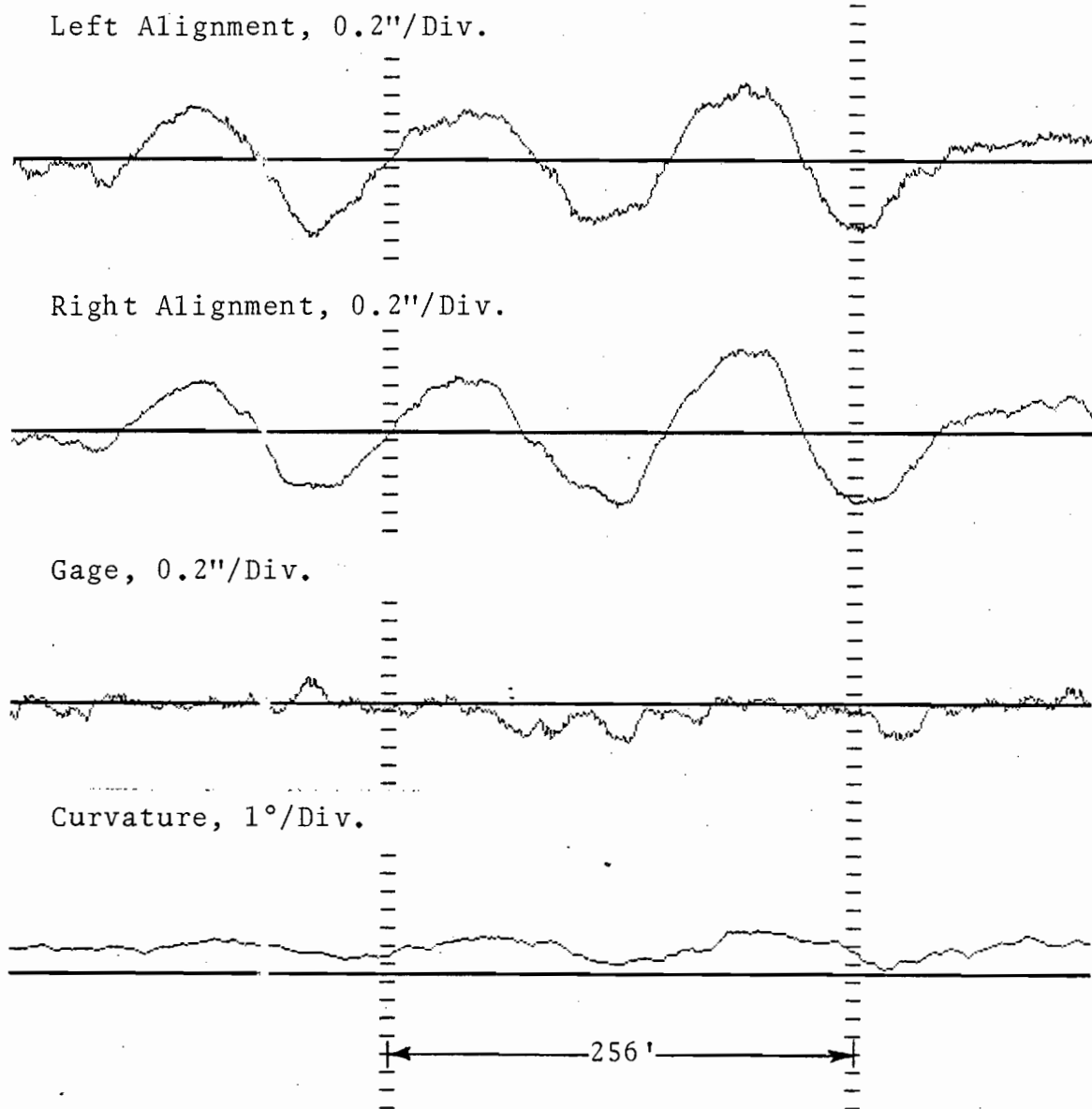


Figure C.2.b.5. Periodic Sinusoidal Variations in Mean Alignment Near a Creek Bridge (Class 6).

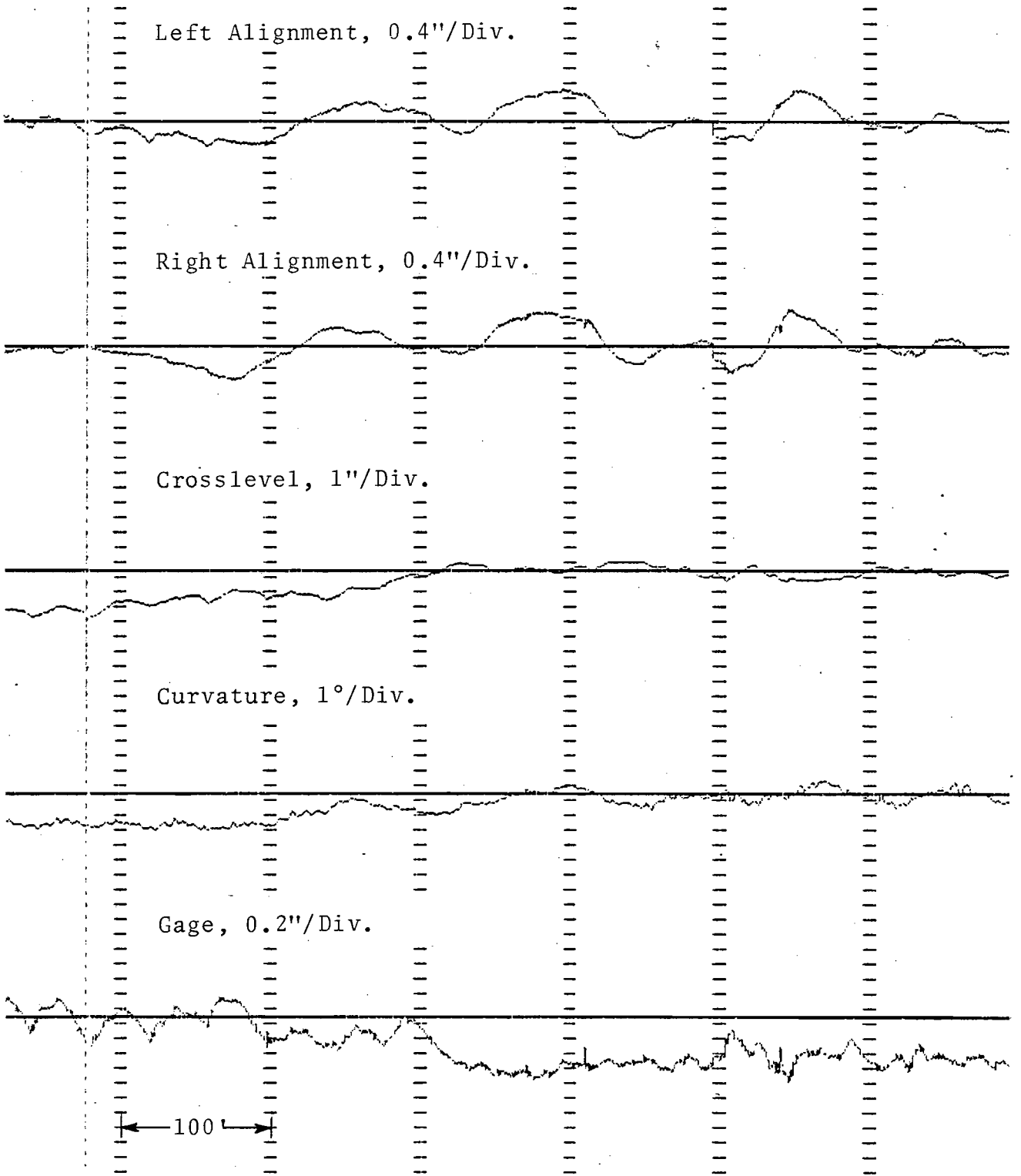


Figure C.2.b.6. Medium Wavelength (120') Sinusoidal Alignment in a Spiral (Class 3, Spiral).

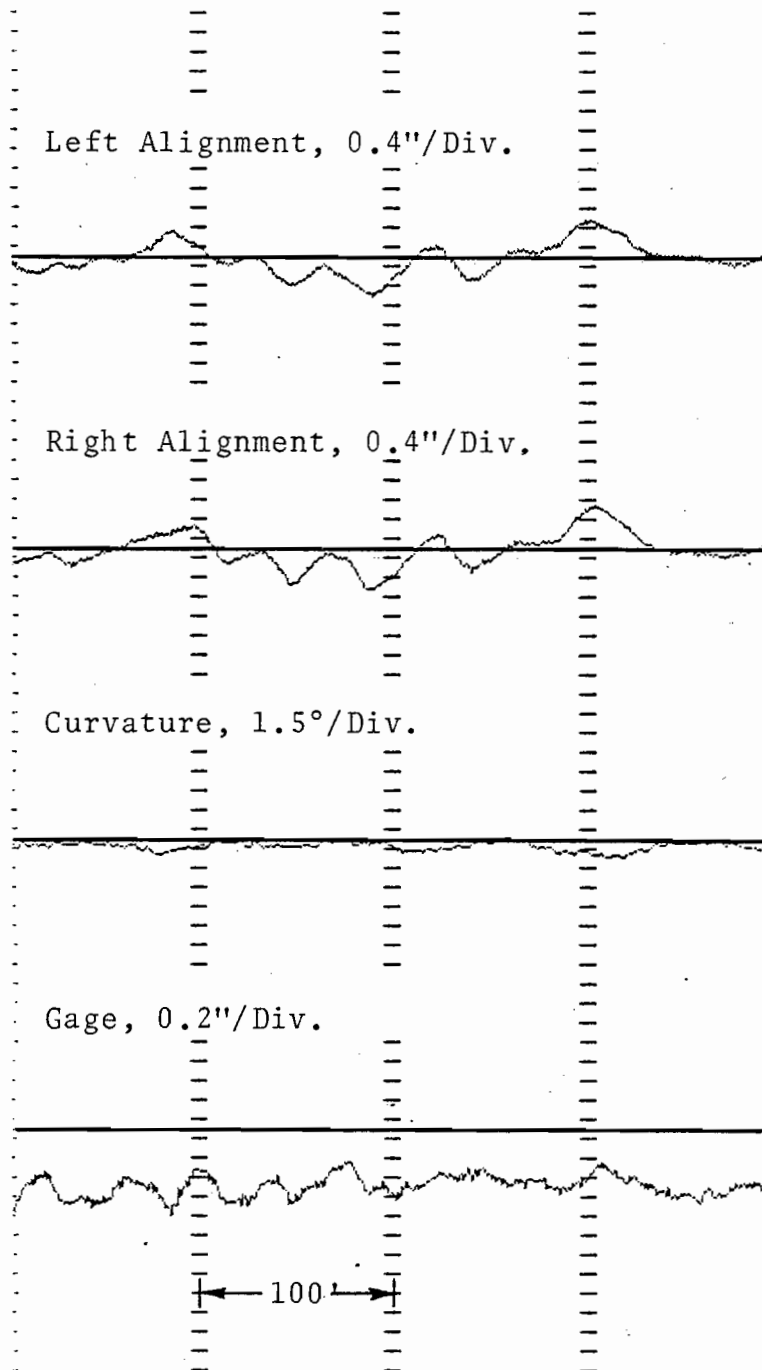


Figure C.2.b.7. Rail Length Sinusoidal Alignment (Class 4, Curve).

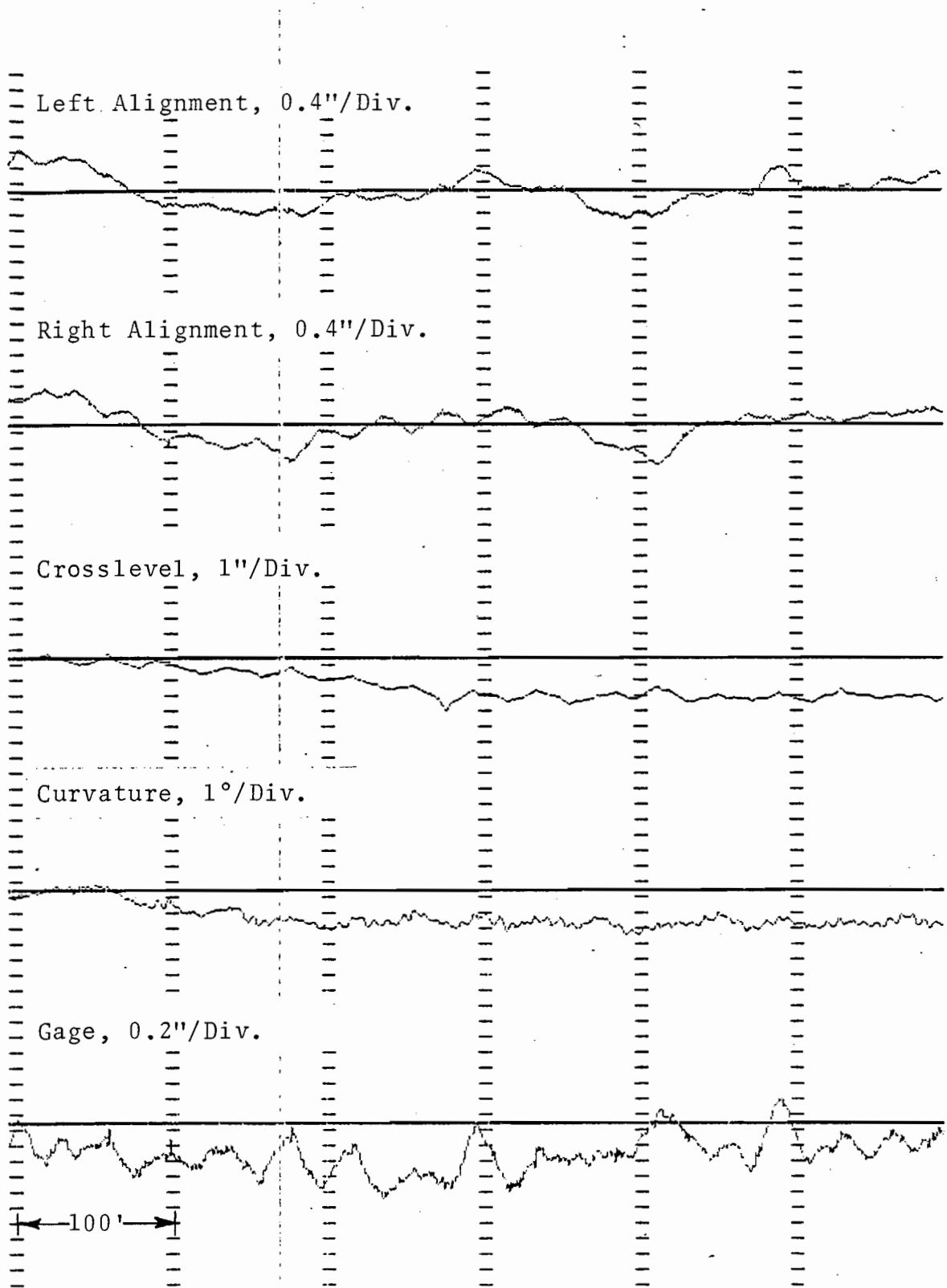


Figure C.2.b.8. Combined Short (39') and Long (250') Wavelength Alignment Sinusoids and Gage Cusps (Class 3, Spiral).

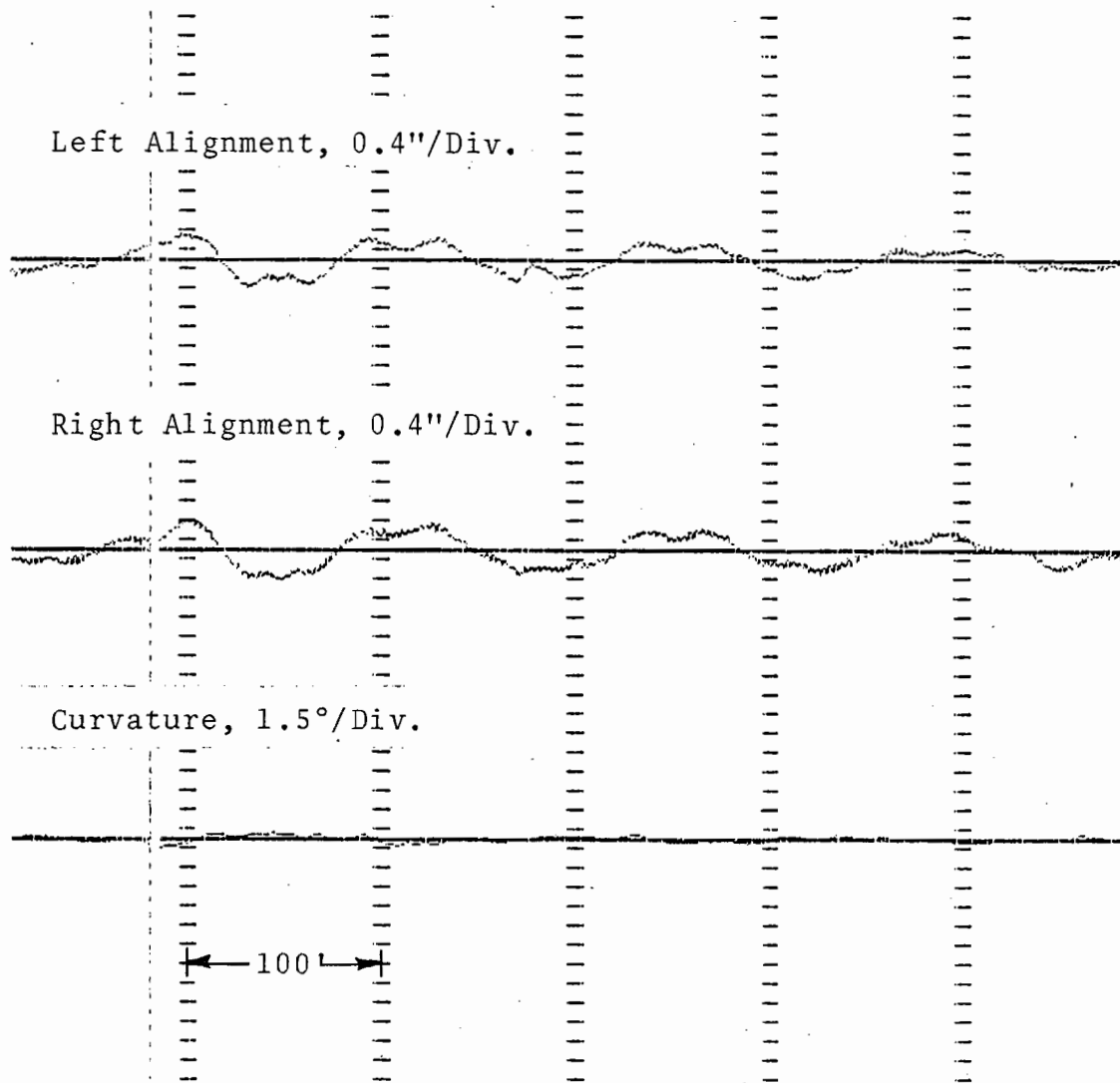
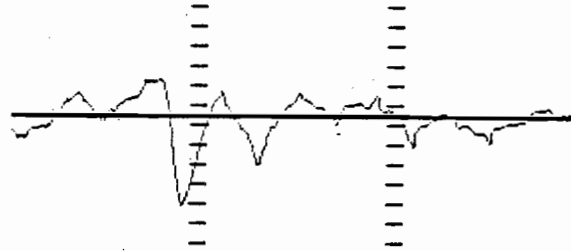


Figure C.2.b.9. Long Wavelength (150') Periodic Alignment (Class 6, Tangent).

Crosslevel Deviation, 0.2"/Div.



Crosslevel, 1"/Div.

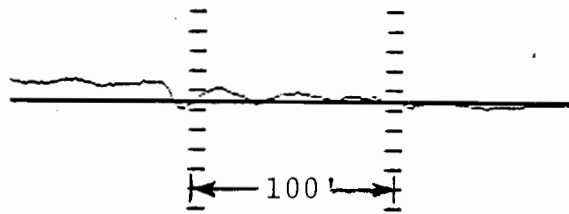
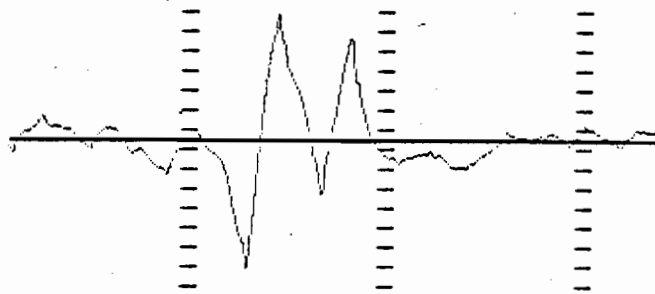


Figure C.2.c.1. Decaying Periodic Crosslevel
(Class 3, Bolted, Spiral).

Crosslevel Deviations, 0.2"/Div.



Crosslevel, 1"/Div.

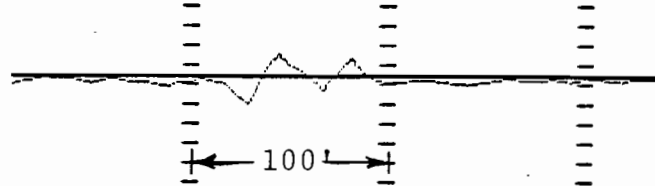


Figure C.2.c.2. Decaying Periodic Crosslevel
(Class 3, Bolted, Tangent).

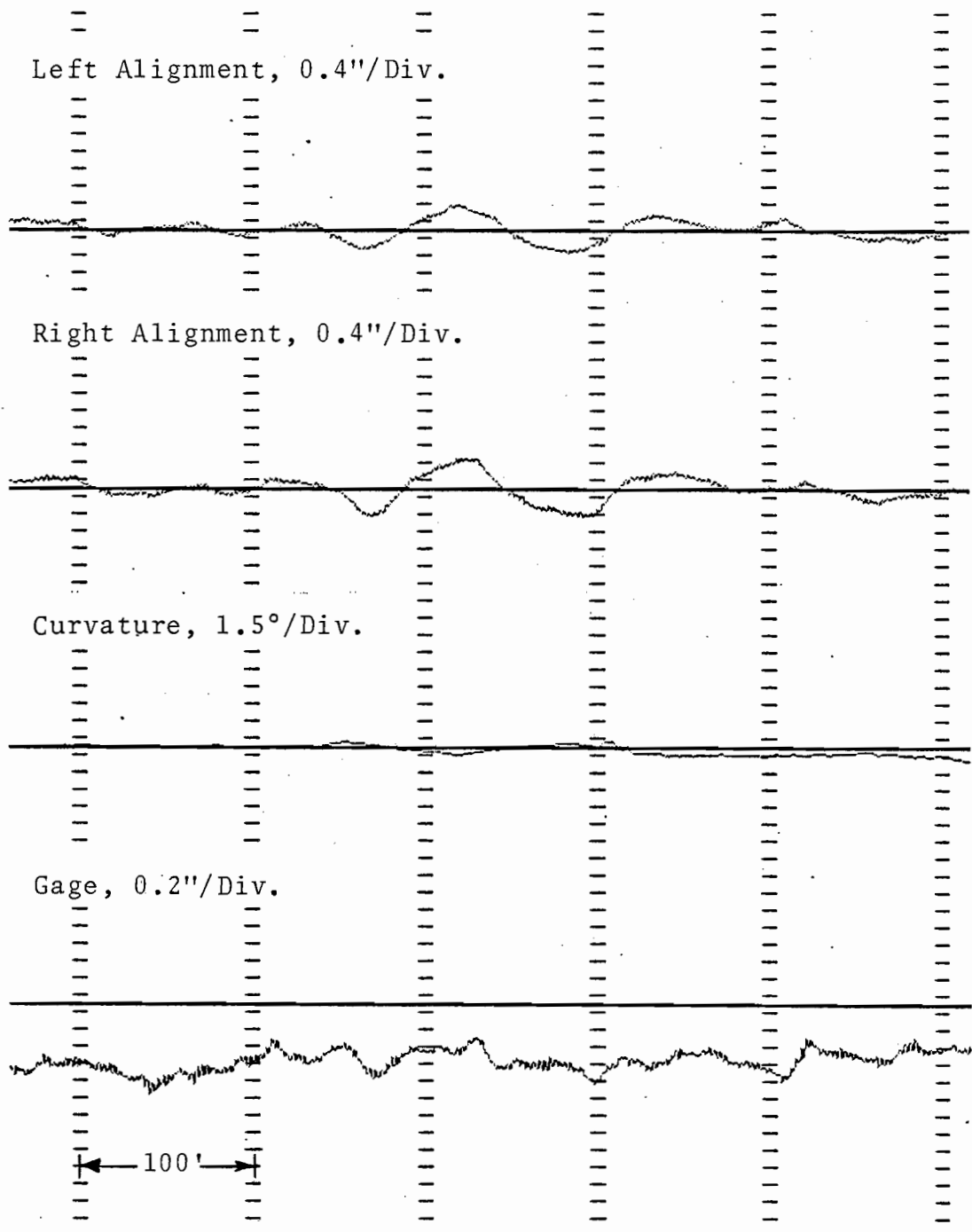


Figure C.2.c.3. Sinusoidal Alignment With Decay (Class 5, Spiral).

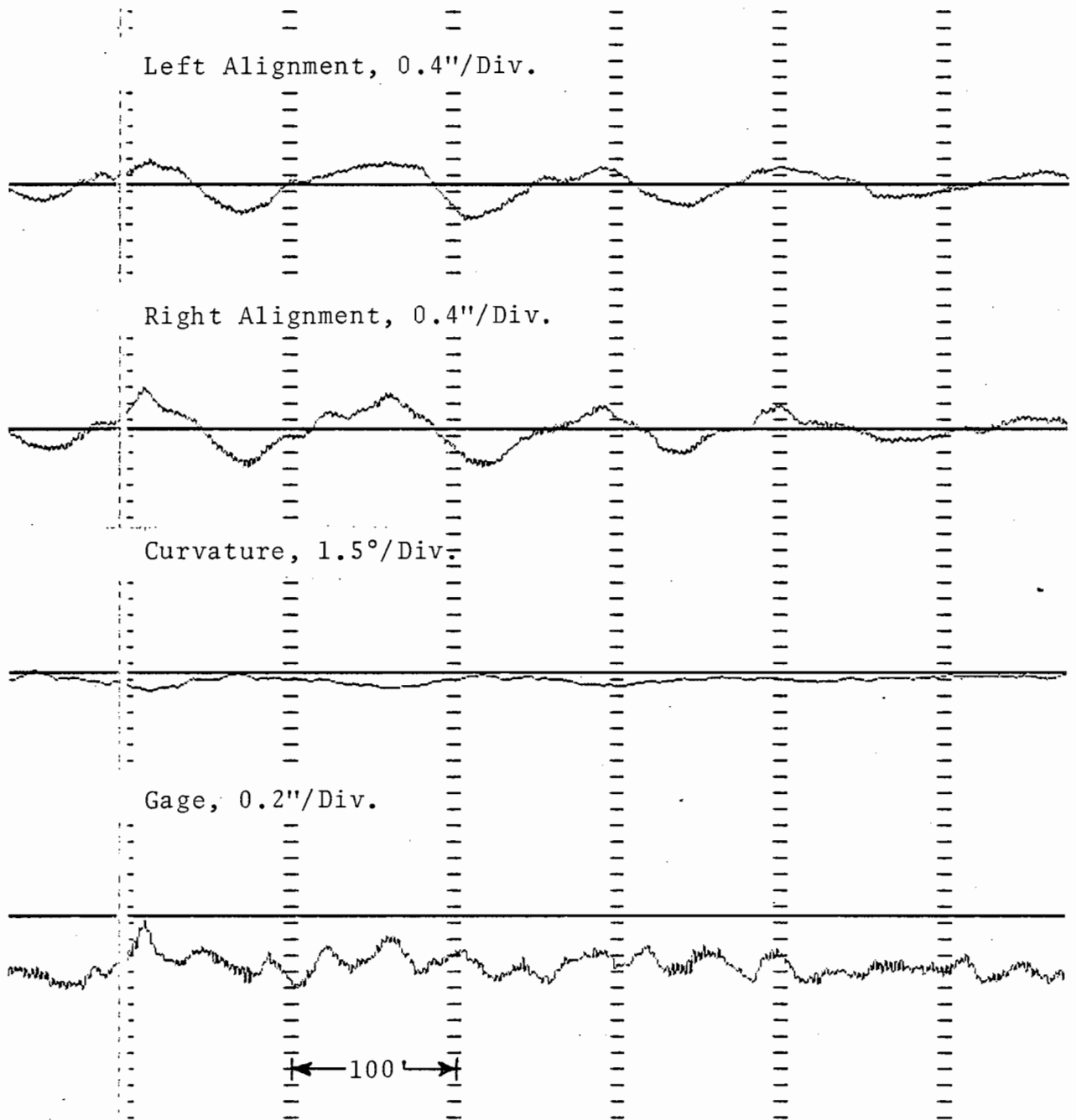


Figure C.2.c.4. Sinusoidal Alignment (150') With Decay and Sinusoidal Gage (39') (Class 5, Curve).

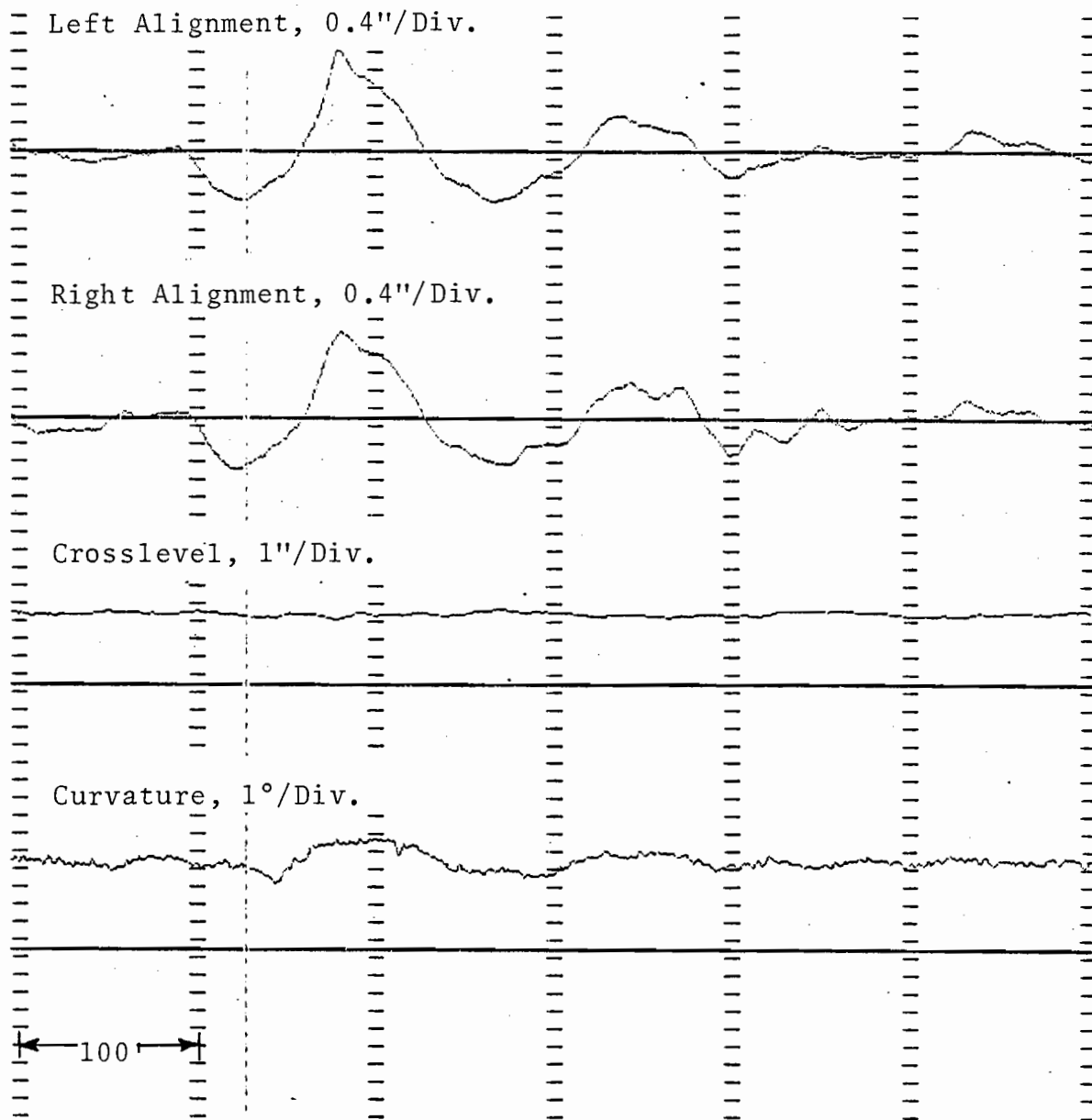


Figure C.2.c.5. Decaying Periodic Sinusoid in Alignment (Class 3, Curve).

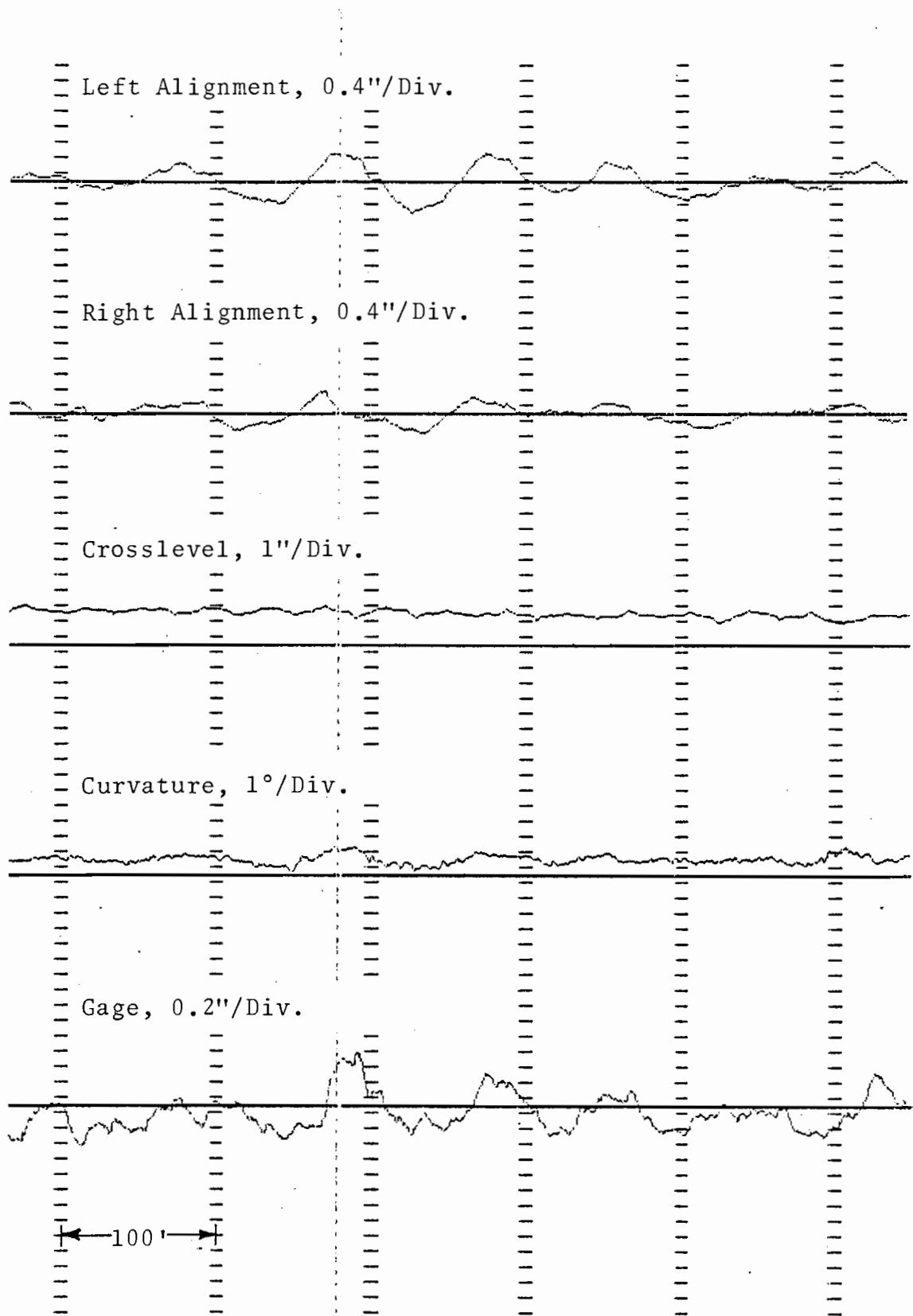


Figure C.2.c.6 Combined Medium Wavelength (90') Gage and Alignment Decaying Sinusoids (Class 3, Curve).

C.3 COMBINED VARIATIONS

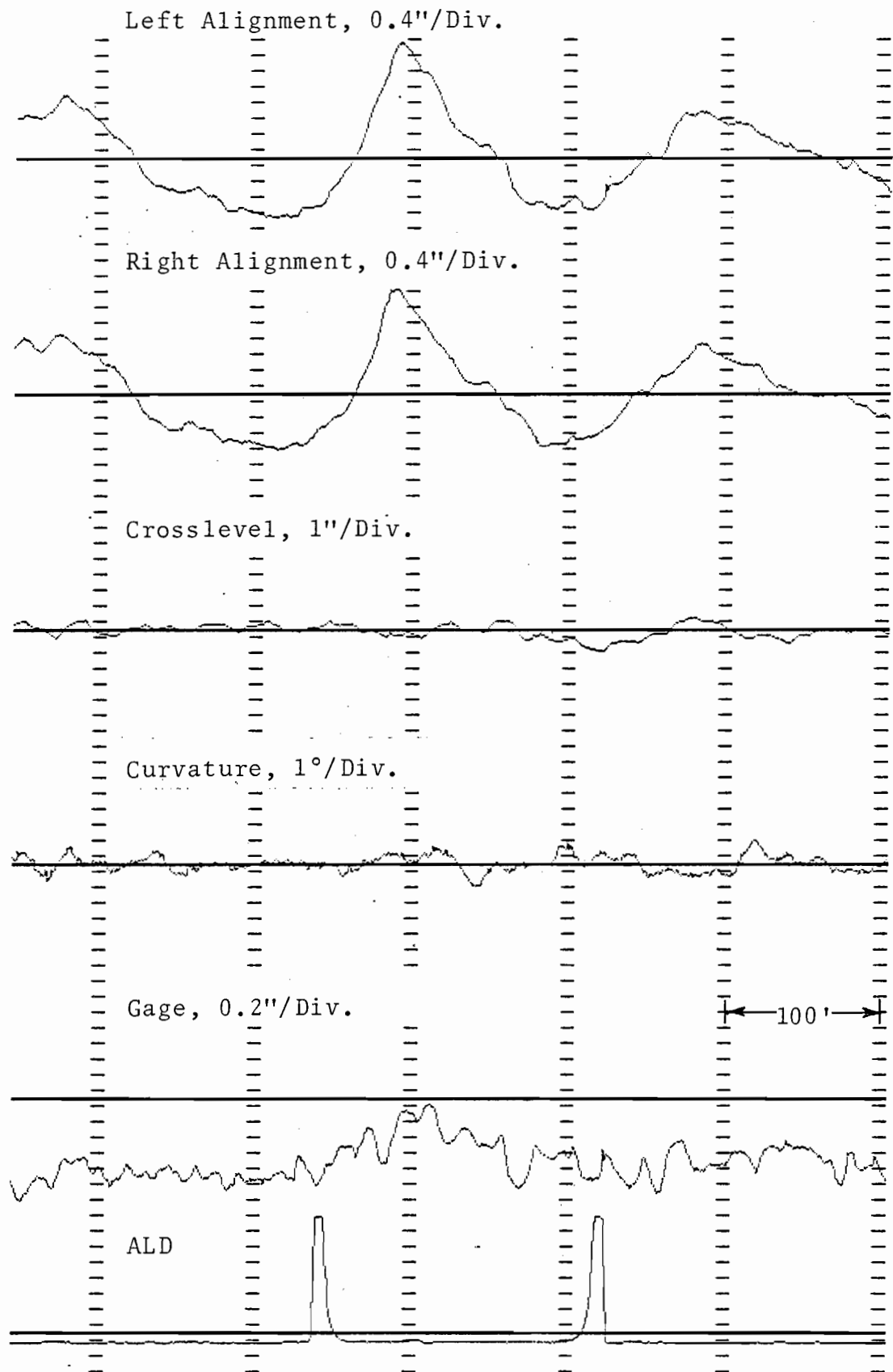


Figure C.3.a.1. Alignment Cusp and Significant Change in Gage Through a Track Structure (Class 2, Tangent).

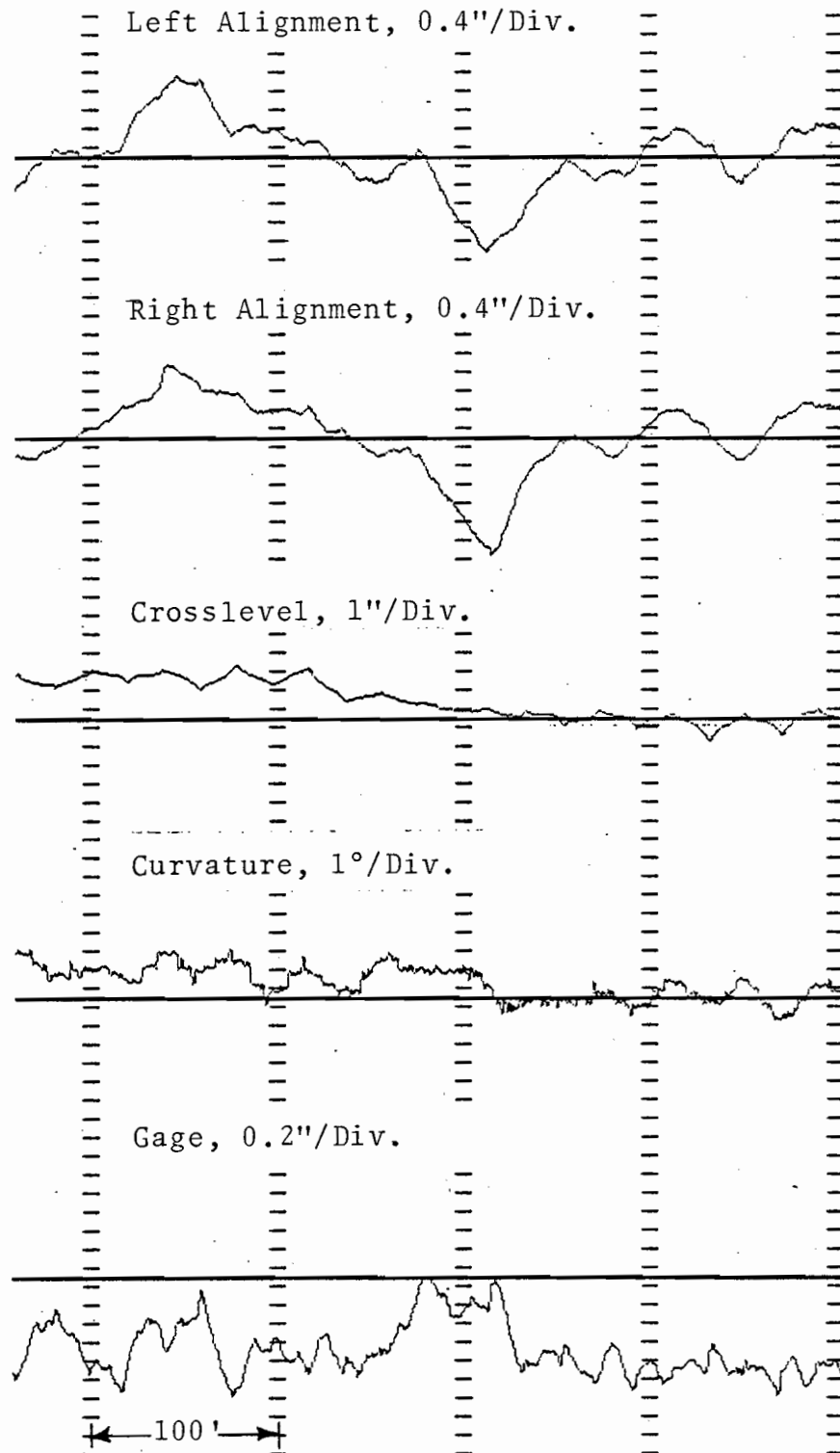


Figure C.3.a.2. Alignment Cusp and Gage Plateau
(Class 2, Spiral).

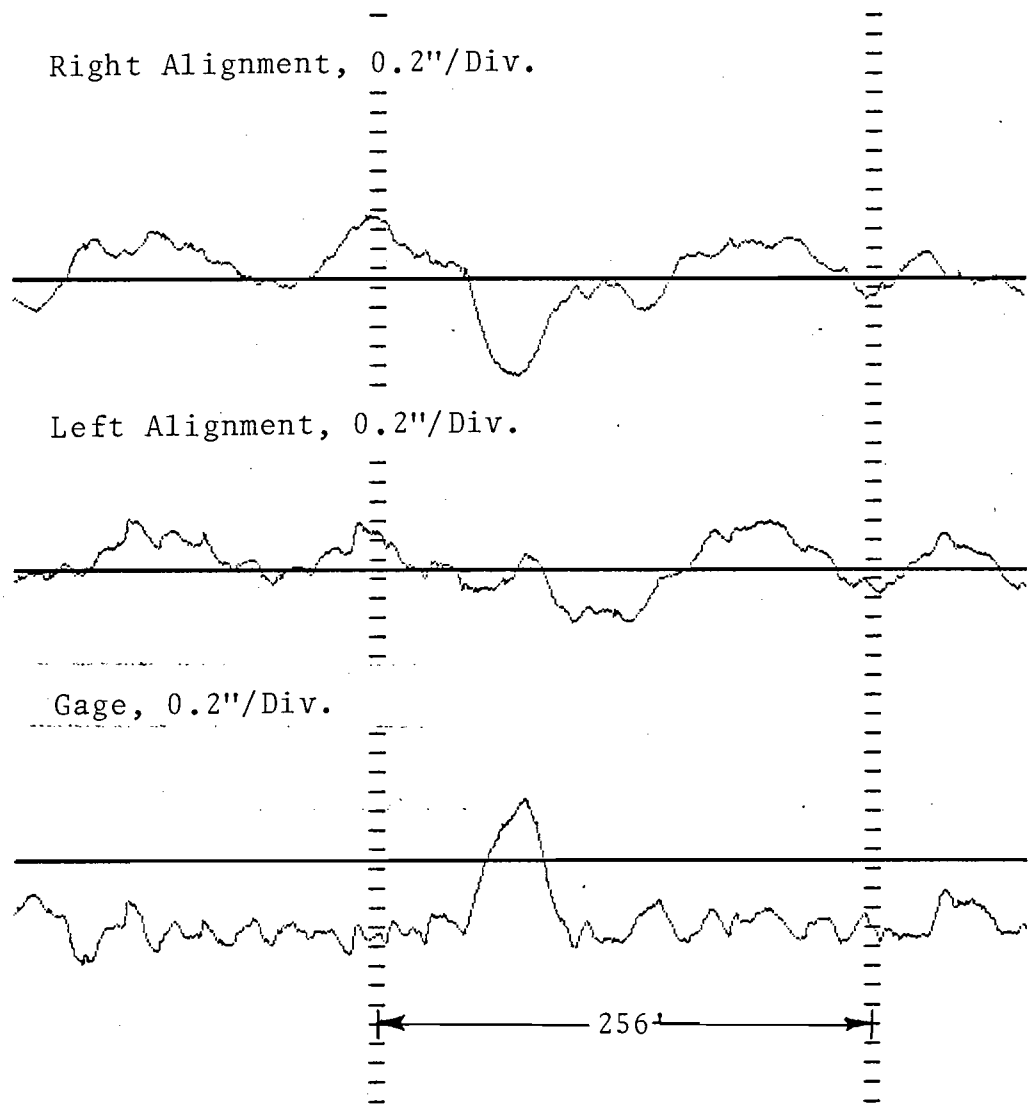


Figure C.3.a.3. Combined Gage and Right-Rail Alignment Bump (Class 2, Tangent).

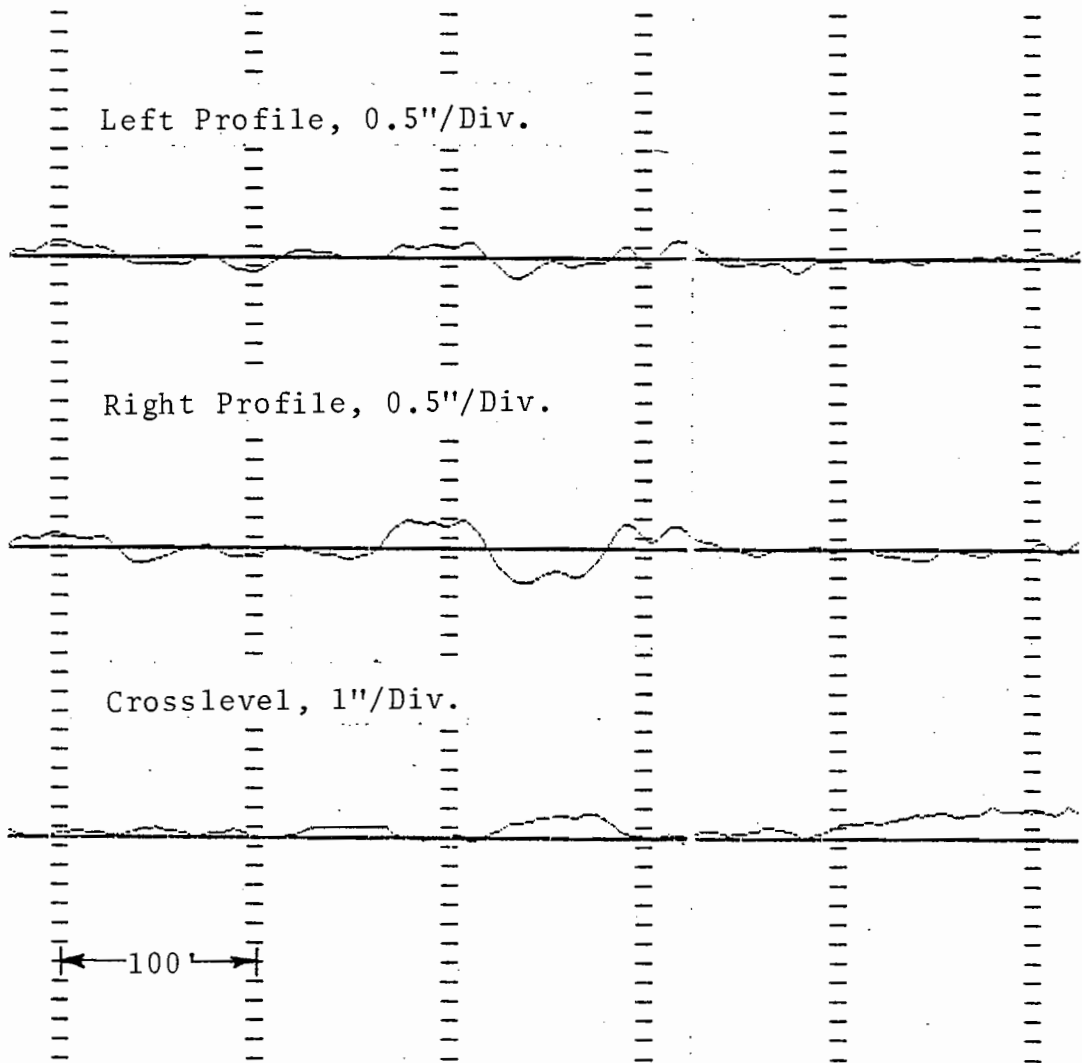


Figure C.3.a.4. Combined Profile and Crosslevel Plateau at Spiral Entry (Class 2).

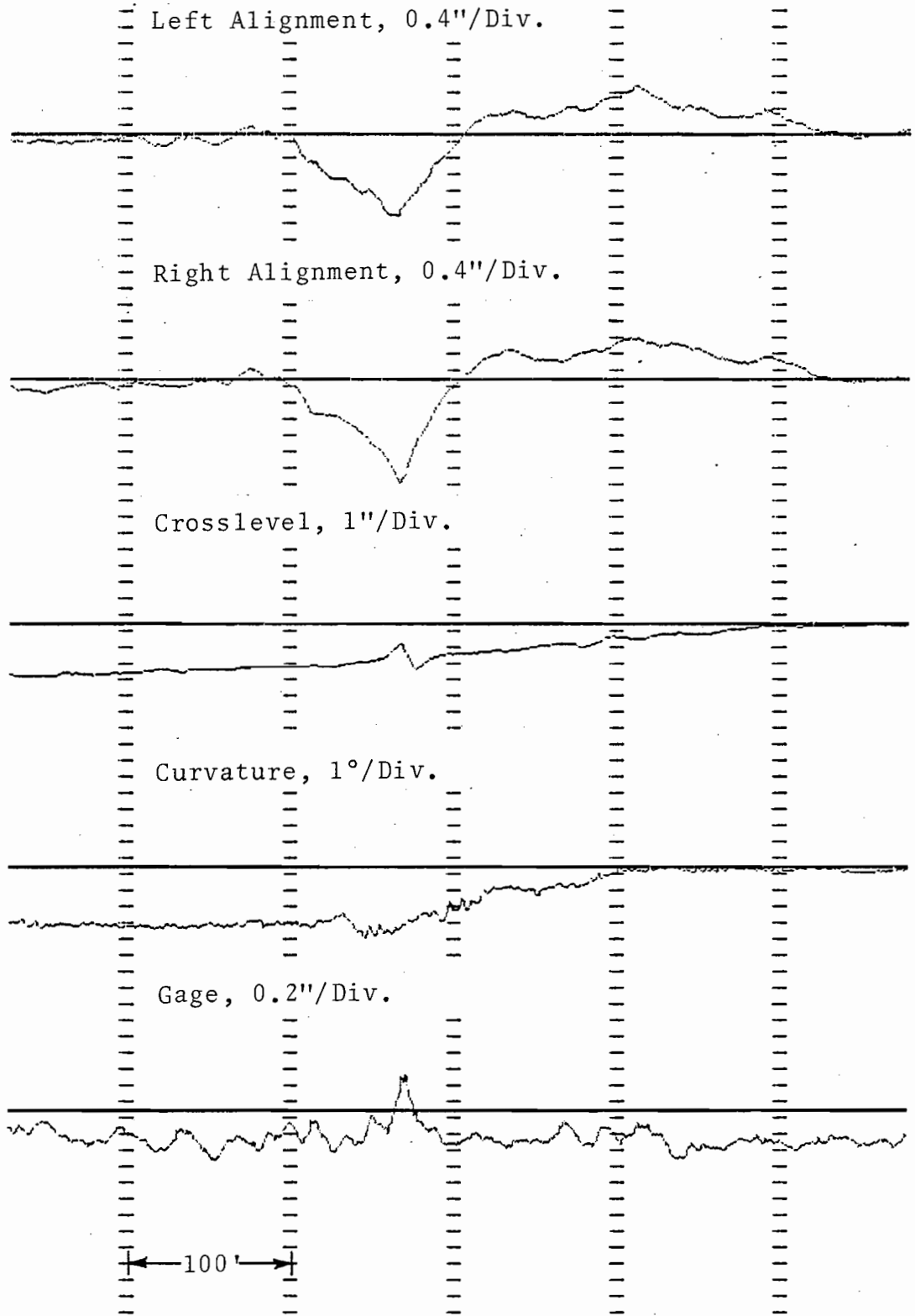


Figure C.3.a.5. Combined Gage, Crosslevel and Alignment Cusp (Class 3, Spiral).

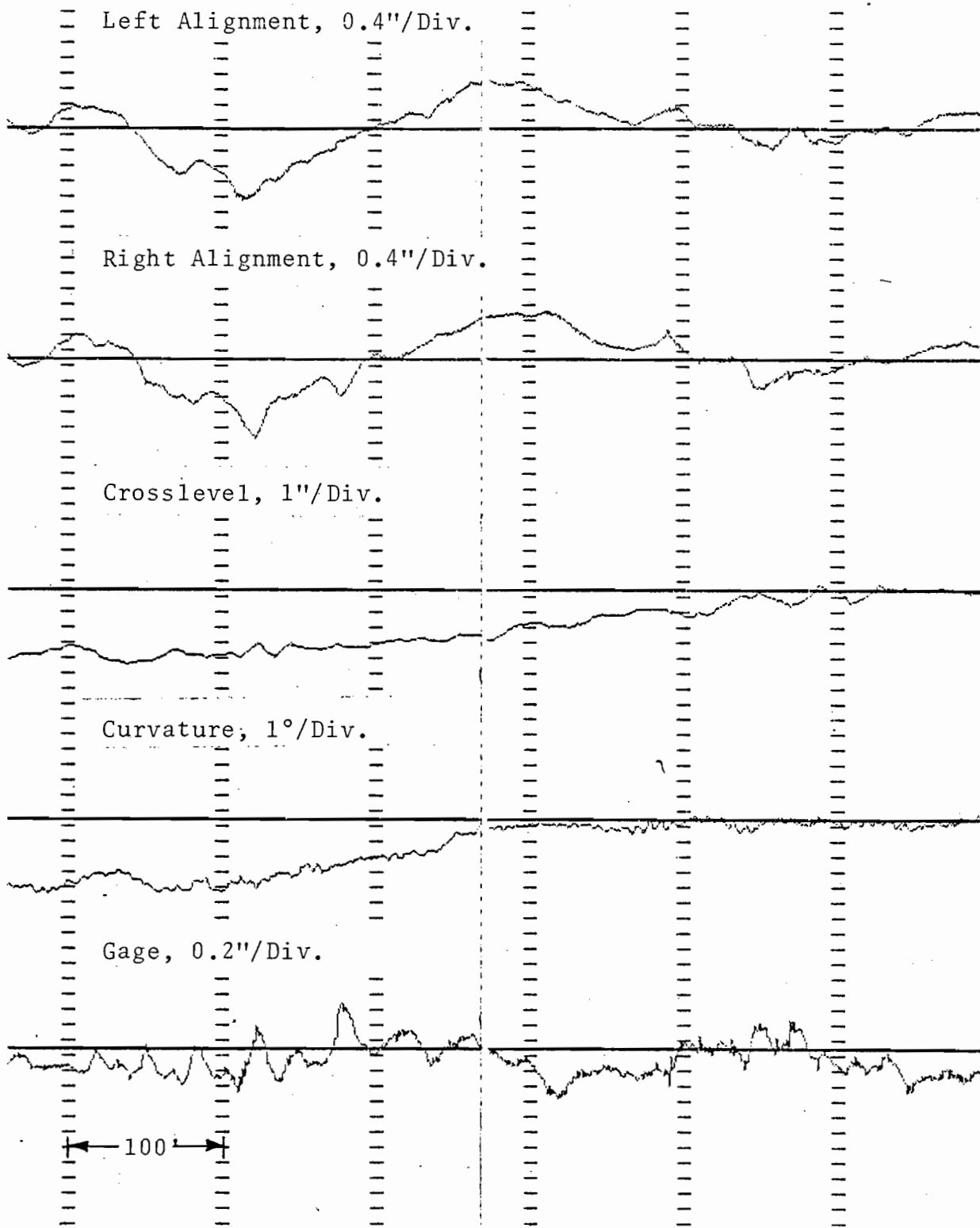


Figure C.3.a.6. Long Wavelength (300') Alignment Jog in a Spiral and Combined Short Wavelength (25') and Alignment Cusps (Class 3, Spiral).

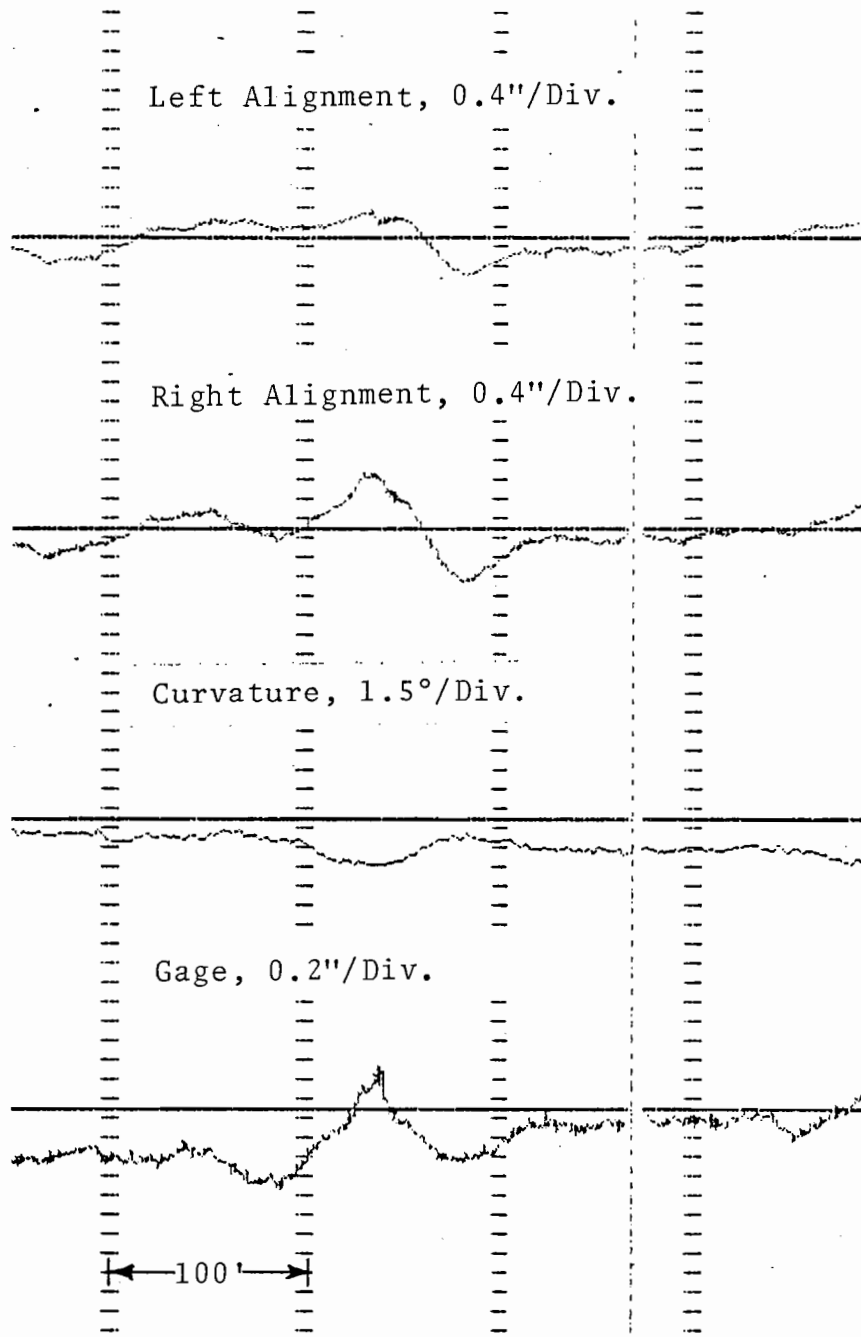


Figure C.3.a.7. Combined Gage Cusp and Alignment Jog
(Class 6, Curve).

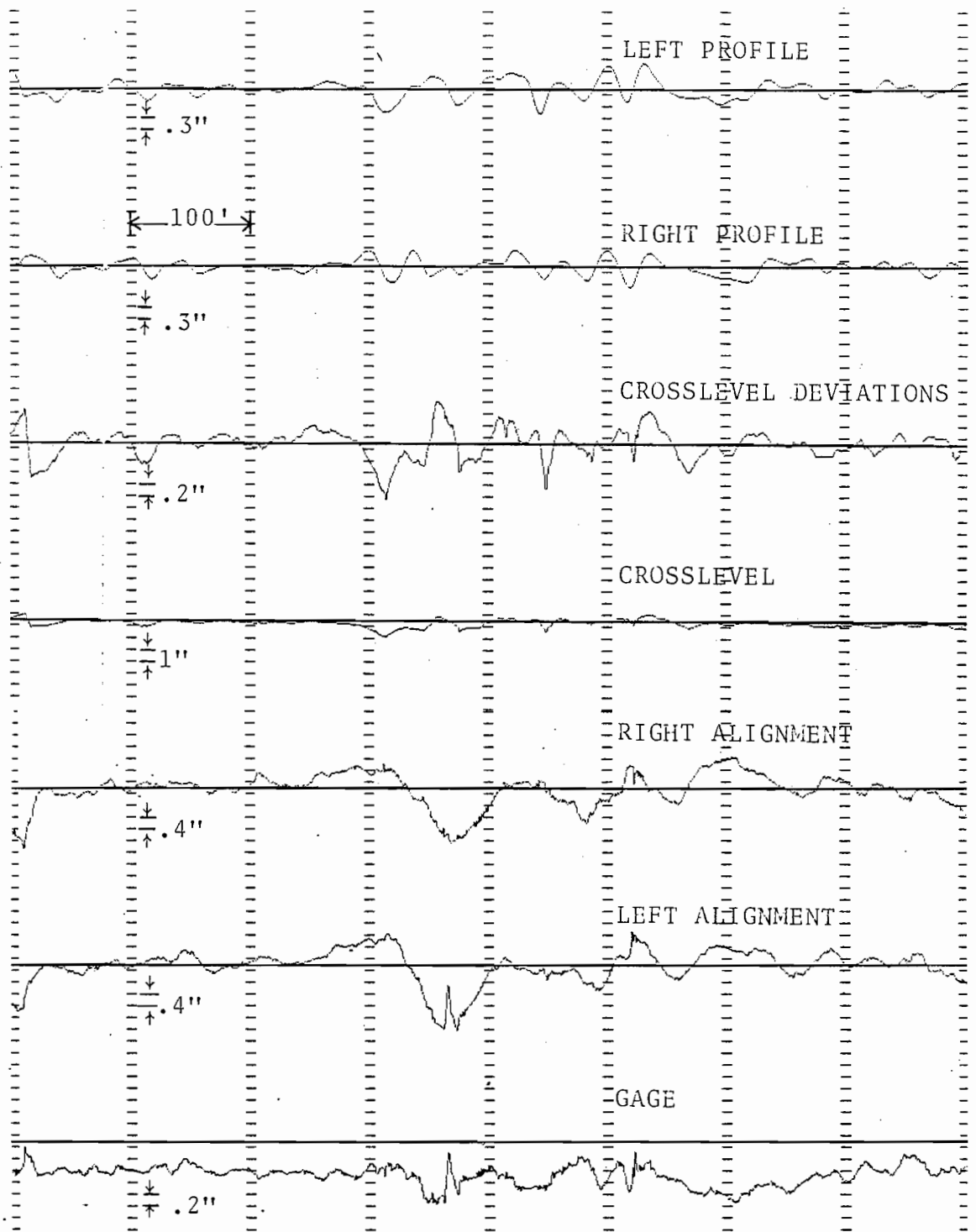


Figure C.3.b.1. Combined Track Geometry Variation in All Parameters at an Interlocking (Class 3, Welded, Tangent).

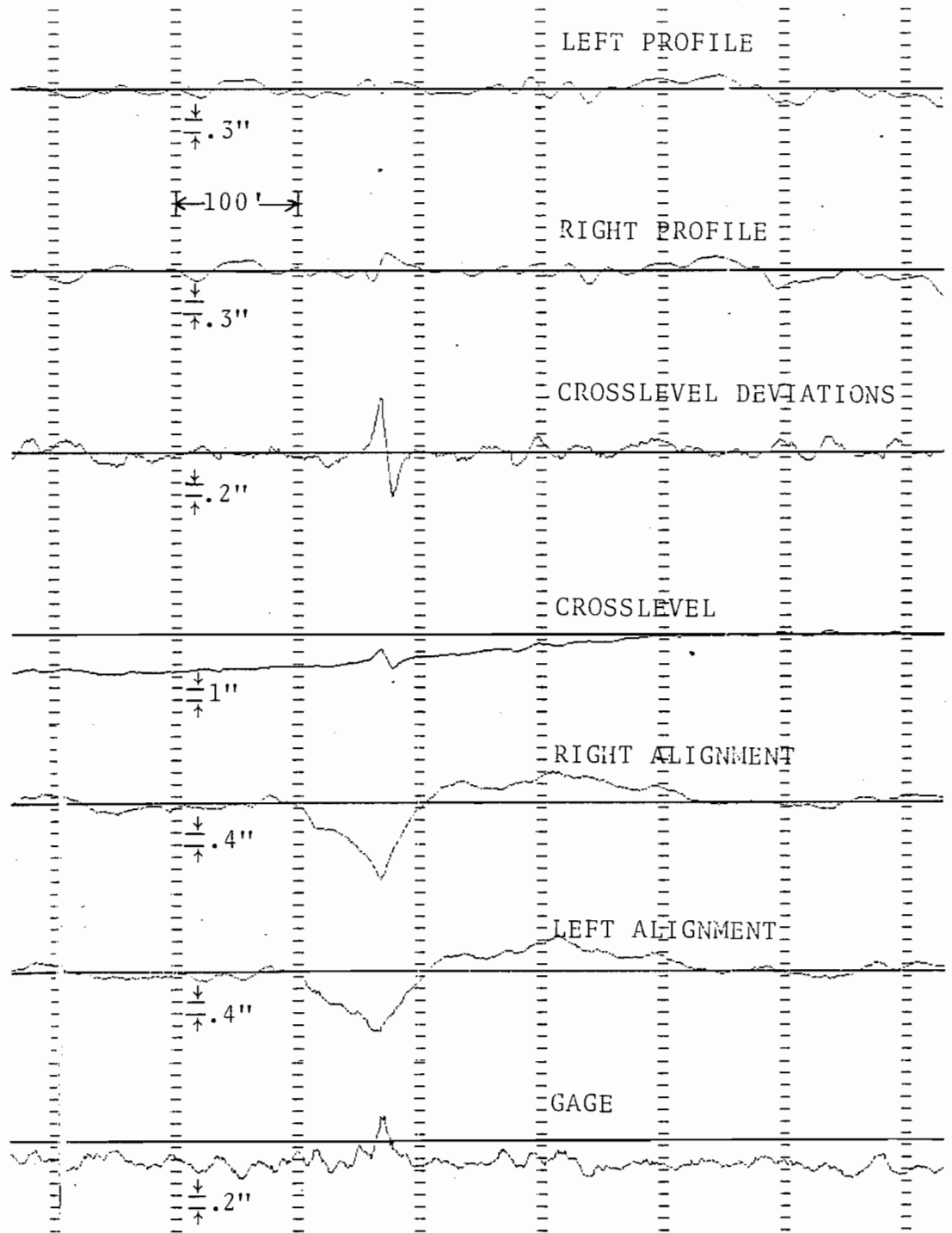


Figure C.3.b.2. Combined track Geometry Variations in All Parameters (Class 3, Welded, Spiral).

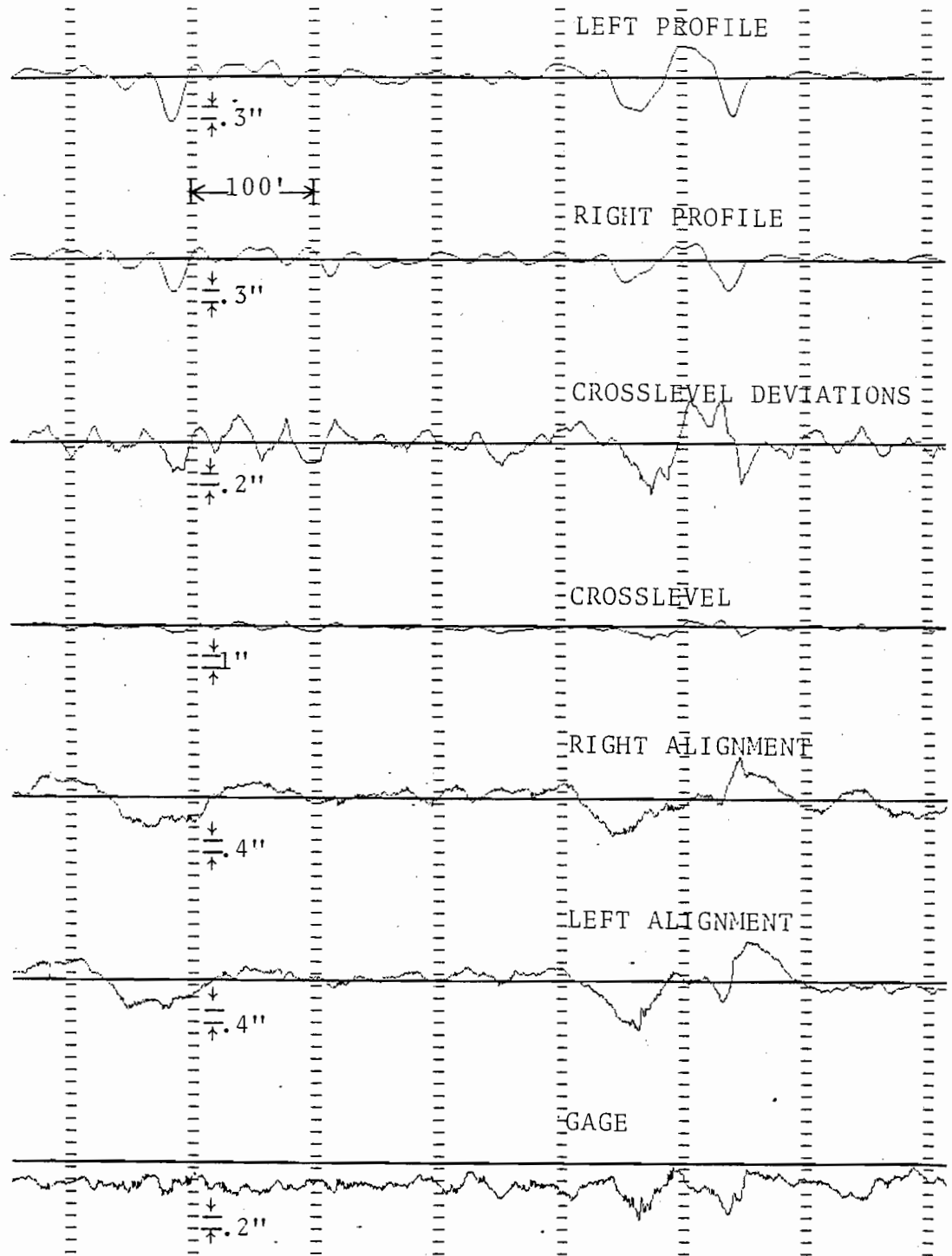


Figure C.3.b.3. Combined Track Geometry Variations in All Parameters at a Switch (Class 3, Bolted, Tangent).

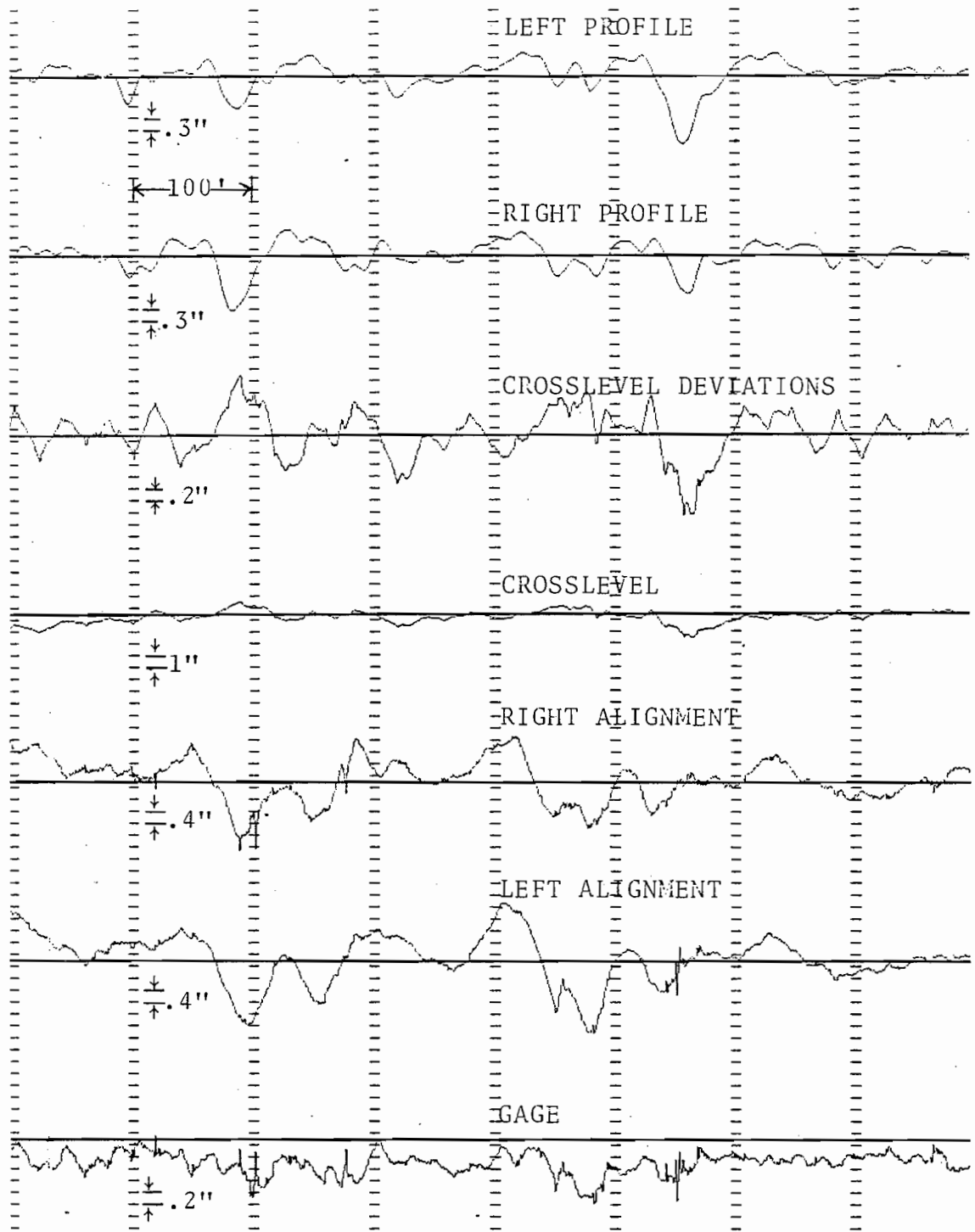


Figure C.3.b.4. Combined Track Geometry Variations in all Parameters at a Switch (Class 3, Bolted, Tangent).

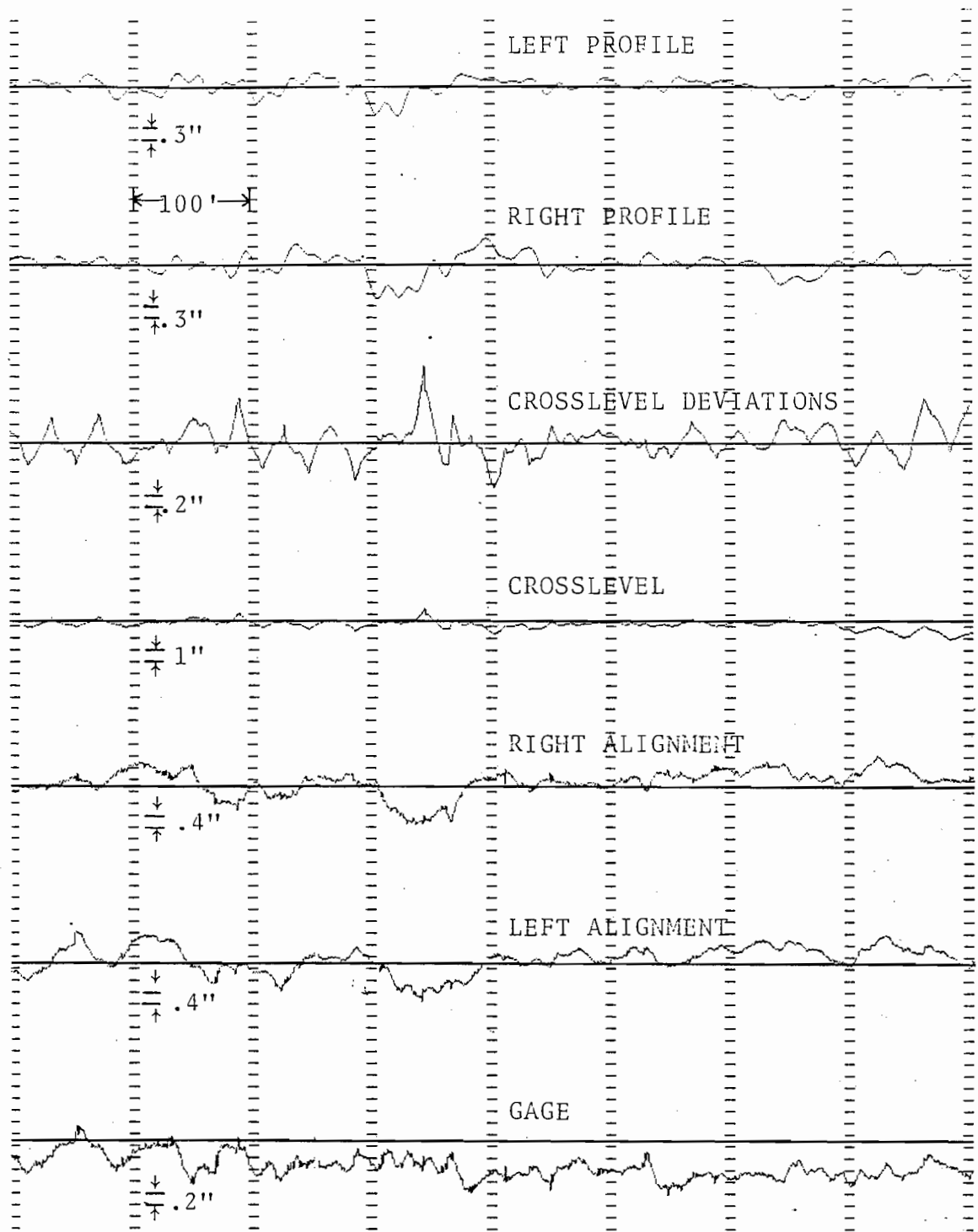


Figure C.3.b.5. Combined Profile Plateau, Crosslevel Cusp and Alignment Trough (Class 3, Tangent).

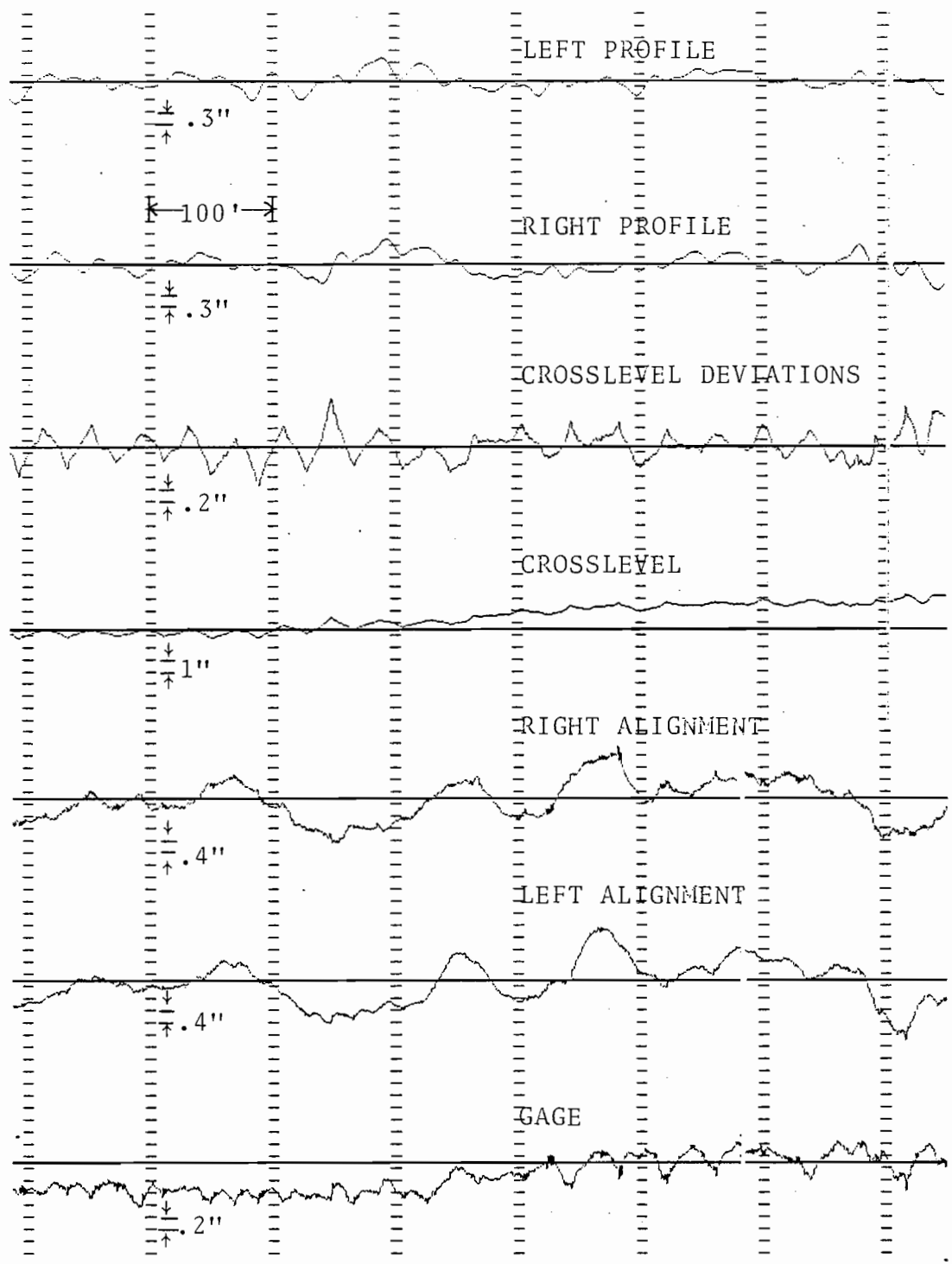


Figure C.3.b.6. Combined Periodic and Isolated Track Geometry Variations in all Parameters (Class 3, Bolted, Spiral).

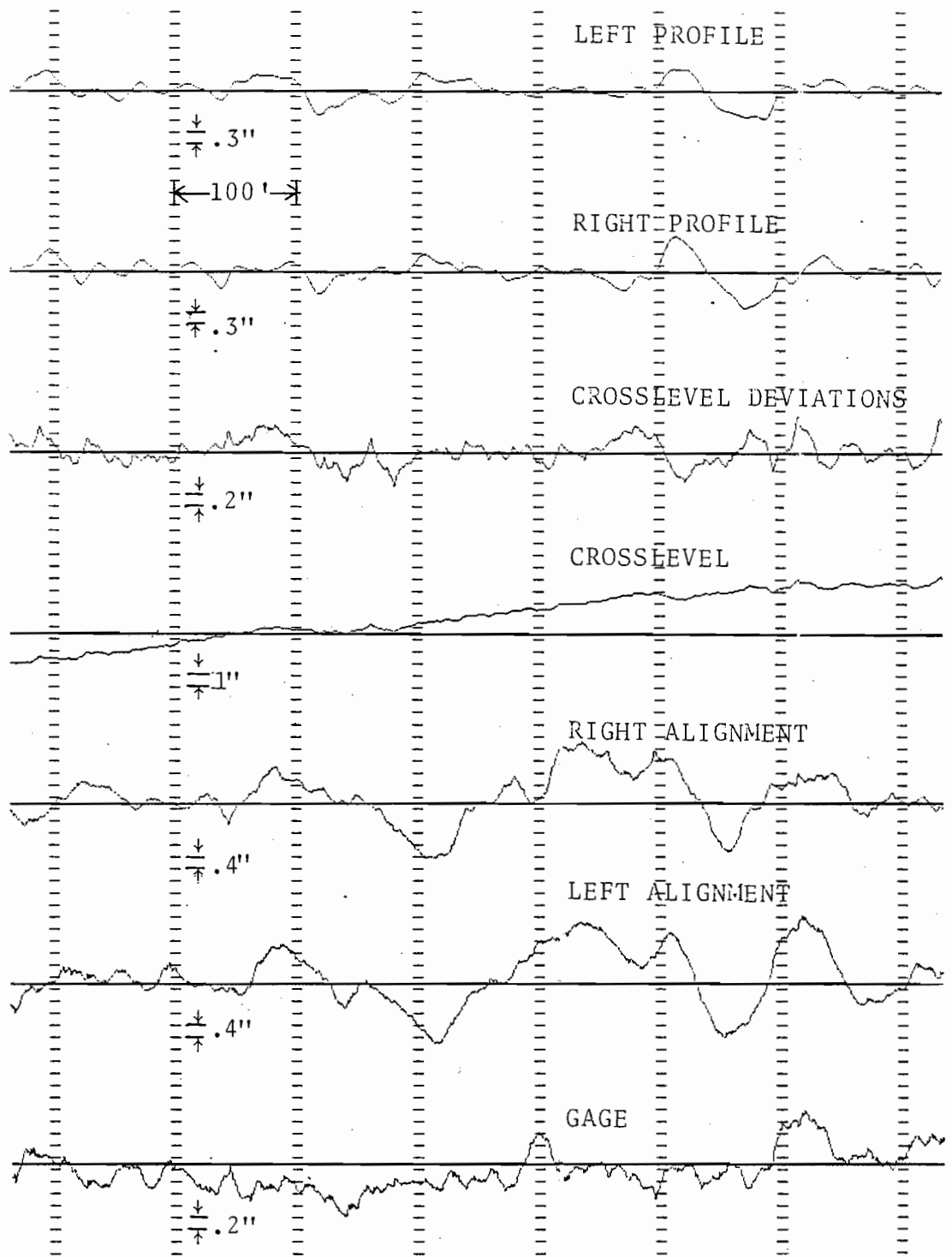


Figure C.3.b.7. Combined Short Wavelength (40') Bumps in Gage, Alignment and Profile and a 100' Jog in Alignment (Class 3, Bolted, Spiral).

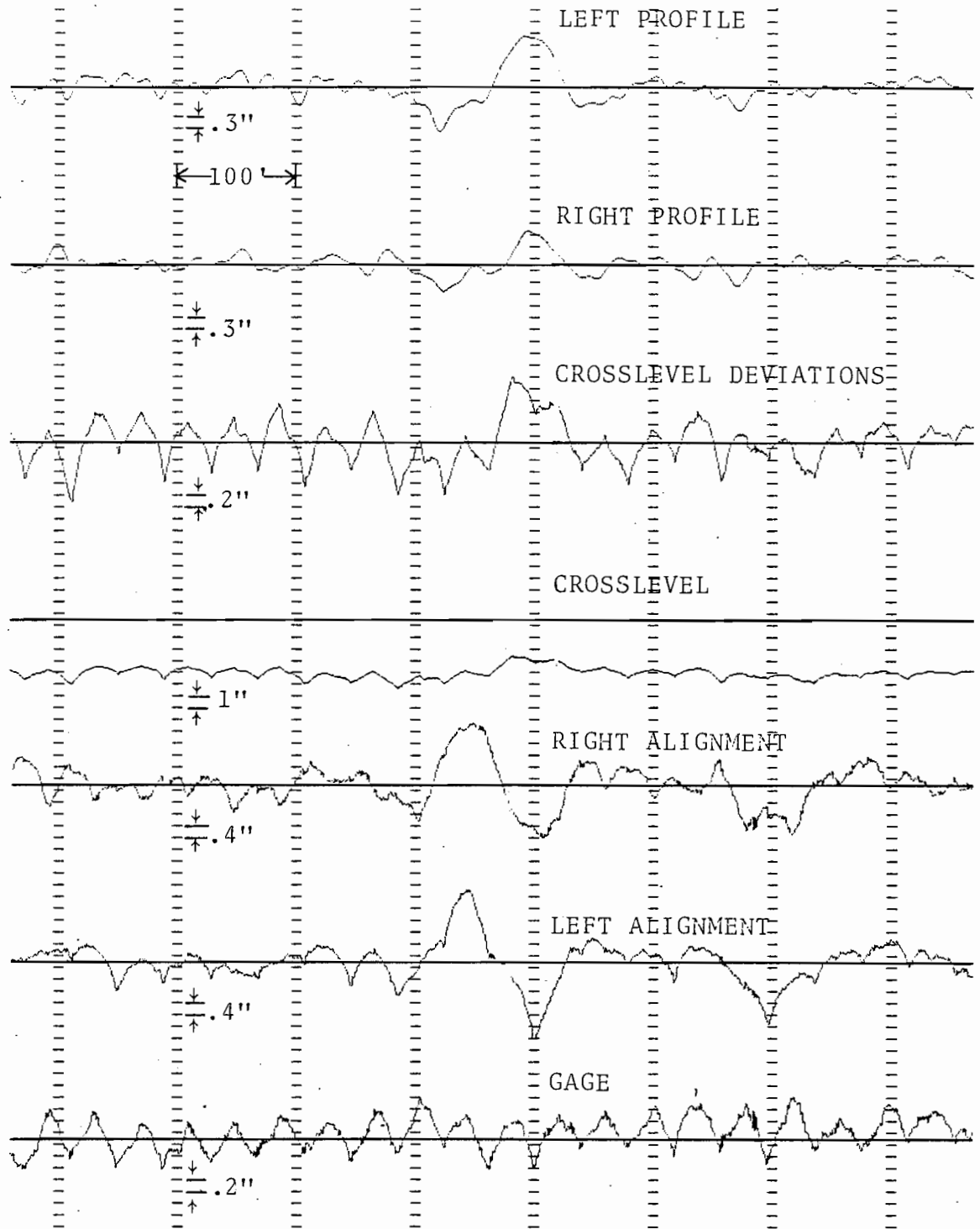


Figure C.3.b.8. Combined Periodic Signature in Gage and Alignment and Isolated Bump in Profile, Crosslevel and Alignment (Class 3, Curve).

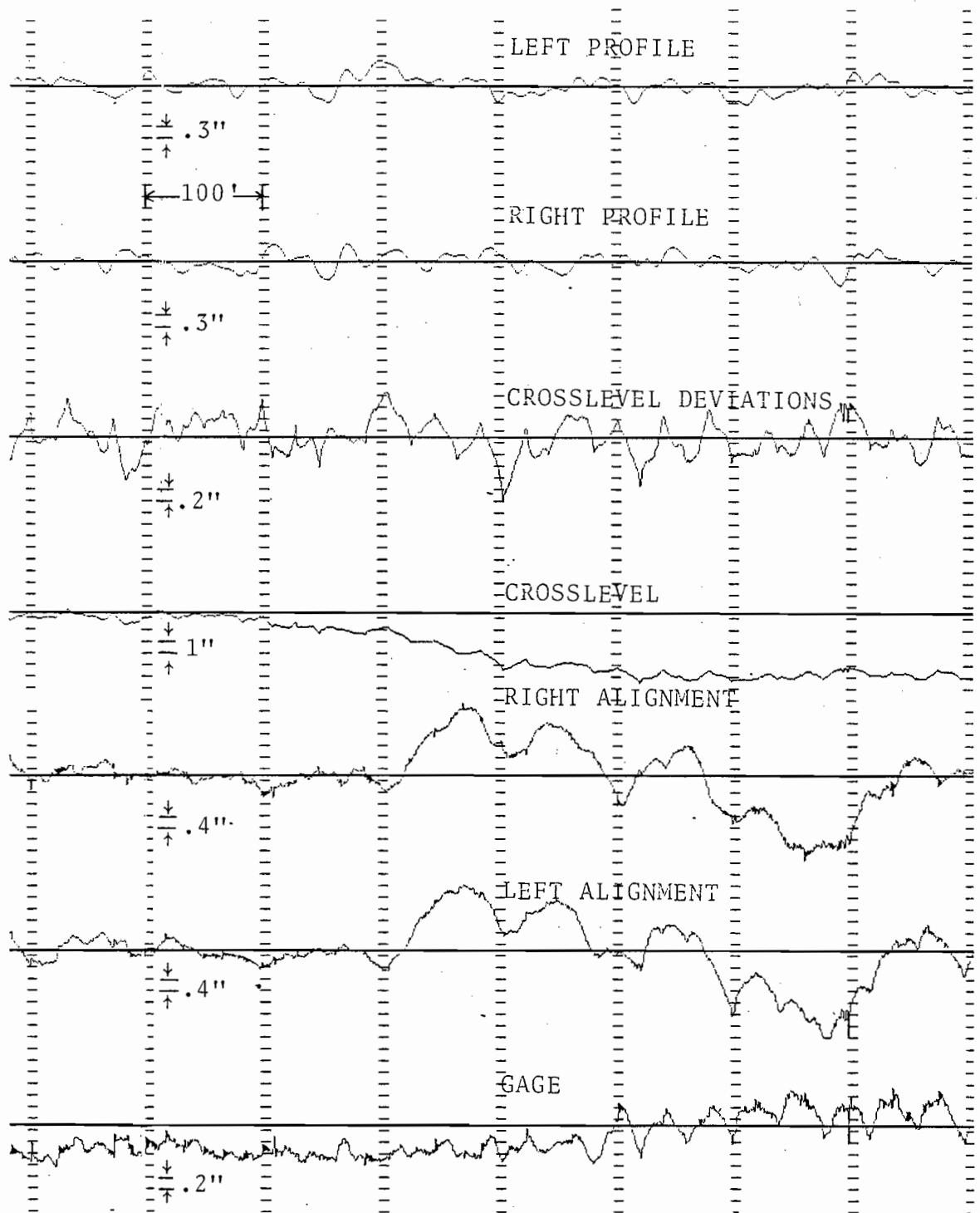


Figure C.3.b.9. Combined Periodic Gage and Crosslevel Cusps (39') and Periodic (100') Alignment (Class 3, Spiral).

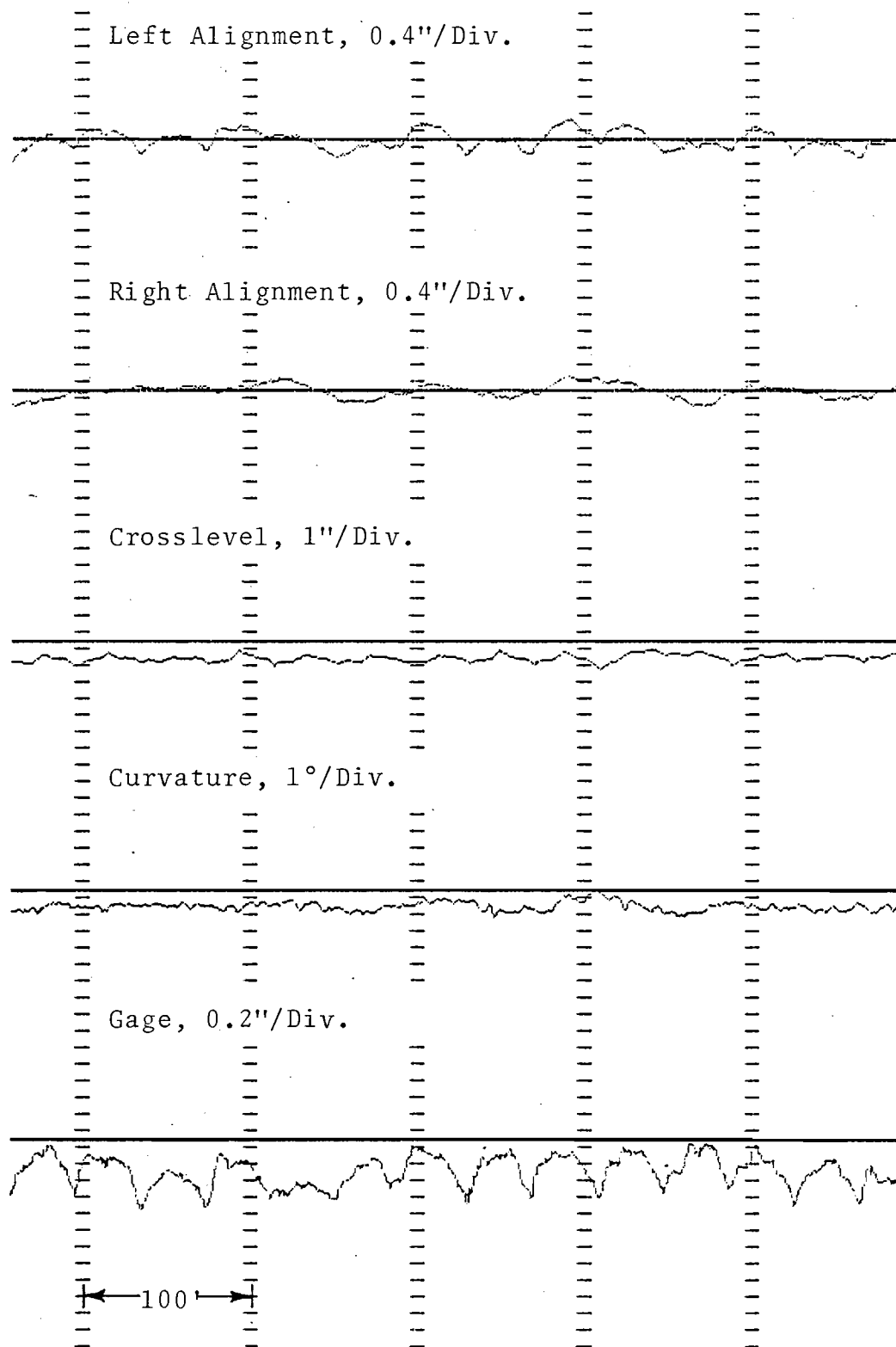


Figure C.3.c.1. Combined Rail-Length Gage and High Rail Alignment Periodic Cusps (Class 3, Curve).

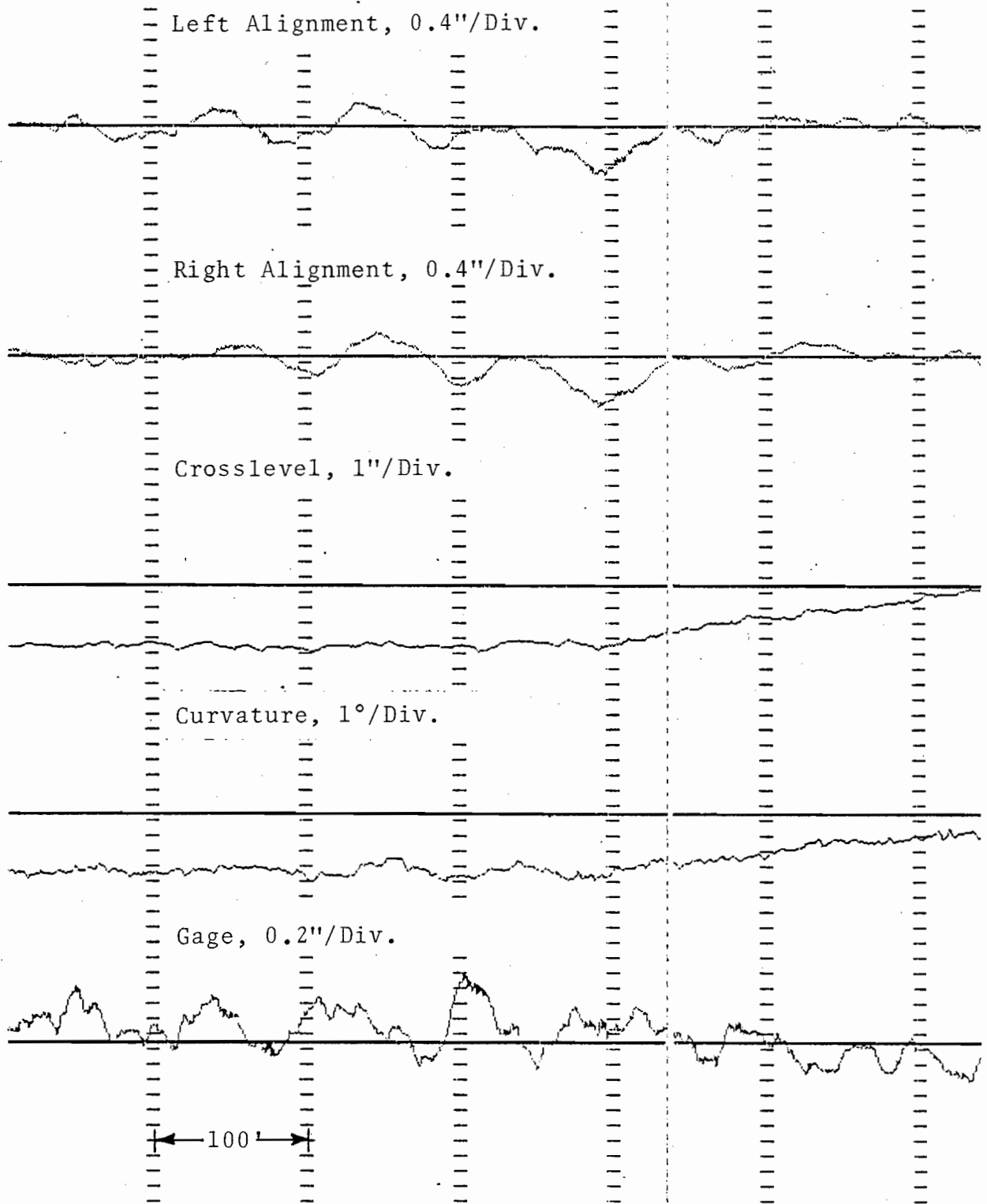
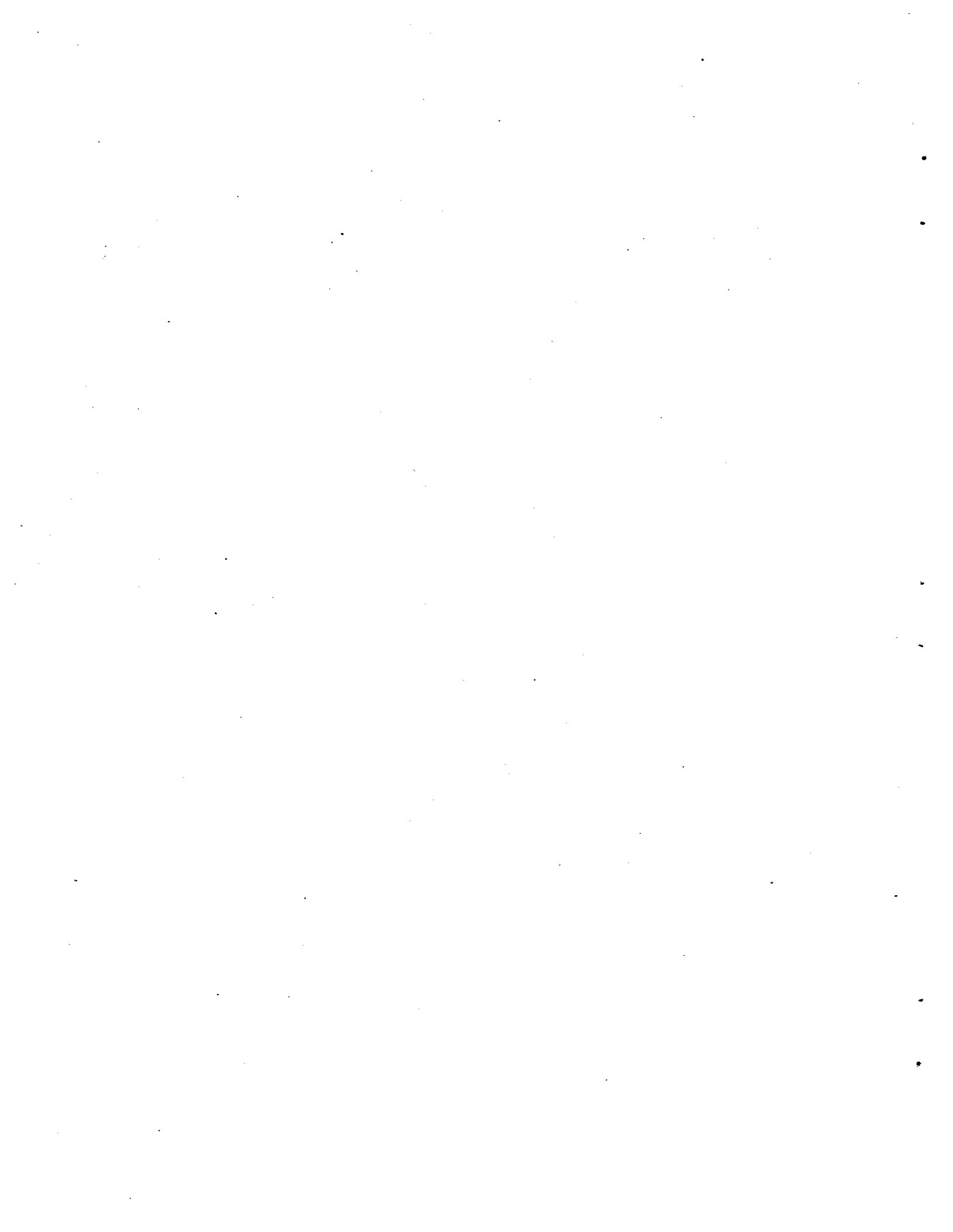


Figure C.3.c.2. Combined Long Wavelength (100') Gage and Alignment Sinusoids (Class 3, Curve/Spiral).



APPENDIX D
FREQUENCY DOMAIN ANALYSIS

An analysis of the power spectra of track geometry parameters can provide useful information about the relationship between track geometry parameters. The following sections provide a discussion of the auto-spectra, cross spectrum and transfer function between two track geometry parameters.

D.1 POWER SPECTRAL DENSITY

D.1.1 DEFINITION

The Power Spectral Density (PSD) of a signal describes the intensity of power as a function of frequency. The PSD plots are commonly used in the characterization of electrical signals varying randomly with time. The area contained under PSD curve between any two frequencies is equal to the total electrical power delivered by the random signal within that bandwidth. In mathematical terms, this can be expressed as:

$$P_x(f_1, f_2) = \int_{f_1}^{f_2} G_x(f) df \quad (1)$$

where

$G_x(f)$ = the PSD of function x.

$P_x(f_1, f_2)$ = power (mean square energy per unit time) between frequencies f_1 and f_2

The total power is given by

$$P_x = \int_0^{\infty} G_x(f) df \quad (2)$$

For small Δf a PSD function can be defined such that Equation (1): -

$$P_x(f, f\Delta f) \approx G_x(f)\Delta f \quad (3)$$

or more precisely:

$$G_x(f) = \lim_{\Delta f \rightarrow 0} \frac{P_x(f, \Delta f)}{\Delta f} \quad (4)$$

Thus, the power spectral density function of random data describes the general frequency composition of data in terms of the spectral density of its mean square value.

The nature of the PSD plot is illustrated in terms of two extreme cases in Figure D-1 and D-2. The PSD of a perfect sine wave of frequency f_0 is given by (2)

$$G_x(f) = \frac{x^2}{2} \int (f - f_0) \quad (5)$$

where

x = amplitude of the sine wave

$\int (f - f_0)$ = delta function at frequency f_0

In other words, PSD of a sine wave is an infinite spike at the frequency of the sine wave (Figure D-1). The integral of the power spectral density over any frequency range that includes f_0 has a finite value equal to the mean square value (x^2/w) of the sine wave.

On the other extreme of the sine wave is the white noise. The white noise has a uniform (flat) power spectrum across all frequencies. Thus, the theoretical PSD plot for perfectly white noise a constant denoted by a horizontal line in Figure D-2.

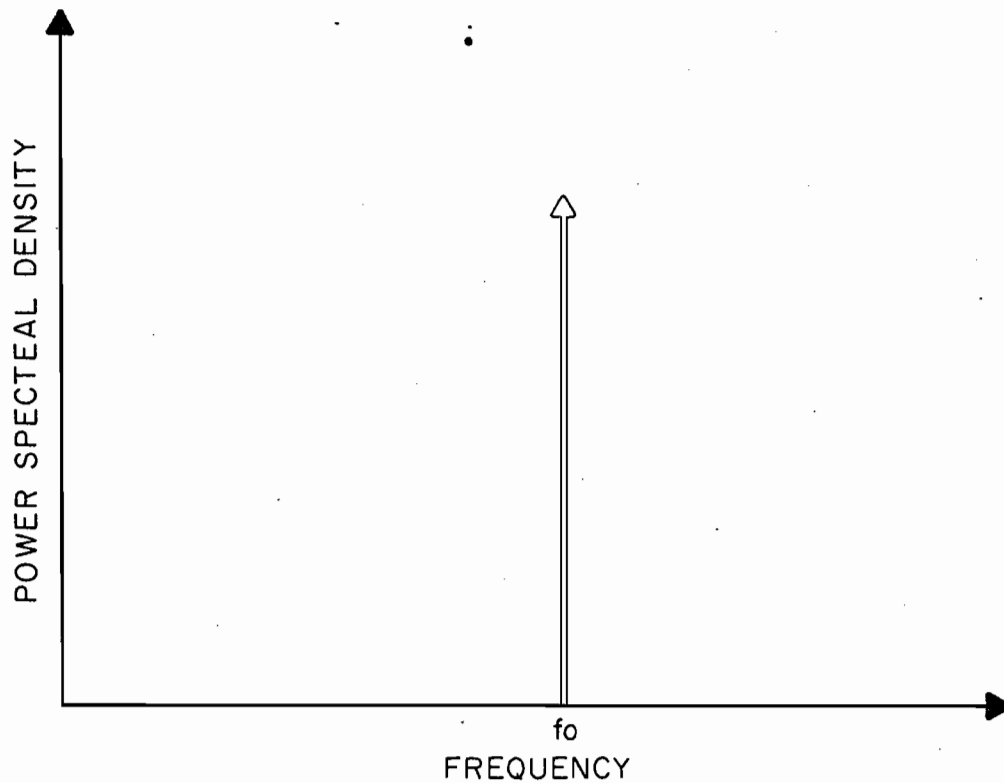


Figure D-1. PSD of a Perfect Sine Wave of Frequency f_0

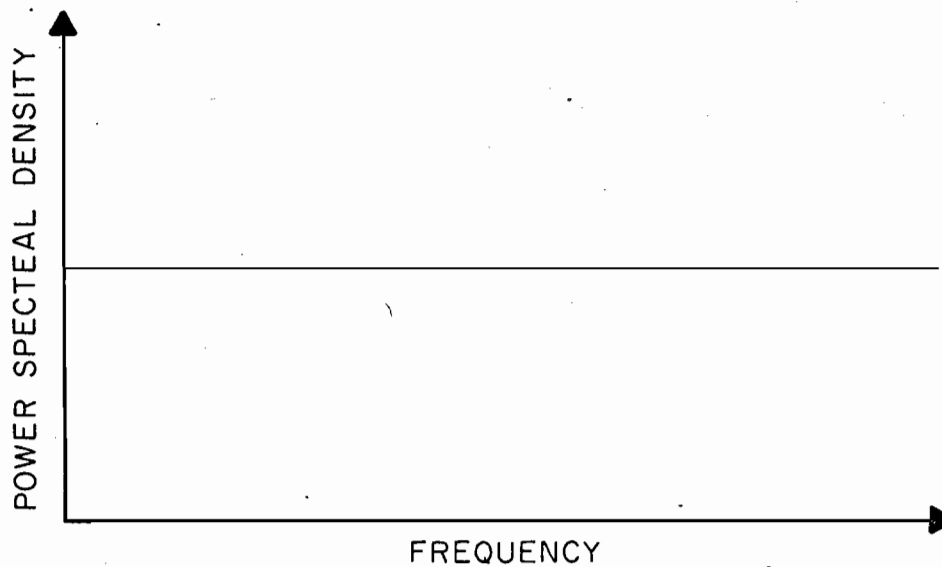


Figure D-2. PSD of White Noise

The principal application of a PSD function is to determine the frequency composition of data. This, in turn, can be used to establish the basic characteristics of the physical system involved. For example, the PSD of the output of an electrical circuit ($G_Y(f)$) is given by (1):

$$G_Y(f) = |H(f)|^2 G_X(f) \quad (6)$$

where

$G_X(f)$ = PSD of the input signal

$H(f)$ = frequency response function of the electrical circuit

A track geometry parameter such as alignment is usually described as a function of distance along the track. The independent parameter in this case is the distance rather than time. Thus, the temporal frequency, f , normally given in units of cycles/second, should be converted to a spatial frequency, ϕ , given in units of cycles/foot.

When the PSD concept is applied to track geometry parameters varying randomly with distance, the area under the PSD curve between any two frequencies does not have a direct power interpretation but it is closely related to the dynamic energy delivered to a traveling vehicle by the track. Because of the amplitude versus frequency information contained in the track geometry PSD's, they are useful both as track quality indicators and as input to dynamic models for vehicle response analysis. A comparison of profile PSD's for different sections of track is provided in Figure D-3. The following points should be noted with reference to Figure D-3.

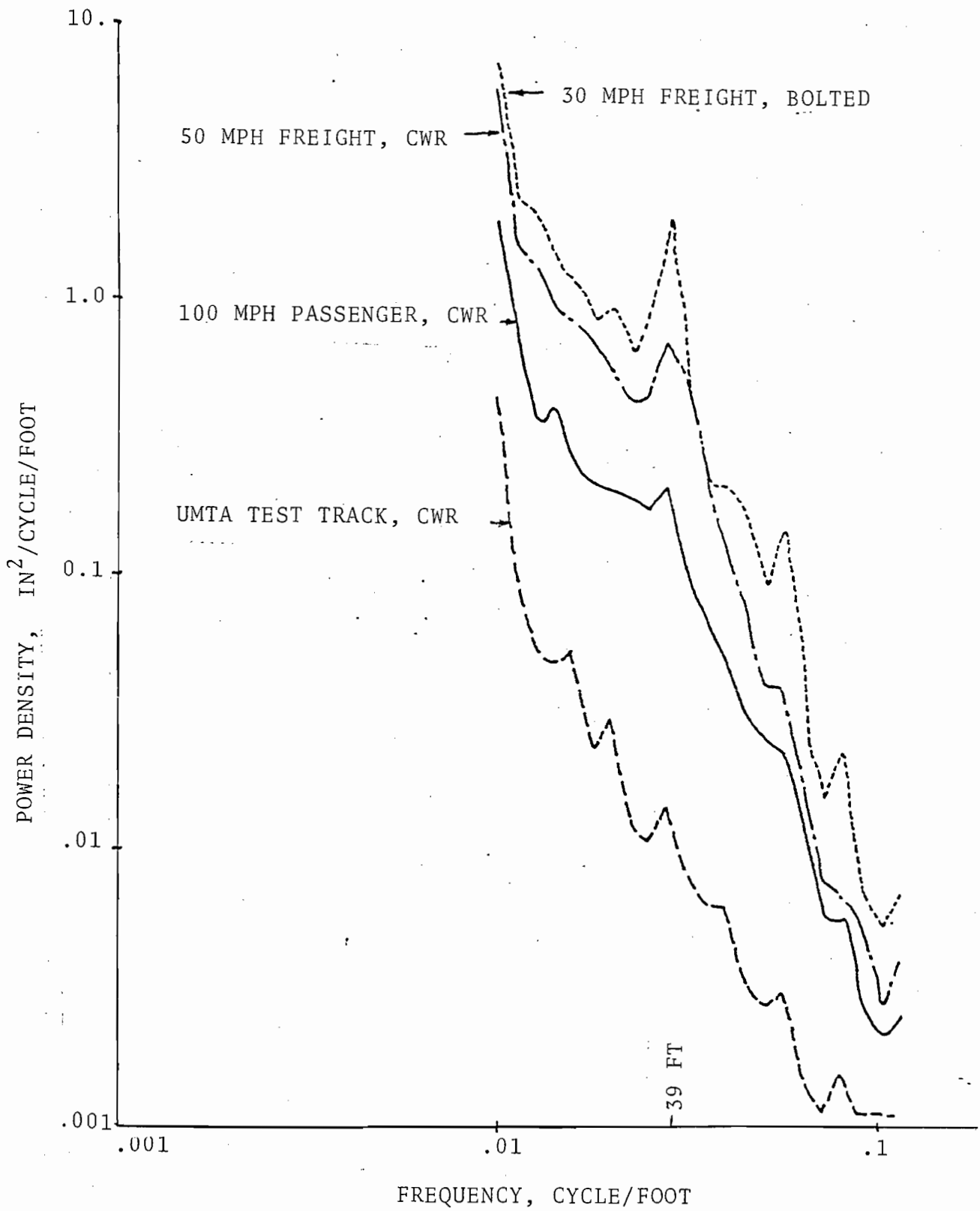


Figure D-3. Profile PSD Comparisons

- o A track section of perfectly smooth surface will have zero density at all frequencies.
- o Tracks of better quality have lower density value.
- o Peaks at 39-foot wavelength and its harmonics appear in all PSD's, indicating the existence of a periodic component at that wavelength.
- o The 39-foot periodic component is especially pronounced in the bolted track.

D.1.2 COMPUTATION OF PSD

The PSD's may be computed by three methods (3). Each of the three methods is based on a different but asymptotically equivalent definition. The first procedure utilized filtering. A bandpass filter with a center frequency, f_k , and bandwidth, B_k , is designed for each frequency. Data are passed through the bandpass filter, squared and then summed and normalized.

Thus,

$$G_k = \frac{1}{B_k N} \sum_{i=1}^{N-r} y_i^2(k) \quad (7)$$

where G_k = PSD at frequency f_k , $0 \leq f_0 \leq f_k \leq f_c$

F_c = cutoff frequency (0.5/sample interval)

N = number of data points

y_i = data points

The second procedure is the standard Blackman-Tukey method. In this method the PSD is computed by taking the Fourier transform of the correlation function. The correlation function, R_r , is given by

$$R_r = \frac{1}{N-r} \sum_{i=1}^{N-r} x_i x_{i+r} \quad (8)$$

where $r = 0, 1, \dots, m$

(x_i) = data (assumed zero mean)

m = number of delays

The PSD, G_k , is computed from:

$$G_k = 2h \left(R_0 + 2 \sum_{r=1}^{m-1} R_r \cos \frac{kr}{m} + R_m \cos \frac{k}{m} \right) \quad (9)$$

where $k = 0, 1, \dots, m$

h = sample interval

m = number of lags

G_k = corresponds to the power near $k/2mh$ Hz.

The third procedure is the direct Fourier transform method.. Let X_k be the Fourier transform of data given by:

$$X_k = \sum_{i=0}^{N-1} x_i e^{-j \frac{2\pi}{N} ik}, \quad k = 0, \dots, N-1 \quad (10)$$

Then PSD is obtained as follows:

$$G_k = \frac{2h}{N} |X_k|^2, \quad k = 0, 1, \dots, \frac{N+1}{2} \quad (11)$$

Here, the frequency interval $(0, 0.5/h)$ is broken into $N/2$ parts, so that the frequency increment, Δf , is given by:

$$\Delta f = \frac{1}{Nh} \quad (12)$$

All three methods produce results that are nearly the same but in general, they are not identical. Since the advent of the Fast Fourier Transform (FFT) algorithms, the finite Fourier transform method of computing PSDs is most efficient. Therefore, further discussion will be limited to this method.

Care should be taken in computing PSD's since problems may arise in direct application of Equation 11 (3). The following sections describe some of the problems and the methods to handle these problems.

D.1.3 TREND REMOVAL

A trend in the data is a frequency component whose period is longer than the record length. Proper handling of data requires that long-term biases and trends in the data be removed, otherwise the distortion can occur in the estimation of the low-frequency end of the spectrum.

The long-term trends may exist even after high-pass digital filtering. Therefore, special techniques are required to remove such trends. The least square procedures can be applied for the removal of linear as well as higher order polynomials.

Let (u_n) , $n = 1, 2, \dots, N$ be the data values. The trend in these data can be approximated by equation of the type (1):

$$\hat{u}_n = b_0 + b_1 n, \quad n = 1, 2, \dots, N \quad (13)$$

where

$$b_0 = \frac{2(2N+1) \sum_{n=1}^N u_n - 6 \sum_{n=1}^N nu_n}{N(N-1)} \quad (14)$$

$$b_1 = \frac{12 \sum_{n=1}^N nu_n - 6(N+1) \sum_{n=1}^N nu_n}{N(N-1)(N+1)} \quad (15)$$

Then the data after trend removal, x_n , is given by

$$x_n = u_n - \hat{u}_n, \quad n = 1, 2, \dots, N \quad (16)$$

Trend removal should be performed only if trends are physically expected or clearly apparent in the data (1). In terms of track geometry measurements, we might expect such trends to arise as a result of extremely long wavelength phenomenon associated with changes in elevation such as those encountered in traversing mountains or valleys. However, these changes are in fact eliminated from inertial measurement of data by means of high-pass filters. This is especially true for alignment and profile space curve. Therefore, trend removal may not be necessary for track geometry data.

D.1.4 TAPERING DATA

The power spectral density estimates are found by first computing the Fourier coefficients of a finite length data record. The specified length records are obtained by truncating a data sequence after specified number of points. The abrupt truncation of data gives rise to a type of distortion known as "leakage" in spectrum computations. The problem of "leakage" is the one in which the estimate of spectral density calculated for a particular frequency contains some additional elements of power derived from adjacent frequencies. This leakage has the effect of reducing the accuracy and value of the estimate (2).

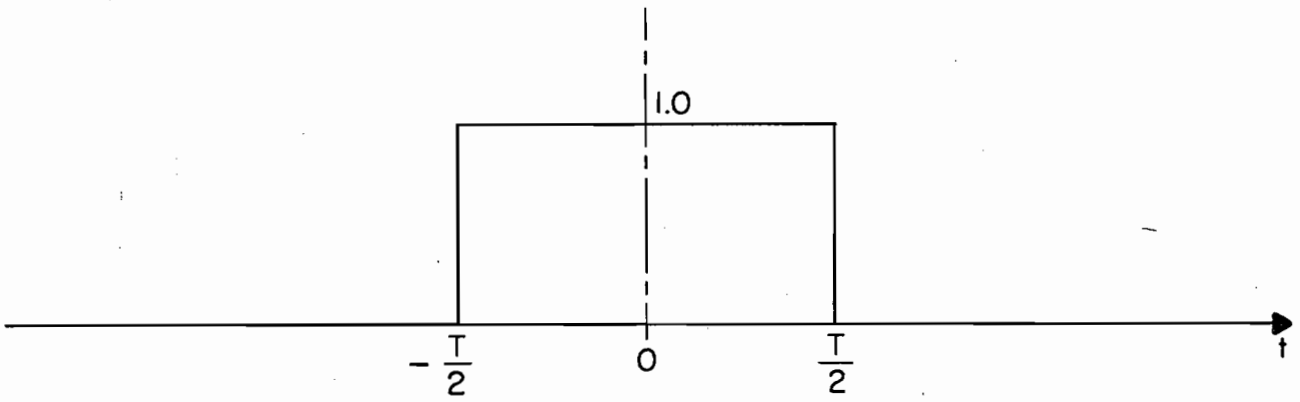


Figure D-4. Rectangular Window

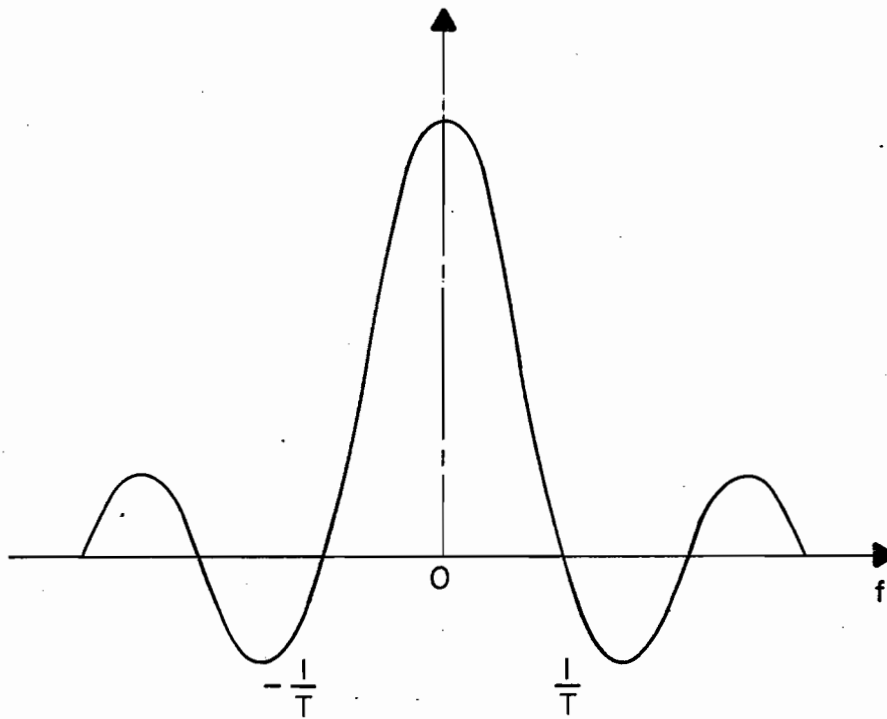


Figure D-5. Fourier Transform of Rectangular Window

The finite Fourier transform is equivalent to the infinite transform obtained by convolving the infinite length data record with a rectangular window (Figure D-4). A finite length record is in effect obtained by multiplying the infinite length process with a rectangular window. The specific effects of this truncation are function of the Fourier transform of the window function. The Fourier transform of the rectangular window is shown in Figure D-5. The presence of large side lobes (Figure D-5) make it difficult to distinguish between the lobe of a large signal and the spectrum response of a low level signal which is close in frequency. This is further illustrated by the PSD of a truncated sinusoid in Figure D-6 (3). Because of the finite value of the record, T ; what would have been a delta function for infinite T has become a sine x/x function centered about f_0 . Thus, the power which was concentrated at a single point has been spread over a much broader range. It is this spreading of power that is termed as leakage.

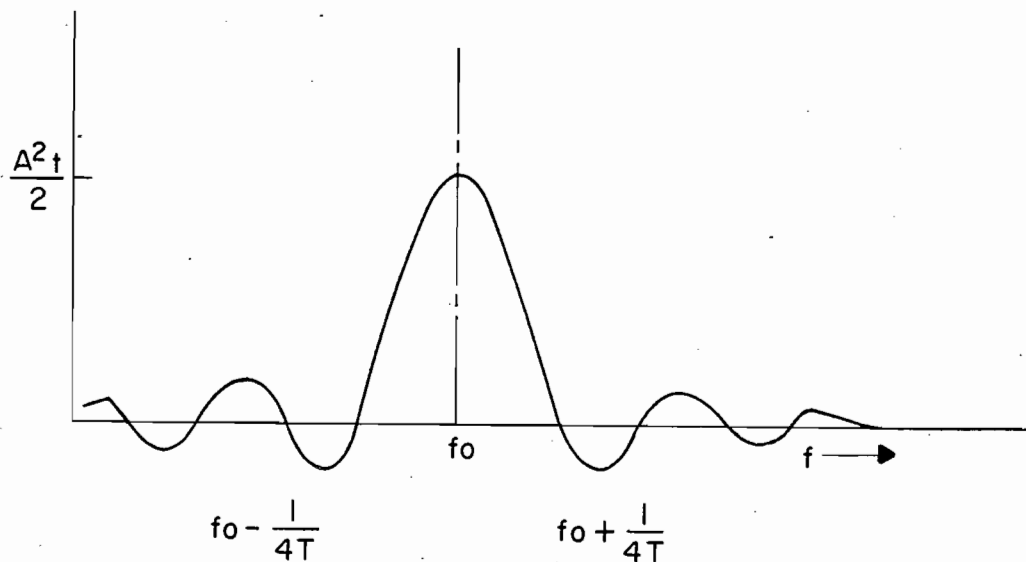


Figure D-6. Power Spectral Density of a Truncated Sinusoid of Frequency f_0

Since the large side lobes arise as a result of the abrupt corners on the rectangular window, the suppression of the side lobes (or reduction of leakage) can be obtained by rounding off these corners. This can be done by multiplying the data with a suitable window other than the rectangular window.

This process is known as "tapering" and its objective is to "round off" potential discontinuities at each end of the finite segment of data being analyzed.

The reduction in leakage can be obtained by tapering the data with a split-cosine-bell window (4). This window is defined as:

$$w_t = \begin{cases} \frac{1}{2} \left(1 - \cos \frac{\pi(t - \frac{1}{2})}{m} \right) & , t = 0, \dots, m-1 \\ 1, & t = m, \dots, n-m-1 \\ \frac{1}{2} \left(1 - \cos \frac{\pi(n-t+\frac{1}{2})}{m} \right) & , t = n-m, \dots, n-1 \end{cases} \quad (17)$$

where m is chosen so that m/n is the desired proportion of data to be tapered on each end. It is suggested that the cosine taper be used over one-tenth of each end of the data (1). This tapering has the effect of reducing the variance of the tapered data relative to the original data. Therefore, the spectrum estimates should be multiplied by a scale factor. The scale factor can be calculated by taking the ratio of the area of the rectangular window to that of the cosine window. Specifically, for the above case, this scaling factor is $(1/0.875)$.

The filter shape corresponding to the cosine taper of Figure D-7 is shown in Figure D-8. Note that the width of the main lobe is greater than that for the rectangular window. Also, the half-power bandwidth is approximately equal to $1/T$, and side lobes are significantly suppressed.

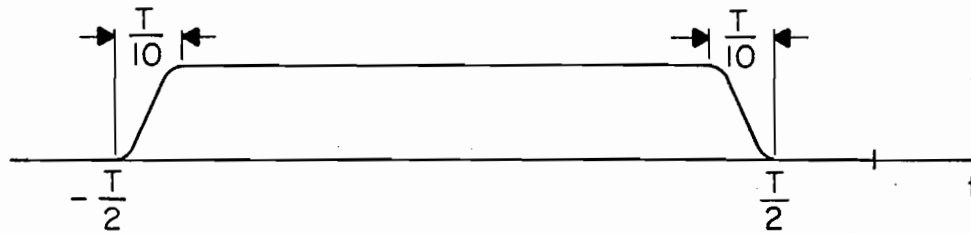


Figure D-7. A Split-Cosine Taper Window

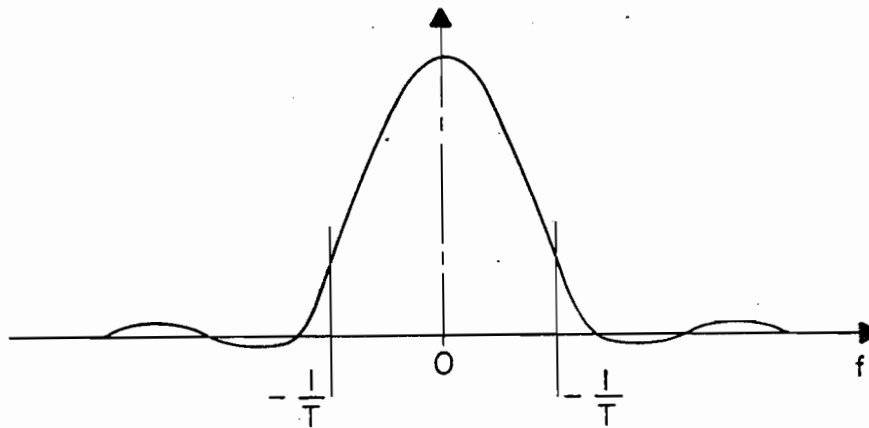


Figure D-8. Effective Filter Shape with Split-Cosine Taper

D.1.5 ADDING ZEROS

Most of the FFT routines usually handle the data records of length $N = 2^P$. In practice, the data sequence is either truncated or zeros are added to obtain the desired number of points. The effect of adding zeros is to reduce the frequency resolution of the spectral estimates. For example, if N_z zeros are added to M data points so that $N = M + N_z$ is 2^P , the effective resolution, $\Delta f'$, becomes

$$\Delta f' = \frac{1}{(M + N_z)h} \quad (18)$$

where h is the sample interval.

D.1.6 SEGMENTATION OF DATA

A raw power spectral density estimate is a CHI^2 variable with two degrees of freedom (each spectral estimate is obtained by squaring and adding the real and imaginary parts). It has been shown that the normalized standard error for the PSD estimate of white noise is greater than or equal to unity (3). In other words, the standard deviation of the estimate is greater than or equal to the quantity being estimated.

The standard error can be reduced by averaging the results from the separate time slices, each of N data points. The smooth spectral estimate is given by:

$$\hat{G}_k = \frac{1}{q} (G_{k,1} + G_{k,2} + \dots + G_{k,q}) \quad (19)$$

where $G_{k,1}$ is the raw PSD estimate at frequency f_k and G_k is the smoothed PSD estimate.

G_k has CHI^2 distribution with approximately $2q$ degrees of freedom. The normalized standard error is now given by:

$$\epsilon = \sqrt{\frac{1}{q}} \quad (20)$$

The effective resolution bandwidth is determined by the length of each segment and is given by:

$$B = \frac{1}{Nh} \quad (21)$$

where N = number of points in a segment
 h = sample interval.

It can be seen from Equations (20) and (21) that good frequency resolution and low variance are conflicting requirements since increasing the length of a segment will decrease the number of segments. An improvement in results can be obtained by dividing the available data sequence into K overlapping segments of length, L . For example, if the segments overlap by $L/2$ samples, the total number of segments is given by

$$K = \frac{N' - L/2}{L/2} \quad (22)$$

where N' equals total length of data sequence.

The normalized standard error in this case is given by (5):

$$\epsilon' = \sqrt{\frac{11}{9K}} \quad (23)$$

D.1.7 COMPUTATION STEPS

Based on the discussions in the previous paragraphs, the following steps are recommended for computing PSD's.

1. Based on the requirements of accuracy and resolution, divide the available data sequence into disjointed or overlapping segments each of length N .
2. Remove the trends in the data segment using procedures outlined in Section D.1.3 (optional).
3. Taper the segment of data using the procedures outlined in Section D.1.4 (optional).
4. Compute Fourier coefficients X_k , $k = 0, 1, \dots, N-1$ (Equation (10)) using FFT.
5. Compute PSD estimate G_k , $k = 0, 1, \dots, (N+1)/2$ as in Equation (11).
6. Repeat Steps 2 through 5 for all segments and compute the smoothed PSD estimates G_k as in Equation 19.
7. Adjust these estimates for the scale factor due to tapering.

D.2 CROSS POWER SPECTRAL DENSITY

The cross power spectral density characterizes two time series and is traditionally defined as the Fourier Transform of the cross-correlation function. The cross-spectral density is a complex number and can be written as (1):

$$G_{xy}(f) = C_{xy}(f) - jQ_{xy}(f) \quad (24)$$

where the real part C_{xy} , is called the co-spectrum and the imaginary part, Q_{xy} , is called the quad-spectrum.

The cross-spectral density function can also be written as (1):

$$G_{xy}(f) = |G_{xy}(f)| e^{-j\theta_{xy}(f)} \quad (25)$$

where $G_{xy}(f)$ is called the amplitude spectrum and $\theta_{xy}(f)$ is called the phase spectrum. The amplitude and phase spectra are given by:

$$|G_{xy}(f)| = \sqrt{C_{xy}^2(f) + Q_{xy}^2(f)} \quad (26)$$

$$\theta_{xy}(f) = \tan^{-1} \frac{-Q_{xy}(f)}{C_{xy}(f)} \quad (27)$$

The amplitude spectrum shows whether frequency components in one series are associated with large or small amplitudes at the same frequency in other series. Similarly, the phase spectrum shows whether frequency components in one series lag or lead the components at the same frequency in the other series. The cross-spectral density function can be used to determine the complete frequency response function of linear systems since (1):

$$G_{xy}(f) = H(f)G_x(f) \quad (28)$$

The cross-spectral density measurements can also be used to determine the time delay through a system since the time delay, τ , is given by (1):

$$\tau = \frac{Q_{xy}(f)}{2f} \quad (29)$$

The cross-spectral density estimates can be obtained via FFT since (1):

$$G_{xy}(f_k) = \frac{2h}{N} (X_k^* Y_k) \quad (30)$$

where $k = 0, 1, \dots, N-1$

$G_{xy}(f_k)$ = cross-power spectral density at frequency f_k

h = sample interval

N = length of time series x and y

X_k = Fourier transform of (x_n)

Y_k = complex conjugate of X_k

f_k = k/Nh .

The cross spectral density can be computed by the extension of methods given in Section D.1. Assume two data sequences x_n and y_n of arbitrary length. The following are the steps to compute the amplitude and phase spectra of the cross spectral density function.

1. Divide x_n and y_n into K segments each of length N .
2. Remove trends from a segment of both time series (optional).
3. Taper the two resulting sequences (optional).
4. Compute X_k and Y_k using FFT.

5. Compute raw power spectral density estimate using Equation (30).
6. Repeat steps 2 through 5 for all segments and obtain average estimates.
7. Adjust these estimates for the scale factor due to tapering.

D.3 TRANSFER FUNCTION

The transfer function describes the relationship between input and output of a constant parameter linear system. For physically reliable and stable systems, the frequency response function may replace the transfer function with no loss of useful information. The frequency response function $H(f)$ relates the input and output of a linear system by the formula (1):

$$Y(f) = H(f)X(f) \quad (31)$$

where $Y(f)$ = Fourier transform of output

$X(f)$ = Fourier transform of input.

The frequency response function be written as:

$$H(f) = |H(f)| e^{-j\phi(f)} \quad (32)$$

where $|H(f)|$ = system gain factor

$\phi(f)$ = phase angle.

Discrete values of the response function H_k at frequencies $f_k = k/Nh$ can be computed by using FFT procedures using the relationship (3):

$$\hat{H}_k = \frac{\hat{G}_{xyk}}{\hat{G}_{xk}} \quad (33)$$

where \hat{G}_{xyk} = smooth cross-spectral density of x_n and y_n

\hat{G}_{xk} = smooth PSD's of x_n .

The gain factor and phase is given by (1):

$$|\hat{H}_k| = \frac{(\hat{C}_k + \hat{Q}_k^2)^{1/2}}{\hat{G}_{xk}} \quad (34)$$

$$\hat{\phi}_k = \tan^{-1} \left(\frac{-\hat{Q}_k}{\hat{C}_k} \right) \quad (35)$$

where \hat{C}_k = smooth co-spectrum

\hat{Q}_k = smooth quad-spectrum

$\hat{\phi}_k$ = phase in radians.

D.4 COHERENCE FUNCTION

The ordinary coherence function in the frequency domain is analogous to the correlation coefficient in the time domain. The squared coherence function, $\gamma_{xy}^2(f)$ is defined as (3):

$$\gamma_{xy}^2(f) = \frac{|G_{xy}(f)|^2}{G_x(f)G_y(f)} \quad (36)$$

Using FFT procedures to compute smooth spectral estimates of power and cross-spectral densities, the coherence function is estimated as (1):

$$\hat{\gamma}_k^2 = \frac{\hat{C}_k^2 + \hat{Q}_k^2}{\hat{G}_{xk} \hat{G}_{yk}} \quad (37)$$

The coherence function theoretically should satisfy the relationship:

$$0 \leq \hat{\gamma}_k^2 \leq 1$$

However, if raw spectral estimates are used in Equation (36), a value of unity will always be obtained (1). Therefore, it is essential to work with smooth spectral density estimates.

D.5 FEDAL

The software package, FEDAL, is developed for the Frequency Domain Analysis of the track geometry data. The program generates power spectral densities, cross power spectral density, cross spectrum, phase spectrum, coherence spectrum, and the transfer function.

D.5.1 CAPABILITIES AND LIMITATIONS

FEDAL operates on the processed T-6 tapes. Processing can be requested on any section of the tape.

Processing can be done on any three track geometry channels at a time.

Program operates on two data sequences at a time. The first data sequence is taken from the first track geometry channel. The second data sequence is constructed from the second channel, mean of second and third channel, or difference of second and third channel. An option is provided to rectify the second data sequence. Another option provided is to take the square of the first channel and the mean of the square of the second and third channels, for the second data sequence.

The program has an option to remove trends from data. The user can request the removal of mean or both mean and slope from data.

The length of a segment of data can vary up to 1024 points. The length should be given in powers of two. The program has an option to fill the last partial segment with zeros.

The program can work on disjoint or overlapping segments of data. This option is provided to improve the accuracy of spectral estimates.

Any proportion of a segment can be tapered using a split-cosine taper.

The output is in the form of plots. The frequency axis can be either on linear or log scale. Option is also provided to obtain plots on both scales.

Table D-1 gives names and function of subroutines in the program.

D.5.2 OPERATION

FEDAL is in the MOW library on disk RD3.3 and can be queued as follows:

```
:NJ,L
:IO,3,24,5,30,7,16
:QUB,FEDAL/MOW
  Data Cards
:QUB,PLOTP2
:QUB,PLOTP3,,1
:XX
```

The above I/O assignments assumes that the input tape is on unit 0. The input format is given in Table D-2.

Options available to change data sequences are shown in Table D-3.

TABLE D-1
SUBROUTINES IN FEDAL

| Name | Function |
|--------|---|
| REDATA | Data input routine |
| TREND | Removed trends |
| WINDOW | Generates weights for split cosine bell |
| PSDXY | Computes raw spectral estimates |
| COHER | Computes cross spectrum, phase, coherence and transfer function |
| DATOUT | Prepares data for output |
| PLOTER | Plots power spectra and transfer function |
| PHPLOT | Plots phase and coherence |
| FIXLOG | Fixes smallest and largest value for plot, converts data to log |
| LXAXIS | Plot X-axis (log) for power spectra |
| LABLXL | Label X-axis for power spectra |
| LYAXIS | Plot Y-axis for power spectra |
| LABLYL | Label Y-axis for power spectra |
| PAXISX | Plot X-axis linear |
| PXAXIS | Plot X-axis log scale |
| CYAXIS | Plot Y-axis for coherence |
| PYAXIS | Plot Y-axis for phase |
| LINAX | Plot X-axis linear for power spectra |

TABLE D-2
INPUT FORMAT FOR FEDAL

| Card Number | Column Number | Format | Parameter | Description |
|-------------|-------------------------|--------|-----------|---|
| 1 | 1-5 | I5 | IFILE | = File number for processing , 0 defaults to first file |
| | 6-10 | I5 | ISREC | = Starting record , 0 defaults to first record |
| | 11-15 | I5 | IEREC | = Ending record , 0 defaults to last record of file |
| | 16-20 | I5 | NPTS | = Number of points per FFT (powers of 2 only) |
| | 21-25 | I5 | IPLT | = Plotting option = 0 plot log - log = 1 plot log - linear = 2 plot both (log-log, log- linear) |
| | 26-30 | I5 | ITRND | = Trend removal = 0 no trend removal = 1 remove mean = 2 remove mean and slope |
| | 31-35 36-40 41-45 | 3I5 | NCHN | = Channel numbers |
| | 46-50 | I5 | ND | = Number of deletes (max equals 8) |
| | 51-55 | I5 | IPOS | ≠ 0 absolute value of second data sequence |
| | 56-60 | I5 | IZERO | ≠ 0 zero fill last partial segment with zeroes. |

TABLE D-2 (CONT)
INPUT FORMAT FOR FEDAL

| Card Number | Column Number | Format | Parameter | Description |
|--------------|---------------|--------|-----------|--|
| 1 (Cont.) | 61-65 | F5.2 | TAPER | = Percentage of data for tapering on each end |
| | 66-70 | F5.2 | OVLAP | = Percentage of data for overlap |
| | 71-75 | F5.2 | SR | = Sample rate , 0. defaults to 1.0 |
| 2 | 1-5 | I5 | 1TEST | = 0 or 1 read data from tape = 2 generate test data from sub. 'LOAD' = 3 generate test data from sub. 'GETX' |
| | 6-10 | I5 | NDJST | = Number of segments to process for test data = 0 defaults to process 32000 segments |
| 3 | 1-5 | 16I5 | ITH | = Starting record number for first delete |
| | 6-10 | | | = Number of records to delete |
| | 11-15 | | | = Starting record number for second delete |
| | 16-20 | | | |
| | | | | Number of deletes = ND Above parameter has pairs for an input |

TABLE D-3
 OPTIONS AVAILABLE TO CHANGE DATA SEQUENCES

| Data Sequence 1, Channel 1 | Data Sequence 2 | | Interpretation |
|-------------------------------|-----------------|-----------------|---|
| | Channel 2 | Channel 3 | |
| +x | | | |
| +x | +y | | |
| +x | +y ₁ | +y ₂ | Avg. of data sequence 2 |
| -x | | | + x + 3 |
| +x | -y ₁ | +y ₂ | x ² vs 1/2 (y ₁ ²) + (y ₂ ²) |
| +x | +y ₁ | -y ₂ | x vs (y ₁ - y ₂) |

The output is in the form of 12 plots for six parameters: PSD of first data sequence, PSD of second data sequence, magnitude of cross spectrum, phase of cross spectrum, squared coherence and gain of transfer function. Each parameter is first plotted on log frequency axis and then on linear frequency axis. The ordinate for PSD's is on log scale (1 means 10, 2 means 100). The output format is given on the following pages.

FREQUENCY DOMAIN ANALYSIS

FILE= 1 FIRST RECORD= 1 LAST RECORD= 15
POINTS PER SEGMENT= 128 SAMPLE RATE= 1.0 TREND REMOVAL= 0
LINEAR PLOT= 2 TAPER=10.00 OVERLAP= 0.00
CHANNELS= 2 -23 24
NO OF DELETES= 0 ABSOLUTE VALUE= 0 ZERO FILLING= 0

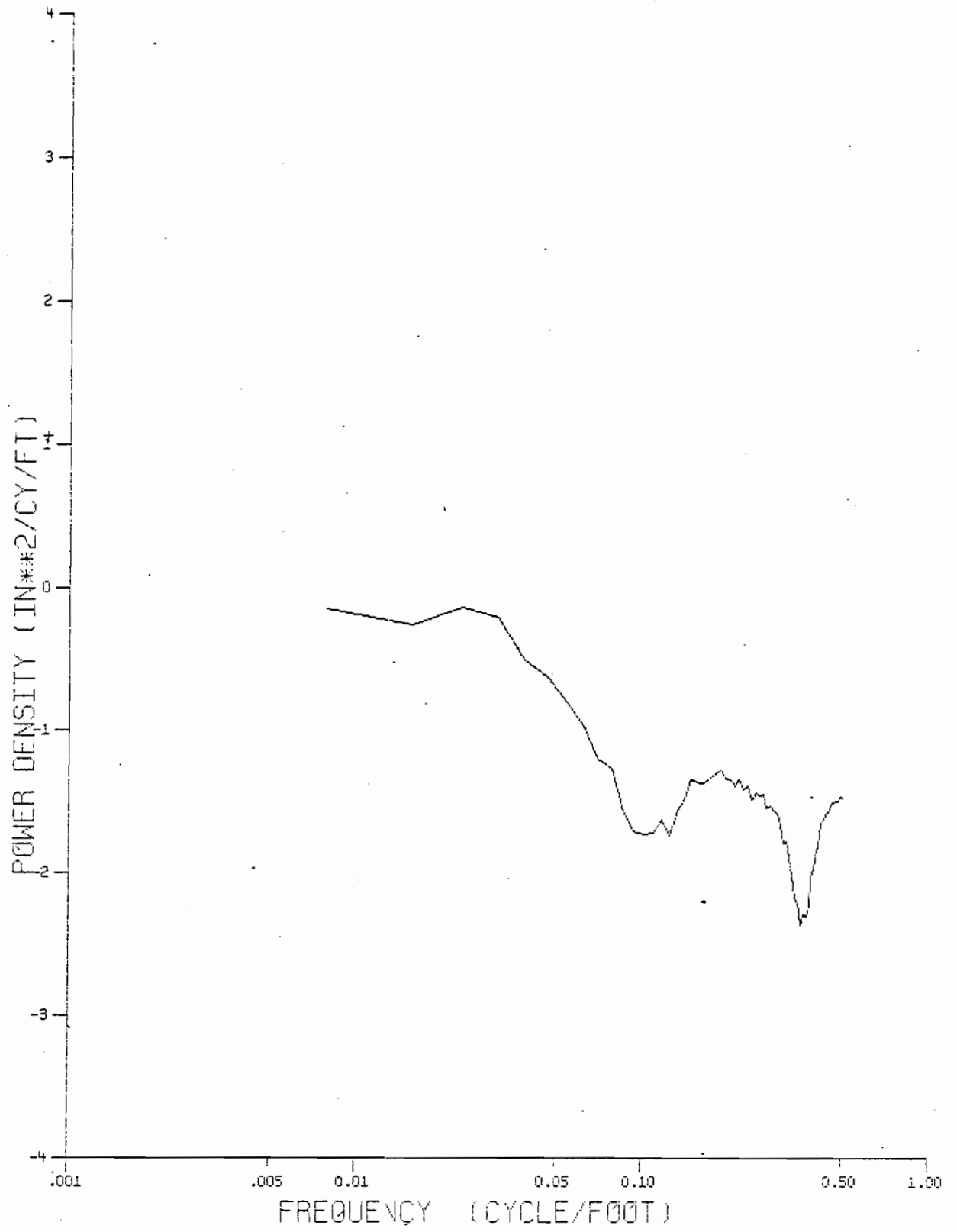
DELETES---

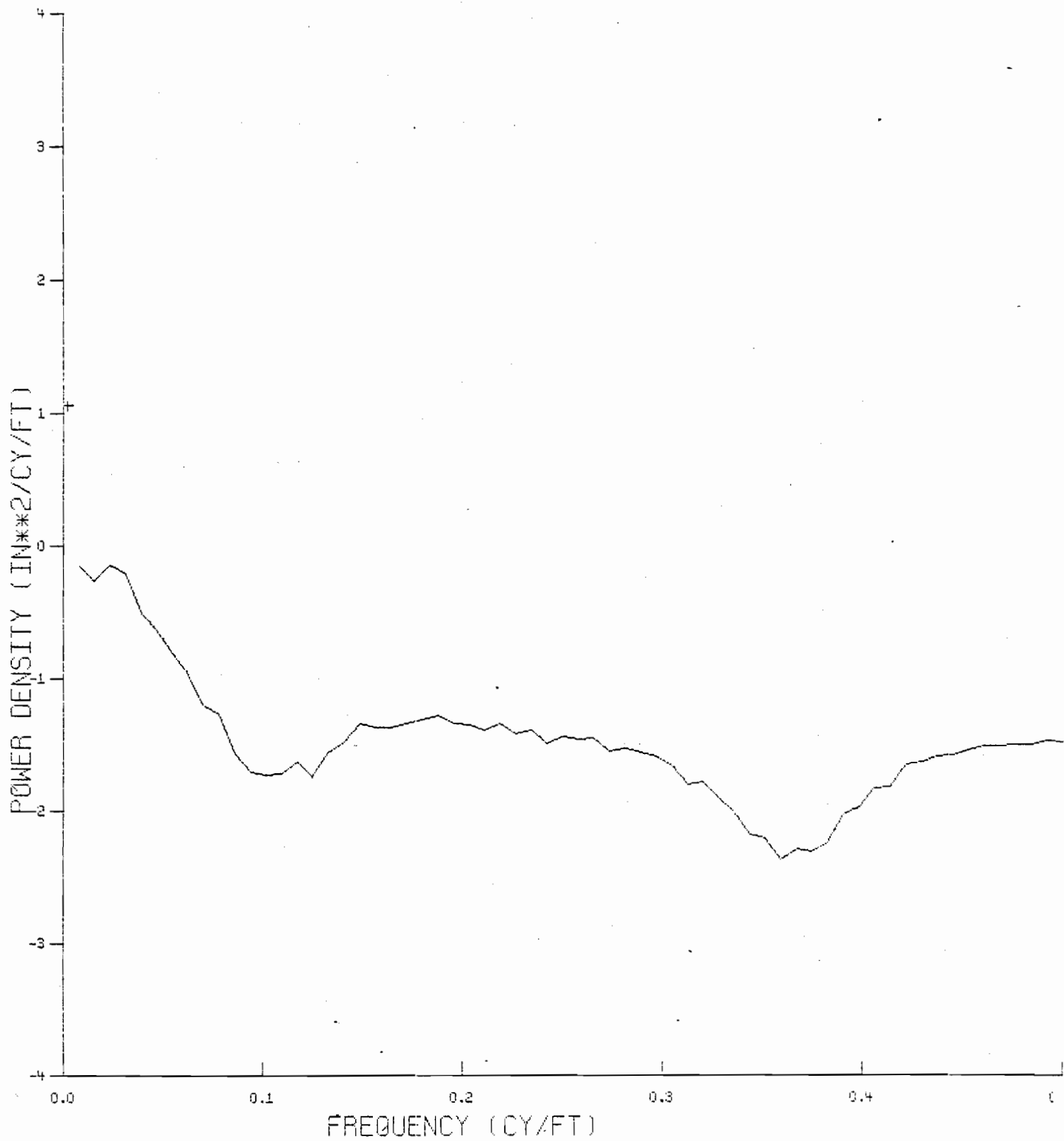
320-241929066 294430792 294630099-3237 15828745 158 8825 2576 304-3071 158

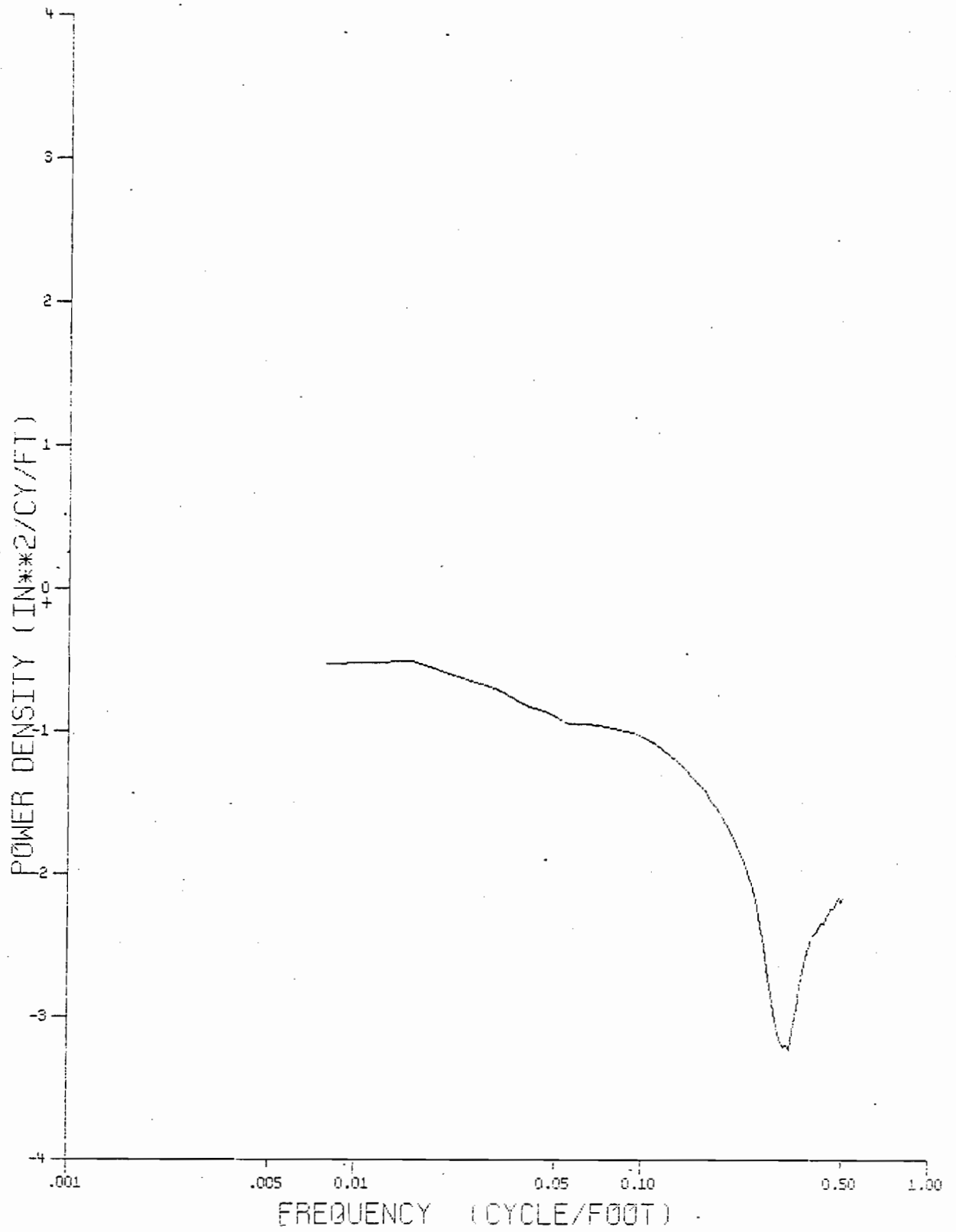
T6P0 M042878T6-318 4/28/78 ELKHORN, KY TO ASHLAND, KY (C&O)

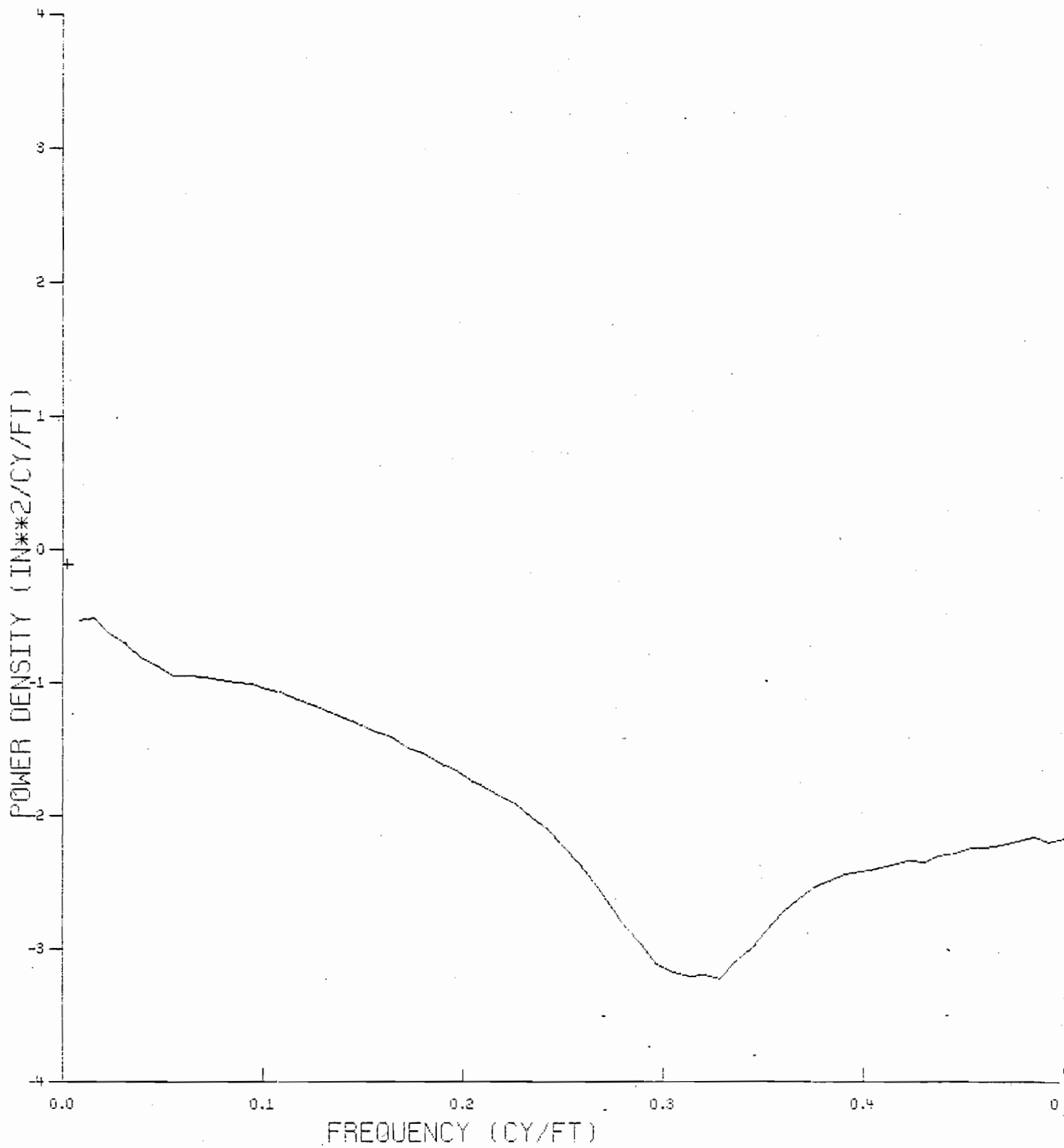
SEGMENTS AVERAGED= 11

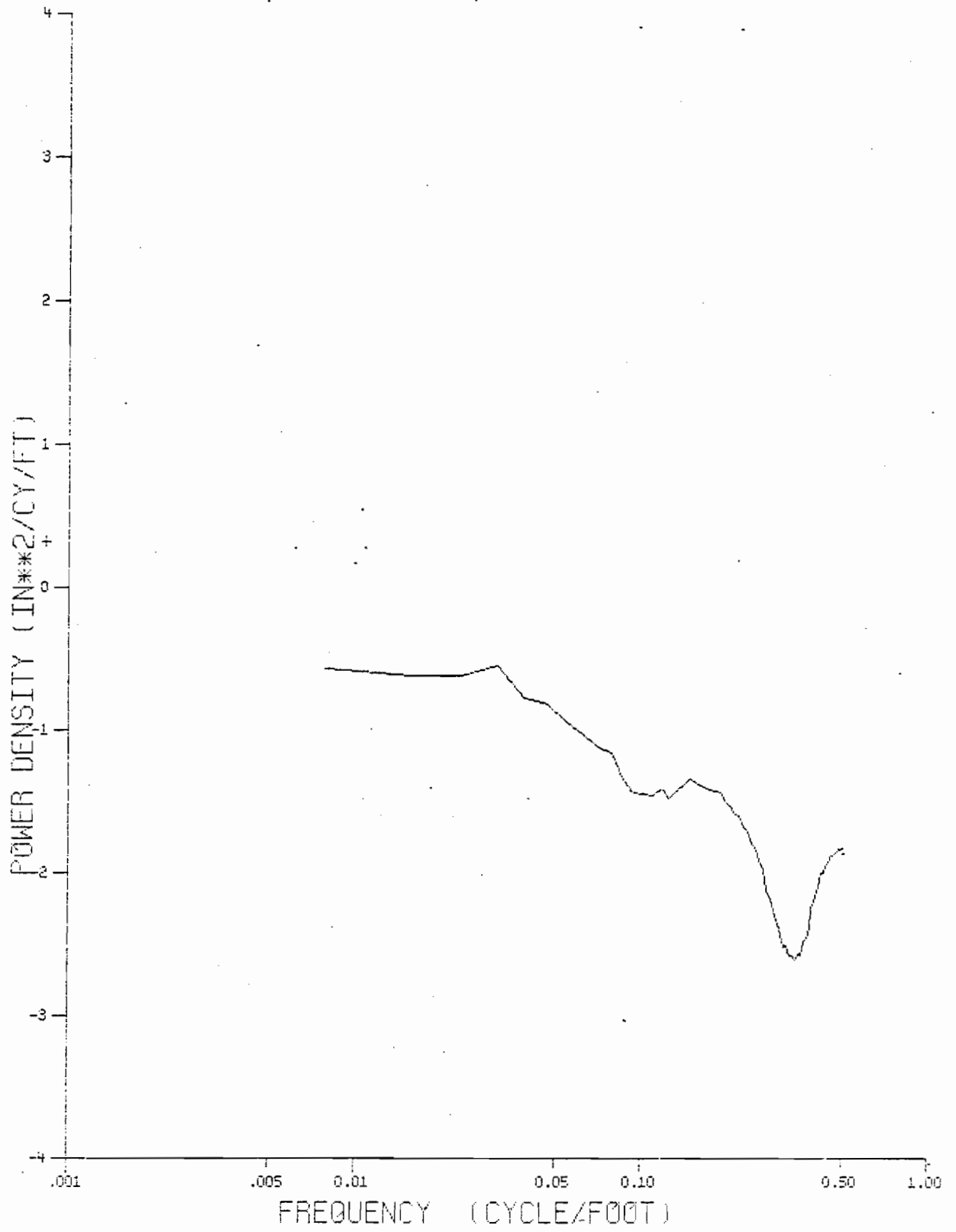
:QUB, PLOTP2
:QUB, PLOTP3, ,1

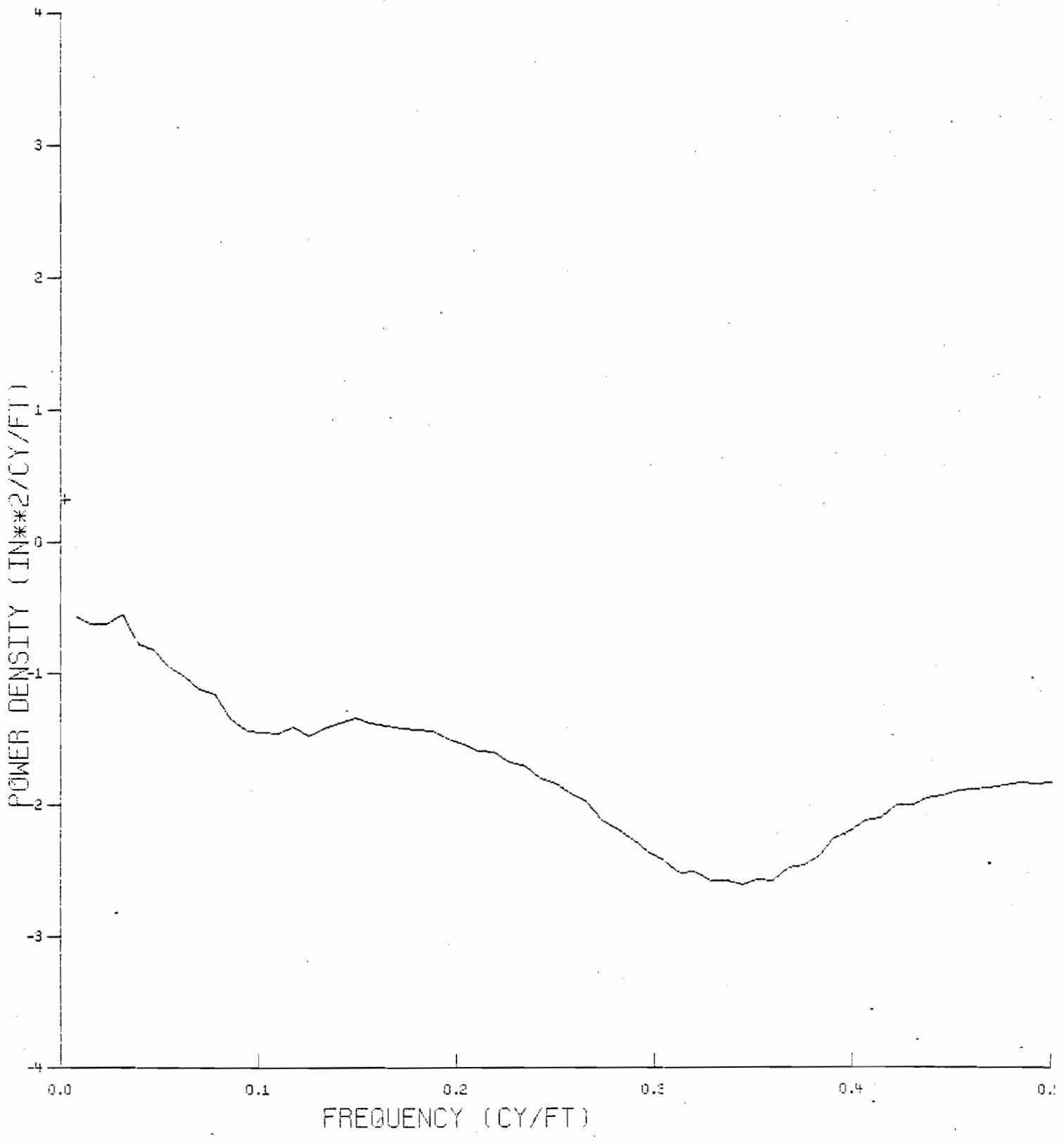


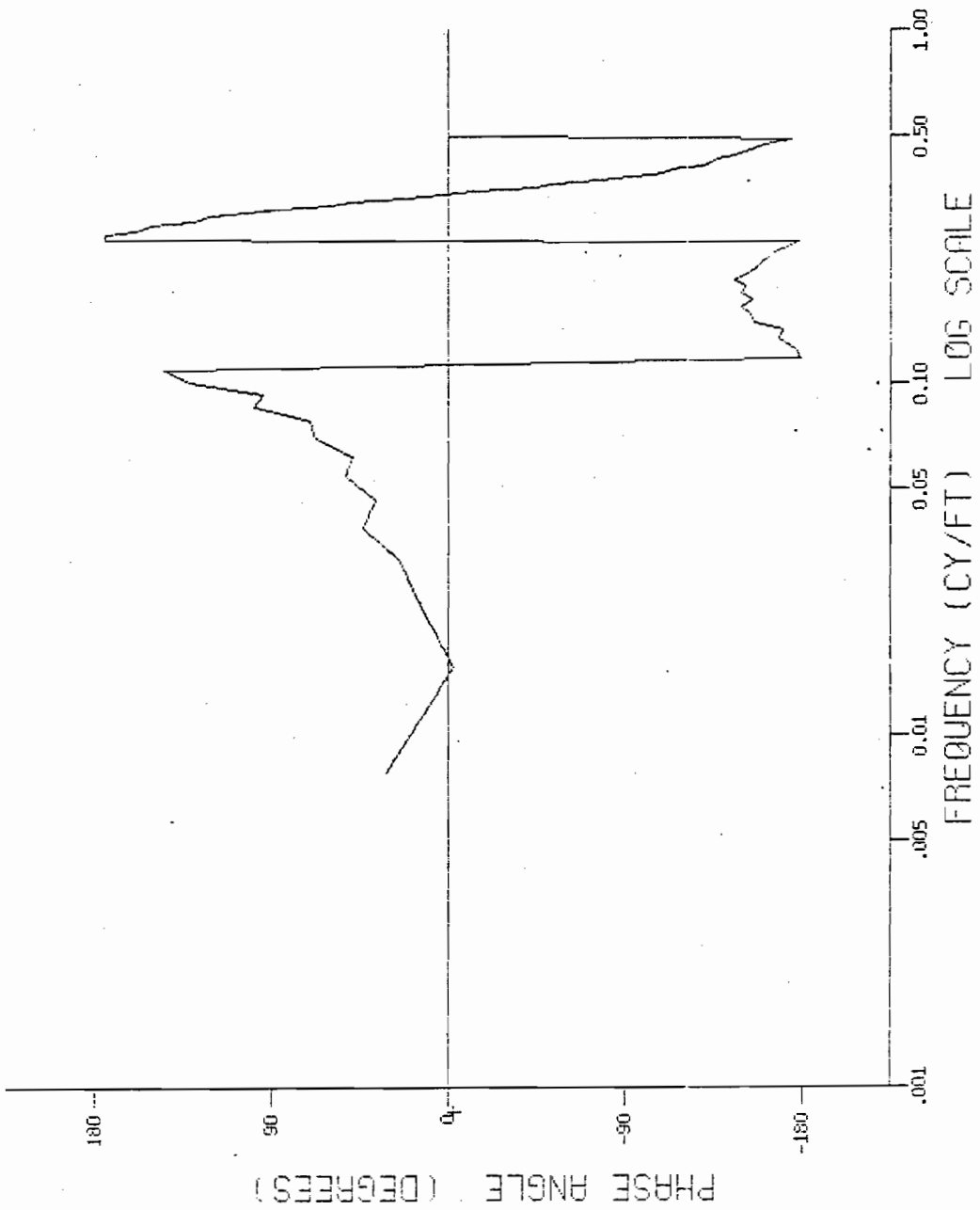


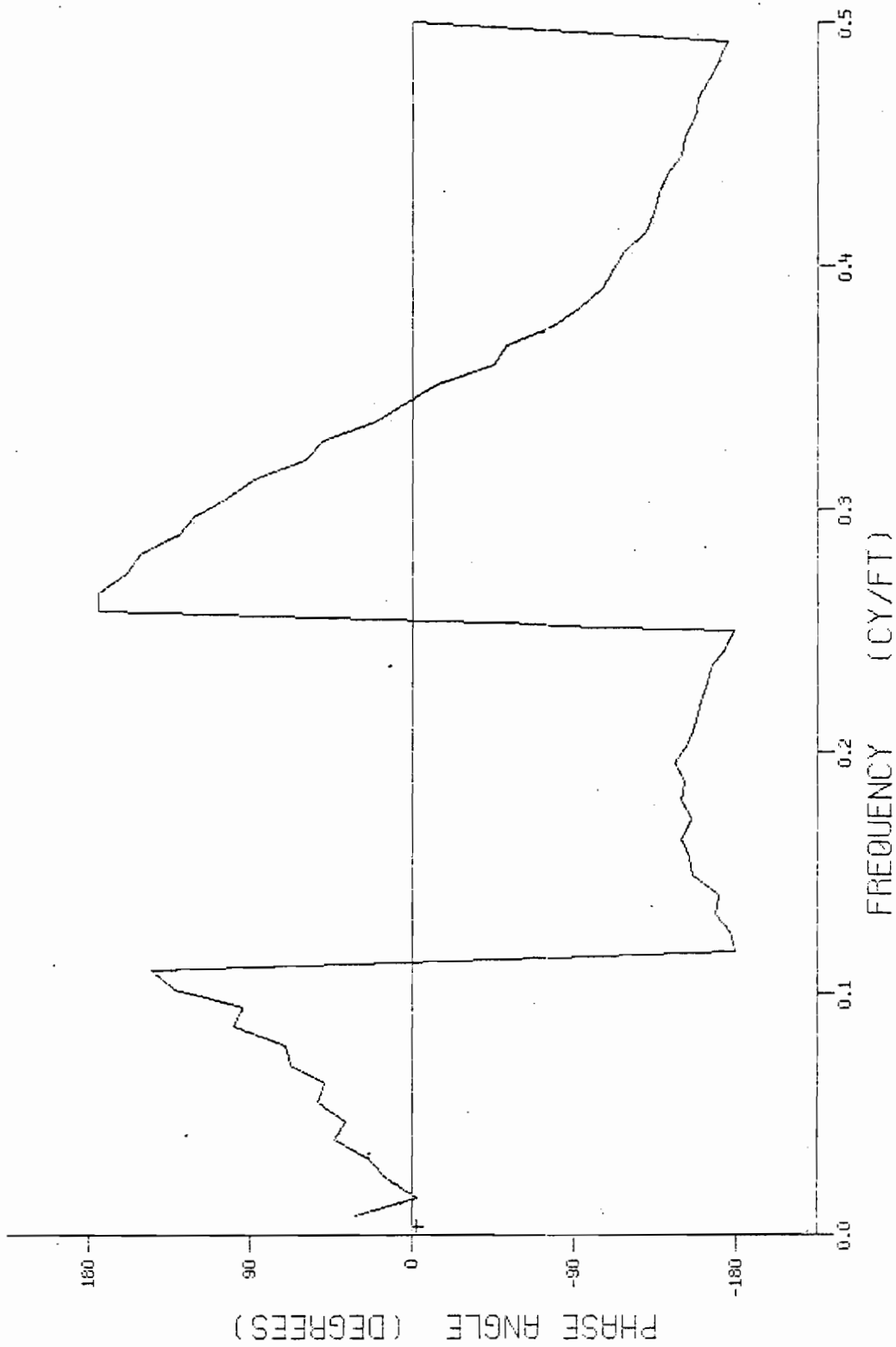


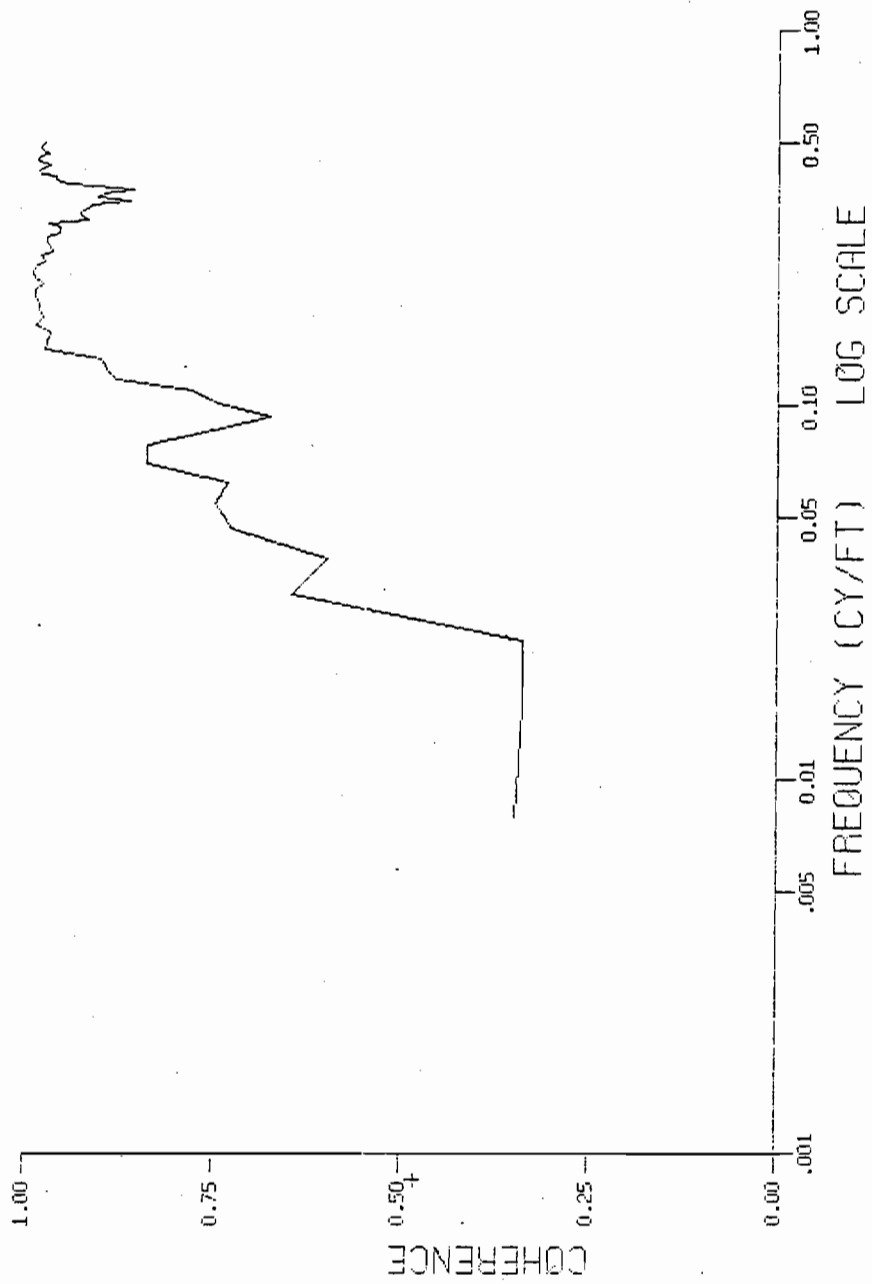


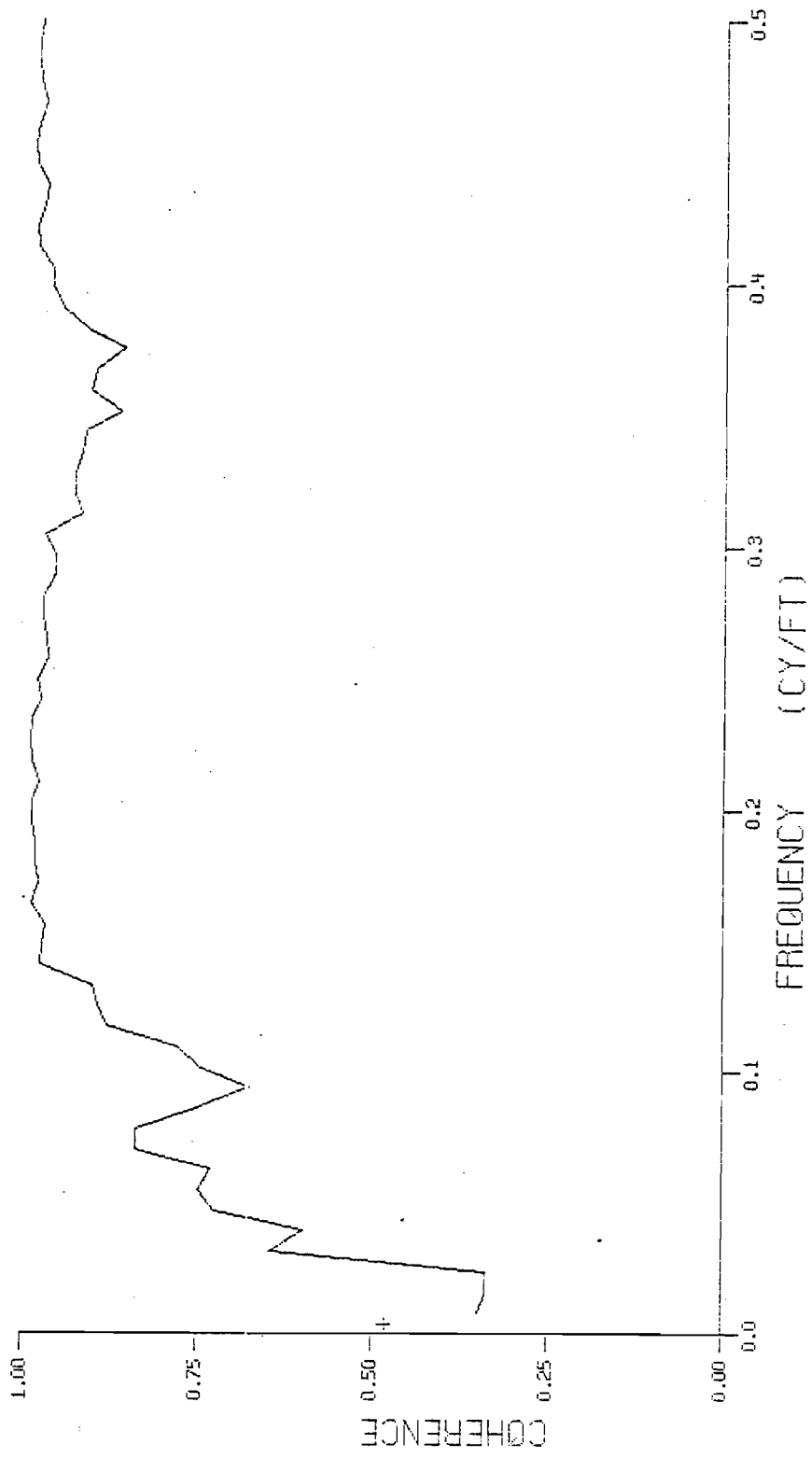


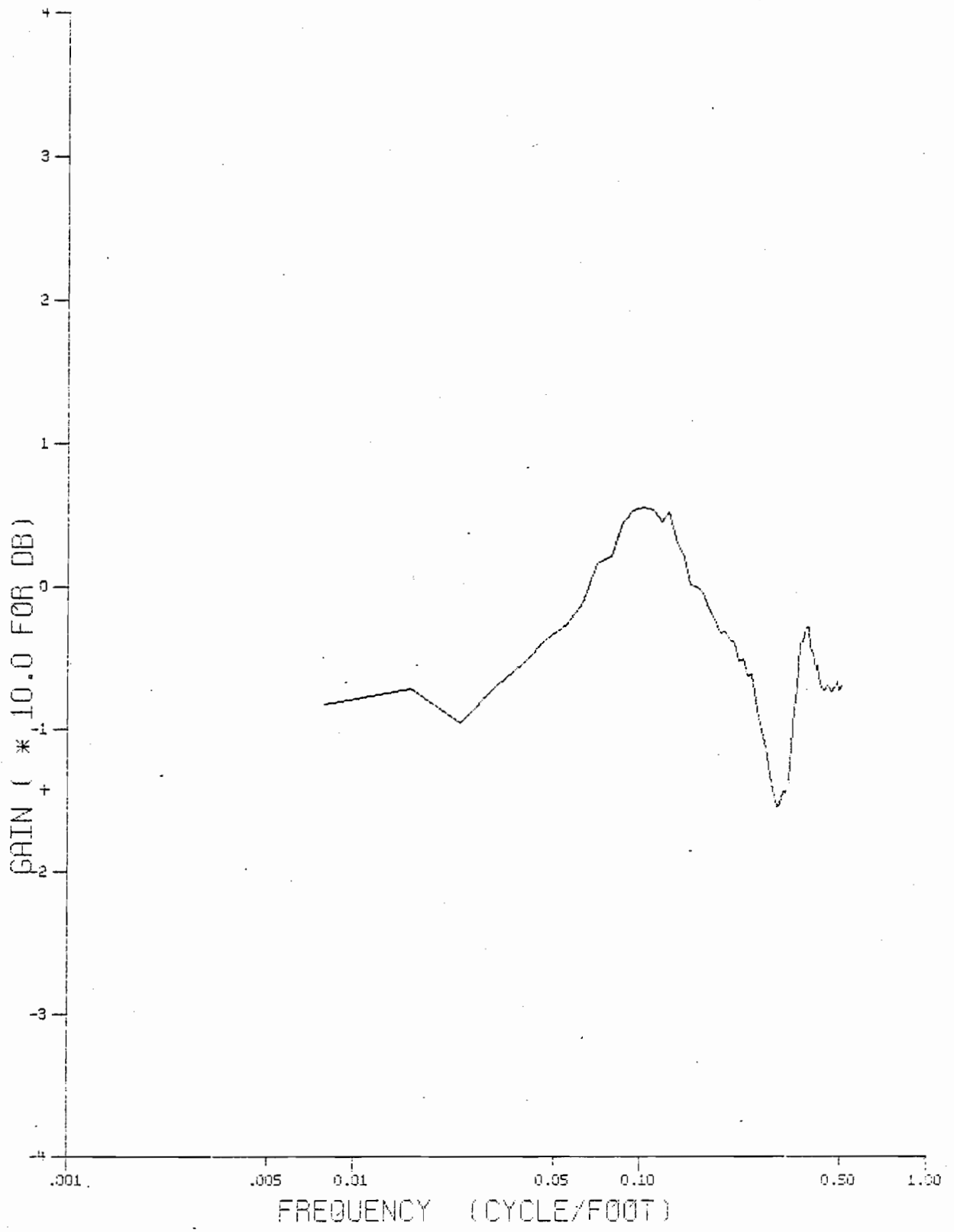


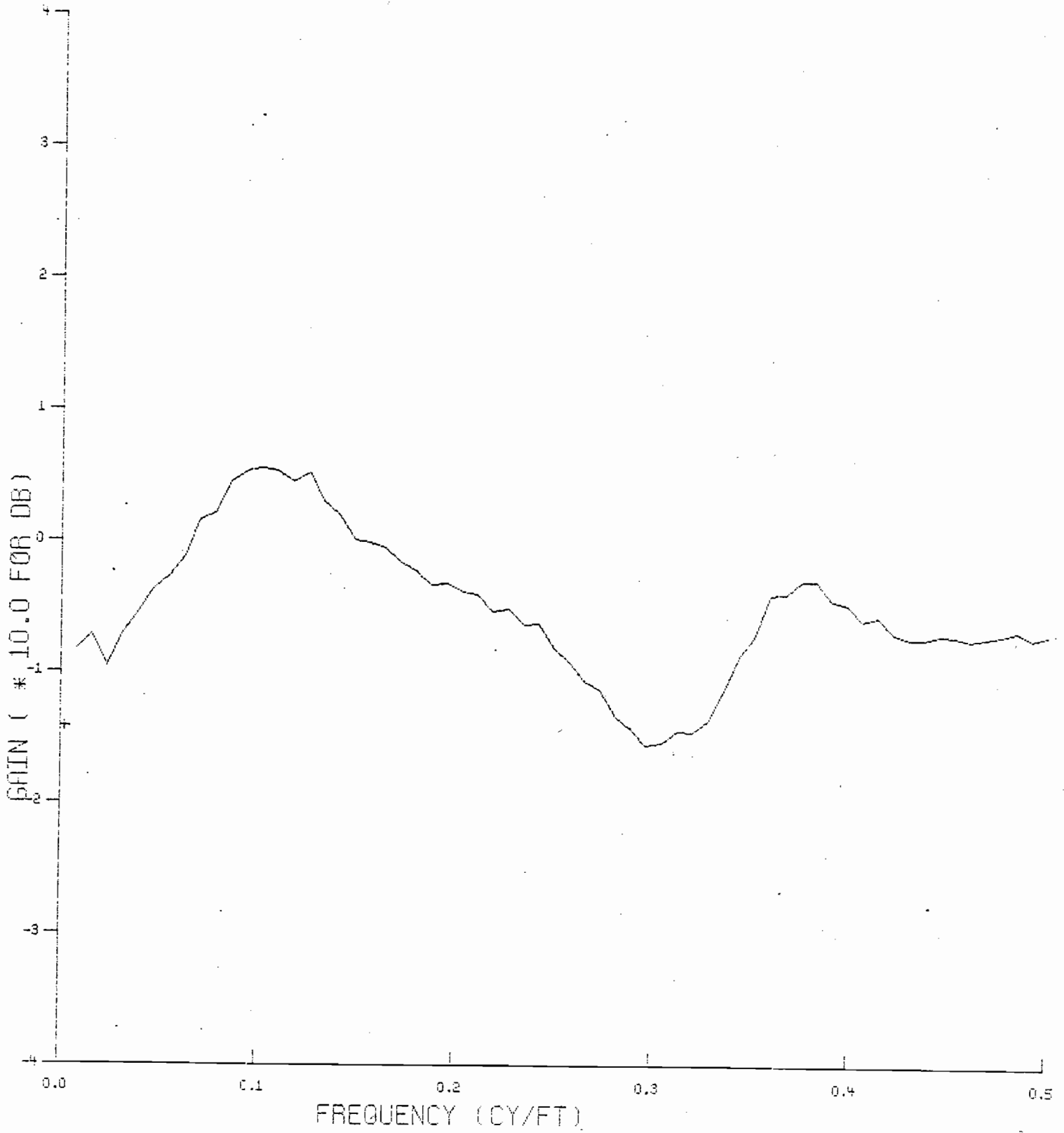












D.6 REFERENCES

1. Bendat, J. S. and Piersol, A.G., "Random Data: Analysis and Measurement Procedures," John Wiley & Sons, Inc., New York, 1971.
2. Anis, Z., "Location of Track Irregularities," prepared for Department of Transportation under Contract DOT-TSC-1206, September 1977.
3. Otnes, R. K. and Enochson, L., "Digital Time Series Analysis," John Wiley & Sons, New York, 1972.
4. Bloomfield, P., "Fourier Analysis of Time Series: An Introduction," John Wiley & Sons, 1976.
5. IEEE, "Programs for Digital Signal Processing," IEEE Press, New York, 1979.

APPENDIX E

CROSS SPECTRAL DENSITY, COHERENCE AND TRANSFER FUNCTION PLOTS

This appendix shows the relationships between different track geometry parameters. The relationships are given in the form of cross spectral densities, phase spectra, coherence spectra, and magnitude of transfer functions. Plots are given for relationships between gage and alignment; crosslevel and profile; crosslevel and alignment; crosslevel and gage; gage and profile; and profile and alignment. These plots are typical of all the current FRA track classes.

These plots were generated by processing the data using the frequency domain analysis software package, FEDAL. Therefore, the reader is referred to Appendix D for terminology and other details.

All the plots are given on log-log scale. The frequency axis covers a dynamic range of 10^{-3} to 1 cy/ft, although the valid data is limited to 0.5 cy/ft. The ordinate for cross spectral densities and transfer function ($|H(\phi)|^2$) cover a range of 10^{-4} to 10^4 .

Ordinate values are indicated in logs, i.e., a value of 2 corresponds to 10^2 and a value of -2 corresponds to 10^{-2} . The phase angle is plotted from -180 to 180 degrees. Values of squared coherence lies between 0 and 1 and accordingly that is the range of the coherence spectrum.

Figure E-1 shows that the coherence between gage and left minus right alignment is almost unity for wavelengths between 2 and 200 feet. This implies that there is a perfect linear relationship between gage and left minus right alignment as one would expect due to physical reasons and the measurement techniques used for gage and alignment. The coherence drops rapidly for wavelengths

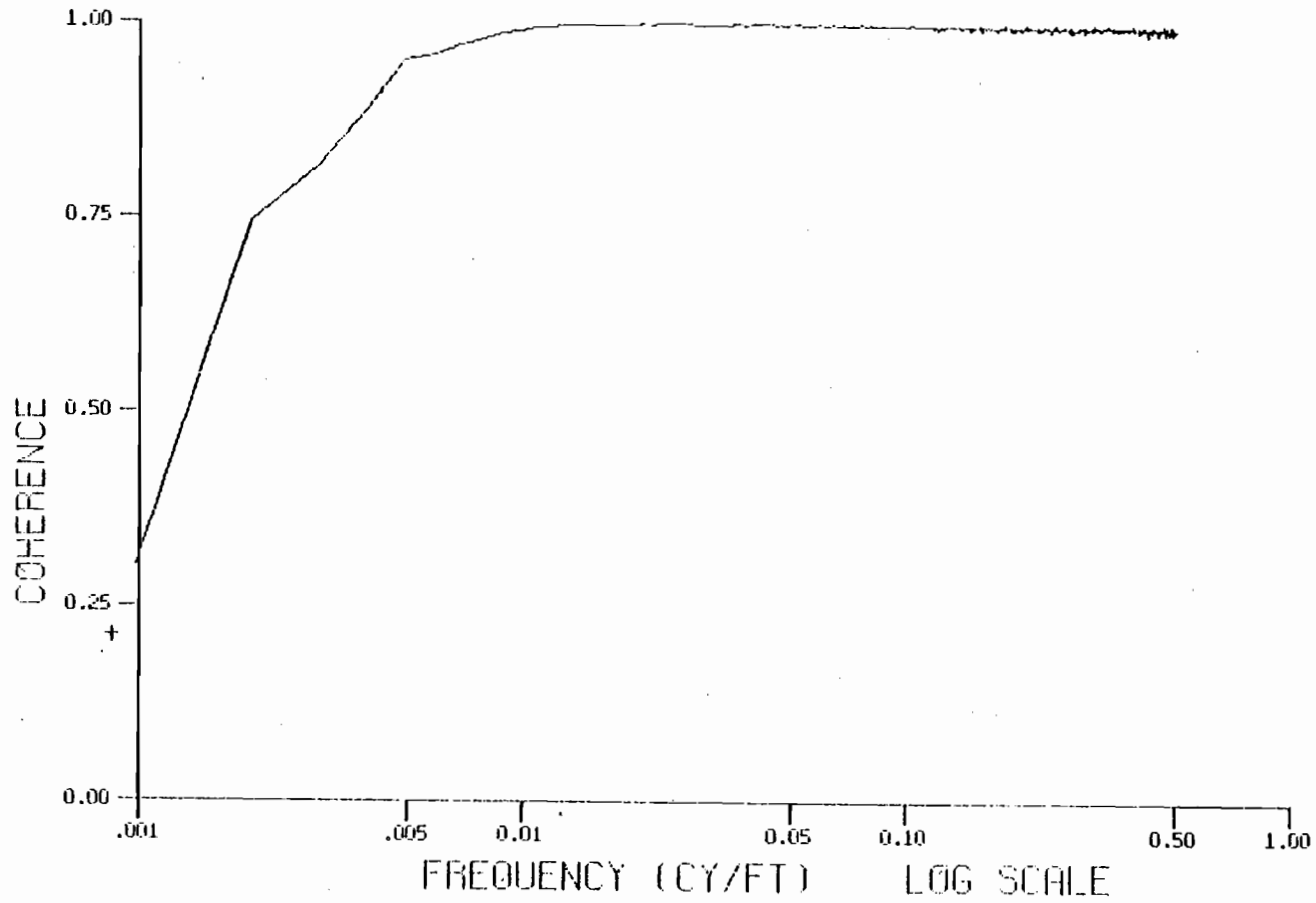


Figure E-1. Squared Coherence Between Gage and Left Minus Right Alignment

longer than 200 feet. This is due to the space curve filter used to process the alignment data. The long wavelength cut-off for the space curve filter used in this study was 208 feet. This is further depicted in Figure E-2 which shows the magnitude (gain) of the transfer function between gage and alignment variations. The gain is plotted on log scale and thus a value of zero indicates a unity gain. Note that the gain curve in Figure E-2 is similar to the gain characteristics of the space curve filter. The oscillations about unity is a characteristic of this filter. These results provide confidence in the measurements and data processing algorithms used to characterize the relationships between gage and alignment variations. It should be noted that the valid wavelength range in gage and alignment plots is from 2 to 200 feet.

Figure E-3 shows an example of coherence between crosslevel and left minus right profile. As expected, the coherence is almost unity for most wavelengths between 8 and 200 feet. The coherence drops for wavelengths shorter than eight feet because of low signal to noise ratio. The cutoff wavelength for the profile space curve filter was also 208 feet. This explains the drop in coherence for wavelengths longer than 200 feet. Some of the sections processed for relationships between crosslevel and left minus right profile showed significant notches in coherence at 78, 39 and 9 feet wavelengths. This situation is typical of system non-linearities. It should be mentioned that the 9 feet wavelength corresponds to the wheel diameters on FRA T-6 car used to collect the track geometry data. However, 39 feet wavelength is typically found in the bolted track and 78 feet wavelength is common in the welded track.

Crosslevel and profile are measured with separate instrumentation on T-6. Therefore, results described in this paragraph provide confidence in the measurements and processing techniques used to develop the relationships between crosslevel and profile variations.

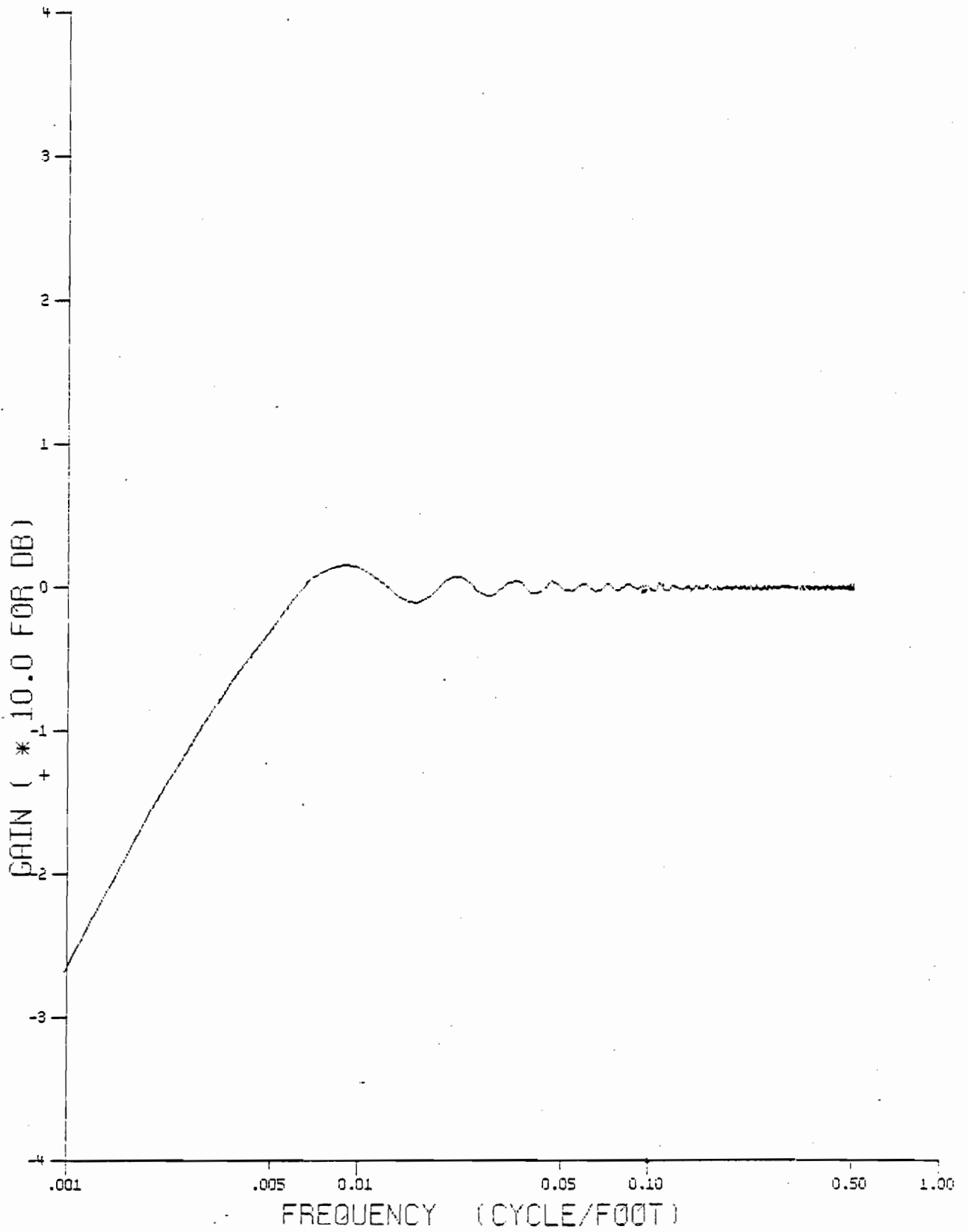


Figure E-2. Magnitude of Transfer Function Between Gage and Left Minus Right Alignment

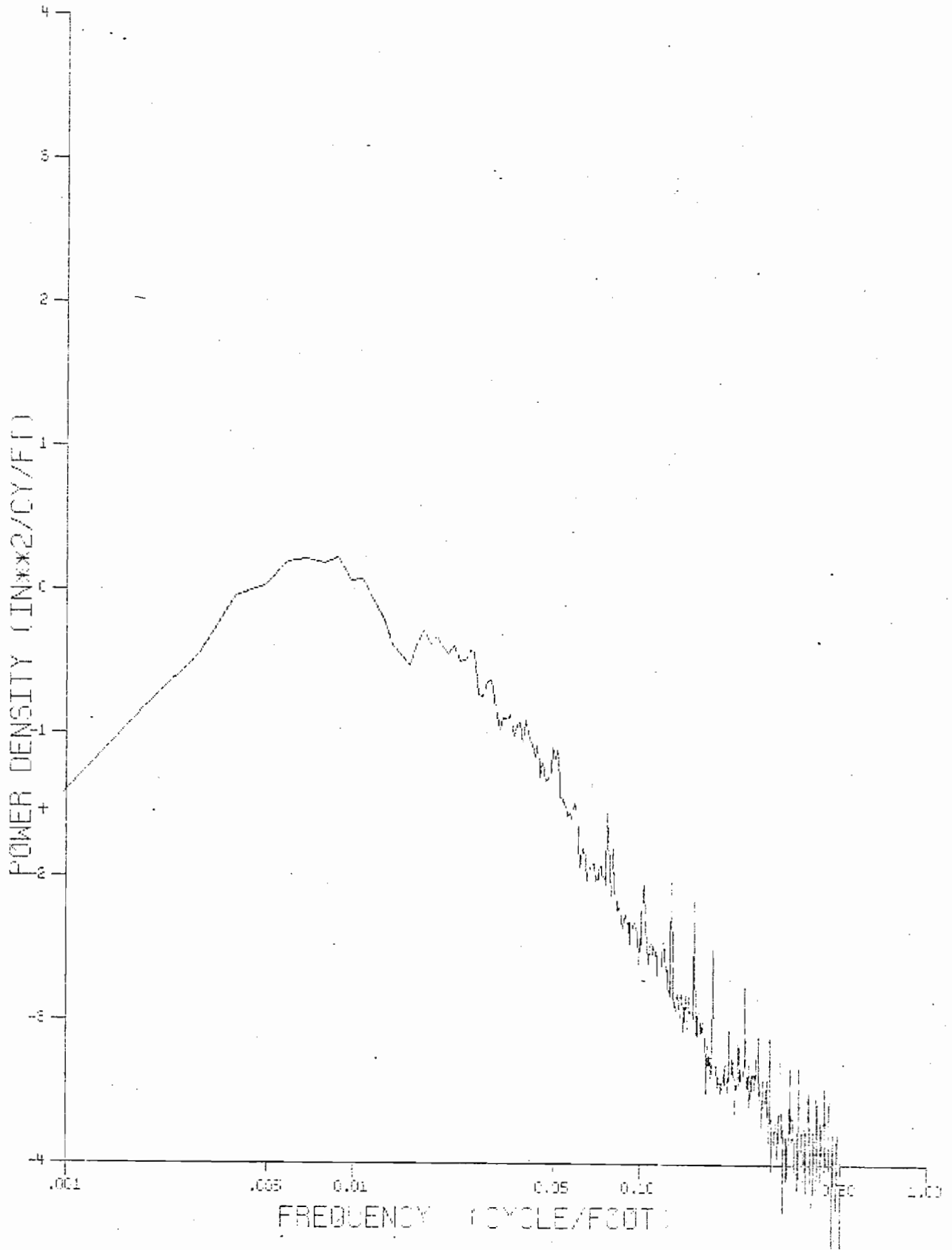
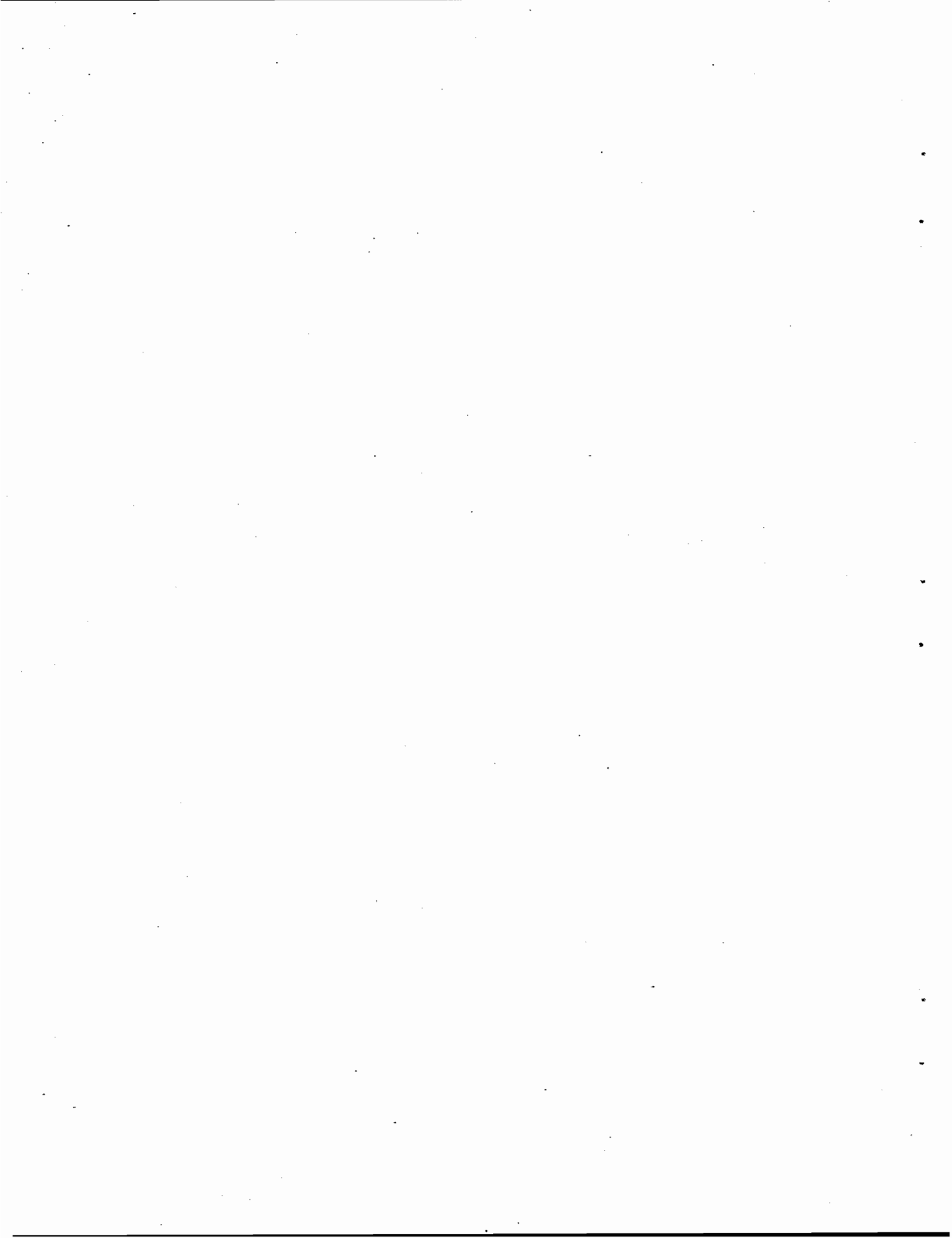


Figure E-3. Cross Spectral Density Between Crosslevel and Left Minus Right Profile

E-5/F-6



E-1. GAGE AND ALIGNMENT

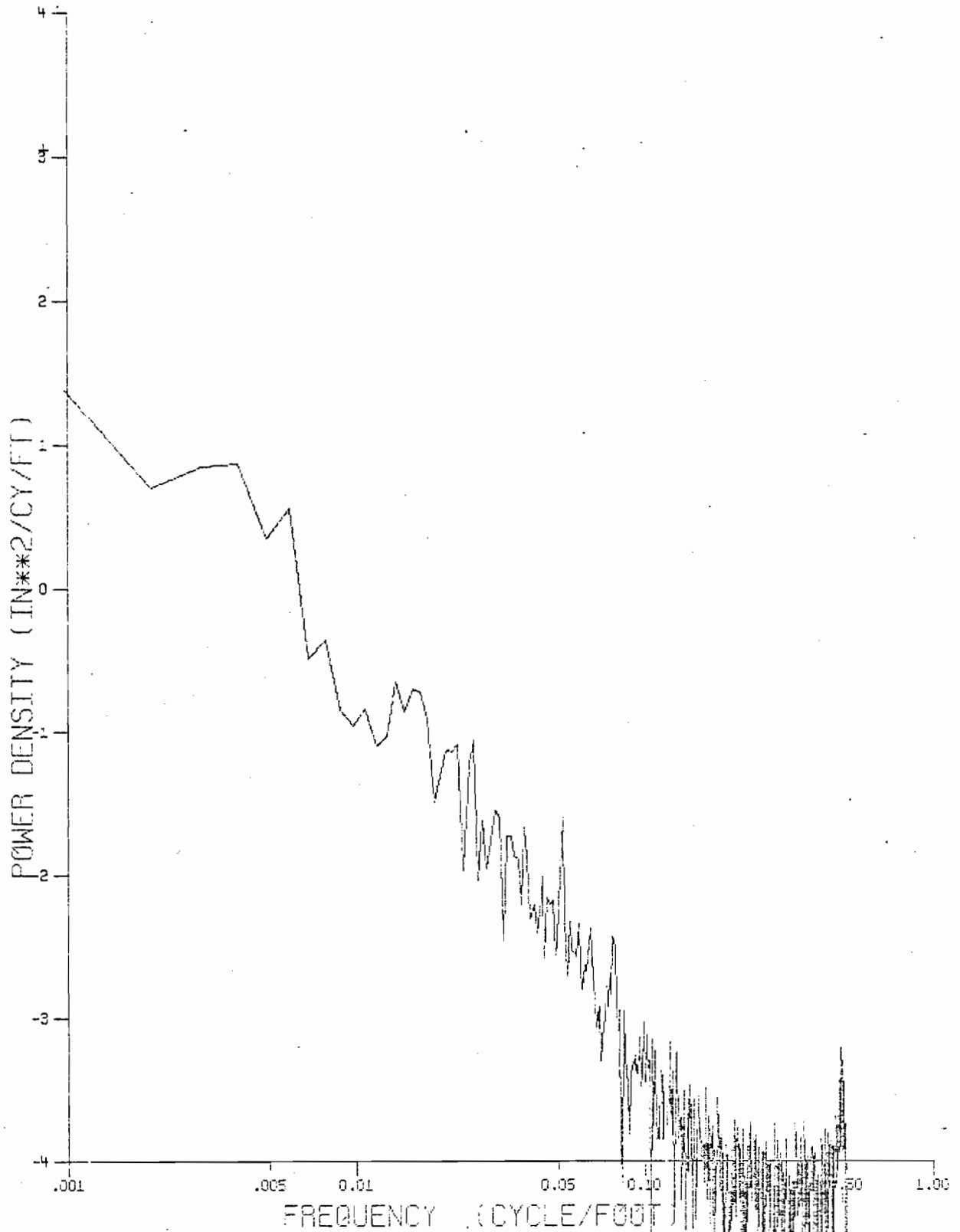


Figure E-4. Cross Spectral Density Between Magnitude of Gage and Mean Alignment (Track Class 3)

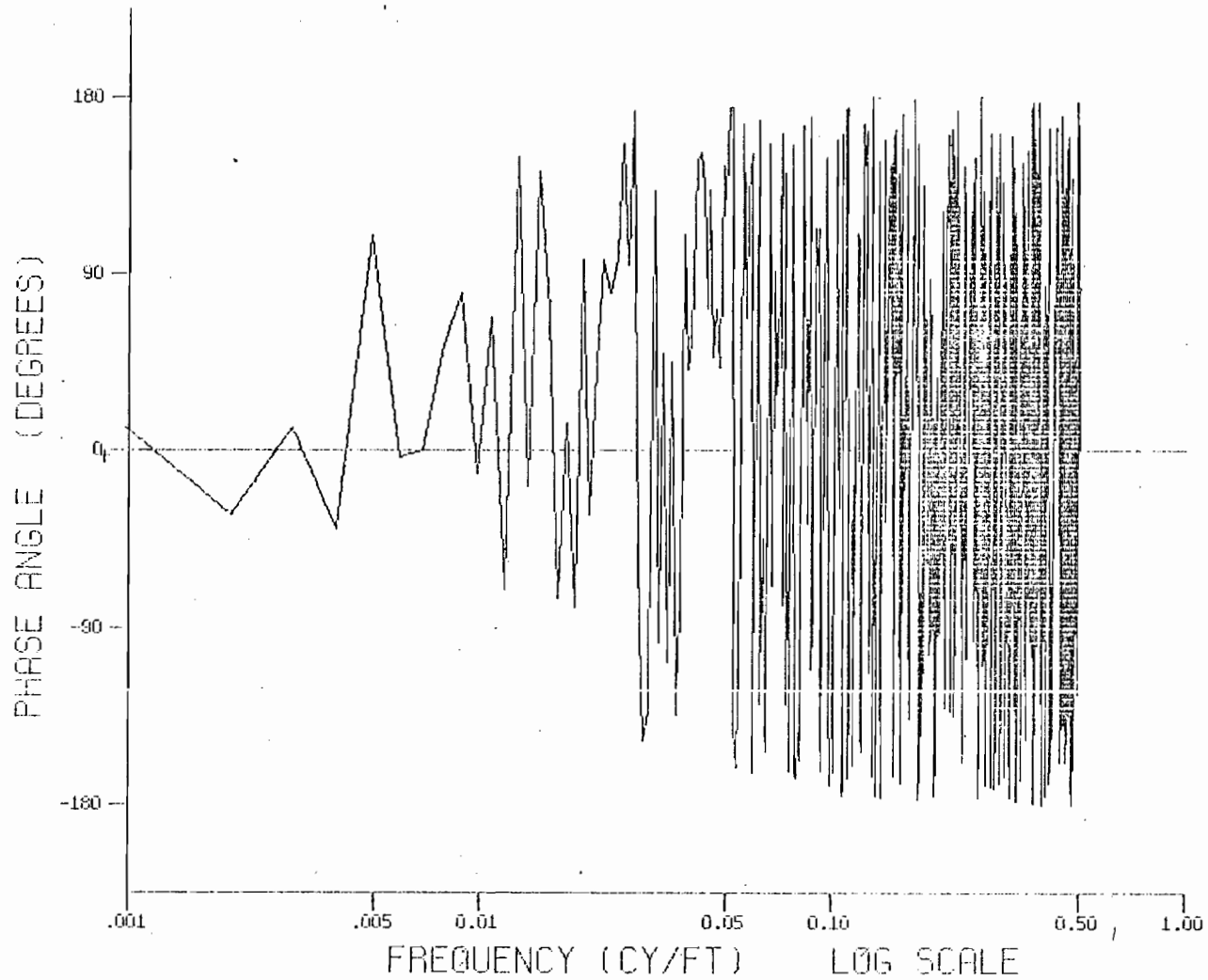


Figure -5. Phase Angle Between Magnitude of Gage and Mean Alignment (Track Class 3)

E-10

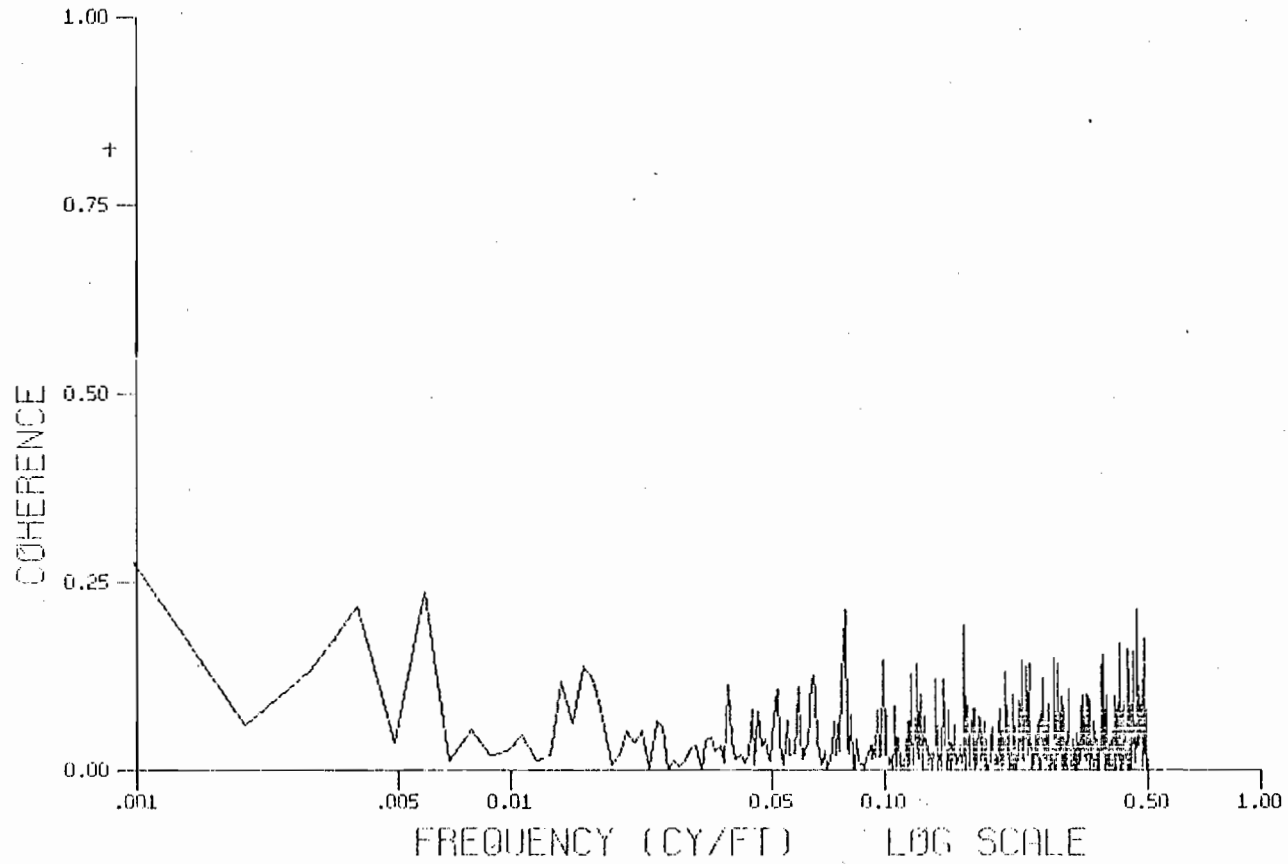


Figure E-6. Squared Coherence Between Magnitude of Gage and Mean Alignment (Track Class 3)

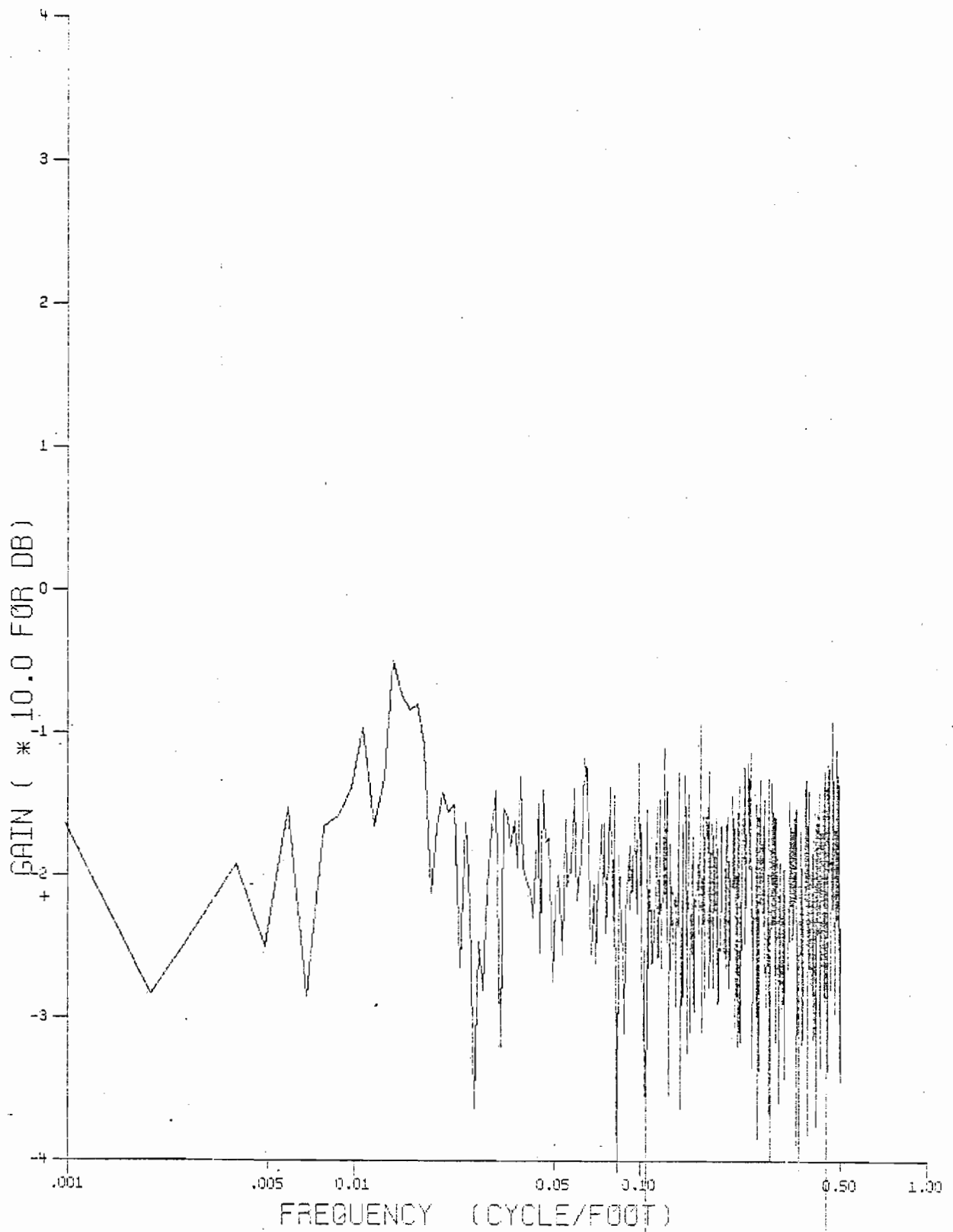


Figure E-7. Magnitude of Transfer Function Between
 Magnitude of Gage and Mean Alignment
 (Track Class 3)

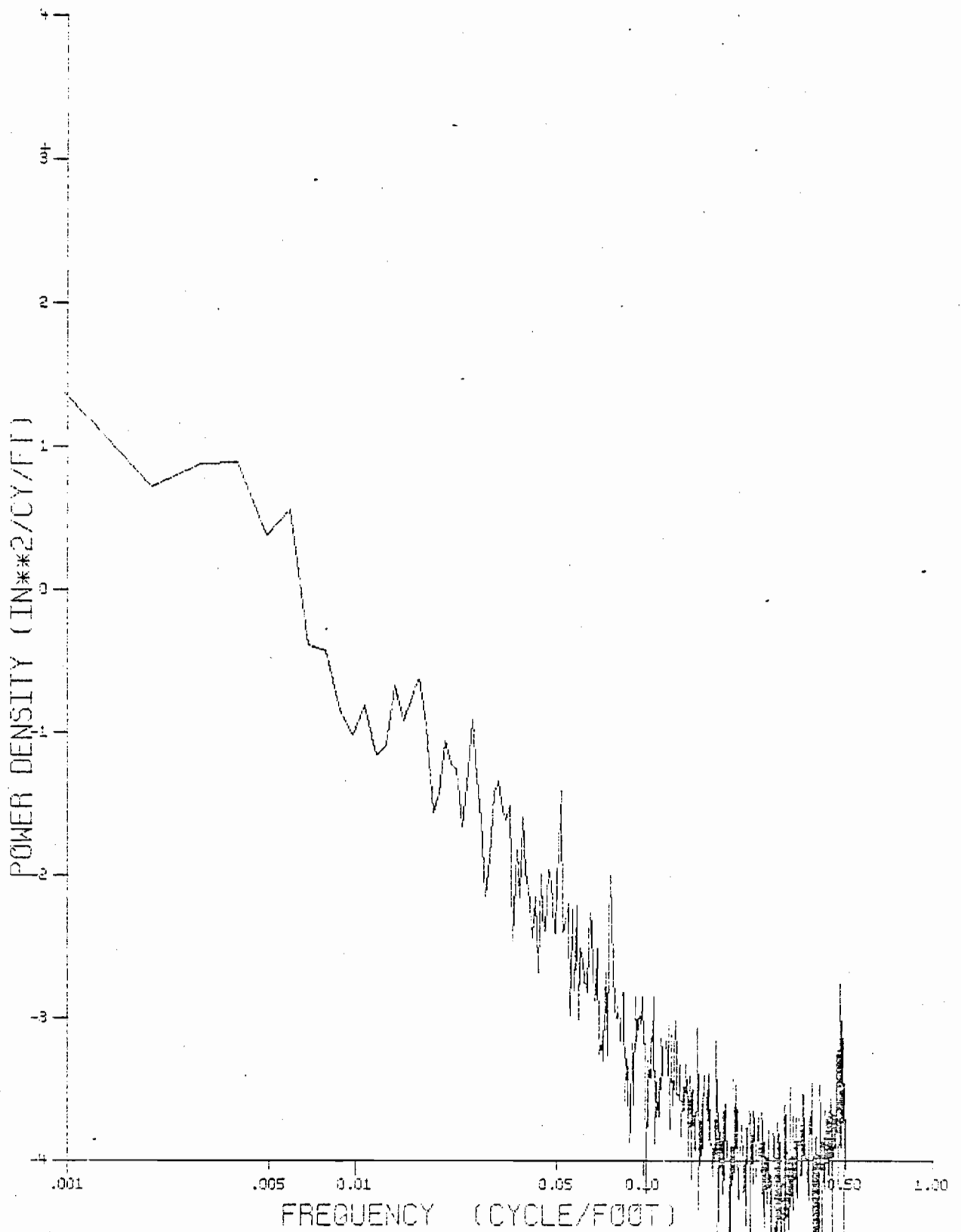


Figure E-8. Cross Spectral Density Between Magnitude of Gage and Right Rail Alignment (Track Class 3)

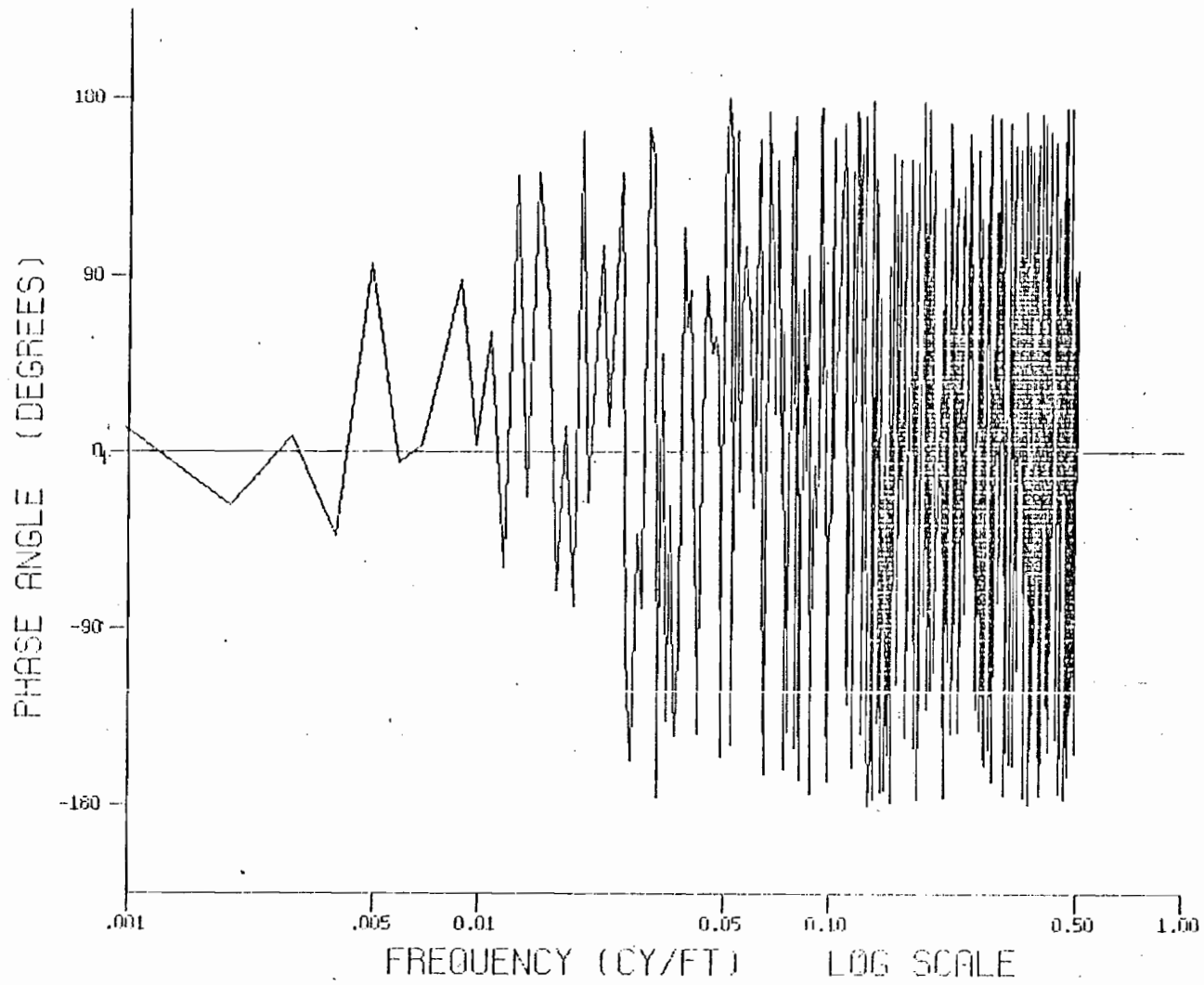


Figure E-9. Phase Angle Between Magnitude of Gage and Right Rail Alignment (Track Class 3)

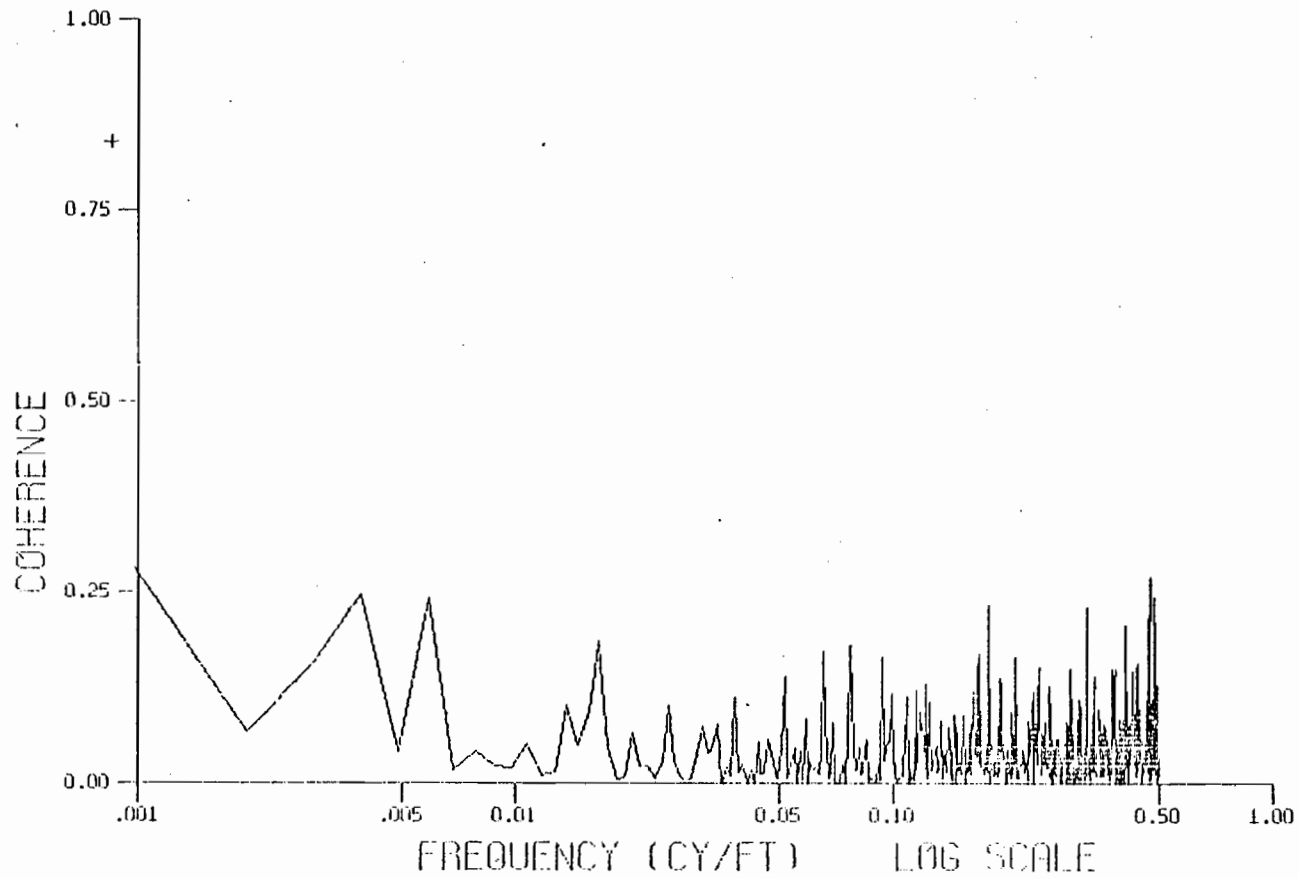


Figure E-10. Squared Coherence Between Magnitude of Gage and Right Rail Alignment (Track Class 3)

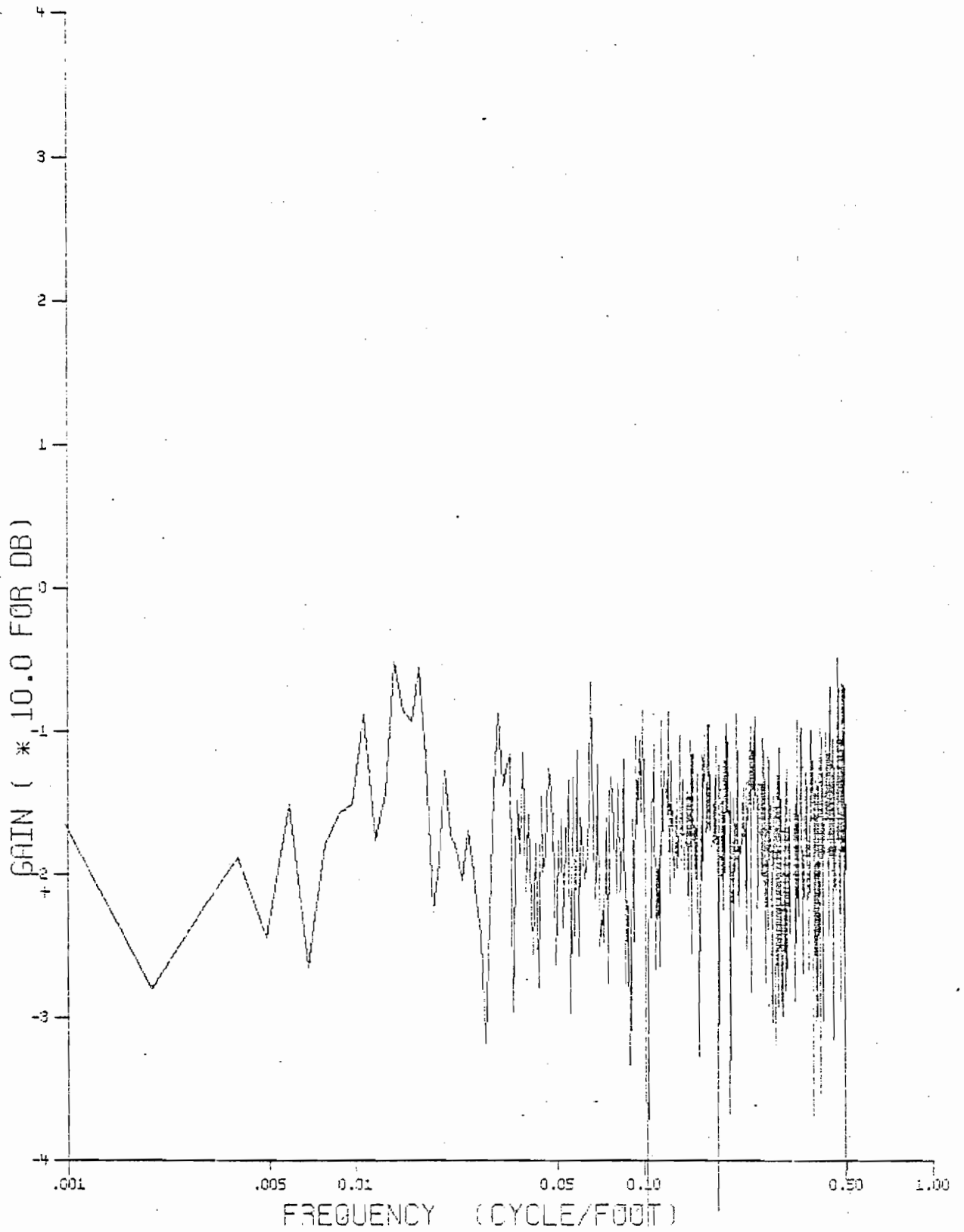


Figure E-11. Magnitude of Transfer Function Between
 Magnitude of Gage and Right Rail Alignment
 (Track Class 3)

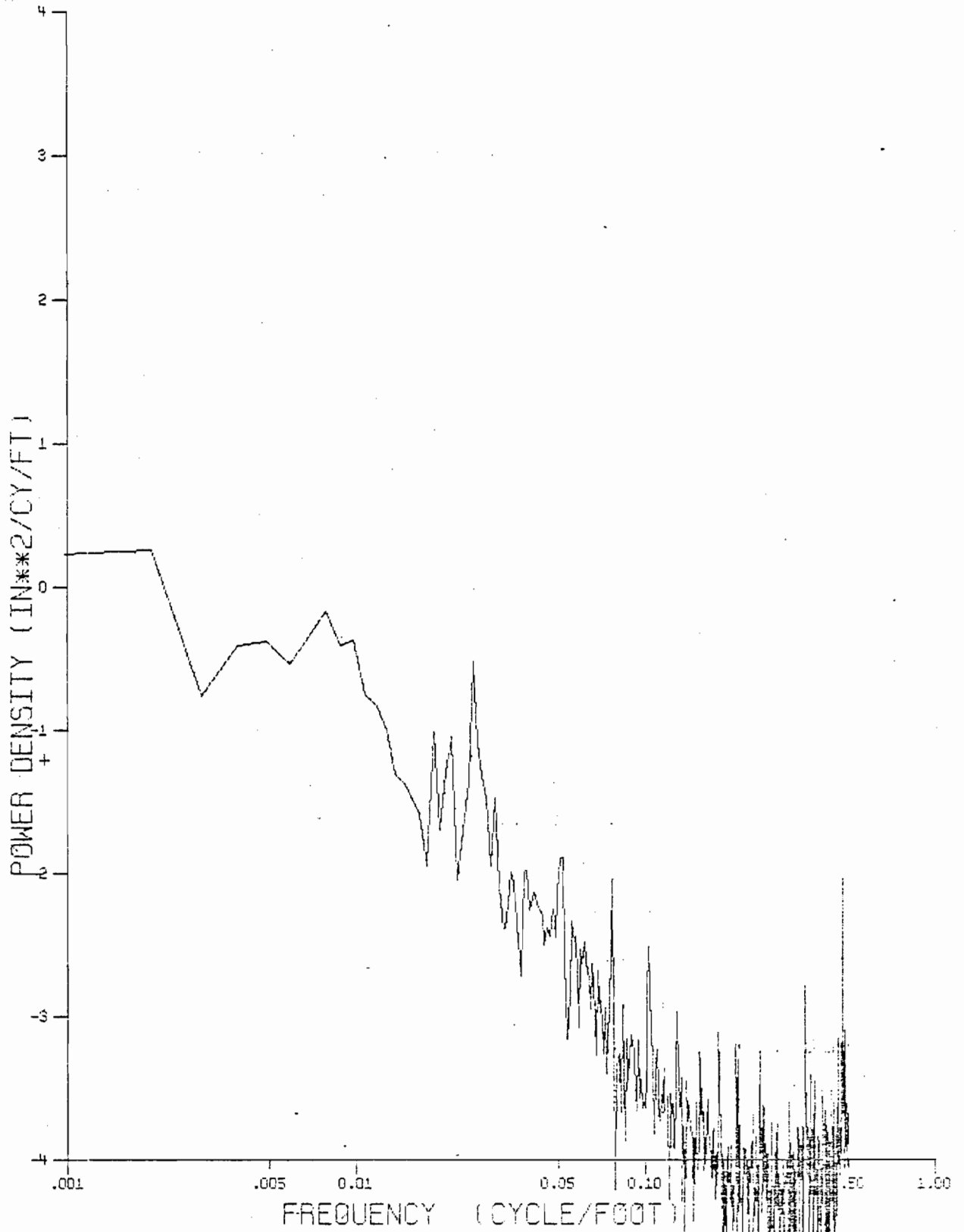


Figure E-12. Cross Spectral Denisty Between
 Gage and Mean Alignment Variations
 (Track Class 3)

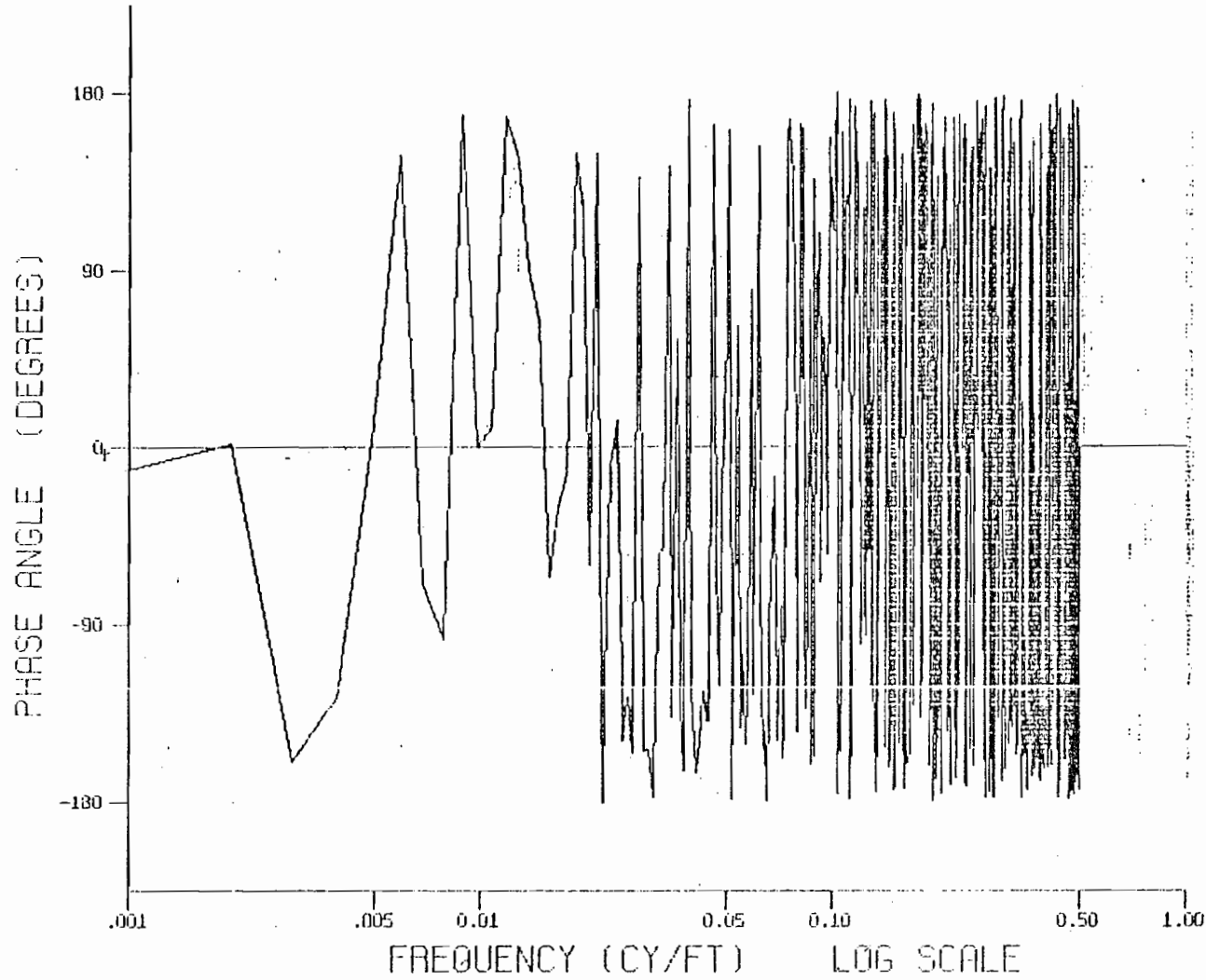


Figure E-13. Phase Angle Between Gage and Mean Alignment Variations (Track Class 3)

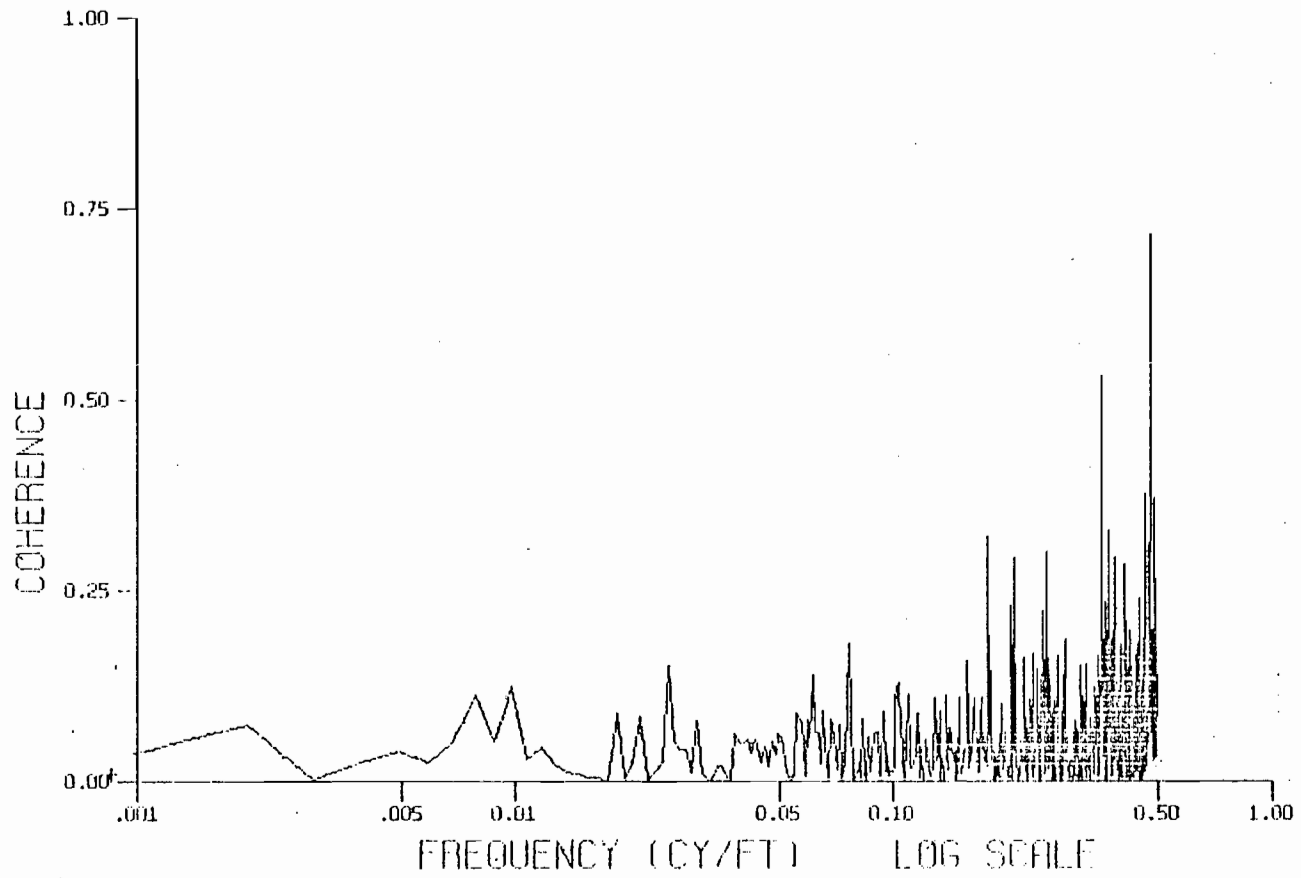


Figure E-14. . Squared Coherence Between Gage and Mean Alignment Variations (Track Class 3)

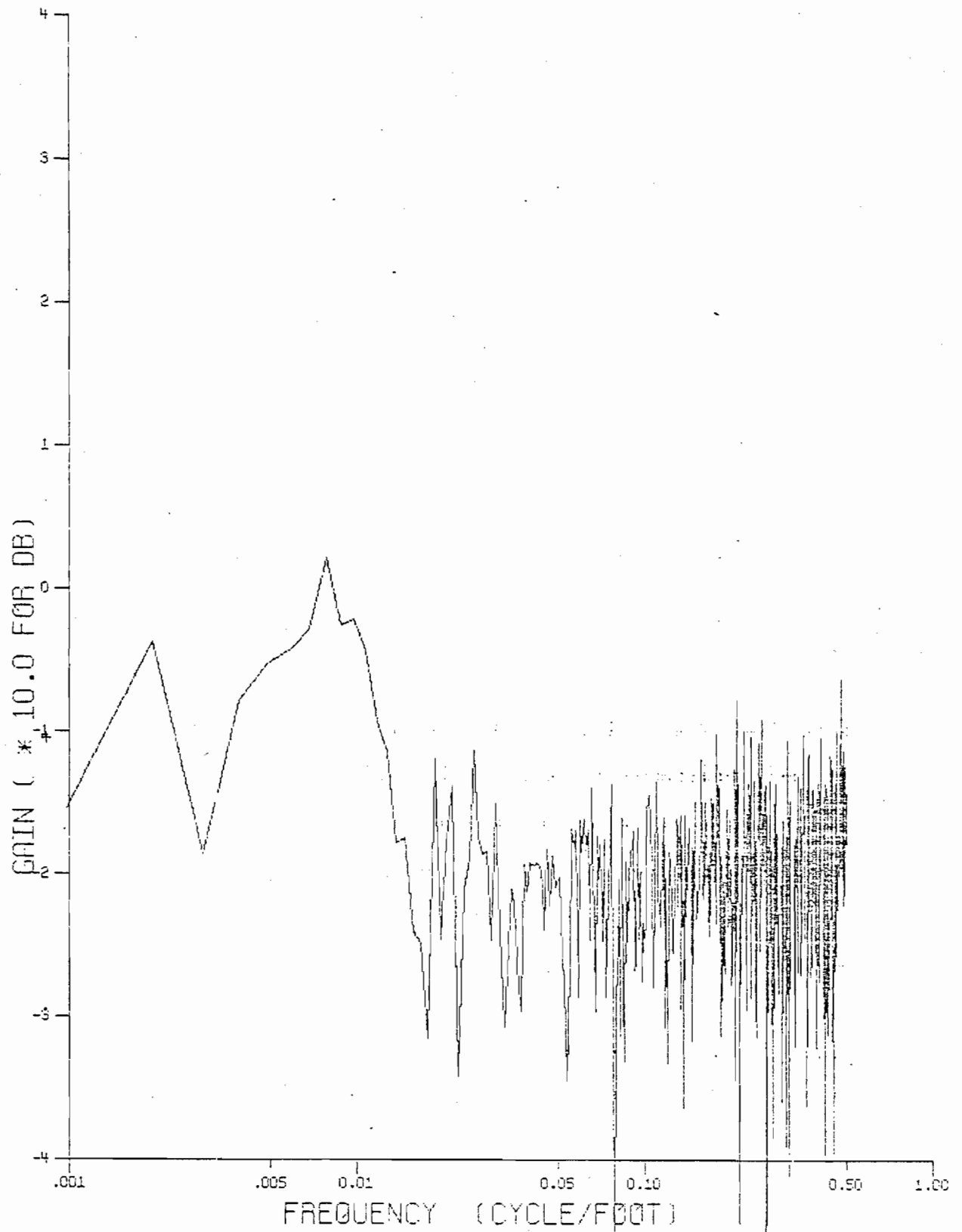


Figure E-15. Magnitude of Transfer Function Between Gage and Mean Alignment Variations (Track Class 3)

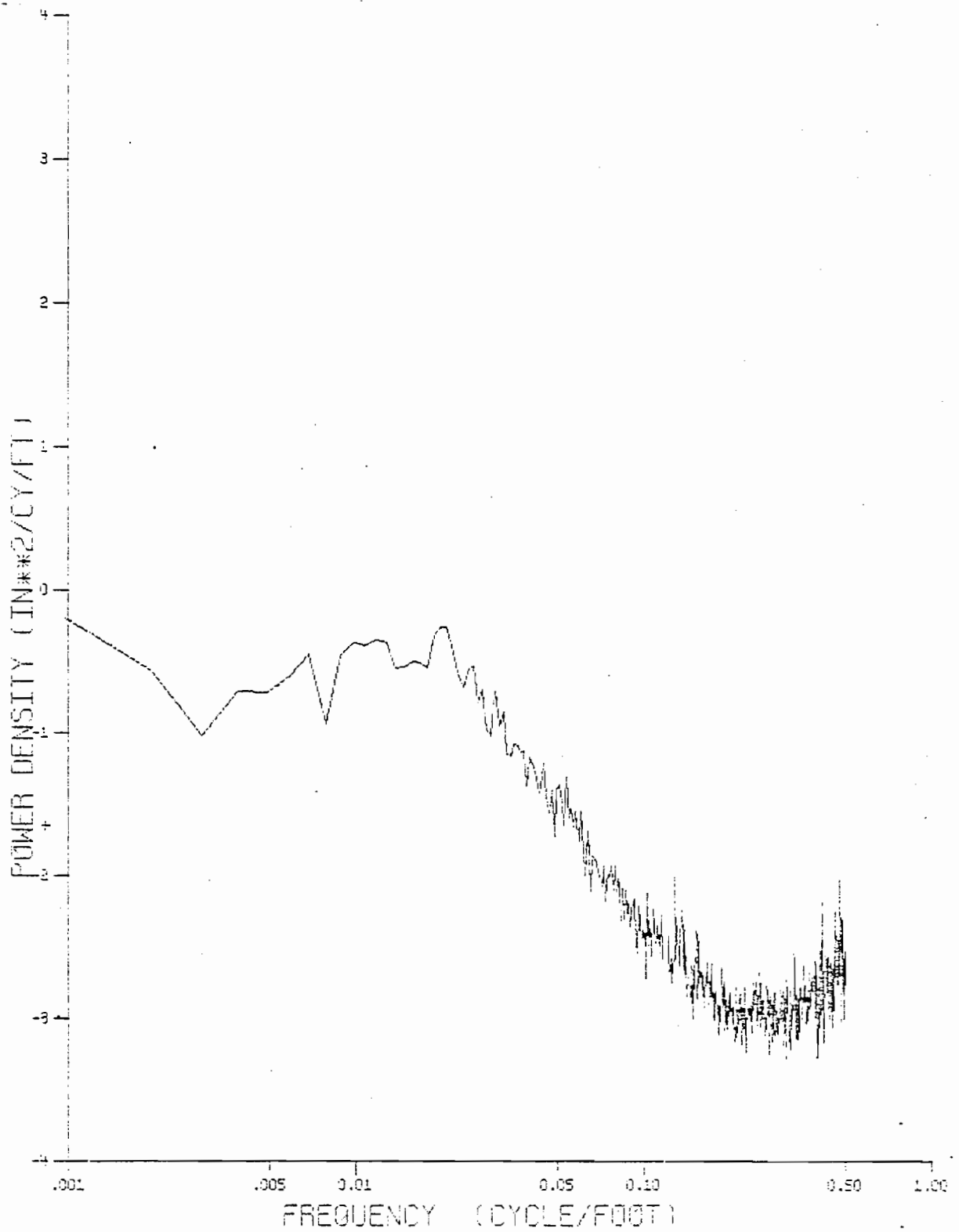


Figure E-16. Cross Spectral Density Between Gage and Right Rail Alignment Variations (Track Class 4)

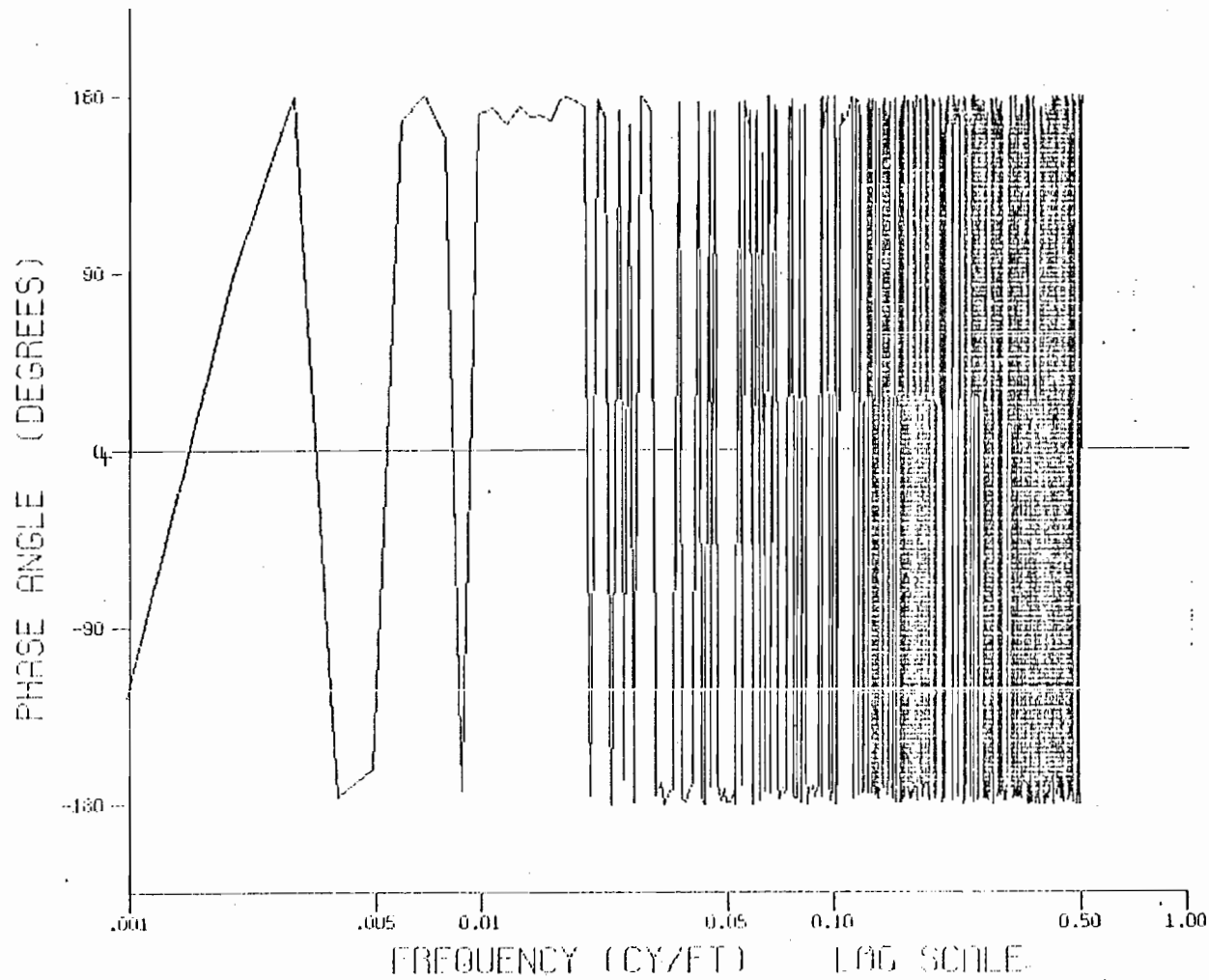


Figure E-17. Phase Angle Between Gage and Right Rail Alignment Variations (Track Class 4)

E-22

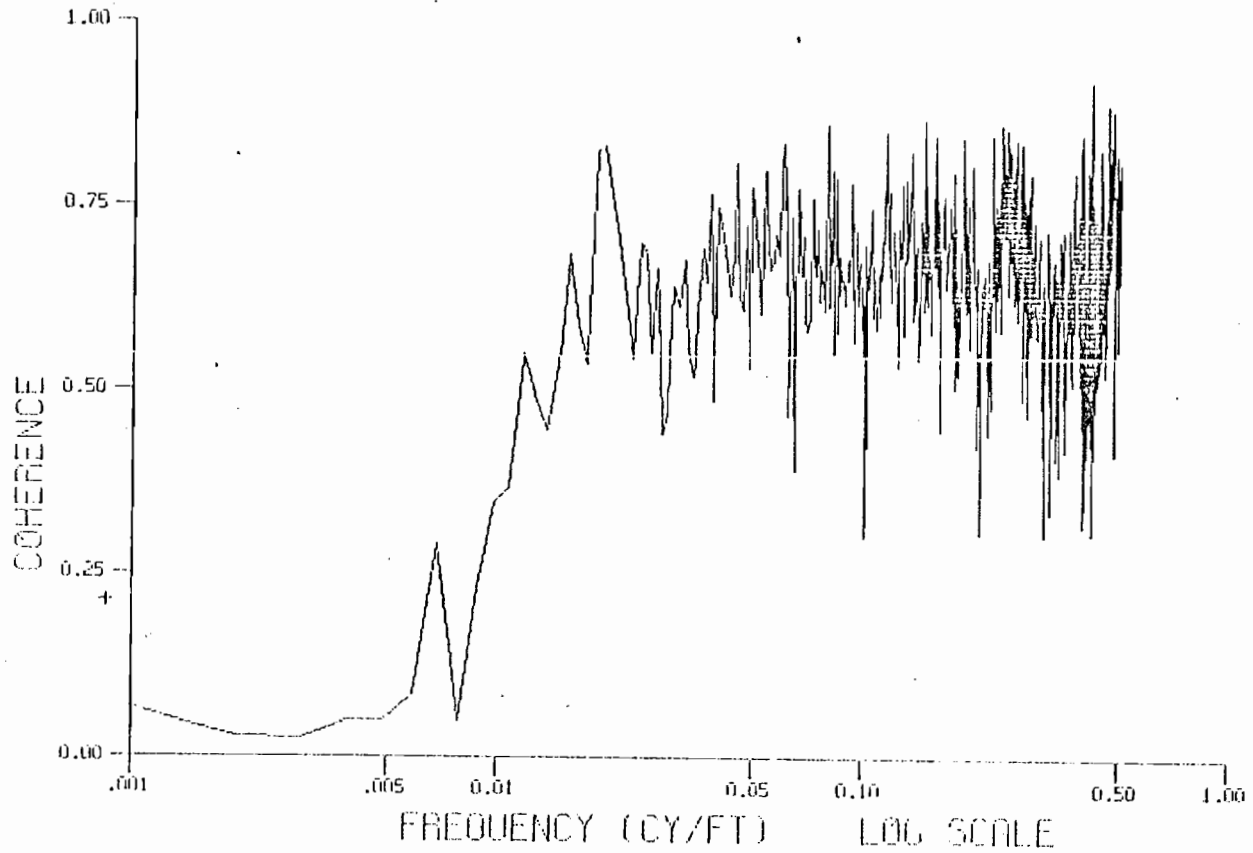


Figure E-18. Squared Coherence Between Gage and Right Rail Alignment Variations (Track Class 4)

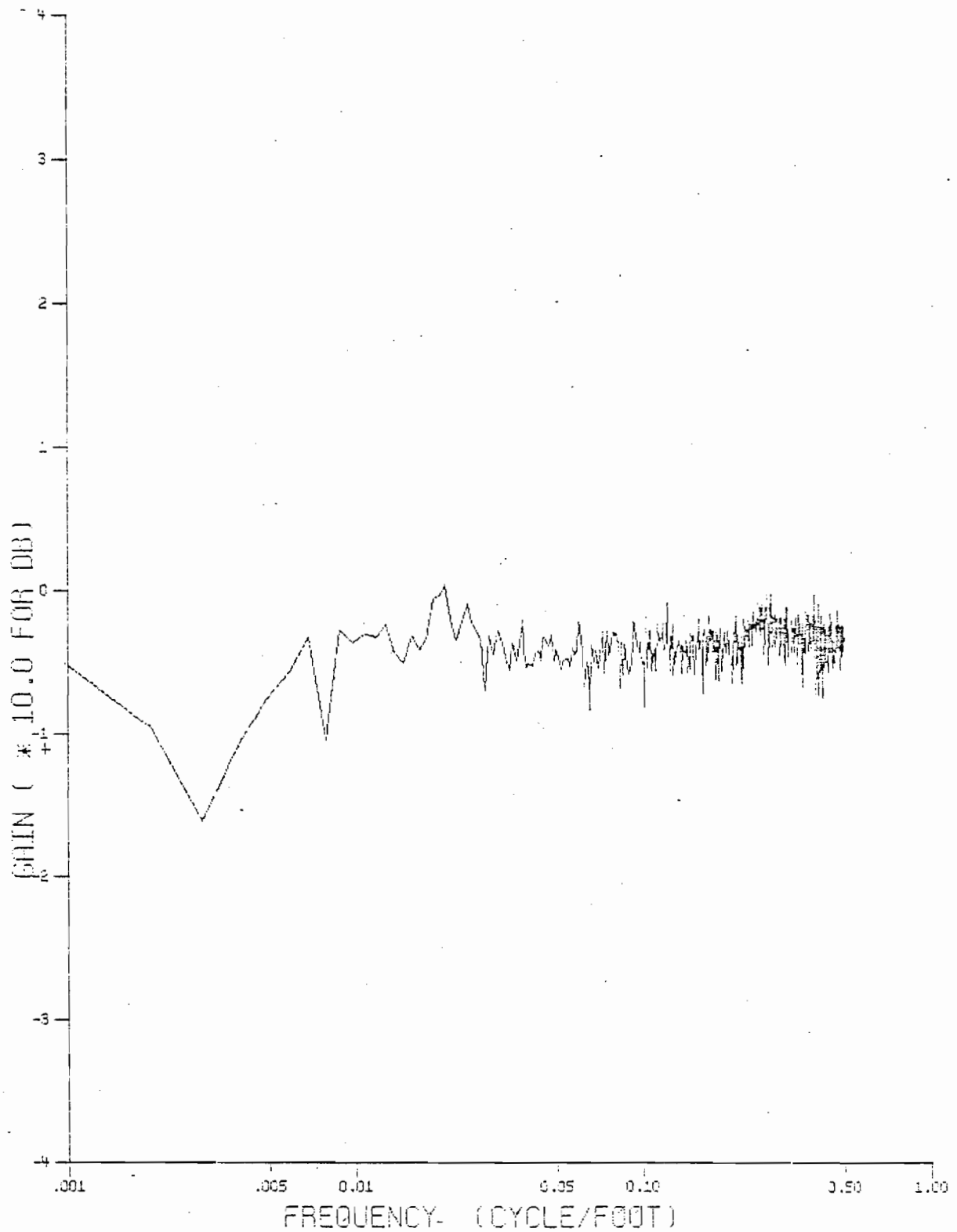


Figure E-19. Magnitude of Transfer Function Between Gage and Right Rail Alignment Variations (Track Class 4)

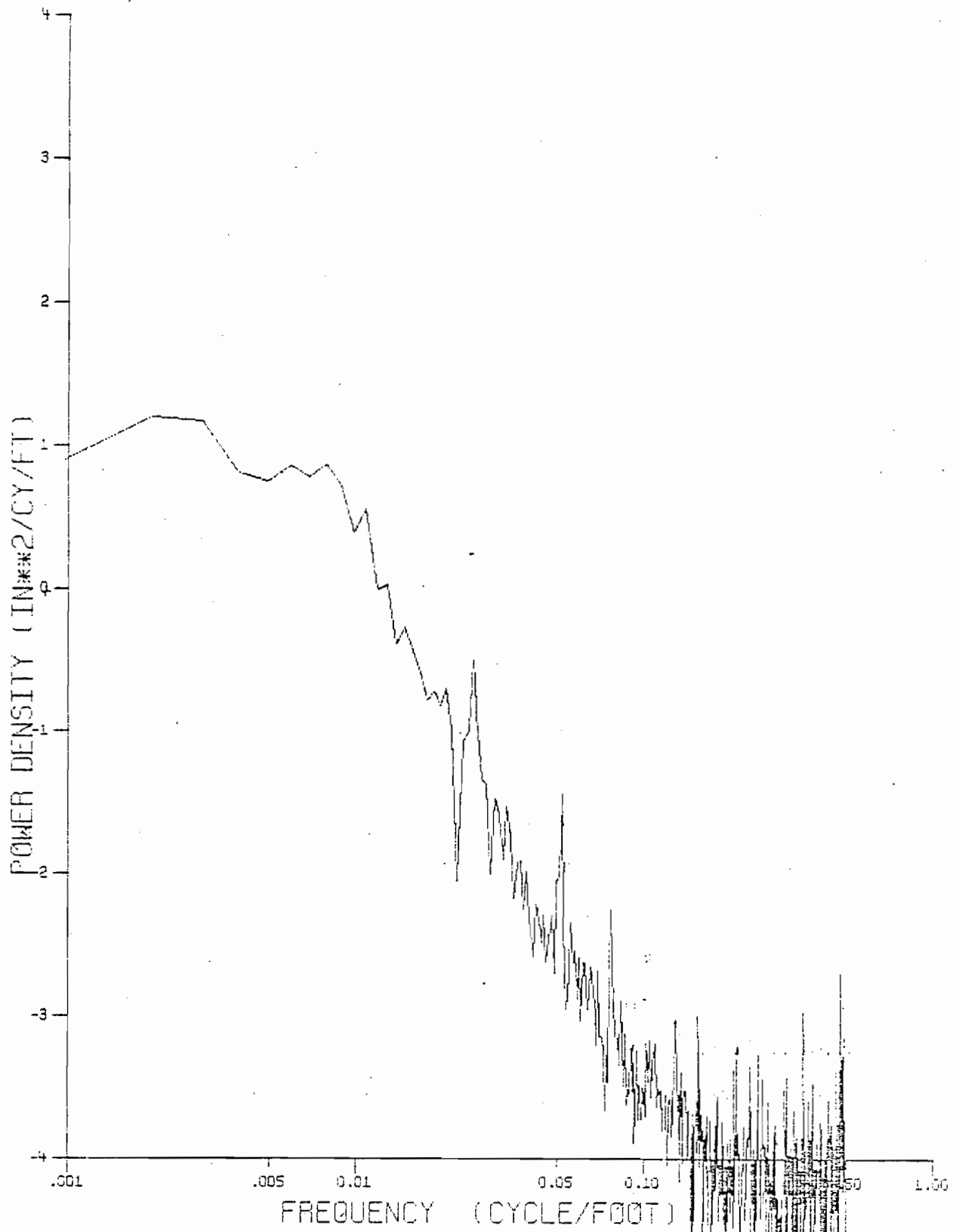


Figure E-20. Cross Spectral Density Between
 Left and Right Alignment (Track
 Class 3)

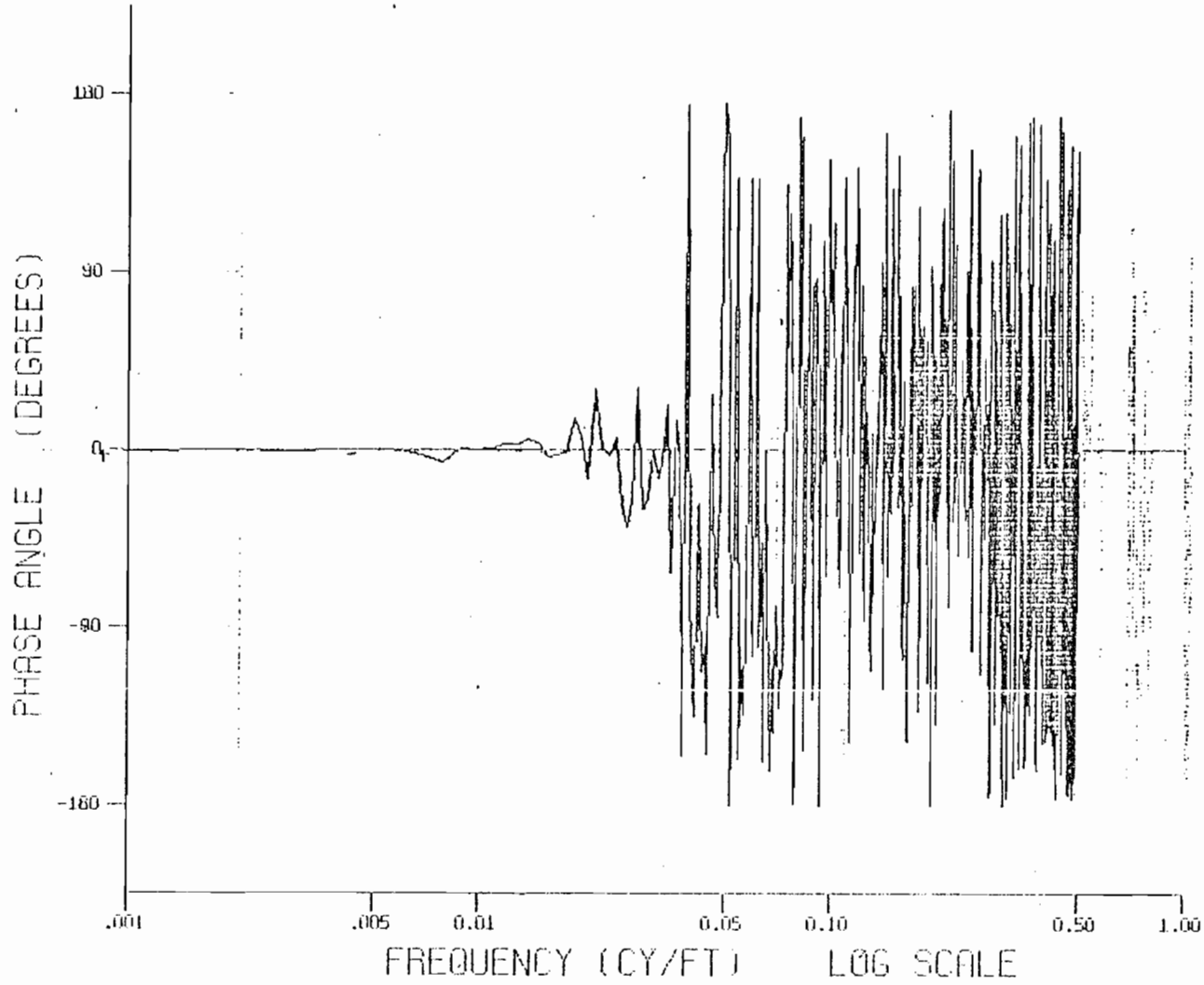


Figure E-21. Phase Angle Between Left and Right Alignment (Track Class 3)

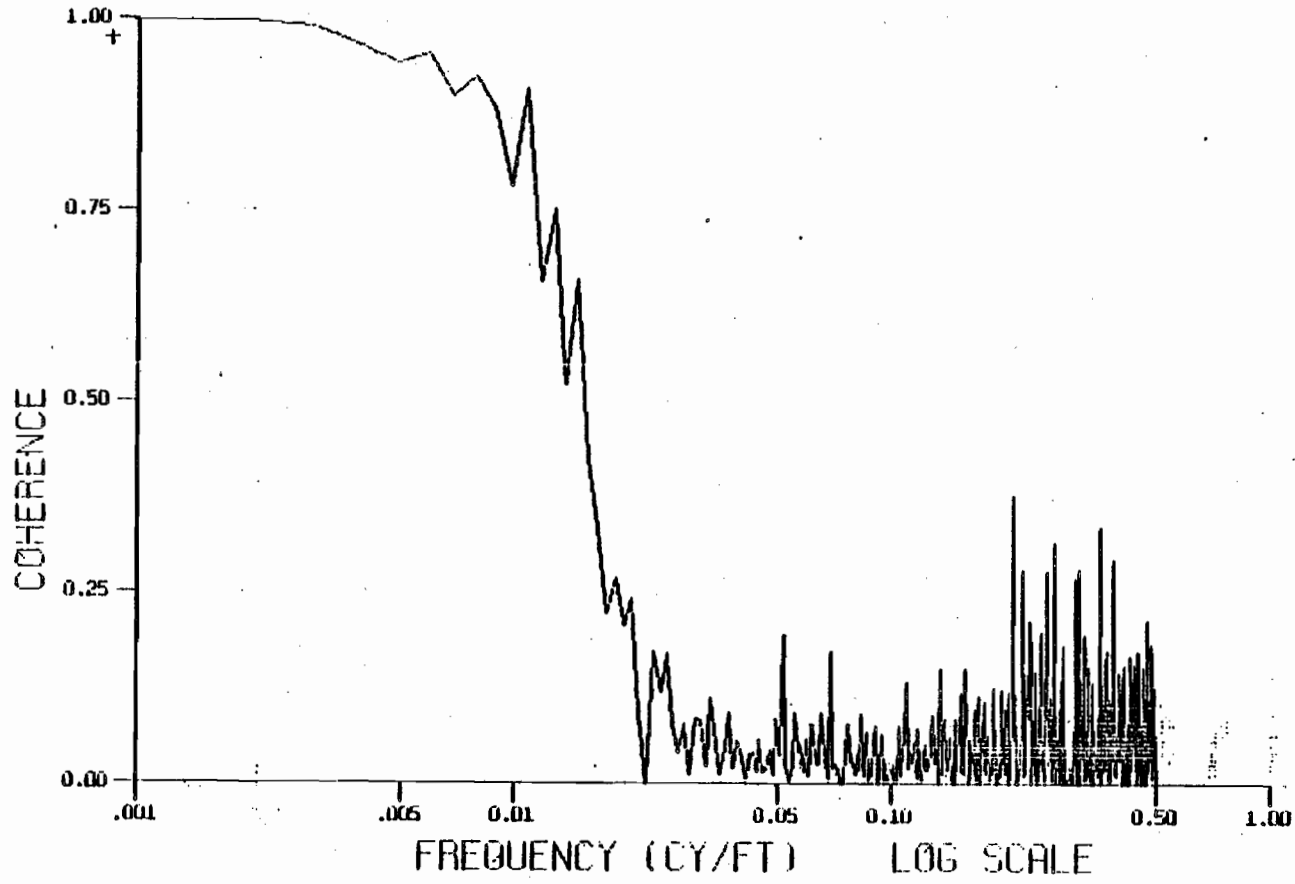


Figure E-22. Squared Coherence Between Left and Right Alignment (Track Class 3)

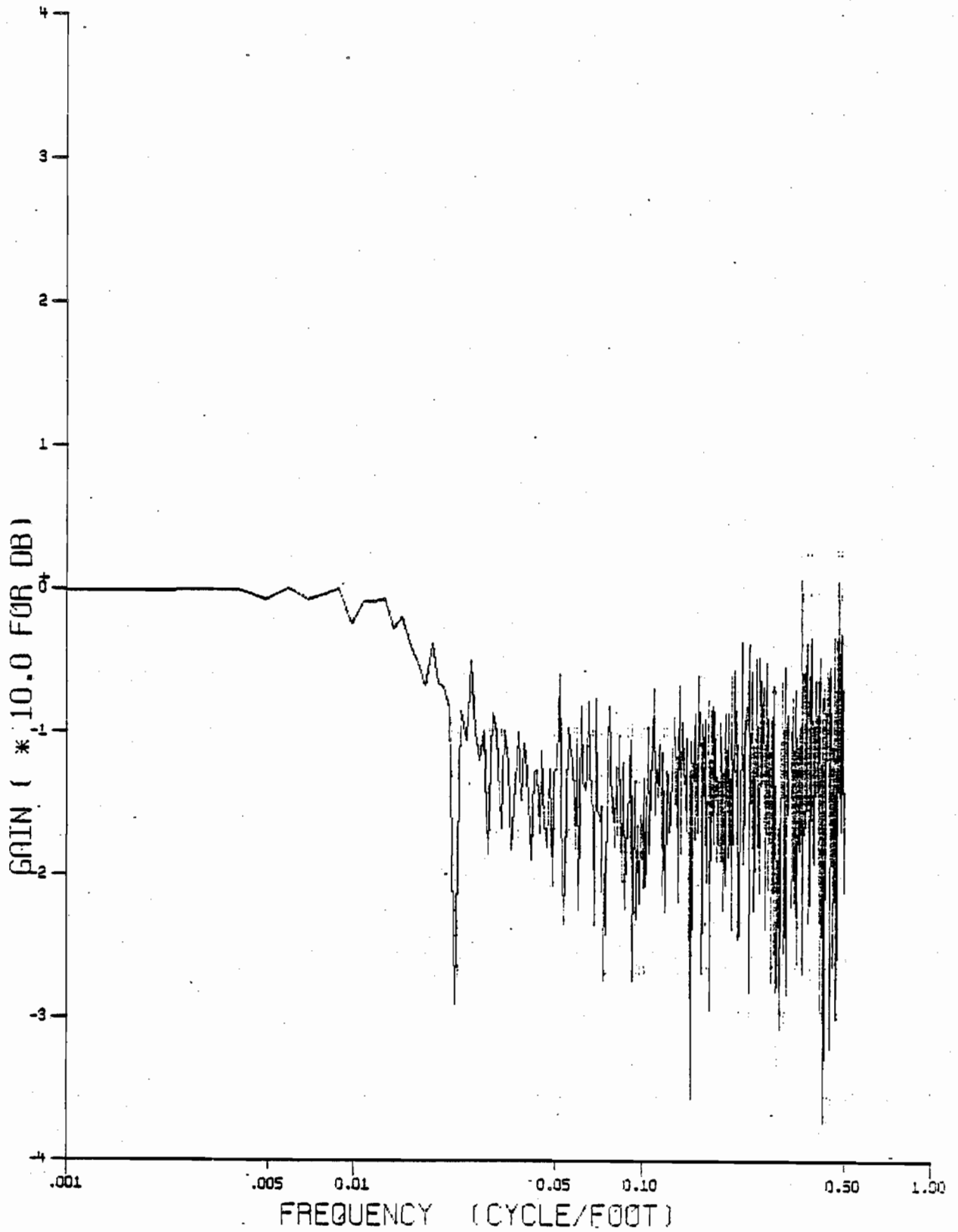


Figure E-23. Magnitude of Transfer Function Between Left and Right Alignment (Track Class 3)

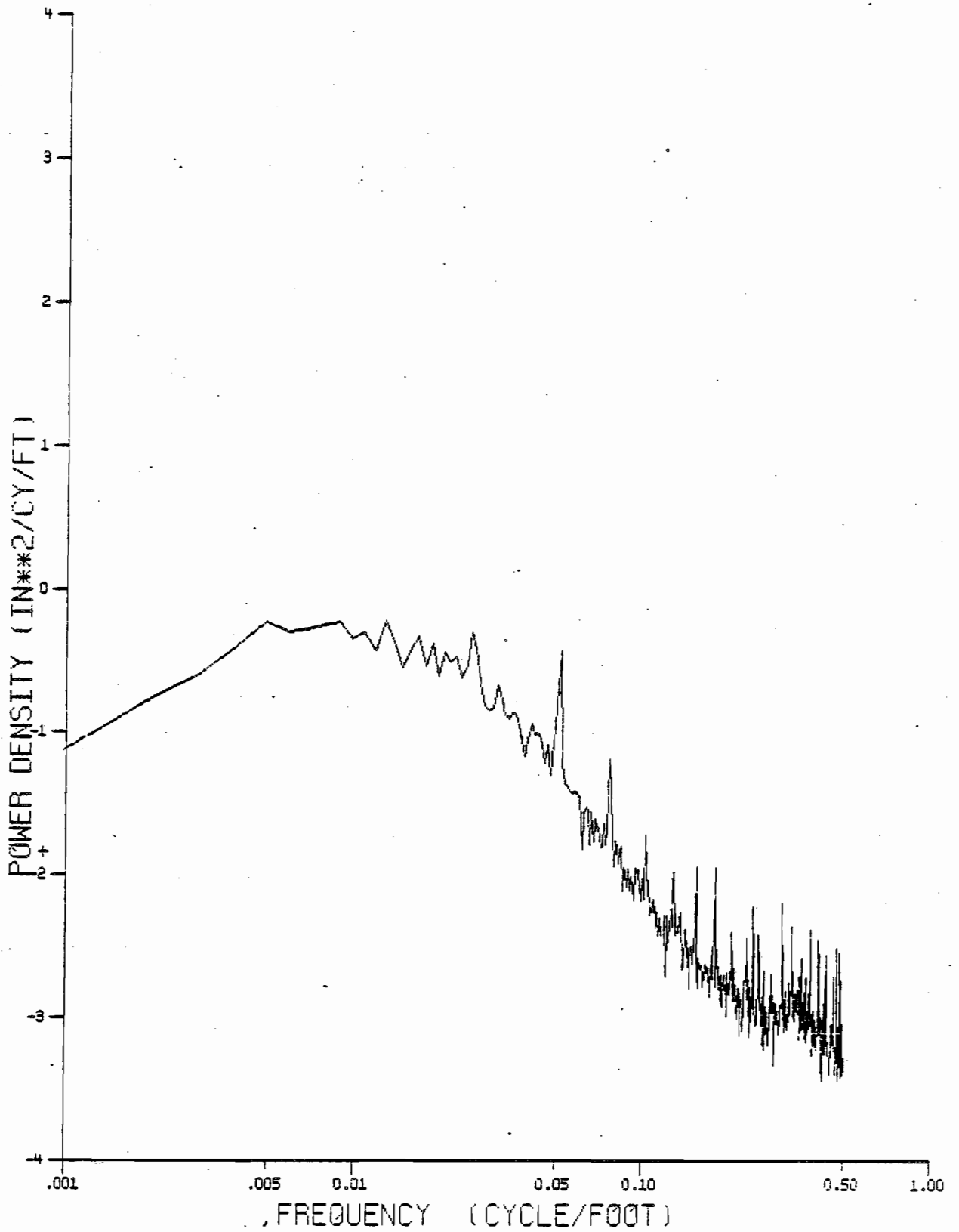


Figure E-24. Cross Spectral Density Between Gage and Left Minus Right Alignment (Track Class 1)

E-29

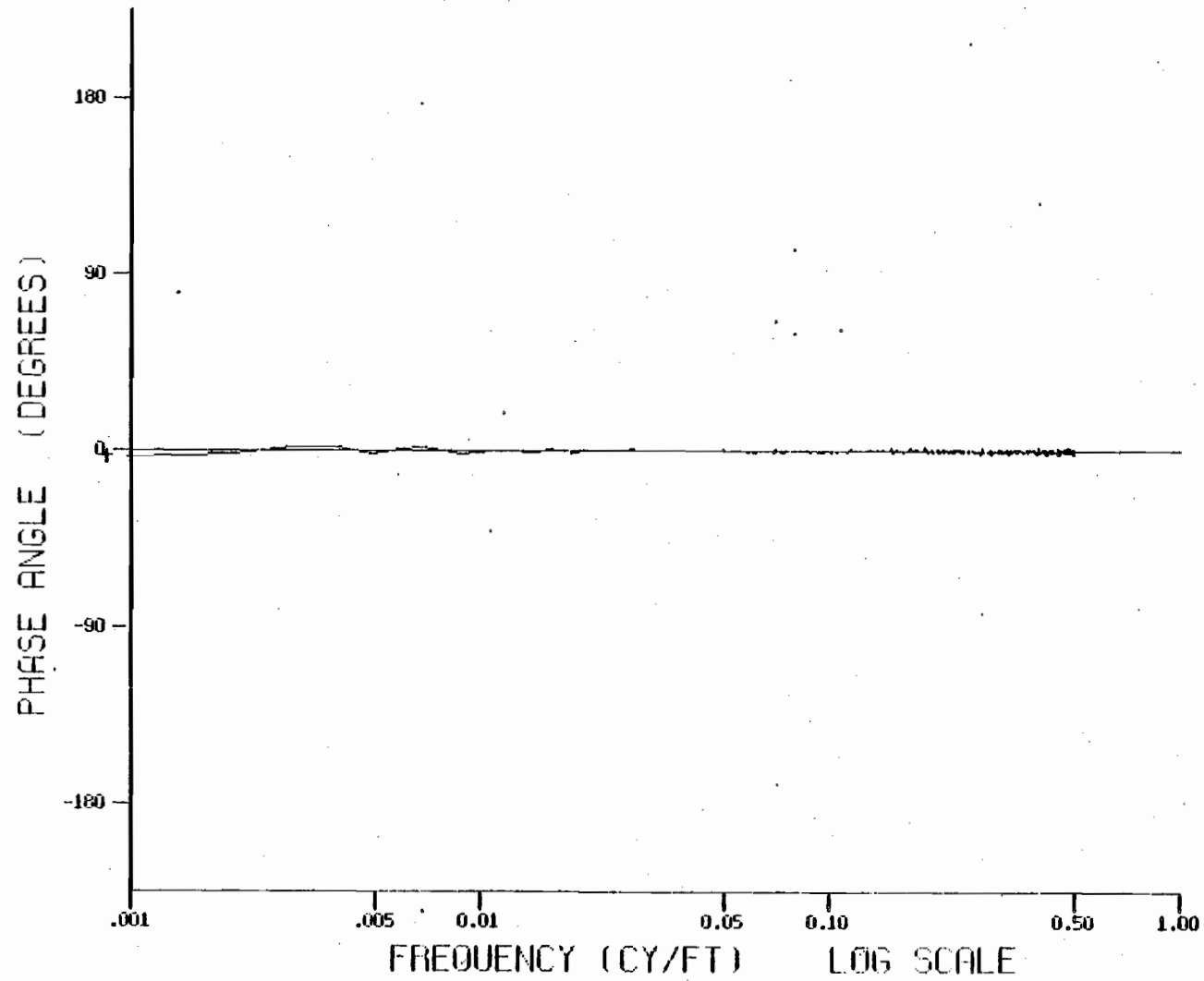


Figure E-25. Phase Angle Between Gage and Left Minus Right Alignment (Track Class 1)

E-30

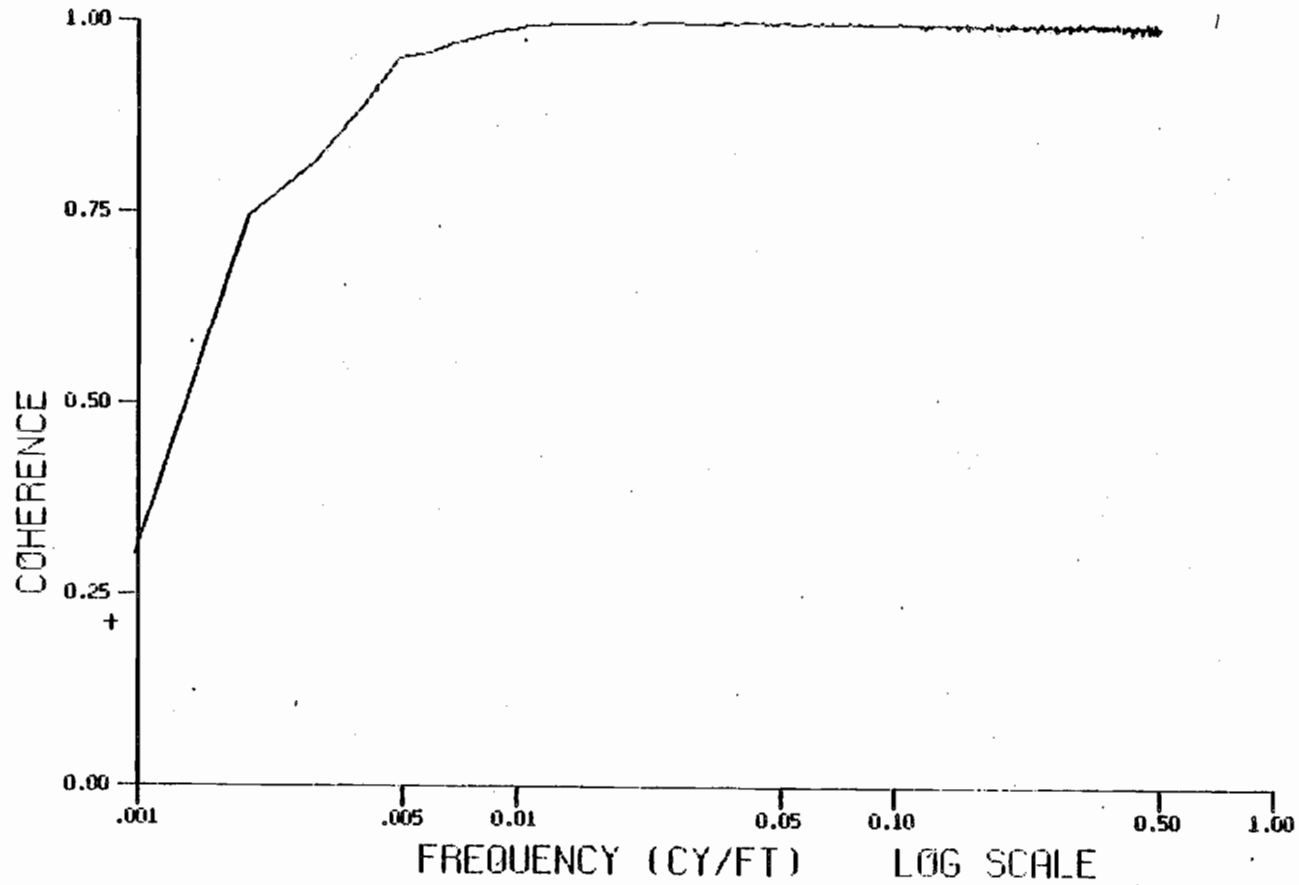


Figure E-26. Squared Coherence Between Gage and Left Minus Right Alignment (Track Class 1)

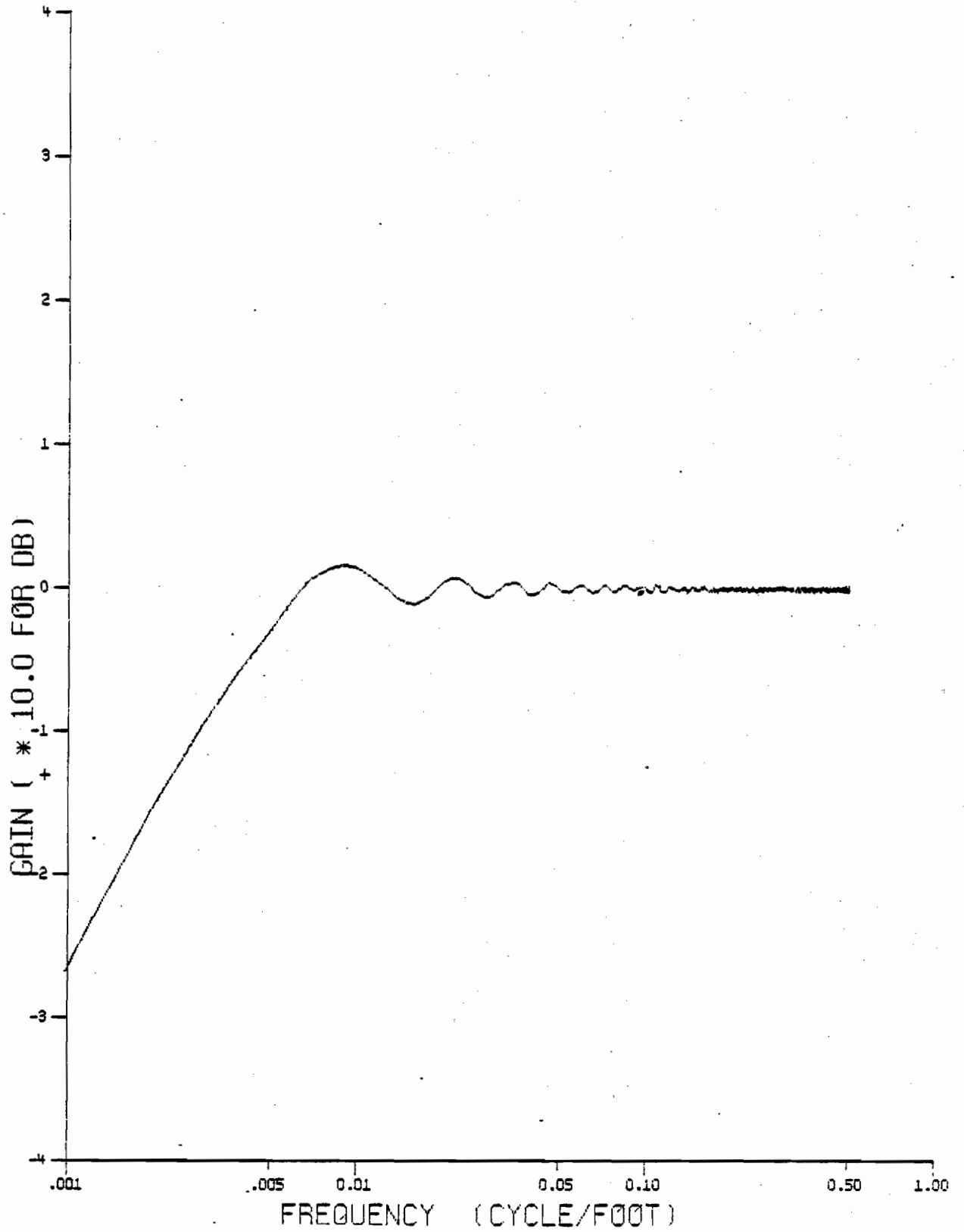
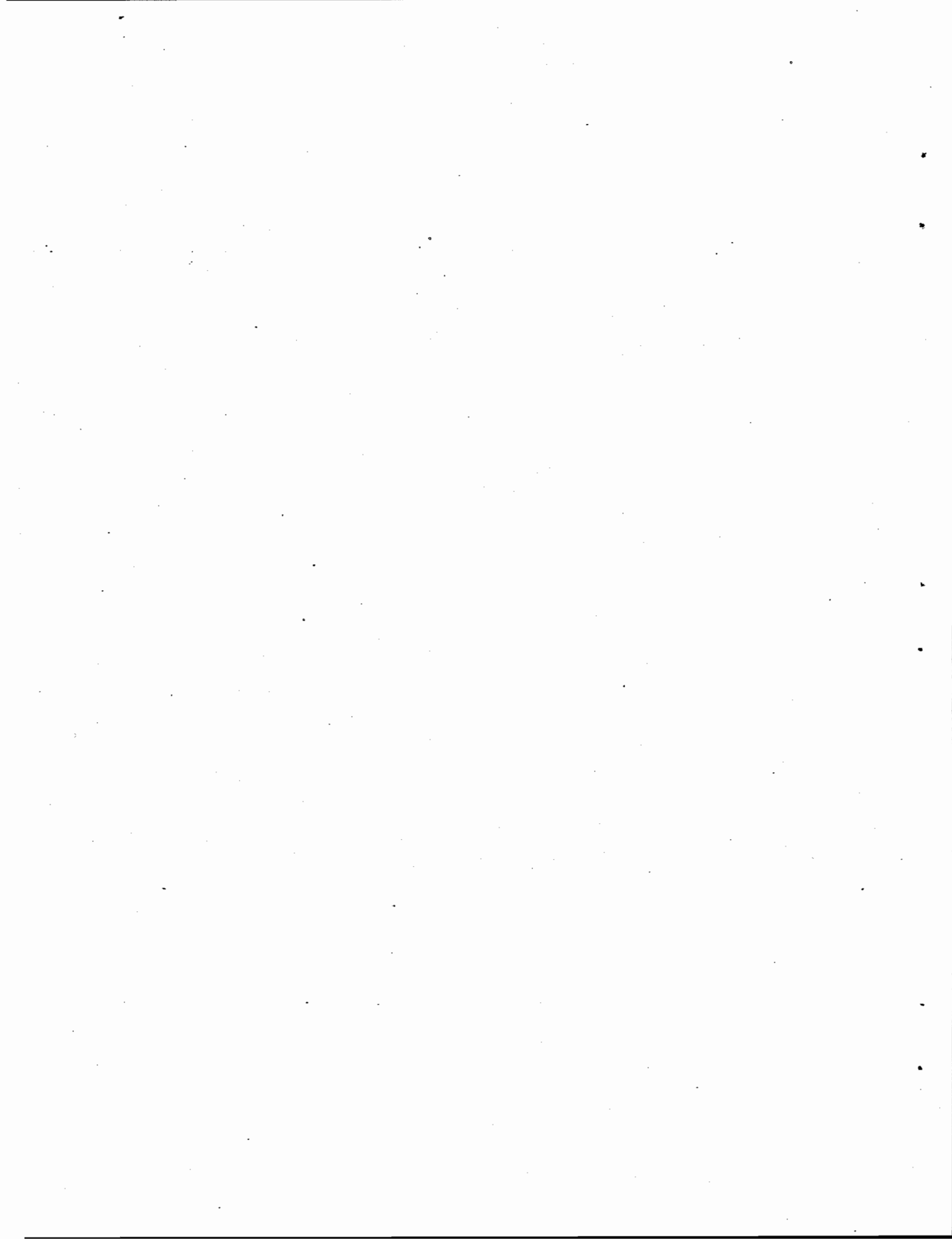


Figure E-27. Magnitude of Transfer Function Between Gage and Left Minus Right Alignment (Track Class 1)



E-2. CROSSLEVEL AND PROFILE

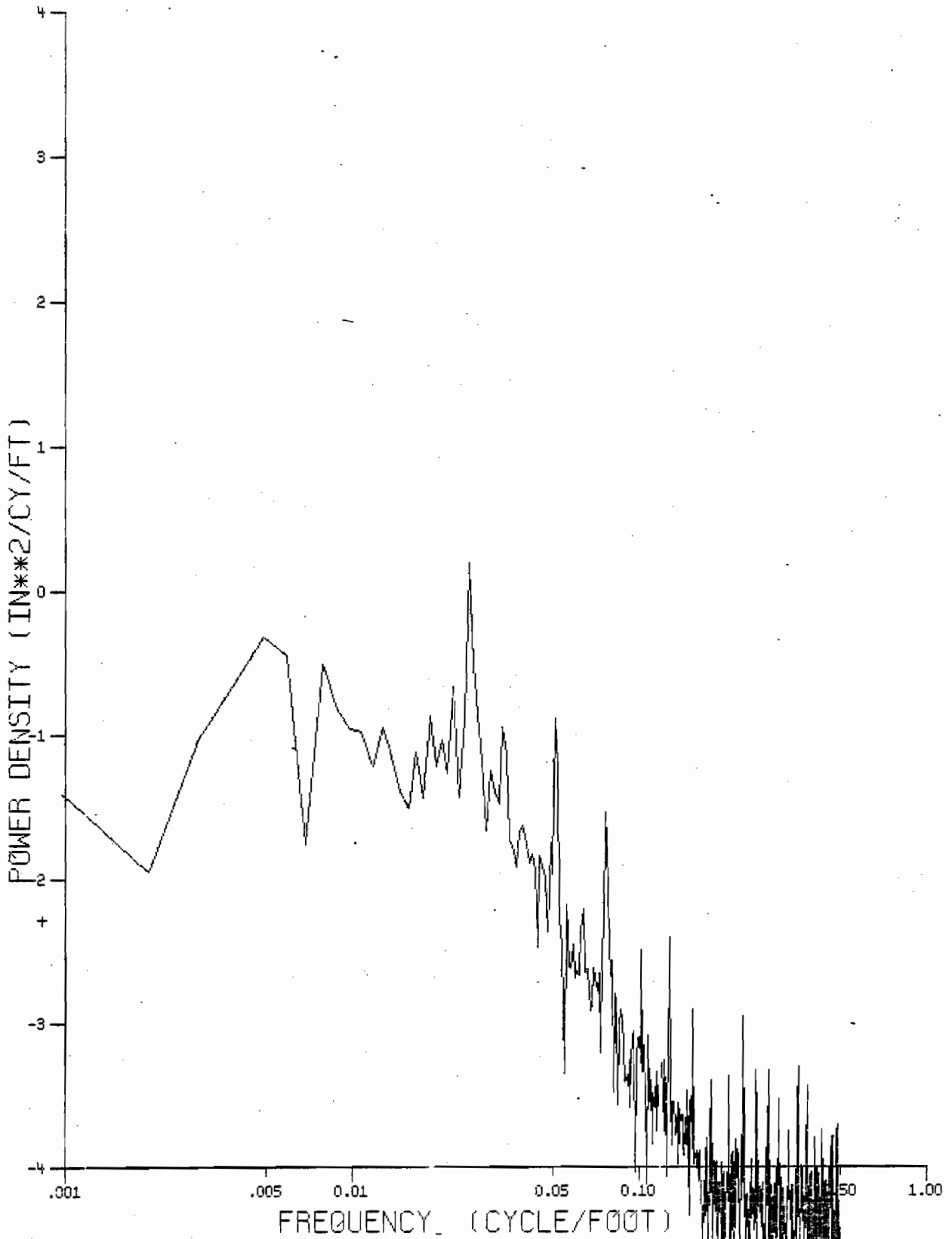


Figure E-28. Cross Spectral Density Between
 Crosslevel and Mean Profile
 (Track Class 3)

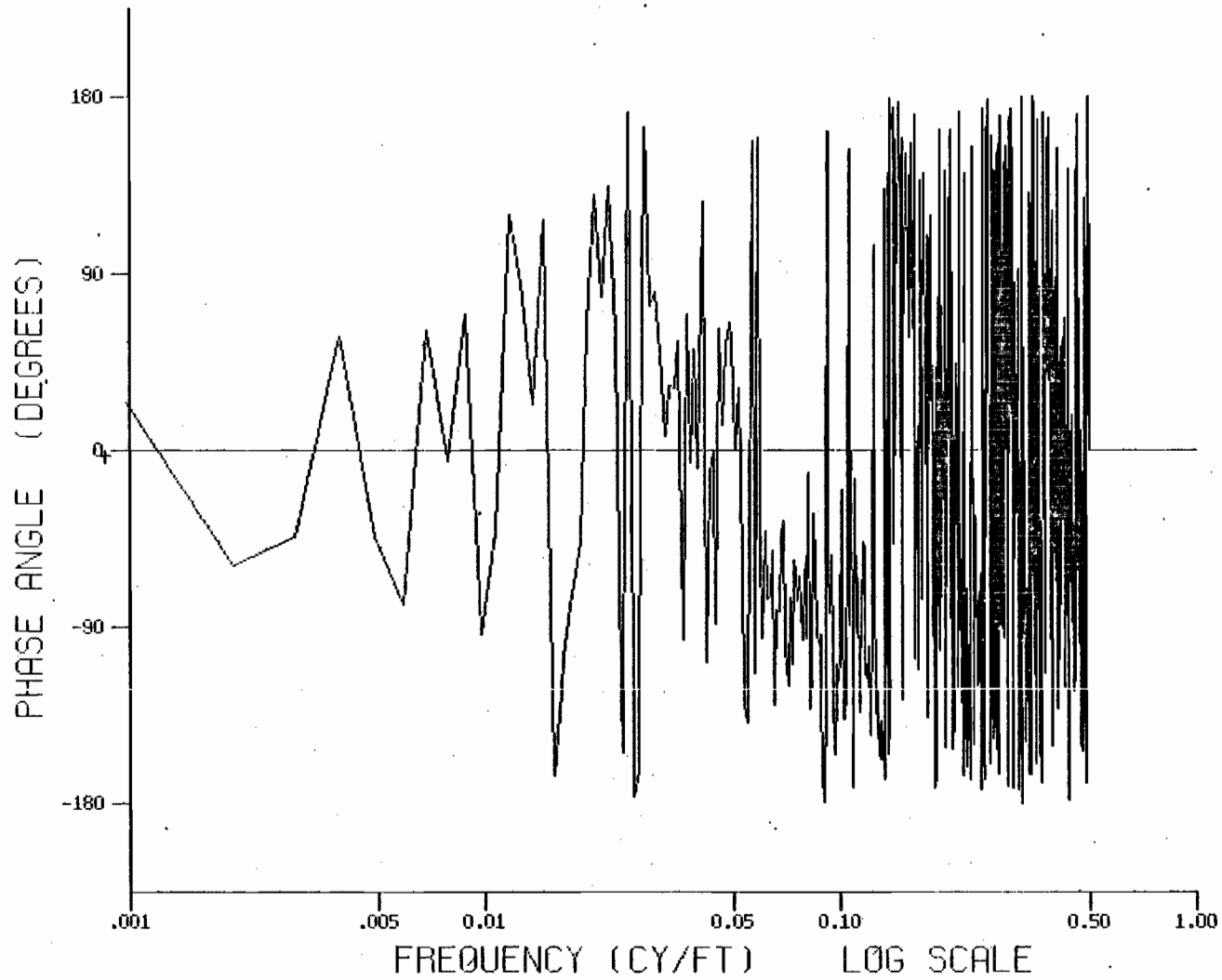


Figure E-29. Phase Angle Between Crosslevel and Mean Profile (Track Class 3)

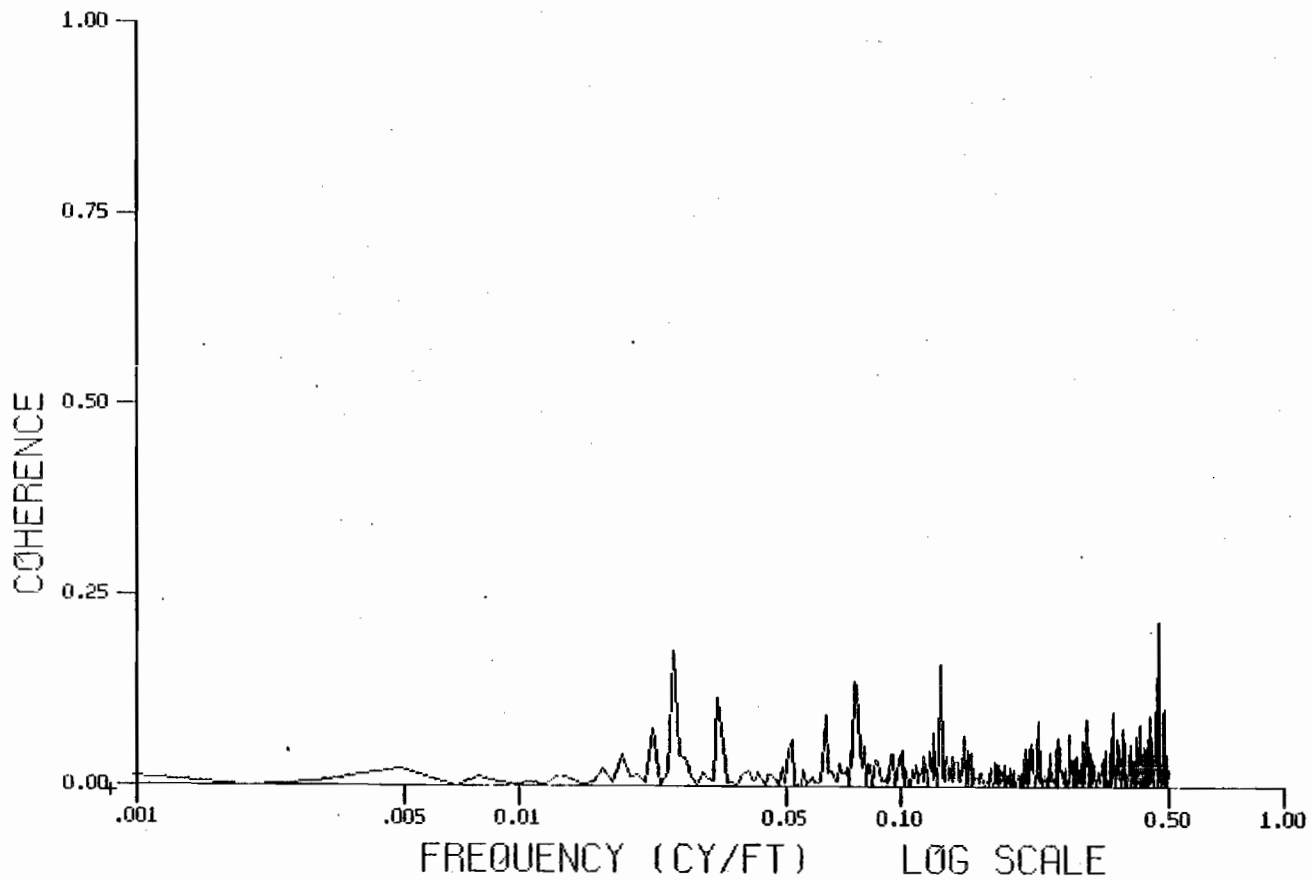


Figure E-30. Squared Coherence Between Crosslevel and Mean Profile (Track Class 3)

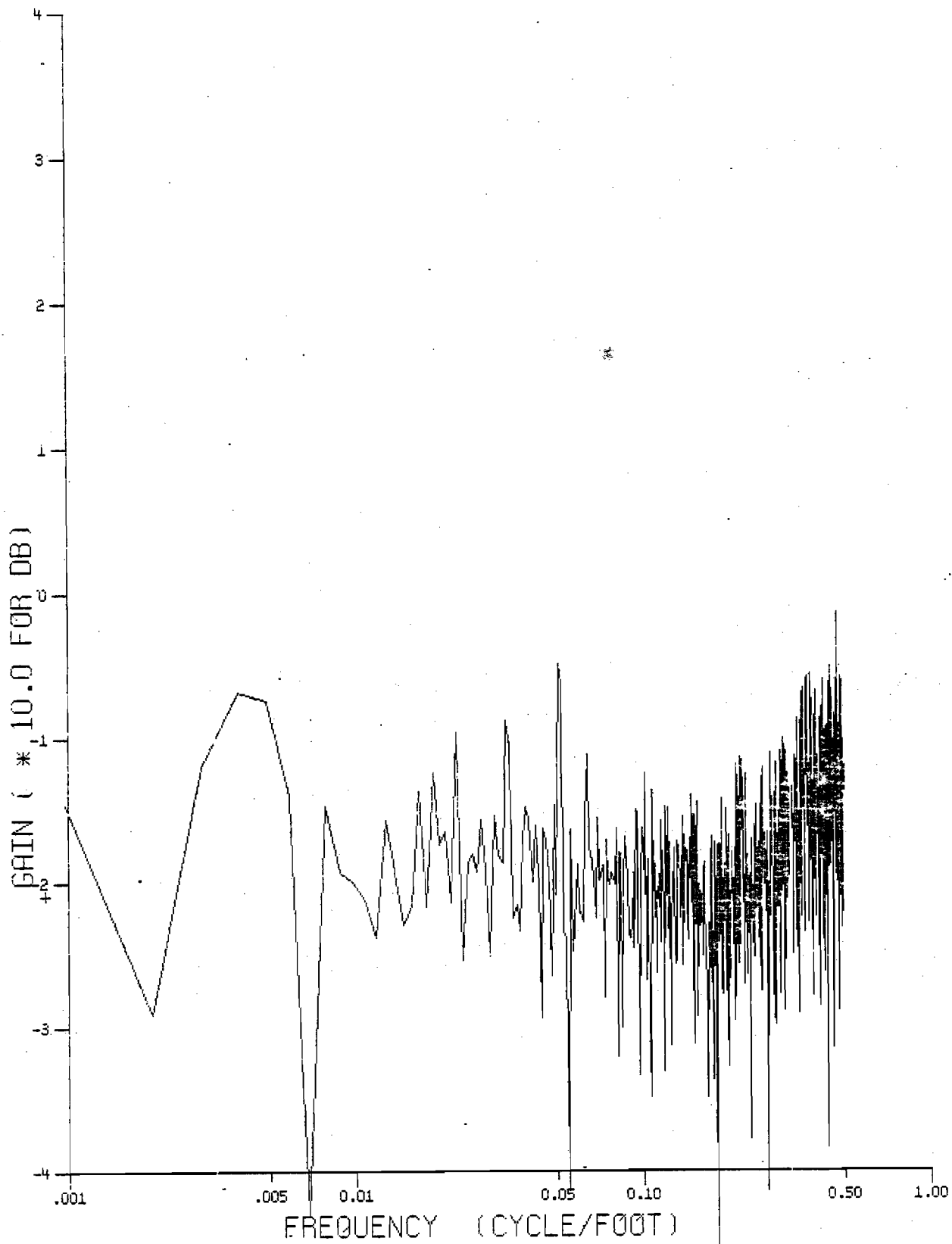


Figure E-31. Magnitude of Transfer Function Between Crosslevel and Mean Profile (Track Class 3)

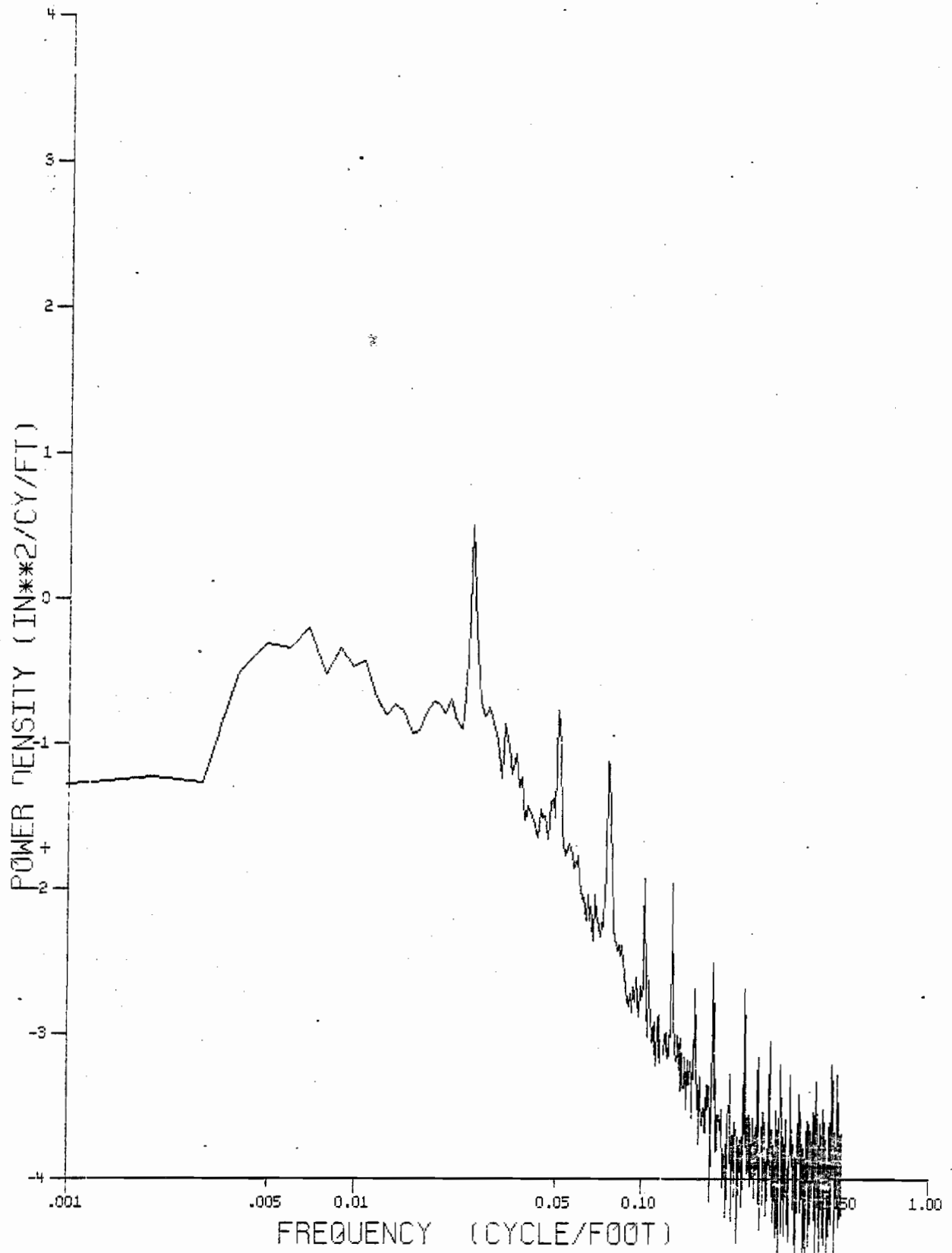


Figure E-32. Cross Spectral Density Between Crosslevel and Left Profile (Track Class 3)
E-38

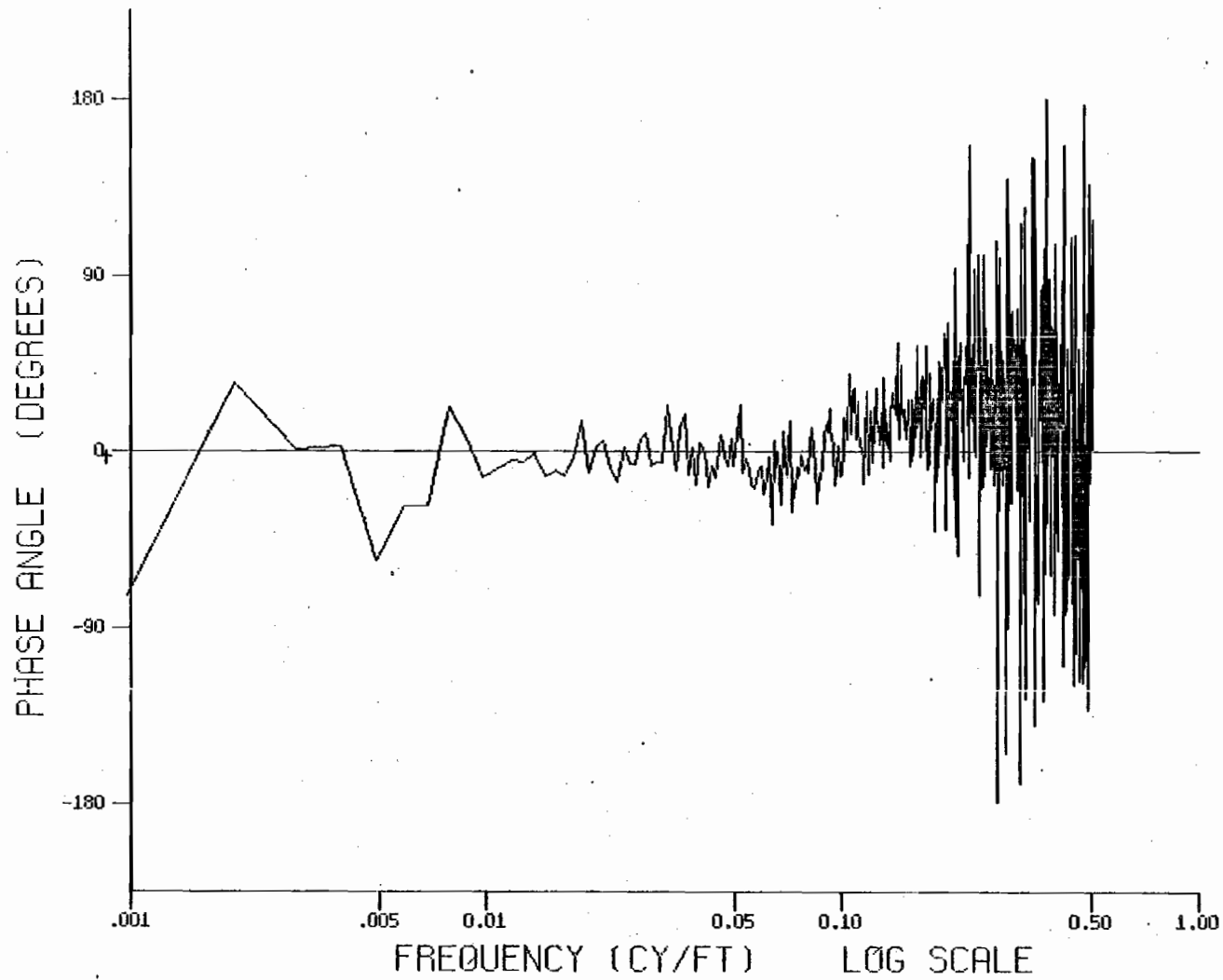


Figure E-33. Phase Angle Between Crosslevel and Left Profile (Track Class 4)

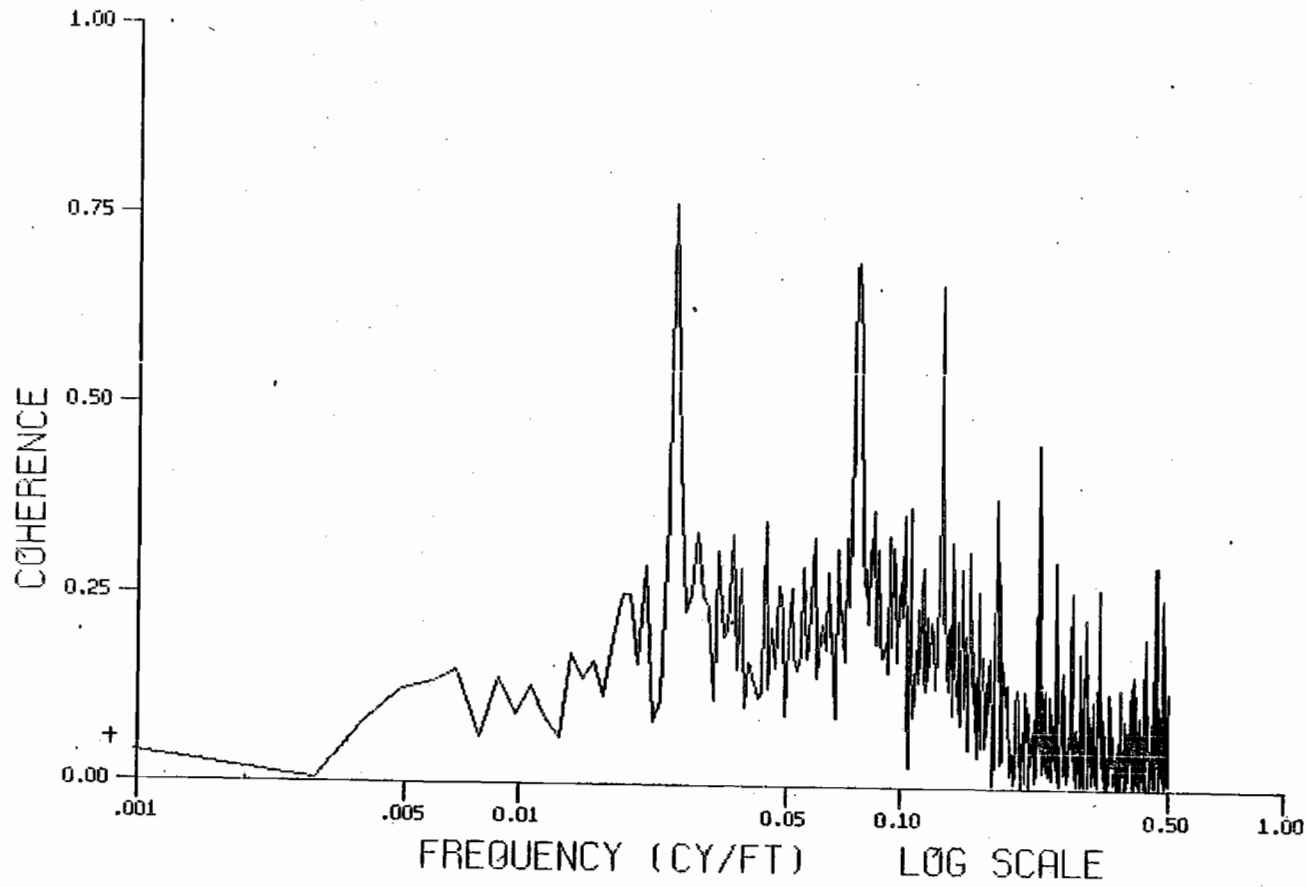


Figure E-34. Squared Coherence Between Crosslevel and Left Profile (Track Class 4)

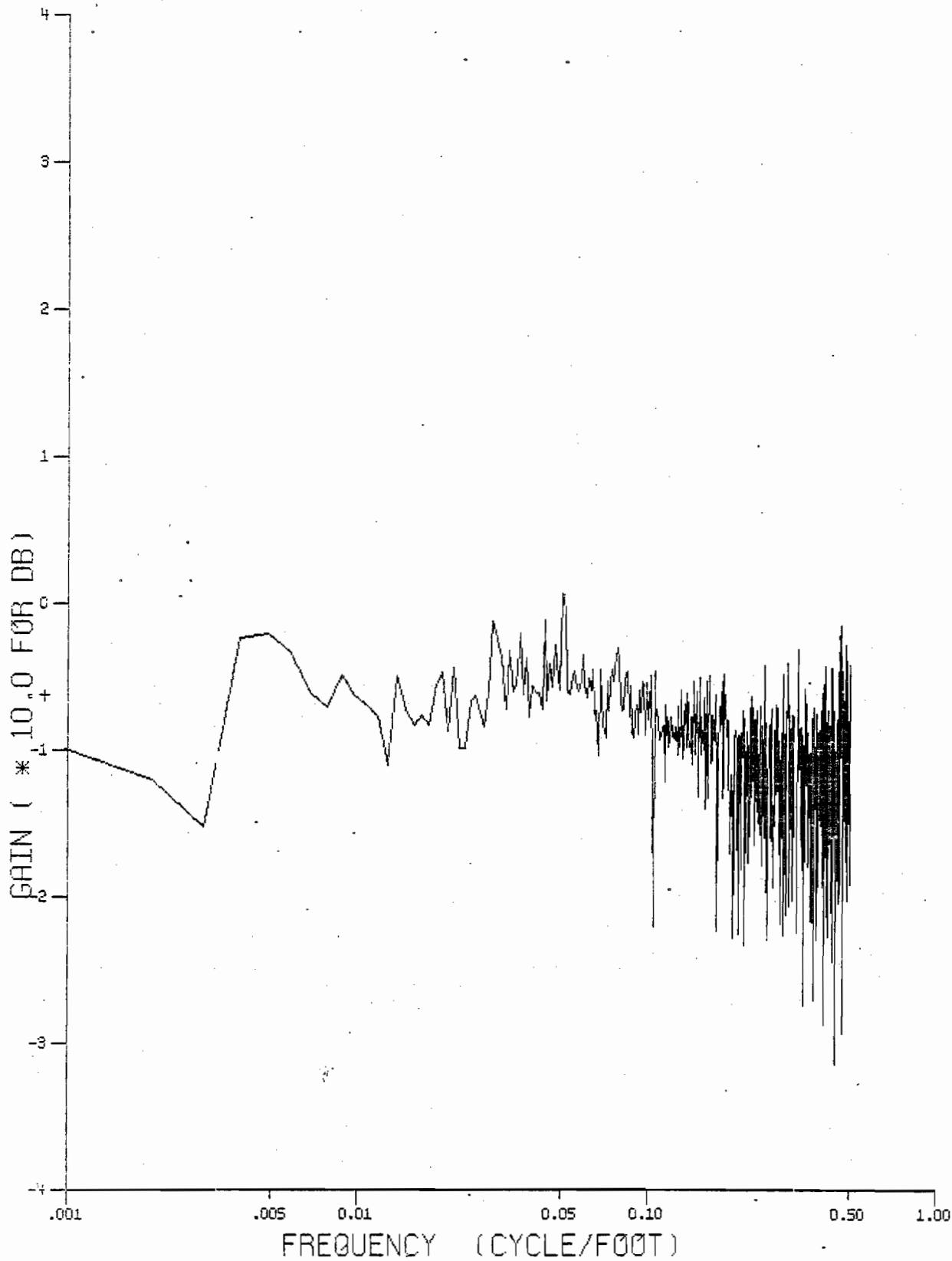


Figure E-35. Magnitude of Transfer Function Between Crosslevel and Left Profile (Track Class 4)

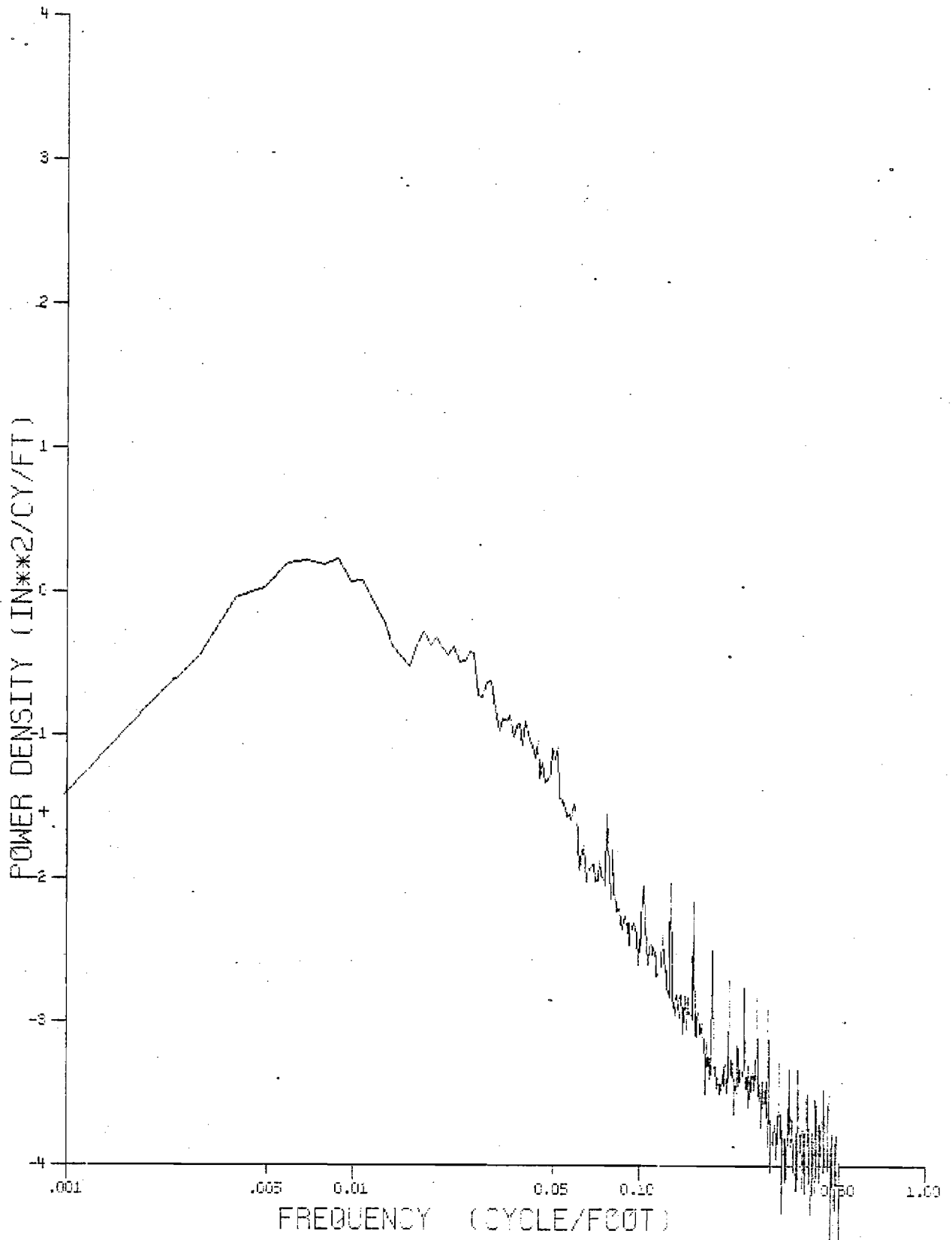


Figure E-36. Cross Spectral Density Between Crosslevel and Left Minus Right Profile (Track Class 4)

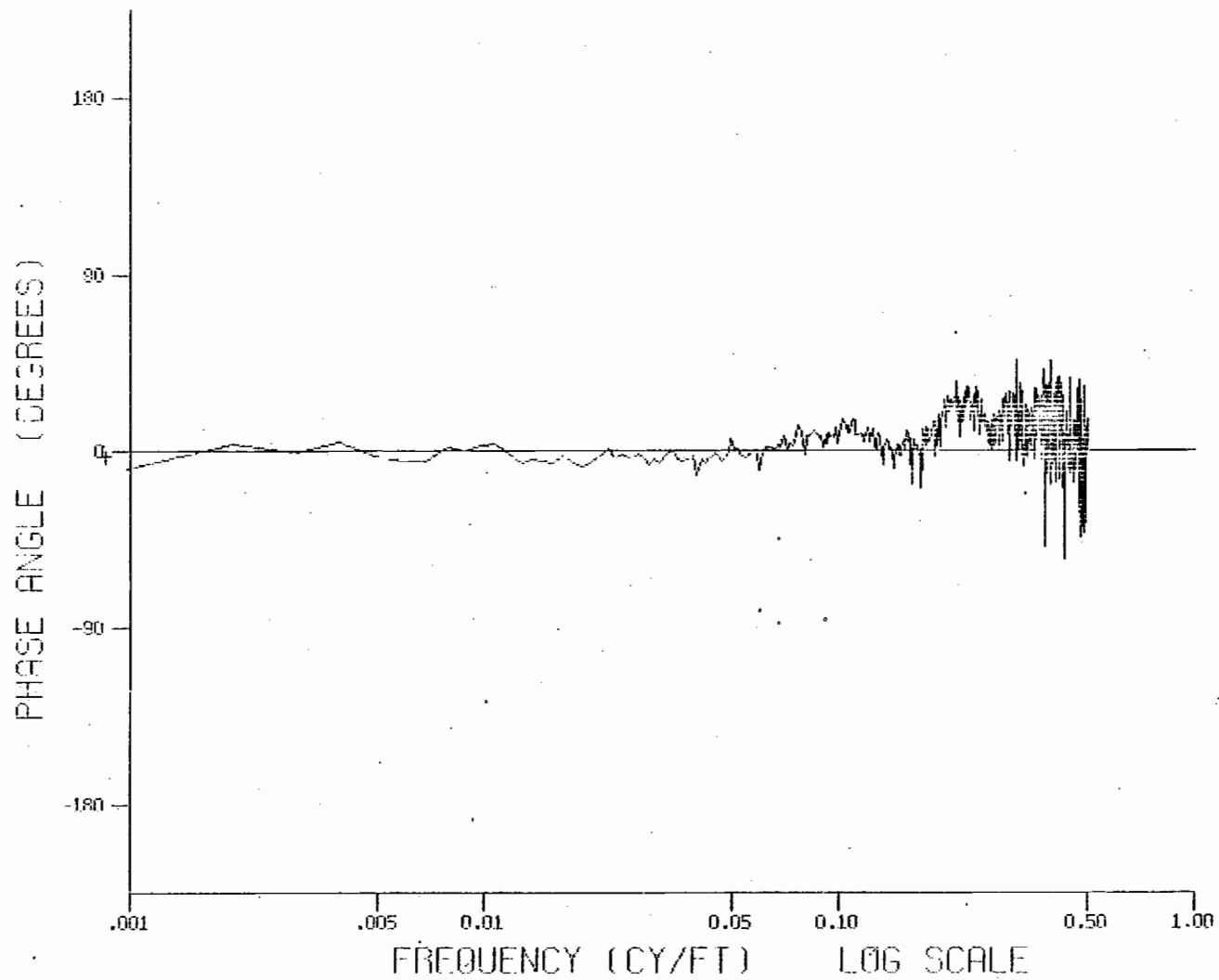


Figure E-37. Phase Angle Between Crosslevel and Left Minus Right Profile (Track Class 4)

E-44

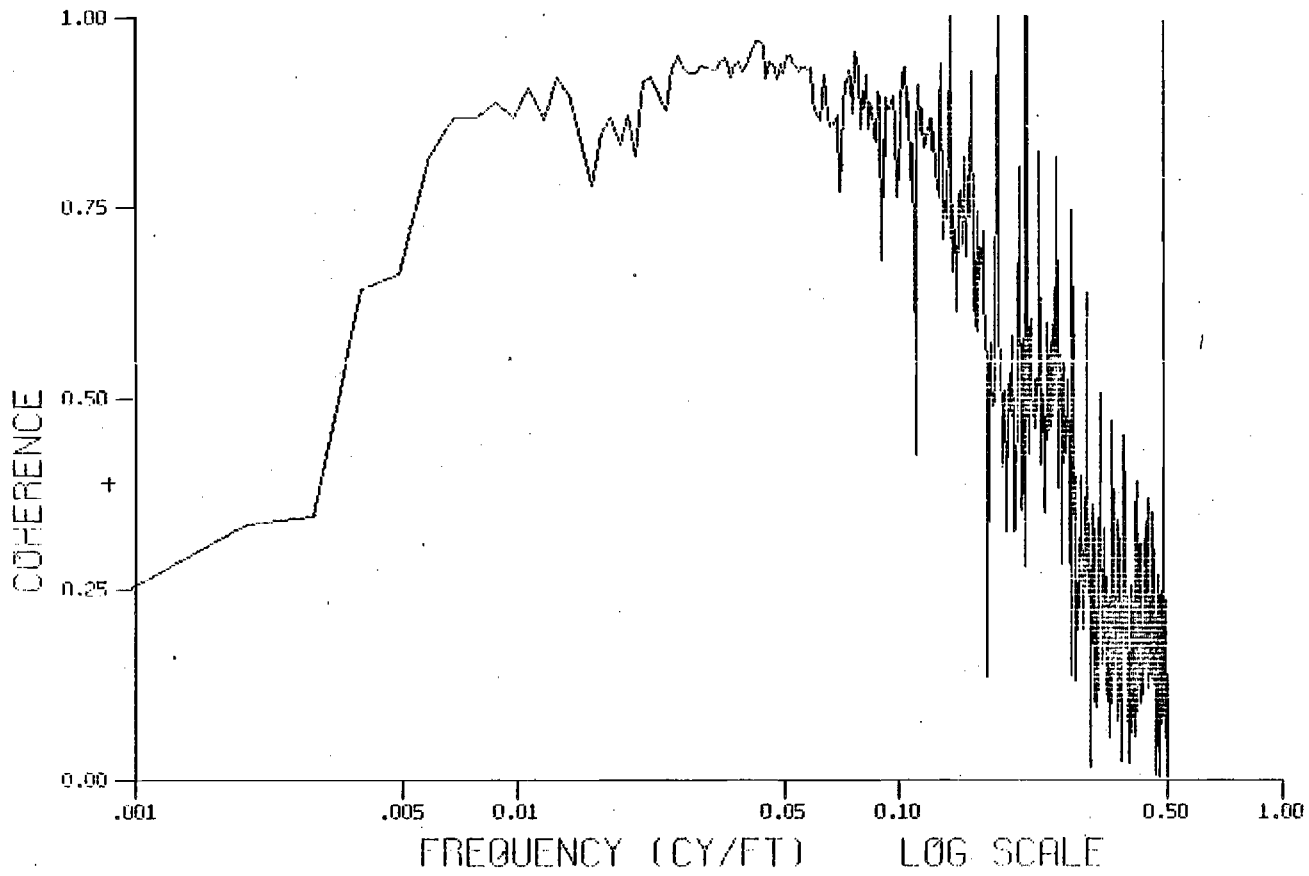


Figure E-38. Squared Coherence Between Crosslevel and Left Minus Right Profile (Track Class 4)

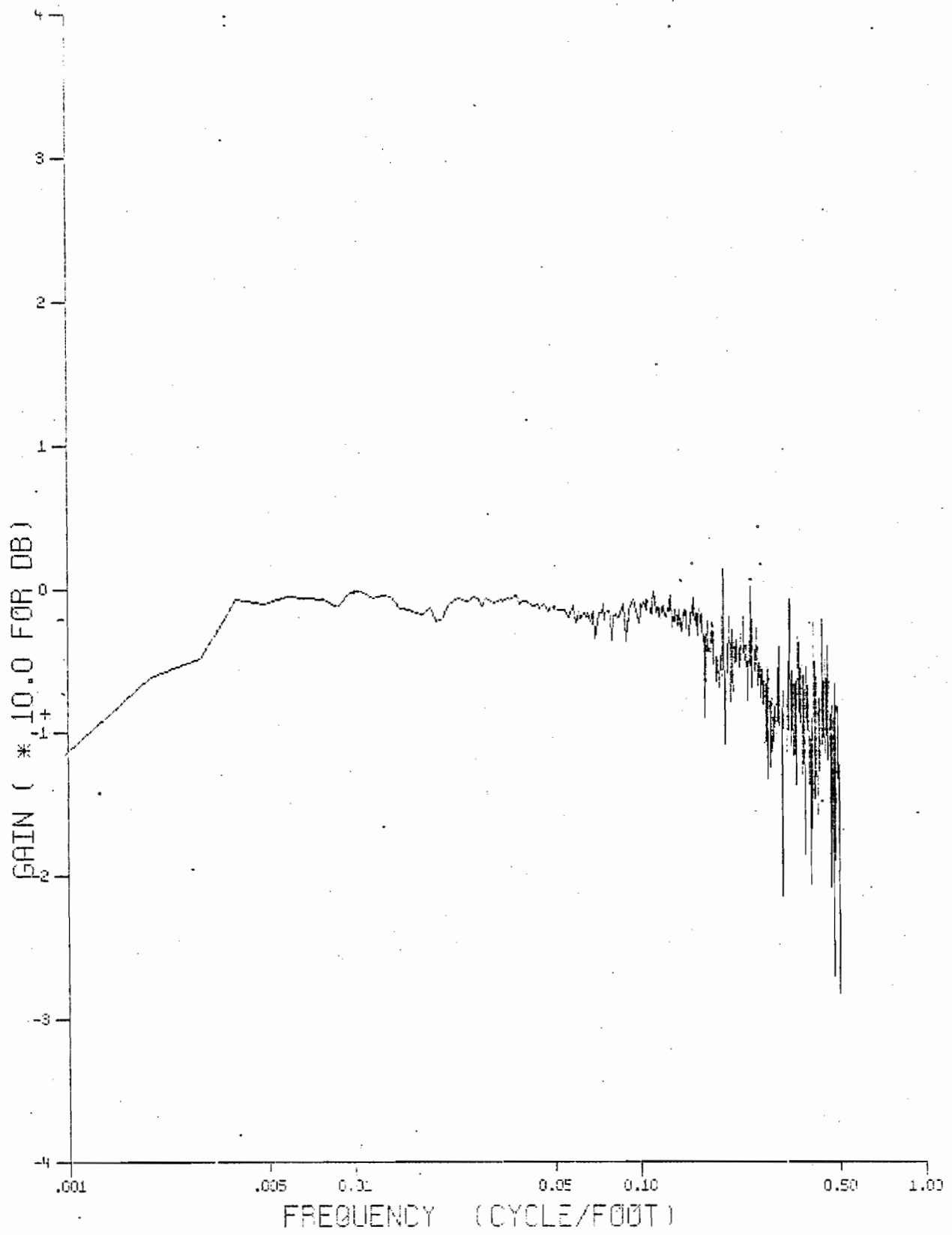


Figure E-39. Magnitude of Transfer Function Between Crosslevel and Left Minus Right Profile (Track Class 4)

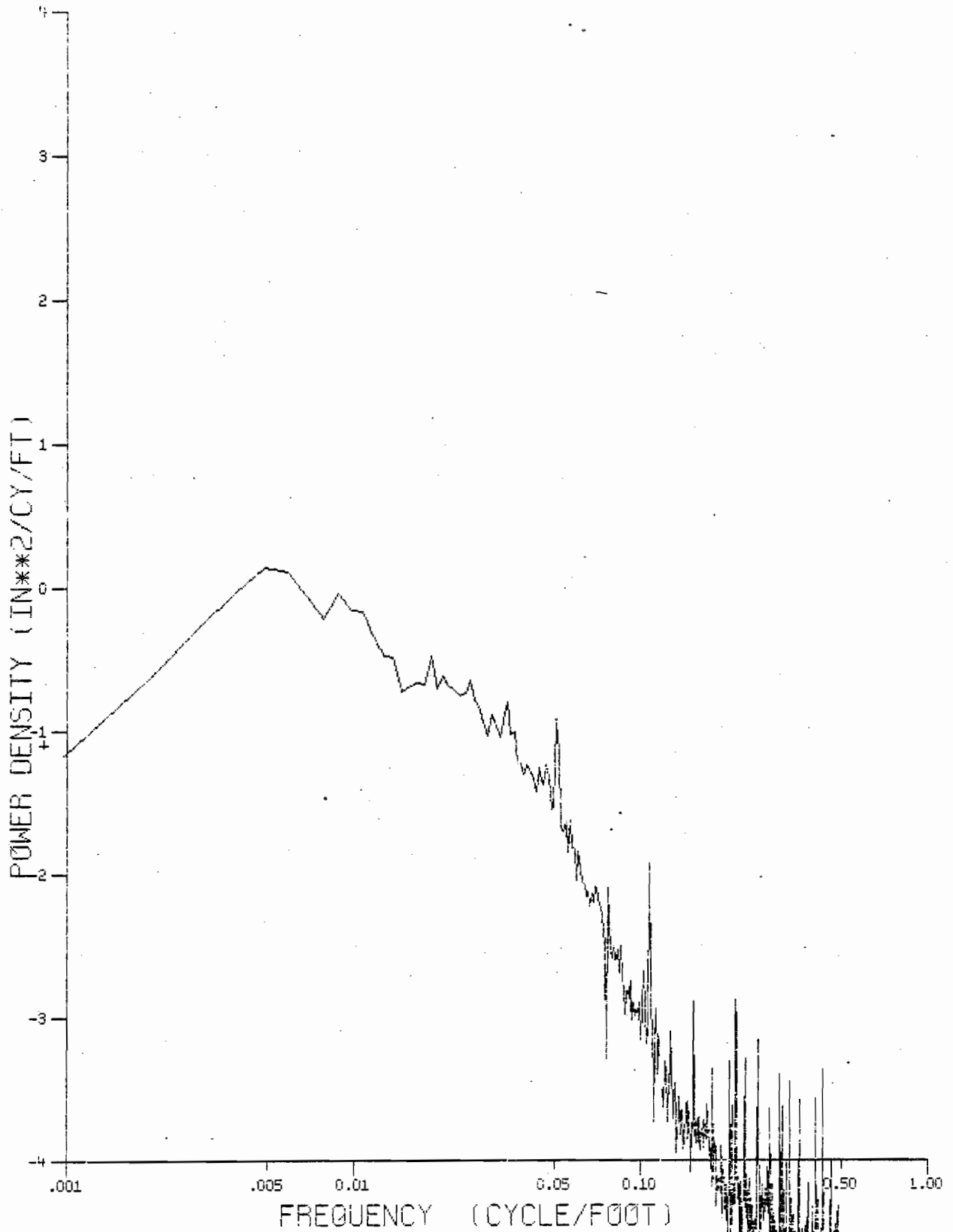


Figure E-40. Cross Spectral Density Between
Left Profile and Right Profile
(Track Class 4)

E-47

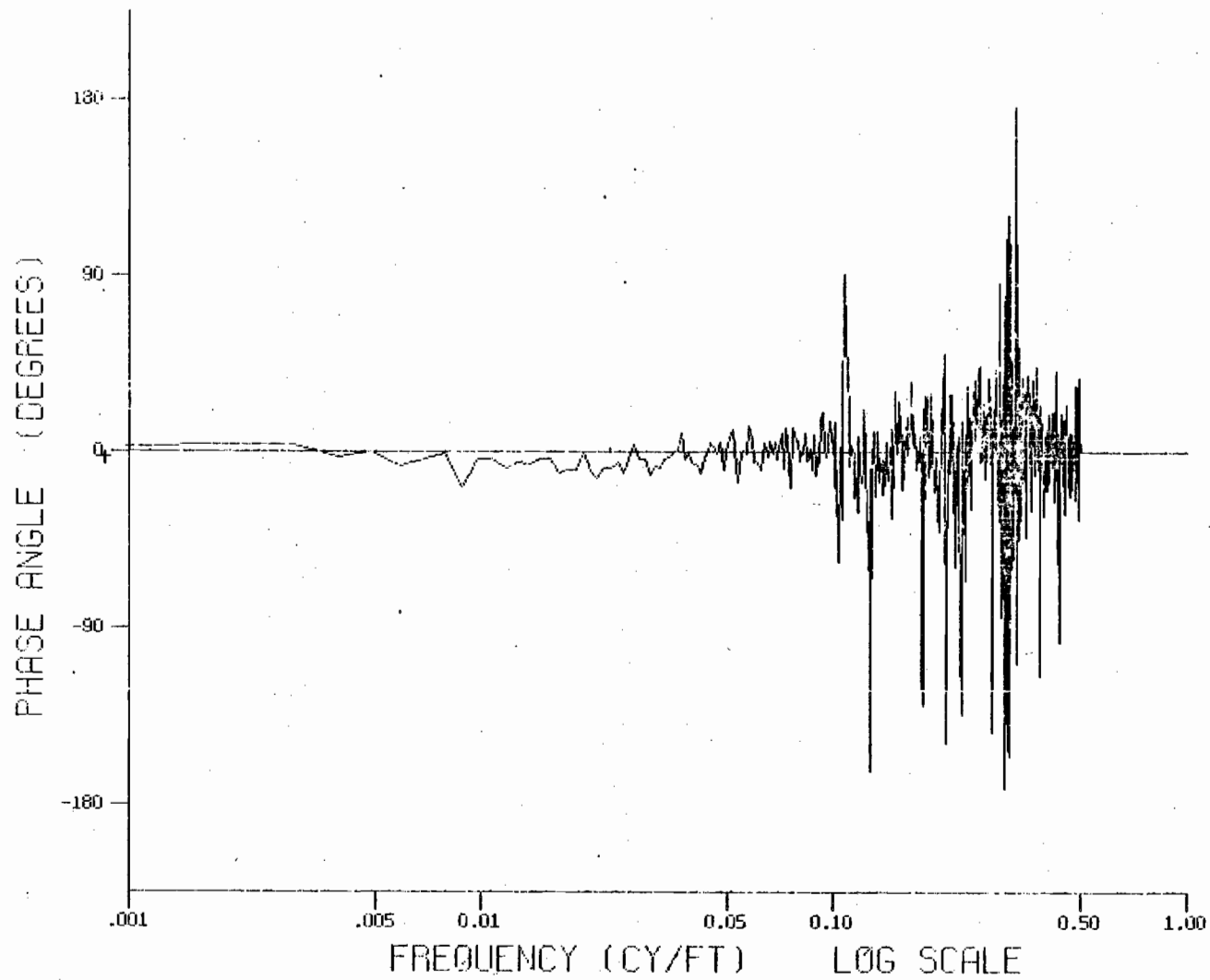


Figure E-41. Phase Angle Between Left Profile and Right Profile (Track Class 4)

E-48

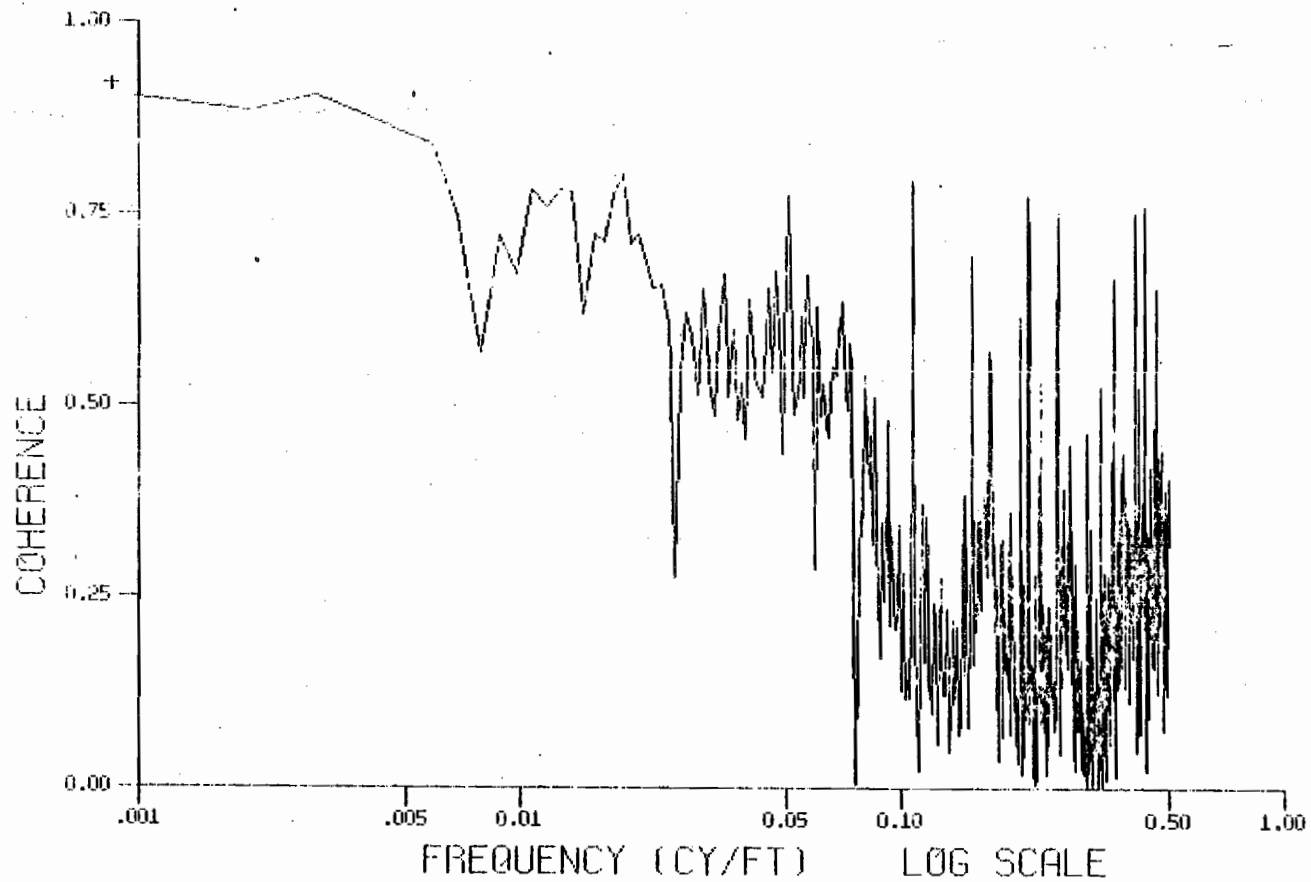


Figure E-42. Squared Coherence Between Left Profile and Right Profile (Track Class 4)

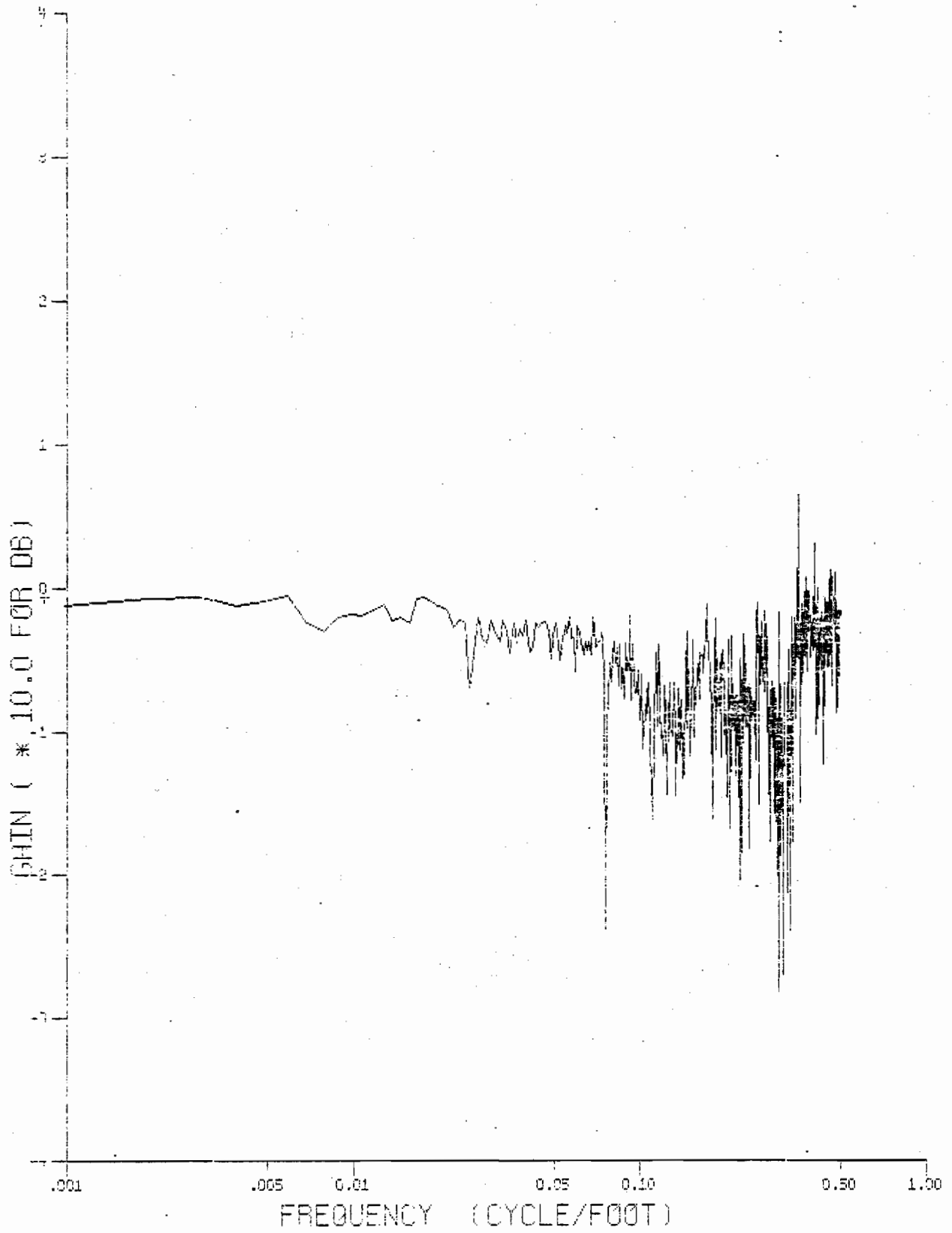
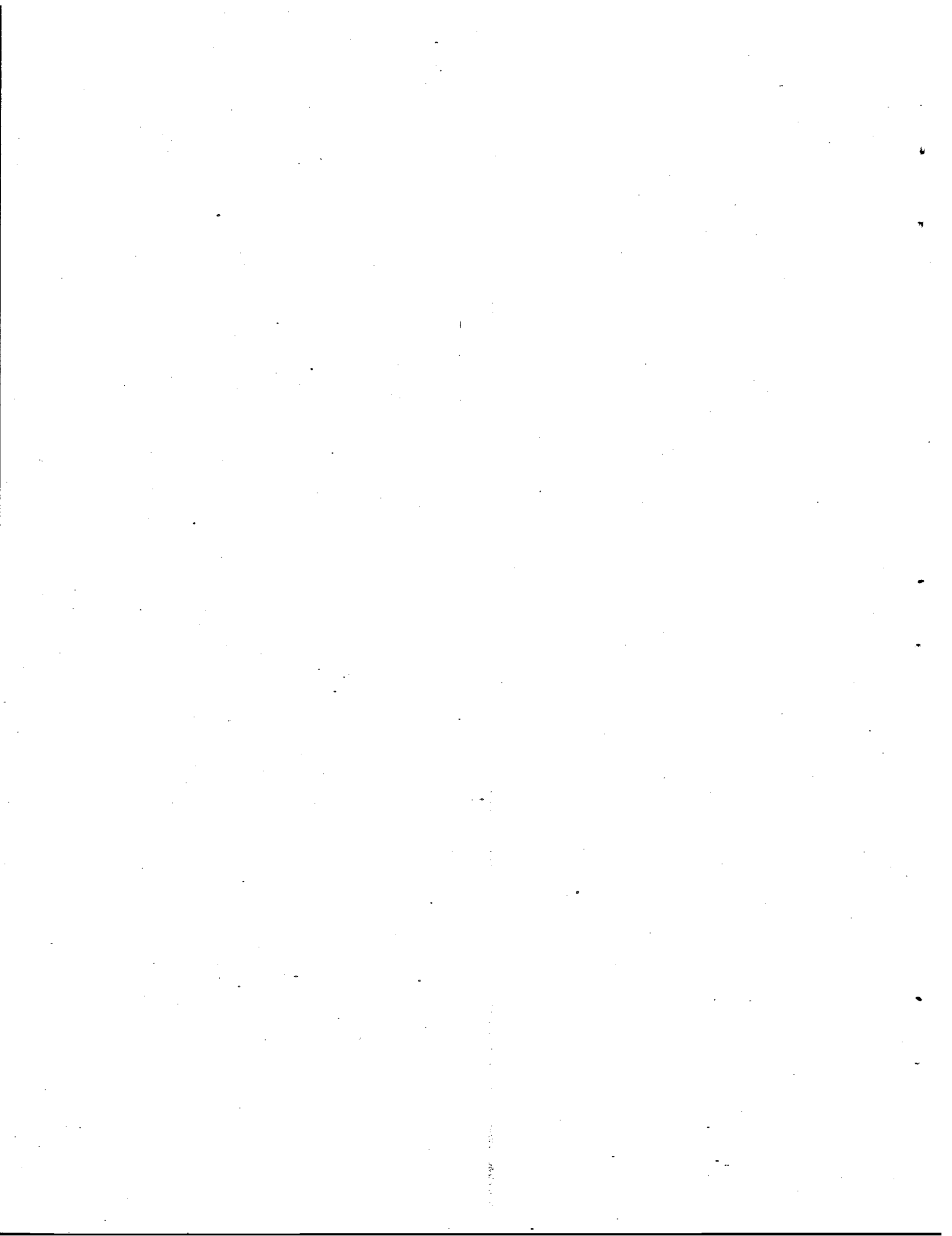


Figure E-43. Magnitude of Transfer Function Between Left Profile and Right Profile (Track Class 4)



E-3. CROSSLEVEL AND ALIGNMENT

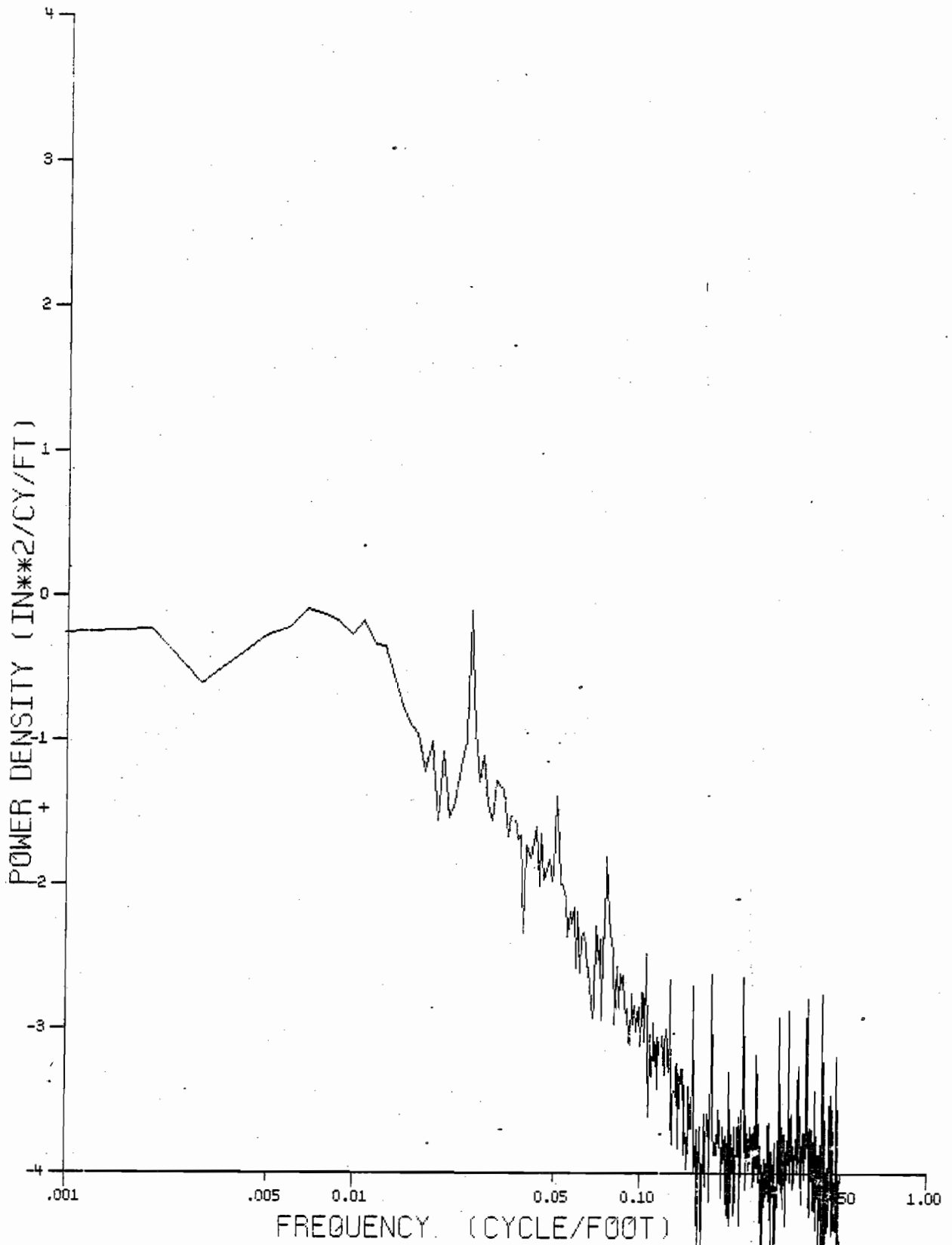


Figure E-44. Cross Spectral Density Between Crosslevel and Right Alignment (Track Class 3)

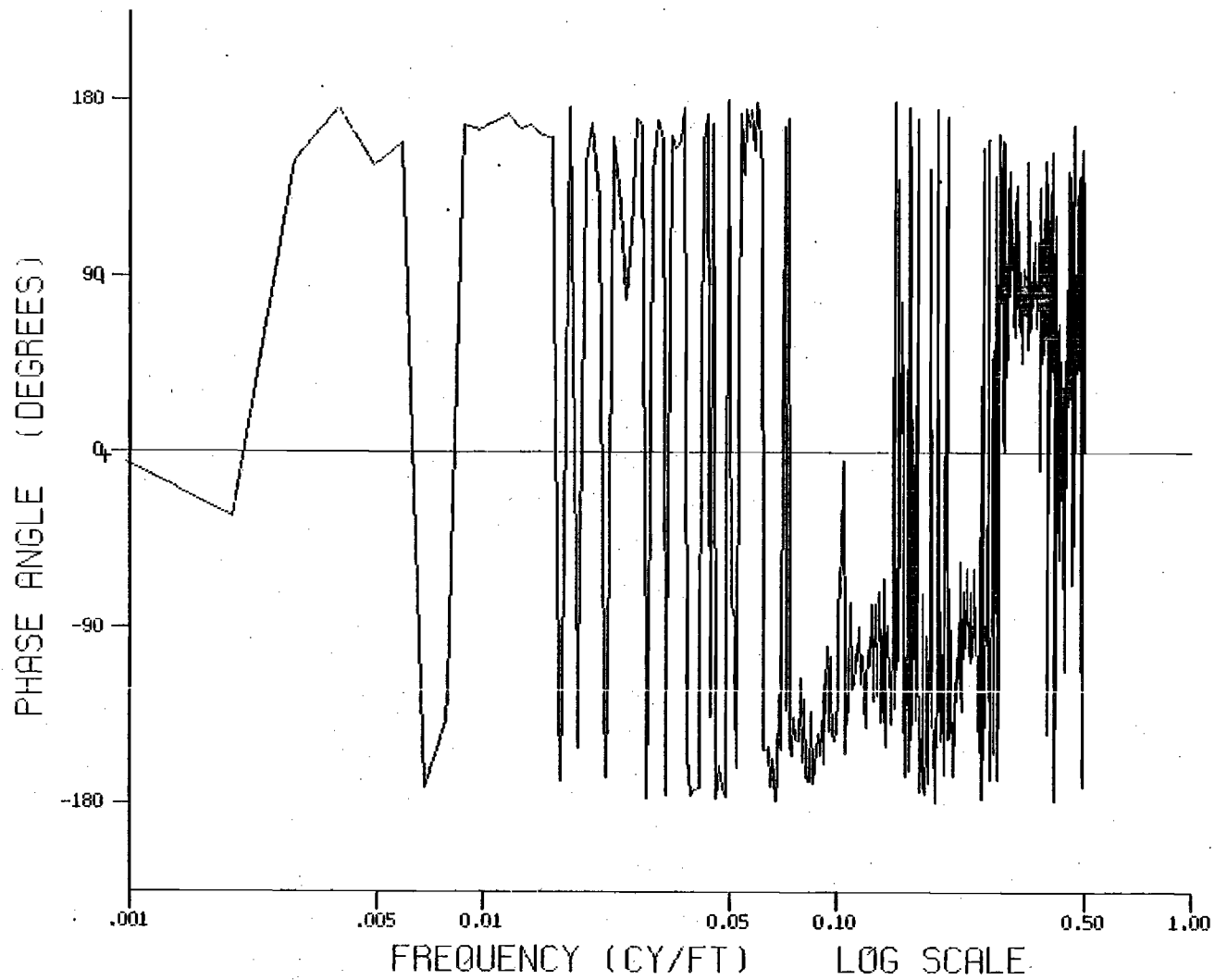


Figure E-45. Phase Angle Between Crosslevel and Right Alignment (Track Class 3)

E-54

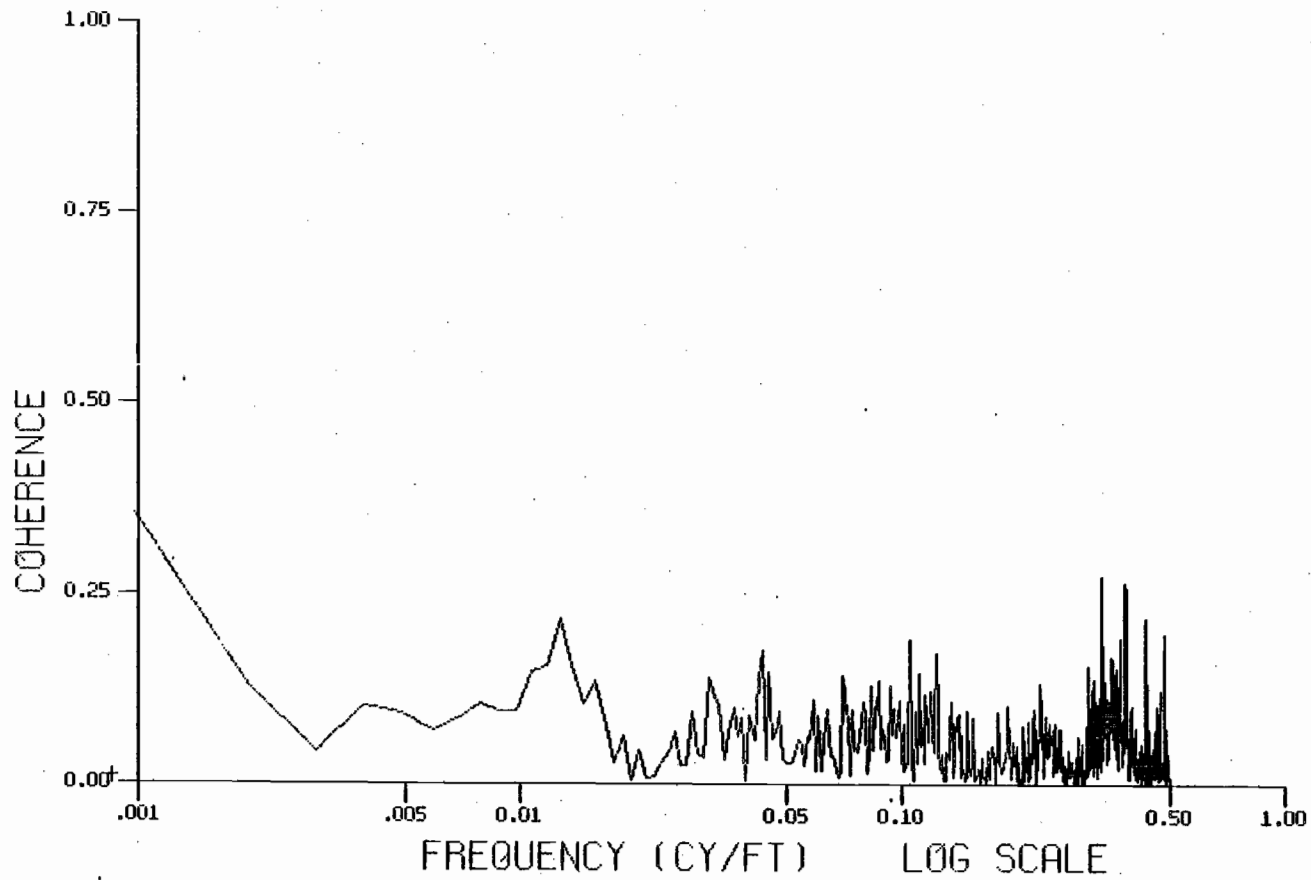


Figure E-46. Squared Coherence Between Crosslevel and Right Alignment (Track Class 3)

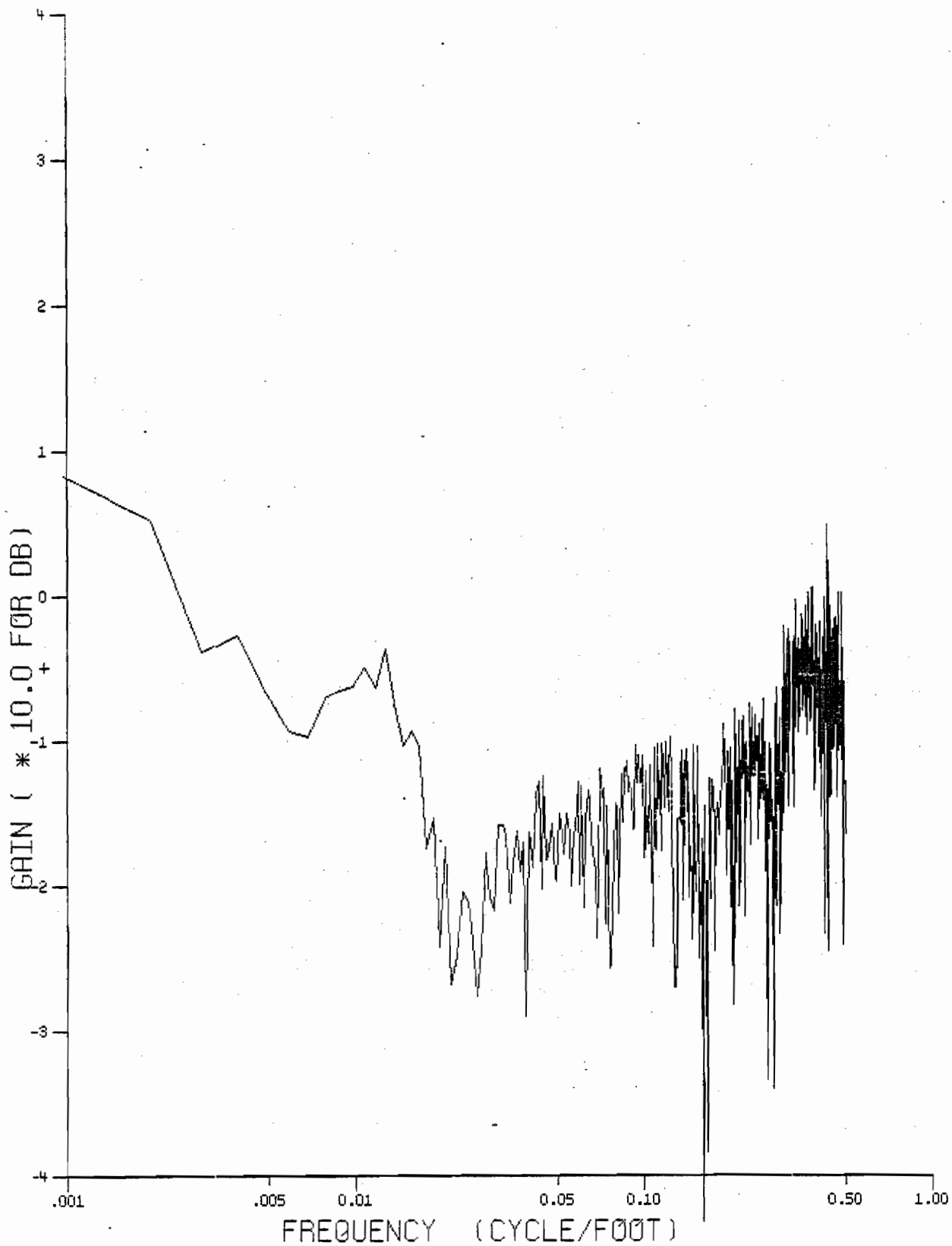
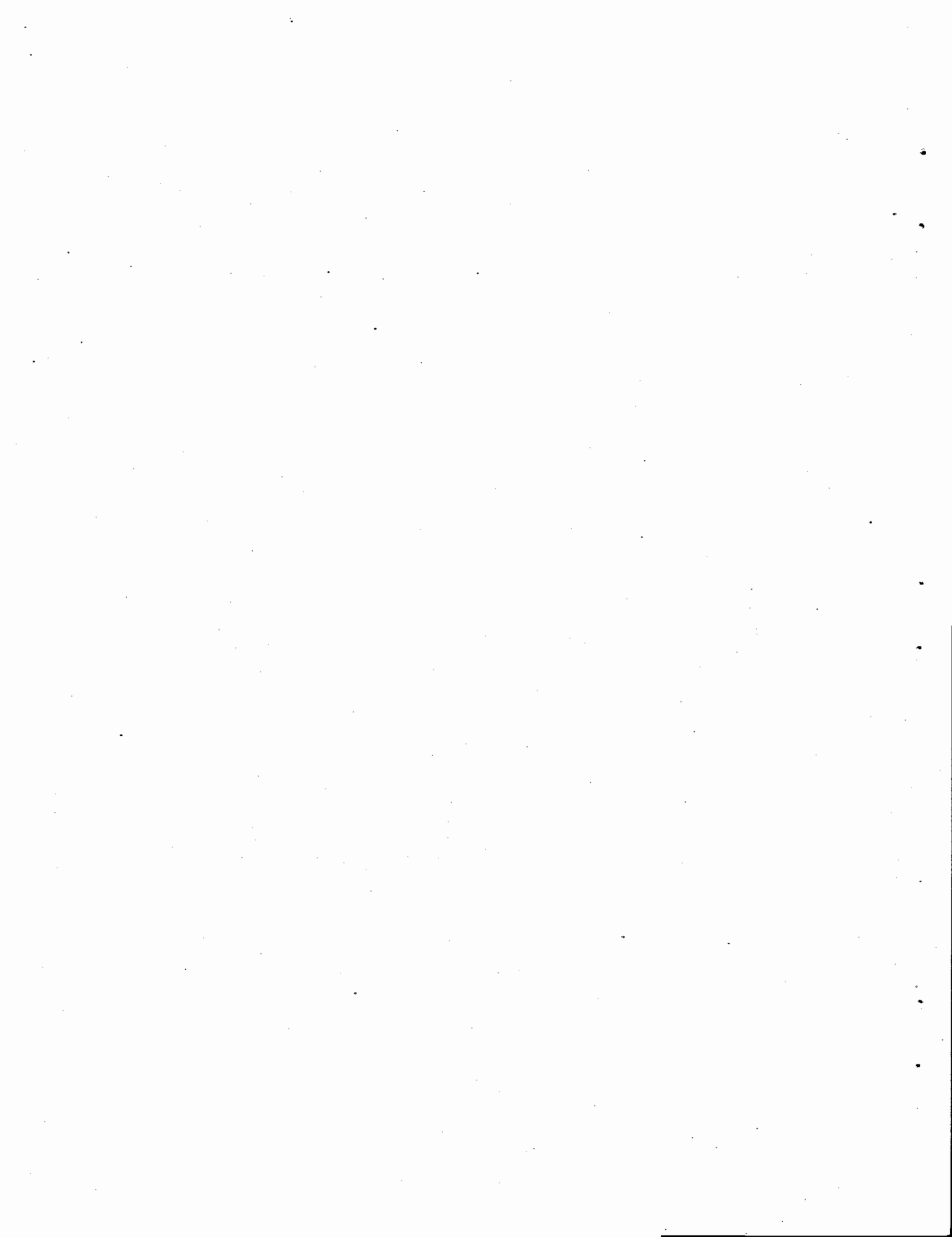


Figure E-47. Magnitude of Transfer Function Between Crosslevel and Right Alignment (Track Class 3)



E-4. CROSSLEVEL AND GAGE, GAGE AND
PROFILE, AND PROFILE AND ALIGNMENT

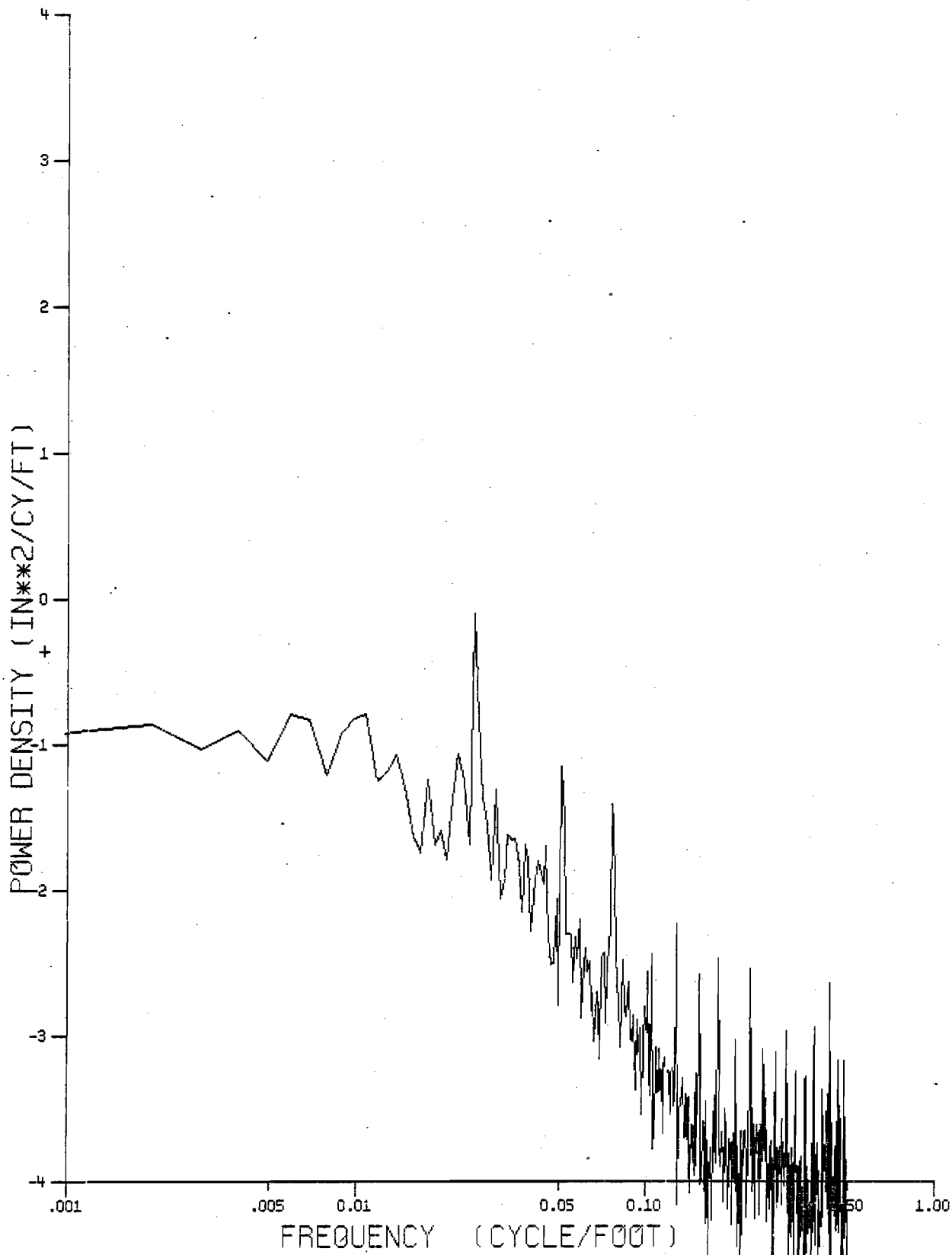


Figure E-48. Cross Spectra Density Between Crosslevel and Gage

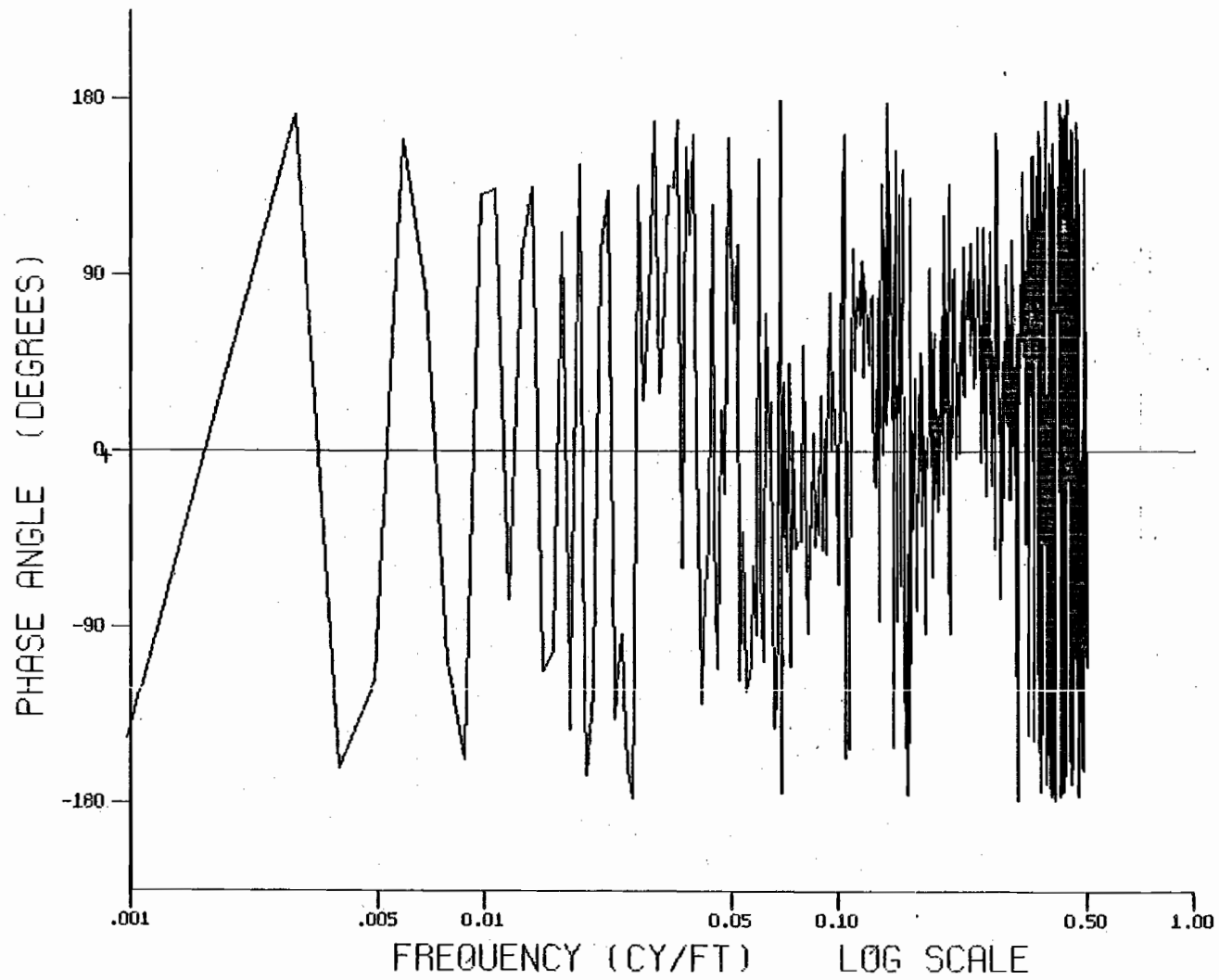


Figure E-49. Phase Angle Between Crosslevel and Gage

E-60

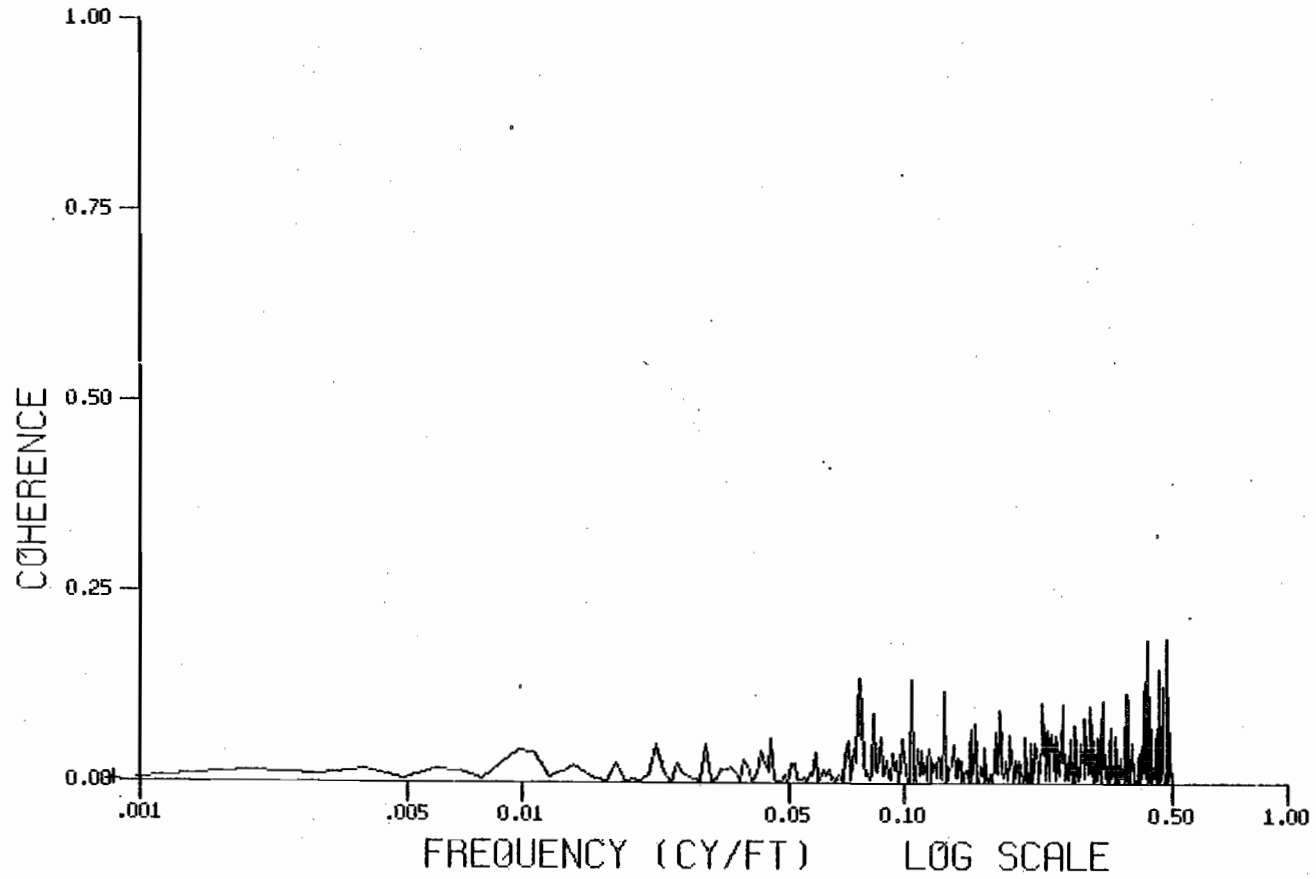


Figure E-50 Squared Coherence Between Crosslevel and Gage

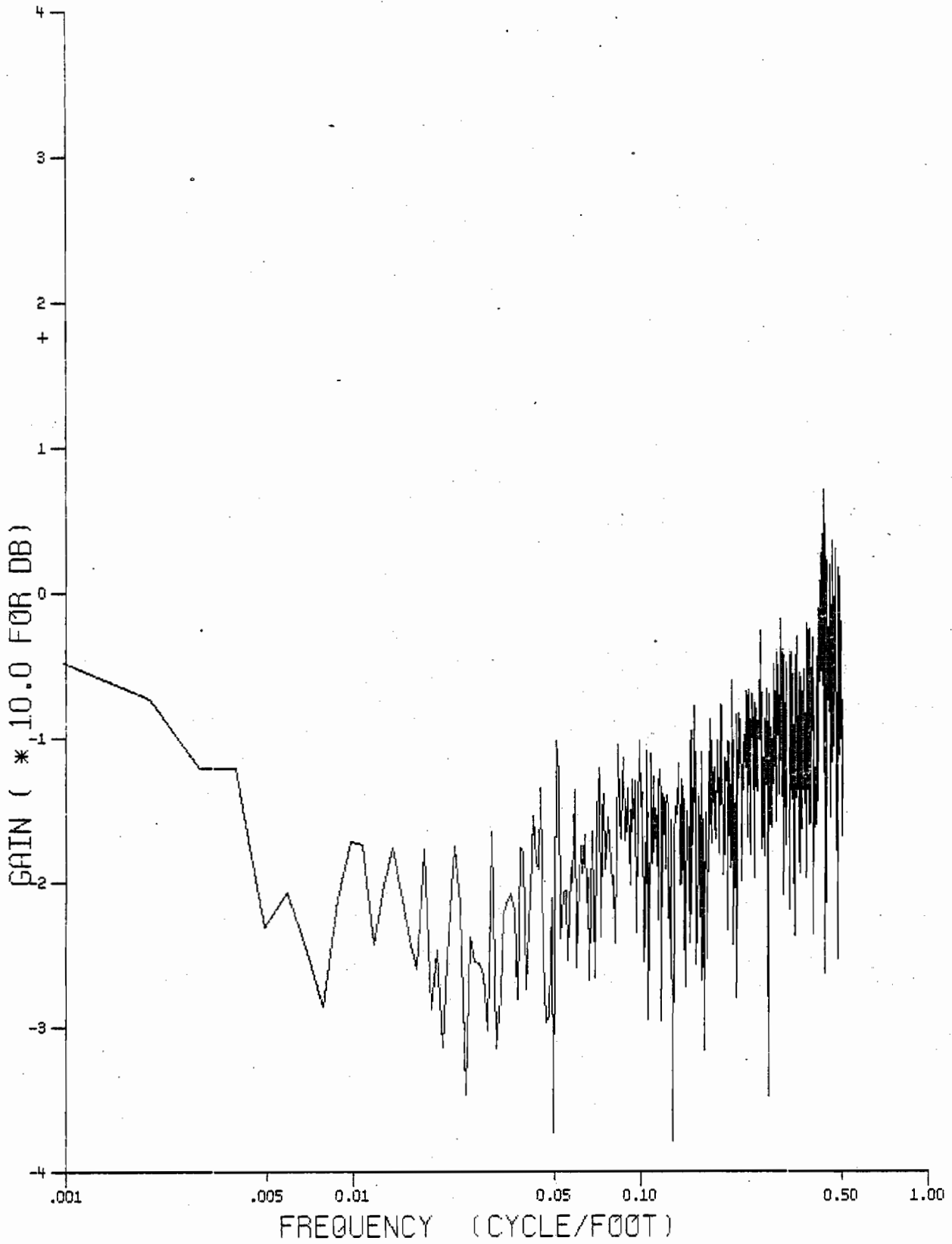


Figure E-51. Magnitude of Transfer Function Between Crosslevel and Gage

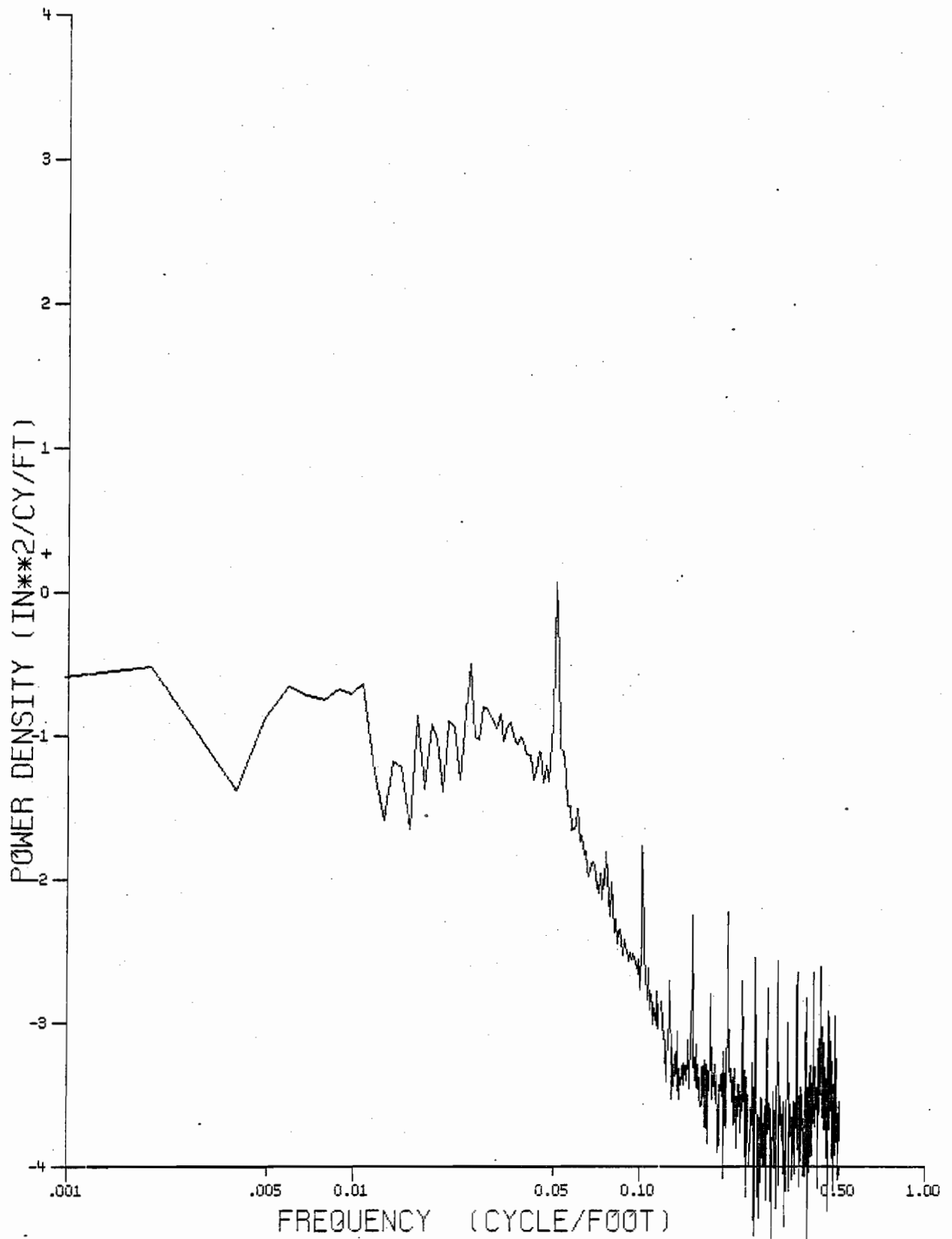


Figure E-52. Cross Spectral Density Between Gage and Left Profile (Track Class 3)

E-63

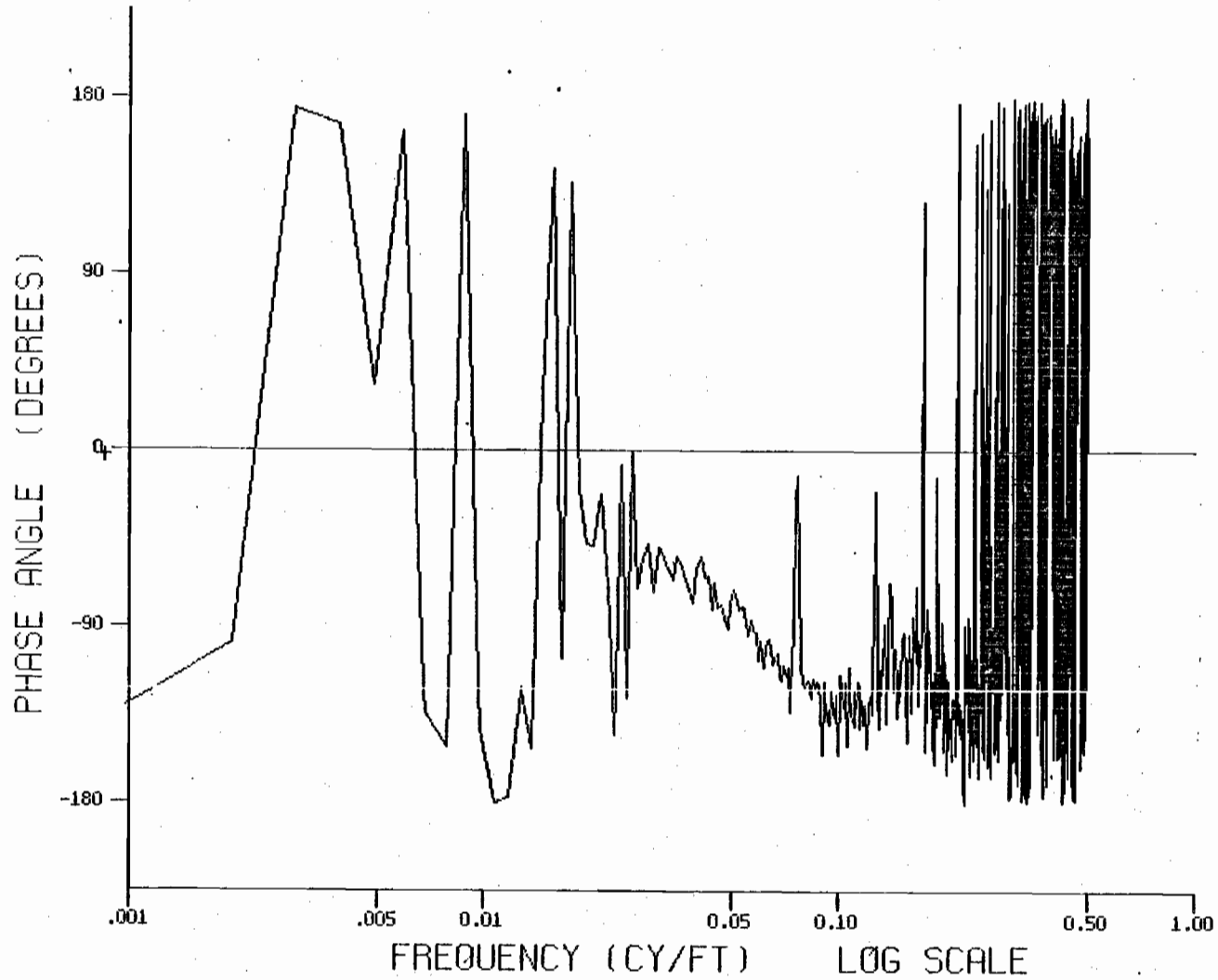


Figure E-53. Phase Angle Between Gage and Left Profile (Track Class 3)

E-64

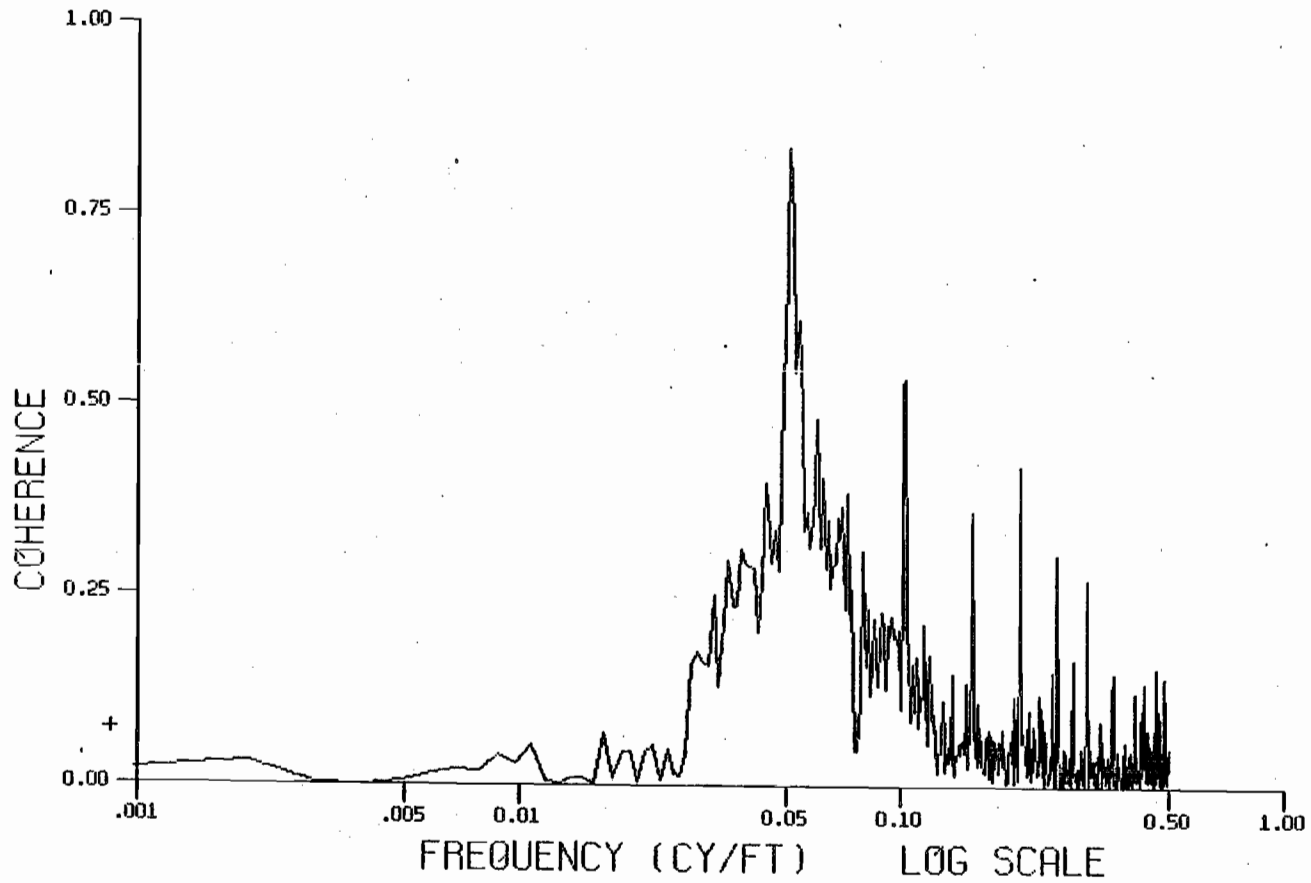


Figure E-54. Squared Coherence Between Gage and Left Profile (Track Class 3)

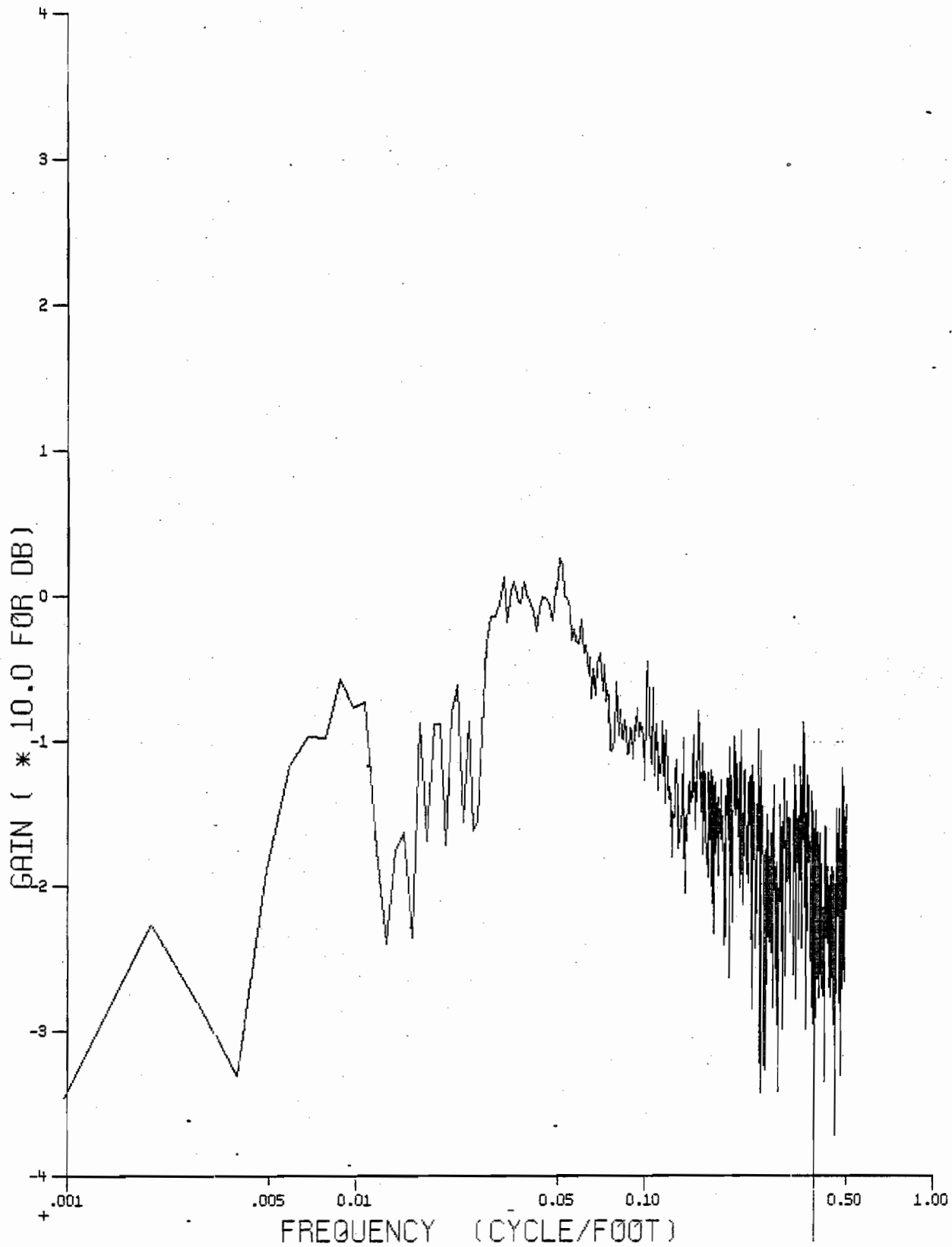


Figure E-55. Magnitude of Transfer Function Between Gage and Left Profile (Track Class 3)

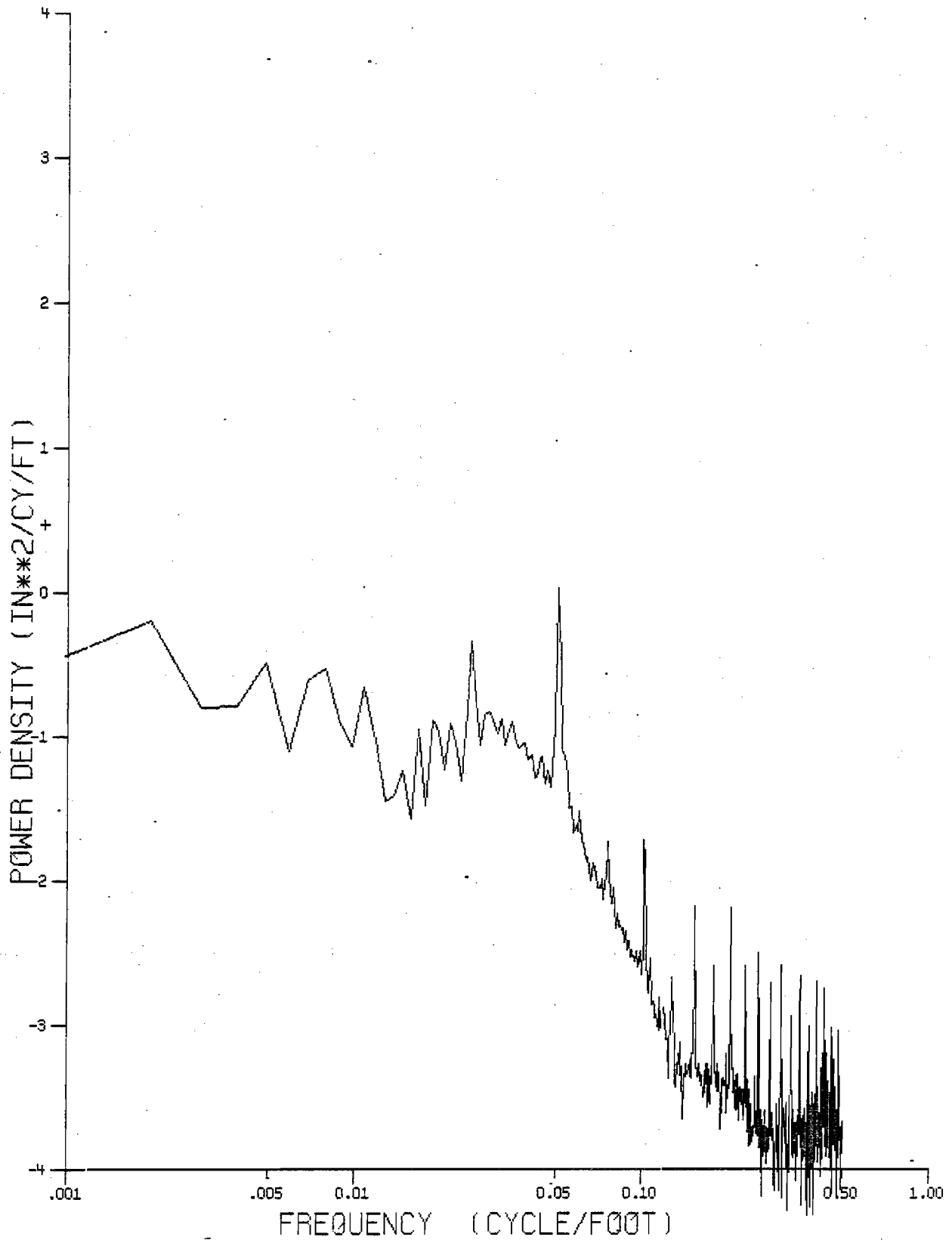


Figure E-56. Cross Spectral Density Between Gage and Mean Profile (Track Class 3)

E-67

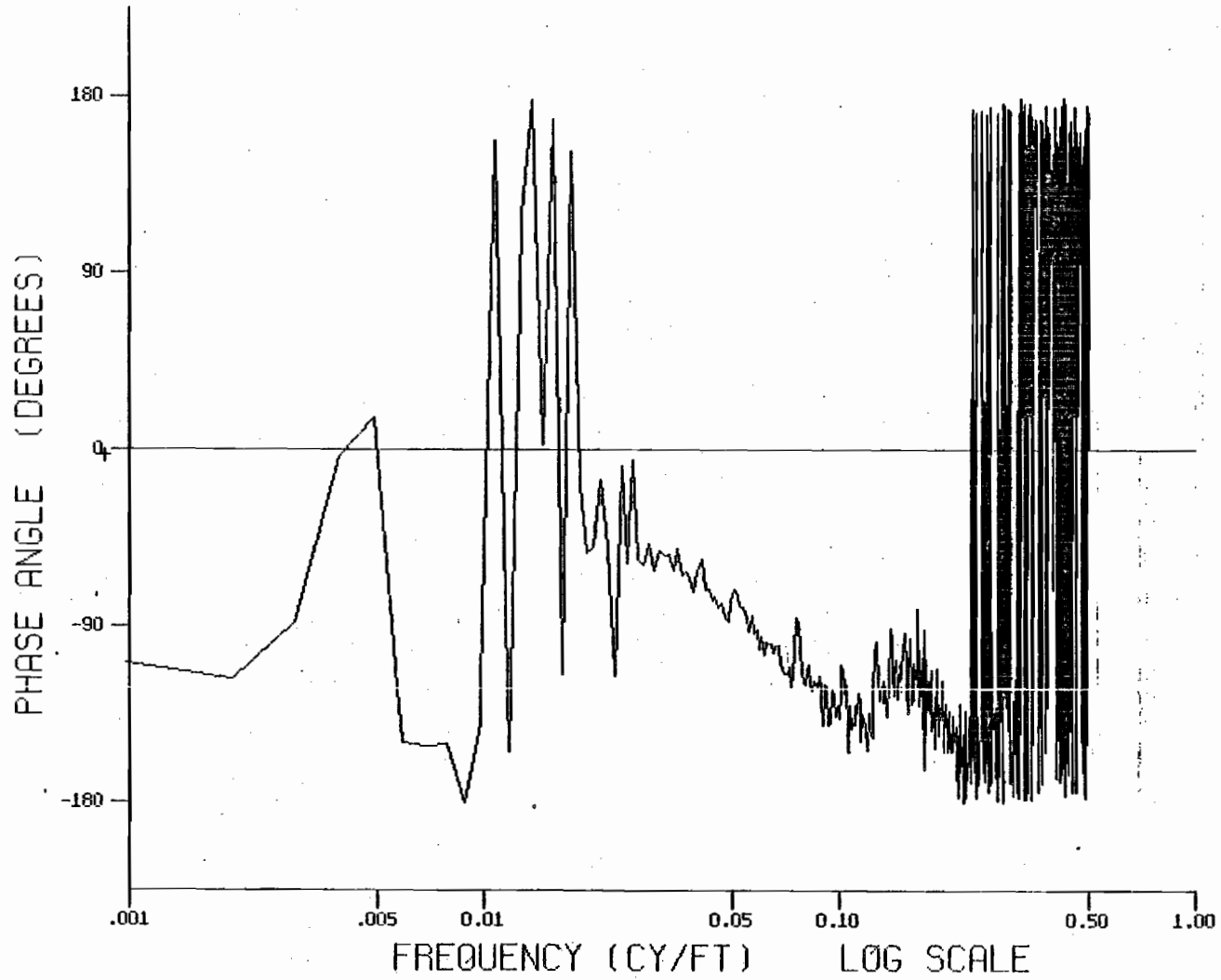


Figure E-57. Phase Angle Between Gage and Mean Profile
(Track Class 3)

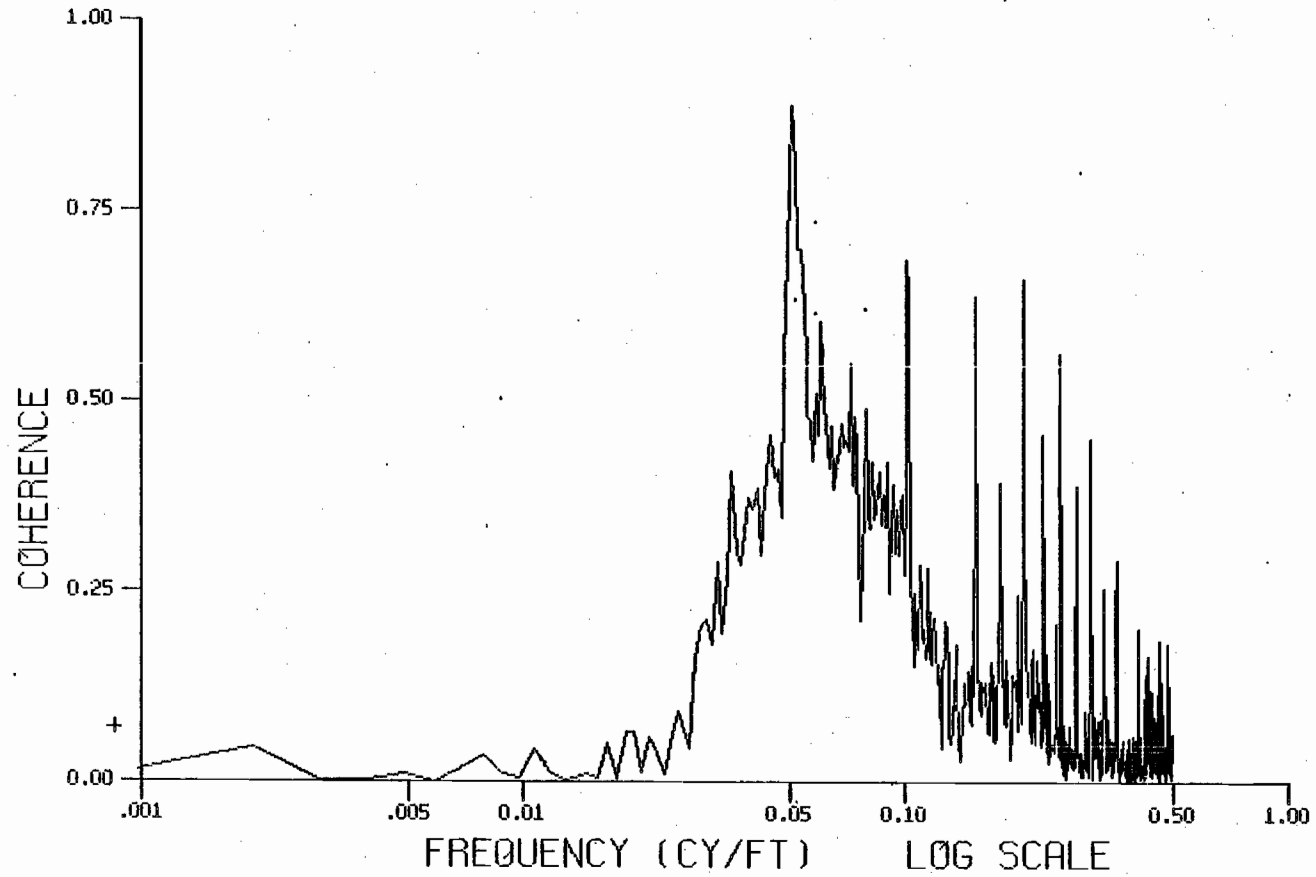


Figure E-58. Squared Coherence Between Gage and Mean Profile (Track Class 3)

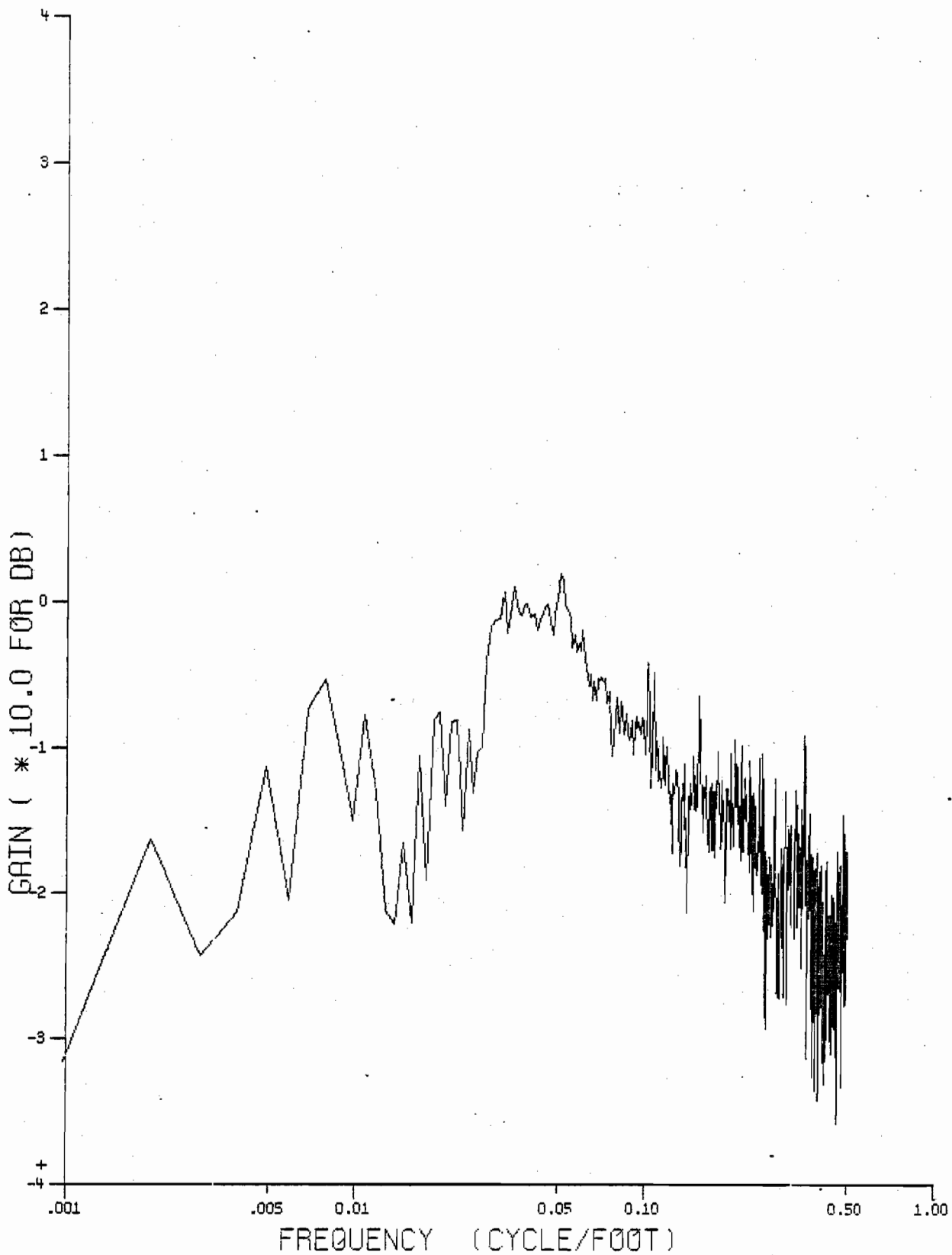


Figure E-59.. Magnitude of Transfer Function Between Gage and Mean Profile (Track Class 3)

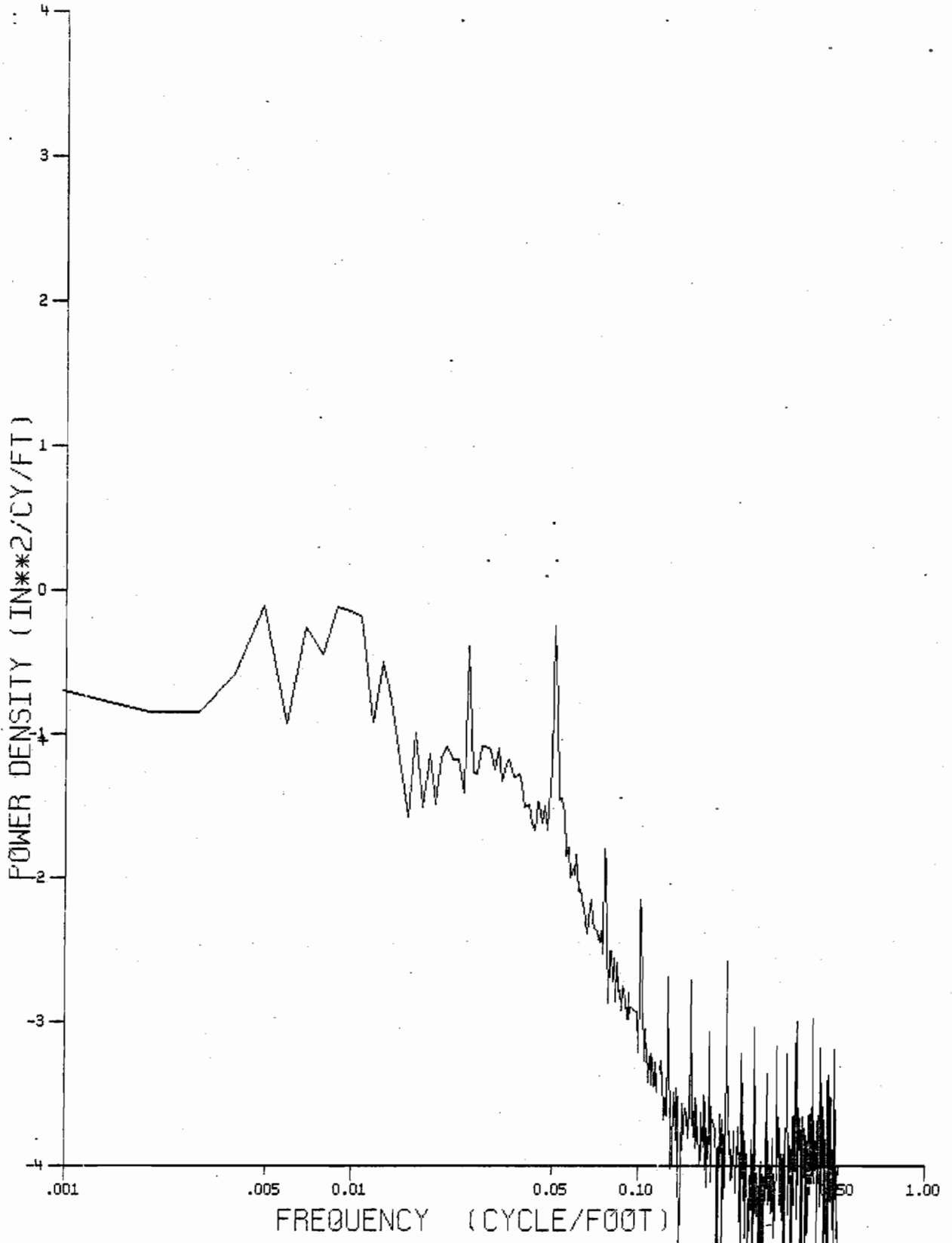


Figure E-60. Cross Spectral Density Between Left Profile and Left Alignment (Track Class 3)

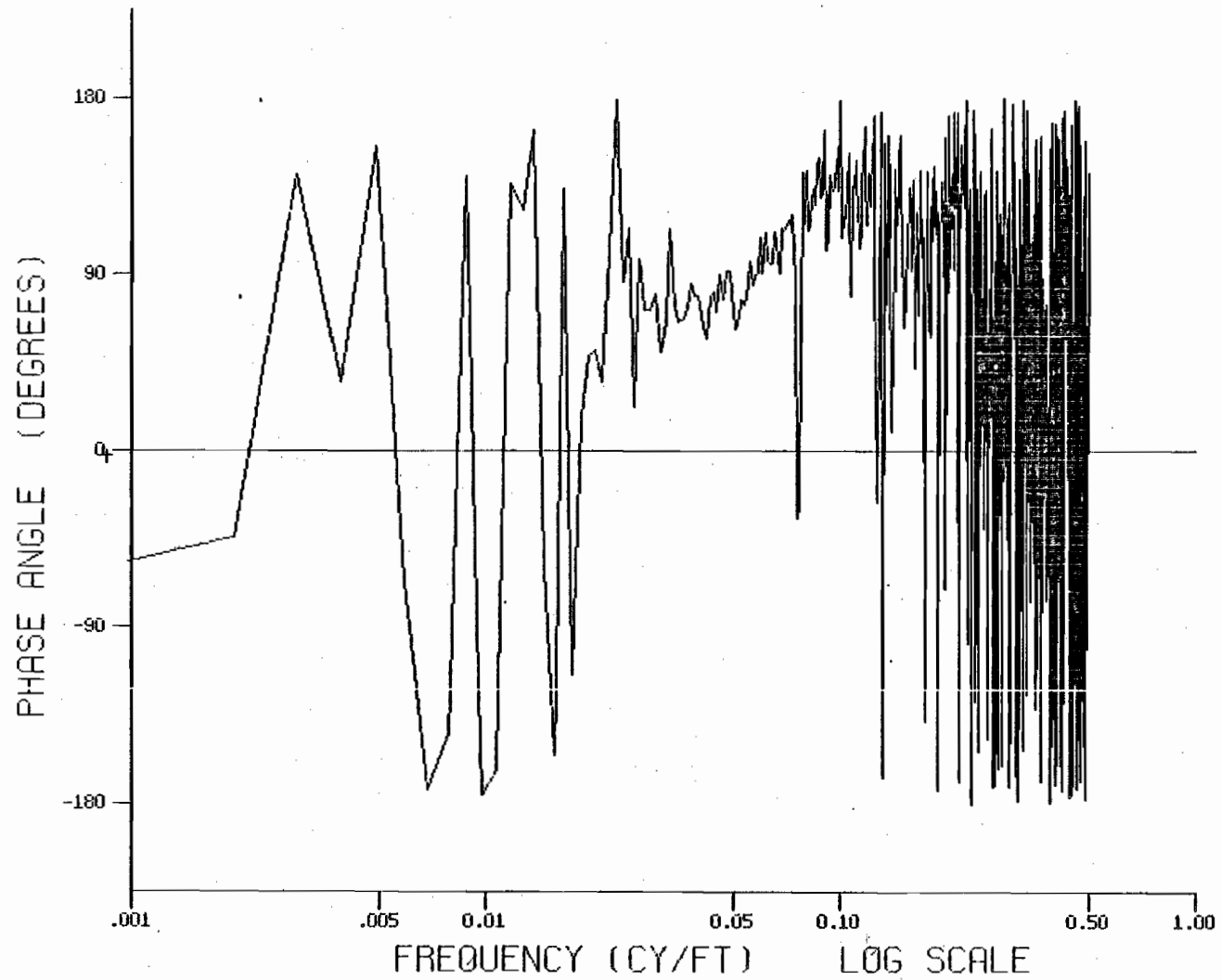


Figure E-61. Phase Angle Between Left Profile and Left Alignment (Track Class 3)

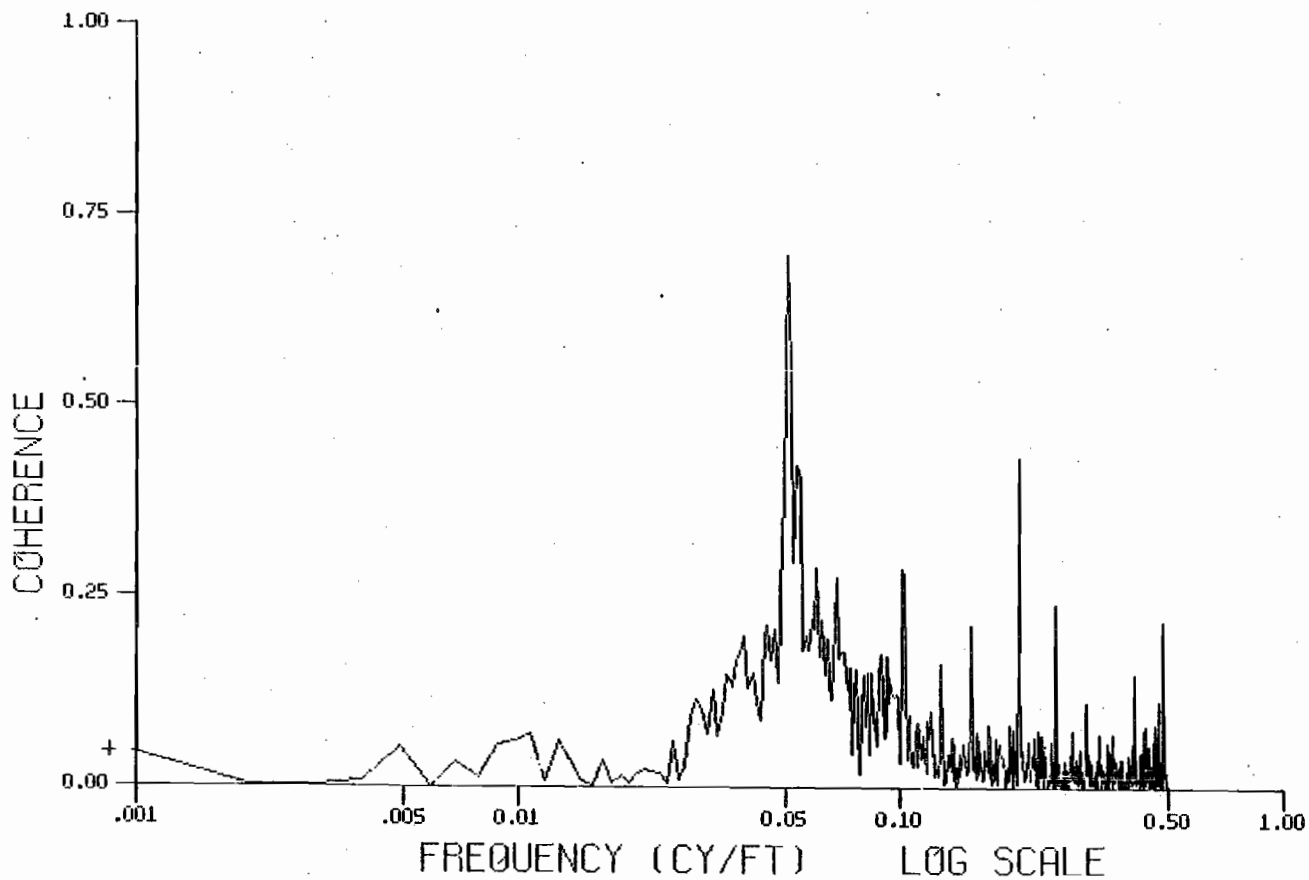


Figure E-62. Squared Coherence Between Left Profile and Left Alignment (Track Class 3)

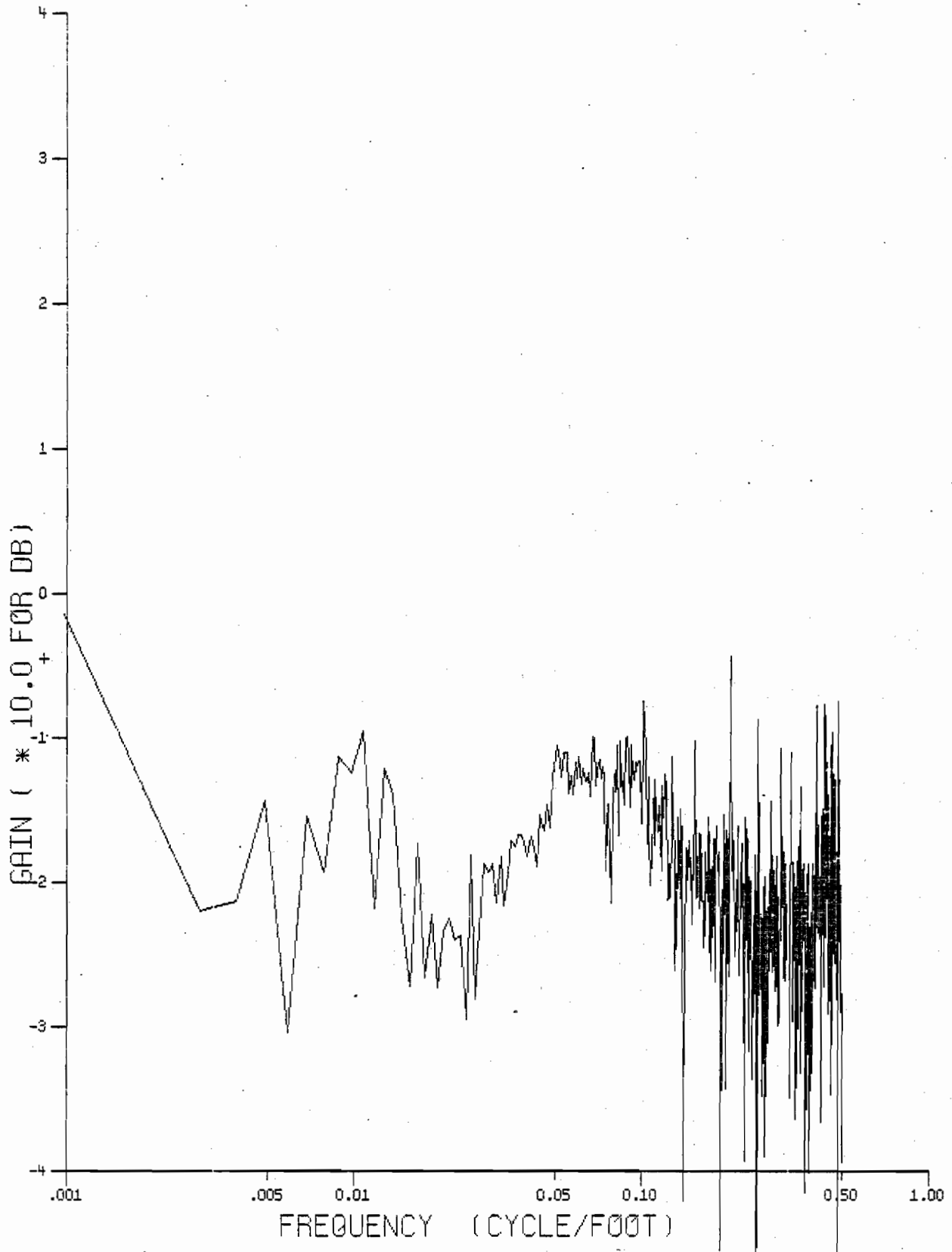
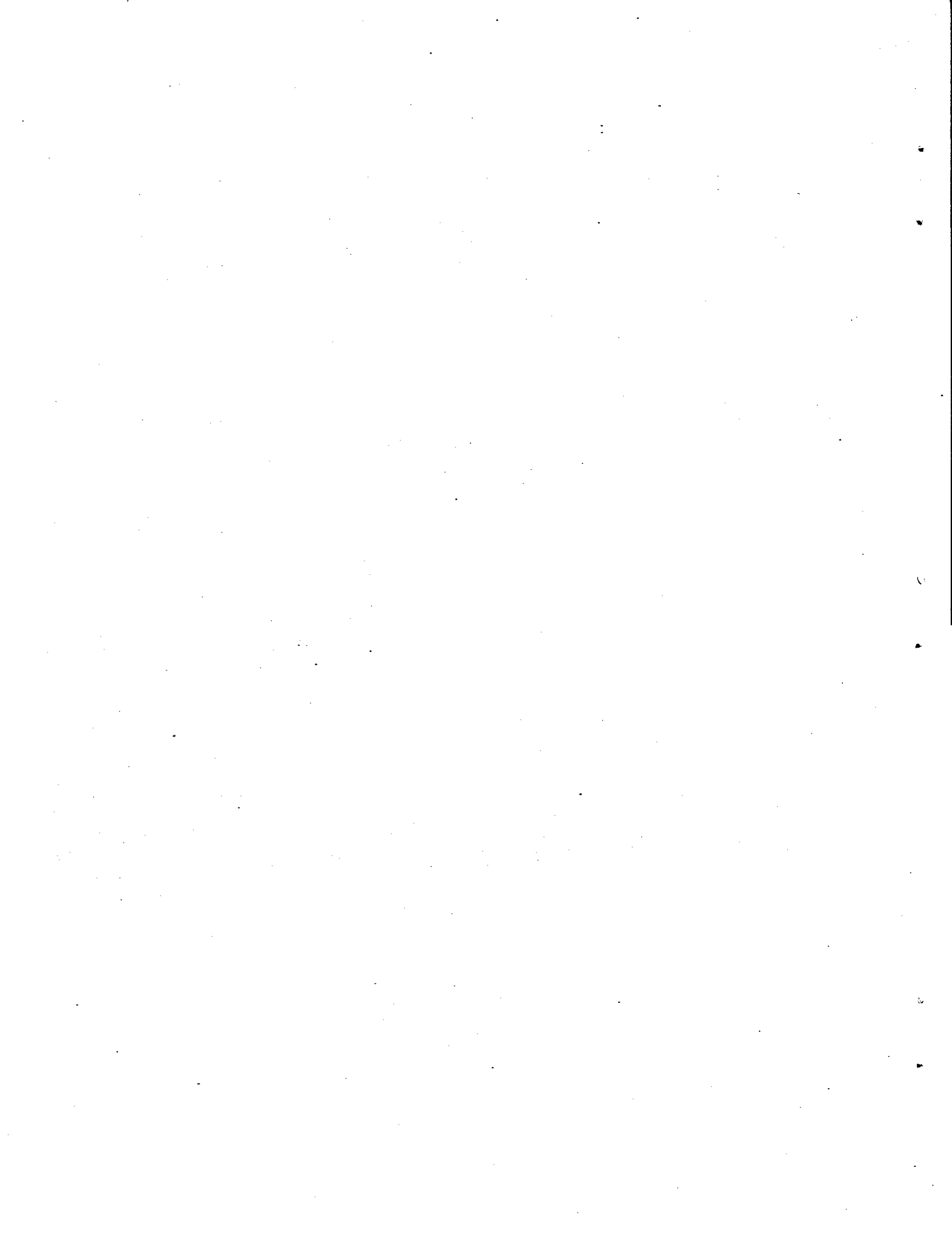


Figure E-63. Magnitude of Transfer Function Between Left Profile and Left Alignment (Track Class 3)



APPENDIX F

RMS VARIATIONS OF GAGE AND ALIGNMENT

This appendix gives the rms variations of gage and alignment as a function of curvature and superelevation. Two methods were used to evaluate these variations. In the first method, the average rms values were computed in the body of curves. Results are presented in Tables F-1 and F-2.

In the second method, a 200-foot moving point window was used to compute the rms variations continuously as a function of distance along the track. This processor was useful to separate the typical and severe variations. Results for typical and severe cases are given in Tables F-3 through F-10.

TABLE F-1
GAGE AND ALIGNMENT VARIATIONS FOR CLASS 2 BOLTED TRACK

| Curvature (Degrees) | Superelevation (Inch) | E - e* (Inch) | Mean Gage (Inch) | RMS Value (Inch) | | |
|------------------------|--------------------------|------------------|---------------------|---------------------|------------------------|-----------------------|
| | | | | Gage | High Rail Alignment | Low Rail Alignment |
| 0.0 | 0.0 | 0.0 | 57.0 | 0.32 | 0.52 | 0.51 |
| 0.1 | 0.0 | 0.0 | 57.0 | 0.33 | 0.41 | 0.41 |
| 1.7 | 1.5 | 0.8 | 58.0 | 0.35 | 0.35 | 0.35 |
| 1.7 | 1.5 | 0.8 | 56.0 | 0.35 | 0.36 | 0.36 |
| 1.8 | 2.0 | 1.3 | 58.0 | 0.35 | 0.39 | 0.40 |
| 1.9 | 1.5 | 0.7 | 58.4 | 0.42 | 0.40 | 0.42 |
| 1.9 | 2.0 | 1.2 | 56.0 | 0.48 | 0.40 | 0.40 |
| 2.2 | 2.5 | 1.6 | 58.5 | 0.41 | 0.39 | 0.40 |
| 2.9 | 3.0 | 1.8 | 55.5 | 0.65 | 0.66 | 0.66 |
| Mean Value | | | | 0.41 | 0.43 | 0.43 |

*E = Measured superelevation
e = Superelevation for the posted speed

TABLE F-2
GAGE AND ALIGNMENT VARIATIONS FOR CLASS 3 BOLTED TRACK

| Curvature (Degrees) | Superelevation (Inch) | E - e (Inch) | Mean Gage (Inch) | RMS Value (Inch) | | |
|------------------------|--------------------------|-----------------|---------------------|------------------|------------------------|-----------------------|
| | | | | Gage | High Rail Alignment | Low Rail Alignment |
| 0.7 | 0.5 | 0.5 | 56.6 | 0.10 | 0.25 | 0.24 |
| 1.0 | 1.0 | -0.7 | 56.6 | 0.13 | 0.19 | 0.17 |
| 1.0 | 1.5 | -0.2 | 56.7 | 0.15 | 0.13 | 0.16 |
| 1.0 | 1.5 | -0.2 | 56.6 | 0.16 | 0.14 | 0.18 |
| 1.0 | 2.0 | 0.3 | 56.8 | 0.16 | 0.24 | 0.24 |
| 1.0 | 2.5 | 0.8 | 56.8 | 0.20 | 0.29 | 0.20 |
| 1.2 | 1.5 | -0.5 | 56.9 | 0.22 | 0.41 | 0.35 |
| 1.8 | 3.0 | 0.0 | 56.9 | 0.21 | 0.33 | 0.33 |
| 2.0 | 2.0 | -0.1 | 56.7 | 0.16 | 0.28 | 0.26 |
| 2.0 | 2.5 | -0.6 | 57.1 | 0.15 | 0.28 | 0.30 |
| 2.1 | 2.5 | -1.0 | 56.9 | 0.21 | 0.26 | 0.22 |
| 3.0 | 4.0 | 0.0 | 56.8 | 0.16 | 0.26 | 0.28 |
| 3.7 | 4.0 | -2.1 | 57.2 | 0.21 | 0.26 | 0.26 |
| 3.8 | 3.5 | -1.6 | 56.8 | 0.15 | 0.40 | 0.40 |
| 4.2 | 5.0 | -1.9 | 57.0 | 0.29 | 0.50 | 0.49 |
| 5.0 | 4.0 | -4.3 | 57.0 | 0.15 | 0.40 | 0.41 |
| 5.4 | 1.5 | -0.7 | 57.0 | 0.24 | 0.19 | 0.26 |
| 6.1 | 3.5 | 1.0 | 56.6 | 0.22 | 0.19 | 0.22 |
| 6.8 | 4.0 | 1.2 | 56.6 | 0.16 | 0.20 | 0.19 |
| 8.2 | 5.0 | 1.6 | 56.8 | 0.22 | 0.52 | 0.56 |
| 9.3 | 2.5 | -0.7 | 57.0 | 0.22 | 0.37 | 0.39 |
| 10.1 | 4.5 | -0.3 | 56.8 | 0.22 | 0.18 | 0.22 |
| 10.5 | 5.5 | 1.2 | 57.2 | 0.24 | 0.33 | 0.34 |
| Mean Value | | | | 0.19 | 0.29 | 0.29 |

F-3

TABLE F-3
NOTES FOR TABLES F-4 THROUGH F-10

Note 1: Symbols

g = mean gage (inch)

C = curvature (degrees)

E = measured superelevation (inch)

e = balanced superelevation for specific values of C and V
 $= 0.00066CV^2$

V = posted speed (mph)

a_g = RMS value of gage (inch)

a_l = RMS value of low rail alignment (inch)

a_h = RMS value of high rail alignment (inch)

a_m = RMS value of mean alignment (inch)

Note 2

RMS values were computed using a 200-foot moving point window.

Note 3

Quotients such as a_g/a_l , a_g/a_h were averaged independently.

TABLE F-4

AVERAGE RMS VALUES OF TYPICAL GAGE AND ALIGNMENT VARIATIONS FOR CLASS 2 BOLTED TRACK

| Curvature | Gage | Crosslevel | E - e | a_g | a_l | a_h | a_m | a_g/a_l | a_g/a_h | a_g/a_m | $a_g^2/a_l^2 + a_h^2$ |
|-----------|------|------------|-------|-------|-------|-------|-------|-----------|-----------|-----------|-----------------------|
| 0.0 | 56.3 | 0.0 | 0.0 | 0.10 | 0.20 | 0.20 | 0.20 | 0.75 | 0.75 | 0.75 | 0.25 |
| 0.0 | 56.2 | 0.0 | 0.0 | 0.15 | 0.20 | 0.20 | 0.20 | 0.62 | 0.62 | 0.62 | 0.25 |
| 0.0 | 56.2 | 0.0 | 0.0 | 0.10 | 0.20 | 0.20 | 0.20 | 0.75 | 0.75 | 0.75 | 0.25 |
| 1.0 | 56.3 | 2.0 | 1.6 | 0.15 | 0.40 | 0.40 | 0.40 | 0.50 | 0.50 | 0.50 | 0.25 |
| 1.0 | 56.4 | 1.5 | 1.1 | 0.10 | 0.25 | 0.25 | 0.25 | 0.50 | 0.50 | 0.50 | 0.12 |
| 1.5 | 57.0 | 3.0 | 2.4 | 0.10 | 0.35 | 0.35 | 0.35 | 0.30 | 0.38 | 0.30 | 0.04 |
| 2.0 | 56.5 | 0.0 | 0.0 | 0.10 | 0.30 | 0.30 | 0.30 | 0.88 | 0.62 | 0.88 | 0.20 |
| 2.0 | 56.4 | 2.0 | 1.2 | 0.10 | 0.30 | 0.30 | 0.30 | 0.62 | 0.50 | 0.50 | 0.25 |
| 2.0 | 56.5 | 2.0 | 1.2 | 0.10 | 0.25 | 0.30 | 0.30 | 0.62 | 0.50 | 0.50 | 0.20 |
| 2.0 | 57.0 | 2.0 | 1.2 | 0.10 | 0.20 | 0.20 | 0.20 | 0.75 | 0.75 | 0.75 | 0.50 |
| 3.0 | 57.0 | 5.0 | 3.8 | 0.10 | 0.40 | 0.40 | 0.40 | 0.30 | 0.30 | 0.30 | 0.03 |
| 3.0 | 57.0 | 4.8 | 3.6 | 0.15 | 0.40 | 0.40 | 0.40 | 0.50 | 0.50 | 0.50 | 0.25 |
| 3.0 | 56.7 | 4.0 | 2.8 | 0.25 | 0.30 | 0.40 | 0.30 | 0.75 | 0.62 | 0.75 | 0.25 |

TABLE F-5

AVERAGE RMS VALUES OF TYPICAL GAGE AND ALIGNMENT VARIATIONS FOR CLASS 3 BOLTED TRACK

| Curvature | Gage | Crosslevel | E - e | a_g | a_ℓ | a_h | a_m | a_g/a_ℓ | a_g/a_h | a_g/a_m | $a_g^2/a_\ell^2 + a_h^2$ |
|-----------|------|------------|-------|-------|----------|-------|-------|--------------|-----------|-----------|--------------------------|
| 0.0 | 5.65 | 0.0 | 0.0 | 0.11 | 0.10 | 0.10 | 0.08 | 1.25 | 1.26 | 1.70 | 0.85 |
| 0.0 | 5.65 | 0.0 | 0.0 | 0.10 | 0.09 | 0.11 | 0.09 | 1.00 | 0.75 | 1.00 | 0.35 |
| 0.0 | 56.4 | 0.0 | 0.0 | 0.09 | 0.09 | 0.09 | 0.08 | 0.88 | 1.00 | 1.10 | 0.35 |
| 0.0 | 56.4 | 0.0 | 0.0 | 0.10 | 0.07 | 0.07 | 0.06 | 1.38 | 1.50 | 1.88 | 1.00 |
| 0.0 | 56.5 | 0.0 | 0.0 | 0.10 | 0.11 | 0.09 | 0.09 | 0.88 | 1.25 | 1.25 | 0.50 |
| 0.0 | 56.5 | 0.0 | 0.0 | 0.09 | 0.10 | 0.10 | 0.10 | 0.88 | 0.75 | 0.80 | 0.25 |
| 0.0 | 56.3 | 0.0 | 0.0 | 0.10 | 0.10 | 0.12 | 0.09 | 0.88 | 1.38 | 1.25 | 0.55 |
| 0.0 | 56.3 | 0.0 | 0.0 | 0.10 | 0.09 | 0.08 | 0.07 | 1.25 | 1.55 | 1.60 | 0.88 |
| 0.0 | 56.3 | 0.0 | 0.0 | 0.11 | 0.10 | 0.12 | 0.11 | 1.00 | 0.75 | 1.00 | 0.50 |
| 0.0 | 56.5 | 0.0 | 0.0 | 0.11 | 0.12 | 0.15 | 0.12 | 0.80 | 0.75 | 0.85 | 0.25 |
| 0.0 | 56.4 | 0.0 | 0.0 | 0.07 | 0.09 | 0.09 | 0.09 | 0.80 | 0.75 | 0.80 | 0.30 |
| 0.0 | 56.5 | 0.0 | 0.0 | 0.09 | 0.15 | 0.11 | 0.12 | 0.50 | 0.63 | 0.63 | 0.13 |
| 0.0 | 56.4 | 0.0 | 0.0 | 0.10 | 0.09 | 0.10 | 0.08 | 1.25 | 0.88 | 1.25 | 0.50 |
| 0.0 | 56.4 | 0.0 | 0.0 | 0.10 | 0.13 | 0.13 | 0.13 | 0.75 | 0.75 | 0.75 | 0.25 |
| 0.0 | 56.3 | 0.0 | 0.0 | 0.10 | 0.15 | 0.13 | 0.13 | 0.63 | 0.75 | 0.75 | 0.25 |
| 0.0 | 56.3 | 0.0 | 0.0 | 0.09 | 0.13 | 0.17 | 0.13 | 0.55 | 0.50 | 0.50 | 0.12 |
| 0.0 | 56.3 | 0.0 | 0.0 | 0.09 | 0.10 | 0.08 | 0.09 | 0.77 | 1.38 | 1.25 | 0.50 |
| 0.0 | 56.3 | 0.0 | 0.0 | 0.10 | 0.10 | 0.10 | 0.09 | 1.00 | 1.00 | 1.12 | 0.50 |
| 0.0 | 56.4 | 0.0 | 0.0 | 0.10 | 0.09 | 0.09 | 0.09 | 1.13 | 1.13 | 1.13 | 0.60 |
| 0.0 | 56.2 | 0.0 | 0.0 | 0.10 | 0.11 | 0.11 | 0.10 | 0.88 | 0.88 | 0.10 | 0.30 |
| 0.0 | 56.2 | 0.0 | 0.0 | 0.11 | 0.10 | 0.10 | 0.09 | 1.38 | 1.13 | 1.63 | 0.75 |
| 0.0 | 56.2 | 0.0 | 0.0 | 0.10 | 0.11 | 0.12 | 0.12 | 0.77 | 0.63 | 0.75 | 0.25 |
| 0.0 | 56.4 | 0.0 | 0.0 | 0.15 | 0.07 | 0.20 | 0.12 | 2.13 | 0.75 | 1.25 | 0.50 |

TABLE F-5 (CONT)

AVERAGE RMS VALUES OF TYPICAL GAGE AND ALIGNMENT VARIATIONS FOR CLASS 3 BOLTED TRACK

| Curvature | Gage | Crosslevel | E - e | a_g | a_ℓ | a_h | a_m | a_g/a_ℓ | a_g/a_h | a_g/a_m | $a_g^2/a_\ell^2 + a_h^2$ |
|-----------|------|------------|-------|-------|----------|-------|-------|--------------|-----------|-----------|--------------------------|
| 0.0 | 56.4 | 0.0 | 0.0 | 0.09 | 0.10 | 0.11 | 0.10 | 0.88 | 0.75 | 0.88 | 0.20 |
| 0.0 | 56.4 | 0.0 | 0.0 | 0.10 | 0.10 | 0.10 | 0.09 | 1.00 | 1.00 | 1.10 | 0.52 |
| 0.0 | 56.4 | 0.0 | 0.0 | 0.15 | 0.12 | 0.09 | 0.10 | 1.13 | 1.75 | 1.75 | 0.88 |
| 0.8 | 56.4 | 0.5 | -0.7 | 0.10 | 0.10 | 0.09 | 0.09 | 0.88 | 1.20 | 1.20 | 0.50 |
| 1.5 | 56.4 | 1.1 | -1.4 | 0.09 | 0.17 | 0.17 | 0.17 | 0.63 | 0.63 | 0.63 | 0.20 |
| 1.7 | 56.3 | 1.3 | -1.5 | 0.11 | 0.10 | 0.09 | 0.08 | 1.25 | 1.38 | 1.75 | 0.75 |
| 2.0 | 57.5 | 2.5 | -0.8 | 0.12 | 0.10 | 0.12 | 0.10 | 1.25 | 1.00 | 1.25 | 0.70 |
| 2.0 | 56.4 | 1.8 | -1.6 | 0.12 | 0.10 | 0.08 | 0.08 | 1.38 | 1.75 | 2.25 | 1.15 |
| 2.0 | 56.3 | 1.5 | -1.8 | 0.12 | 0.20 | 0.25 | 0.20 | 0.63 | 0.72 | 0.75 | 0.22 |
| 2.0 | 56.3 | 1.0 | -2.3 | 0.12 | 0.20 | 0.25 | 0.25 | 0.63 | 0.50 | 0.63 | 0.13 |
| 2.0 | 56.5 | 3.0 | -0.3 | 0.09 | 0.12 | 0.12 | 0.11 | 0.63 | 0.63 | 0.63 | 0.22 |
| 2.5 | 57.3 | 2.5 | -0.1 | 0.12 | 0.20 | 0.12 | 0.15 | 0.73 | 1.00 | 1.00 | 0.30 |
| 2.5 | 57.3 | 2.0 | -2.13 | 0.12 | 0.17 | 0.21 | 0.20 | 0.75 | 0.63 | 0.75 | 0.25 |
| 3.0 | 57.4 | 4.5 | -0.5 | 0.11 | 0.25 | 0.25 | 0.25 | 0.50 | 0.50 | 0.50 | 0.10 |
| 3.0 | 57.3 | 3.8 | -1.2 | 0.12 | 0.25 | 0.25 | 0.25 | 0.50 | 0.50 | 0.50 | 0.13 |
| 3.5 | 57.5 | 3.5 | -0.2 | 0.15 | 0.13 | 0.13 | 0.11 | 1.00 | 1.00 | 1.25 | 0.50 |
| 3.5 | 57.5 | 3.8 | 0.1 | 0.15 | 0.15 | 0.15 | 0.15 | 0.75 | 0.90 | 0.90 | 0.30 |
| 3.5 | 56.5 | 4.0 | -1.8 | 0.17 | 0.20 | 0.20 | 0.20 | 0.88 | 0.88 | 1.00 | 0.35 |
| 3.5 | 57.3 | 6.5 | 0.7 | 0.11 | 0.22 | 0.20 | 0.21 | 0.50 | 0.50 | 0.50 | 0.13 |
| 3.5 | 57.4 | 3.8 | -2.0 | 0.12 | 0.25 | 0.25 | 0.25 | 0.50 | 0.50 | 0.50 | 0.12 |
| 3.5 | 57.4 | 4.0 | -1.8 | 0.11 | 0.15 | 0.15 | 0.15 | 0.75 | 0.75 | 0.75 | 0.25 |
| 4.5 | 57.7 | 4.3 | -0.5 | 0.25 | 0.20 | 0.20 | 0.20 | 1.27 | 1.23 | 1.38 | 0.88 |
| 5.5 | 57.8 | 5.0 | -0.8 | 0.20 | 0.21 | 0.20 | 0.20 | 1.00 | 1.13 | 1.13 | 0.50 |

TABLE F-6

AVERAGE RMS VALUES OF TYPICAL GAGE AND ALIGNMENT VARIATIONS FOR CLASS 3 WELDED TRACK

| Curvature | Gage | Crosslevel | E - e | a_g | a_ℓ | a_h | a_m | a_g/a_ℓ | a_g/a_h | a_g/a_m | $a_g^2/a_\ell^2+a_h^2$ |
|-----------|------|------------|-------|-------|----------|-------|-------|--------------|-----------|-----------|------------------------|
| 0.0 | 56.4 | 0.0 | 0.0 | 0.12 | 0.10 | 0.10 | 0.10 | 1.25 | 1.13 | 1.50 | 0.75 |
| 0.0 | 56.3 | 0.0 | 0.0 | 0.09 | 0.09 | 0.08 | 0.08 | 0.88 | 1.00 | 1.00 | 0.50 |
| 0.0 | 56.3 | 0.0 | 0.0 | 0.12 | 0.18 | 0.13 | 0.13 | 0.75 | 1.00 | 0.88 | 0.25 |
| 0.0 | 56.3 | 0.0 | 0.0 | 0.15 | 0.10 | 0.09 | 0.09 | 1.38 | 1.75 | 2.25 | 1.13 |
| 0.0 | 56.3 | 0.0 | 0.0 | 0.09 | 0.18 | 0.13 | 0.15 | 0.50 | 0.50 | 0.50 | 0.13 |
| 0.0 | 56.5 | 0.0 | 0.0 | 0.09 | 0.09 | 0.08 | 0.08 | 1.00 | 1.00 | 1.13 | 0.50 |
| 0.0 | 56.3 | 0.0 | 0.0 | 0.08 | 0.10 | 0.10 | 0.10 | 0.64 | 9.75 | 0.75 | 0.25 |
| 0.0 | 56.2 | 0.0 | 0.0 | 0.13 | 0.11 | 0.09 | 0.09 | 1.10 | 1.75 | 1.50 | 0.30 |
| 0.0 | 56.3 | 0.0 | 0.0 | 0.10 | 0.11 | 0.10 | 0.10 | 0.63 | 1.00 | 1.00 | 0.50 |
| 0.0 | 56.4 | 0.0 | 0.0 | 0.10 | 0.09 | 0.09 | 0.08 | 1.25 | 1.38 | 1.75 | 0.88 |
| 0.0 | 56.3 | 0.0 | 0.0 | 0.12 | 0.10 | 0.12 | 0.10 | 1.25 | 1.00 | 1.20 | 0.50 |
| 0.0 | 56.4 | 0.0 | 0.0 | 0.10 | 0.10 | 0.10 | 0.09 | 1.00 | 1.00 | 1.13 | 0.50 |
| 0.0 | 56.3 | 0.0 | 0.0 | 0.10 | 0.18 | 0.13 | 0.12 | 0.65 | 0.88 | 0.75 | 0.25 |
| 0.8 | 56.3 | 0.5 | -0.7 | 0.12 | 0.13 | 0.12 | 0.12 | 0.88 | 1.00 | 1.00 | 0.50 |
| 1.0 | 56.3 | 0.1 | -1.6 | 0.12 | 0.11 | 0.10 | 0.10 | 0.88 | 1.13 | 1.38 | 0.75 |
| 1.0 | 56.6 | 0.1 | -1.6 | 0.11 | 0.13 | 0.15 | 0.15 | 0.75 | 0.72 | 0.75 | 0.25 |
| 1.3 | 56.3 | 0.5 | -1.6 | 0.12 | 0.15 | 0.12 | 0.12 | 0.70 | 1.00 | 1.00 | 0.30 |

TABLE F-6 (CONT)

AVERAGE RMS VALUES OF TYPICAL GAGE AND ALIGNMENT VARIATIONS FOR CLASS 3 WELDED TRACK

| Curvature | Gage | Crosslevel | E - e | a_g | a_ℓ | a_h | a_m | a_g/a_ℓ | a_g/a_h | a_g/a_m | $a_g^2/a_\ell^2 + a_h^2$ |
|-----------|------|------------|-------|-------|----------|-------|-------|--------------|-----------|-----------|--------------------------|
| 1.3 | 56.3 | 0.5 | -1.6 | 0.10 | 0.11 | 0.12 | 0.11 | 0.63 | 1.00 | 1.00 | 0.50 |
| 1.6 | 56.5 | 1.3 | -1.3 | 0.15 | 0.13 | 0.15 | 0.13 | 1.25 | 1.10 | 1.25 | 0.70 |
| 2.3 | 56.3 | 2.0 | -1.7 | 0.10 | 0.20 | 0.25 | 0.22 | 0.63 | 0.50 | 0.50 | 0.13 |
| 2.3 | 56.6 | 1.3 | 01.2 | 0.07 | 0.12 | 0.10 | 0.12 | 0.50 | 0.50 | 0.50 | 0.13 |
| 2.5 | 56.3 | 3.0 | -1.1 | 0.10 | 0.10 | 0.12 | 0.10 | 1.13 | 0.53 | 1.00 | 0.50 |
| 3.0 | 56.4 | 3.5 | -1.5 | 0.17 | 0.17 | 0.12 | 0.11 | 1.00 | 1.25 | 1.38 | 0.63 |
| 3.8 | 56.5 | 2.5 | -1.5 | 0.09 | 0.20 | 0.20 | 0.20 | 0.50 | 0.50 | 0.50 | 0.13 |
| 4.0 | 56.7 | 4.0 | -0.22 | 0.10 | 0.15 | 0.15 | 0.15 | 0.75 | 0.63 | 0.75 | 0.25 |
| 5.0 | 56.5 | 3.8 | -1.5 | 0.12 | 0.22 | 0.15 | 0.15 | 0.63 | 0.75 | 0.75 | 0.25 |
| 5.0 | 56.7 | 3.8 | -1.5 | 0.10 | 0.15 | 0.15 | 0.15 | 0.58 | 0.58 | 0.58 | 0.13 |

TABLE F-7
 AVERAGE RMS VALUES OF GAGE AND ALIGNMENT VARIATIONS
 FOR CLASS 2 AND 3 BOLTED TRACK (LARGE/SMALL)

| Curvature | Gage | Crosslevel | E - e | a_g | a_ℓ | a_h | a_m | a_g/a_ℓ | a_g/a_h | a_g/a_m | $a_g^2/a_\ell^2 + a_h^2$ | Remarks |
|-----------|------|------------|-------|-------|----------|-------|-------|--------------|-----------|-----------|--------------------------|---|
| 2.5 | 56.3 | 2.5 | -0.3 | 0.15 | 0.10 | 0.15 | 0.12 | 1.25 | 0.88 | 1.25 | 0.38 | Typical |
| 5.4 | 56.4 | 1.5 | -0.7 | 0.20 | 0.35 | 0.20 | 0.25 | 0.63 | 1.00 | 0.75 | 0.25 | Typical |
| 6.0 | 56.4 | 3.0 | 0.5 | 0.22 | 0.25 | 0.25 | 0.25 | 0.75 | 0.75 | 0.75 | 0.25 | Typical |
| 6.8 | 56.3 | 4.0 | 1.2 | 0.10 | 0.25 | 0.25 | 0.25 | 0.50 | 0.50 | 0.50 | 0.12 | Typical |
| 8.0 | 56.5 | 4.5 | 1.2 | 0.12 | 0.20 | 0.25 | 0.20 | 0.75 | 0.50 | 0.63 | 0.25 | Typical |
| 8.2 | 56.3 | 5.0 | 1.6 | 0.20 | 0.70 | 0.60 | 0.65 | 0.25 | 0.25 | 0.25 | 0.02 | Left and Right With Series of Cusps |
| 8.3 | 56.5 | 4.5 | 1.1 | 0.10 | 0.80 | 0.80 | 0.80 | 0.22 | 0.22 | 0.22 | 0.01 | Jog in Left and Right Alignment |
| 9.3 | 56.3 | 2.8 | -1.1 | 0.25 | 0.30 | 0.25 | 0.25 | 0.80 | 0.85 | 0.92 | 0.38 | Gage, Left and Alignment With Series of Cusps |
| 10.1 | 56.5 | 4.5 | 0.3 | 0.20 | 0.20 | 0.15 | 0.20 | 1.00 | 1.38 | 1.25 | 0.38 | Typical |
| 10.5 | 57.6 | 4.8 | 0.4 | 0.20 | 0.50 | 0.50 | 0.50 | 0.33 | 0.33 | 0.33 | 0.05 | Cusp in Left and Right Alignment |
| 11.0 | 57.3 | 5.0 | 0.5 | 0.20 | 0.20 | 0.20 | 0.20 | 1.00 | 1.00 | 1.00 | 0.50 | Typical |

F-10

TABLE F-8

AVERAGE RMS VALUES OF ISOLATED GAGE AND
ALIGNMENT VARIATIONS FOR CLASS 2 BOLTED TRACK

| Curvature | Gage | Crosslevel | E - e | a_g | a_ℓ | a_h | a_m | a_g/a_ℓ | a_g/a_h | a_g/a_m | $a_g^2/a_\ell^2 + a_h^2$ | Remarks |
|-----------|--------------------|------------|-------|-------|----------|-------|-------|--------------|-----------|-----------|--------------------------|-------------------------------|
| 0.0 | 56.3 | 0.0 | 0.0 | 0.10 | 0.50 | 0.50 | 0.50 | 0.25 | 0.25 | 0.25 | 0.02 | Bump in Alignment |
| 0.0 | 56.2 to 57.6 | 0.0 | 0.0 | 0.40 | 0.40 | 0.30 | 0.30 | 1.00 | 1.50 | 1.25 | 0.64 | Bump in Gage |
| 0.0 | 56.2 | 0.0 | 0.0 | 0.10 | 0.70 | 0.60 | 0.65 | 0.25 | 0.25 | 0.25 | 0.01 | Jog in Alignment |
| 0.0 | 56.2 | 0.0 | 0.0 | 0.10 | 0.80 | 0.80 | 0.80 | 0.25 | 0.25 | 0.25 | 0.01 | Bump in Alignment |
| 0.0 | 56.4 | 0.0 | 0.0 | 0.10 | 0.80 | 0.80 | 0.80 | 0.25 | 0.25 | 0.25 | 0.01 | Jog in Alignment |
| 0.0 | 56.7 to 57.0 | 0.0 | 0.0 | 0.30 | 0.80 | 0.80 | 0.80 | 0.38 | 0.50 | 0.50 | 0.07 | Spiral Exit |
| 0.0 | 55.9 to 56.7 | 0.0 | 0.0 | 0.30 | 1.40 | 1.40 | 1.40 | 0.25 | 0.25 | 0.25 | 0.02 | Cusp in Alignment |
| 0.0 | 56.5 | 0.0 | 0.0 | 1.50 | 1.50 | 1.50 | 1.50 | 0.15 | 0.15 | 0.15 | 0.01 | Severe Alignment Variation |
| 1.5 | 57.0 | 3.0 | 2.4 | 0.10 | 0.80 | 0.80 | 0.80 | 0.25 | 0.25 | 0.25 | 0.01 | Spiral |
| 2.0 | 57.7 | 2.0 | 1.2 | 0.30 | 0.30 | 0.30 | 0.30 | 1.00 | 0.75 | 1.00 | 0.50 | Cusp in Gage |
| 2.0 | 56.2 | 3.5 | 2.7 | 0.20 | 1.20 | 1.30 | 1.20 | 0.20 | 0.20 | 0.20 | 0.01 | Spiral |
| 3.5 | 56.7 | 3.5 | 2.1 | 0.30 | 1.60 | 1.60 | 1.60 | 0.20 | 0.20 | 0.20 | 0.02 | Jog in Alignment |
| 4.0 | 57.4 | 5.0 | 3.3 | 0.20 | 1.20 | 1.20 | 1.20 | 0.20 | 0.20 | 0.20 | 0.01 | Bump in Alignment |

TABLE F-9
 AVERAGE RMS VALUES OF ISOLATED GAGE AND ALIGNMENT
 VARIATIONS FOR CLASS 3 BOLTED TRACK

| Curvature | Gage | Crosslevel | E - e | a_g | a_ℓ | a_h | a_m | a_g/a_ℓ | a_g/a_h | a_g/a_m | $a_g^2/a_\ell^2 + a_h^2$ | Remarks |
|-----------|------|------------|-------|-------|----------|-------|-------|--------------|-----------|-----------|--------------------------|--------------------------------------|
| 0.0 | 56.3 | 0.0 | 0.0 | 0.10 | 0.25 | 0.30 | 0.28 | 0.50 | 0.38 | 0.38 | 0.05 | Jog in Left and Right Alignment |
| 0.0 | 56.0 | 0.0 | 0.0 | 0.20 | 0.25 | 0.30 | 0.28 | 0.75 | 0.50 | 0.75 | 0.30 | Bump in Left Alignment |
| 0.0 | 56.3 | 0.0 | 0.0 | 0.10 | 0.25 | 0.30 | 0.28 | 0.50 | 0.50 | 0.50 | 0.13 | Jog in Left and Right Alignment. |
| 0.0 | 56.3 | 0.0 | 0.0 | 0.15 | 0.20 | 0.35 | 0.30 | 0.75 | 0.50 | 0.63 | 0.13 | Bump in Left and Right Alignment |
| 0.0 | 56.3 | 0.0 | 0.0 | 0.10 | 0.25 | 0.30 | 0.27 | 0.50 | 0.50 | 0.50 | 0.13 | Bump in Left and Right Alignment |
| 0.0 | 56.4 | 0.0 | 0.0 | 0.15 | 0.30 | 0.32 | 0.32 | 0.50 | 0.50 | 0.50 | 0.13 | Jog in Left and Right Alignment |
| 0.0 | 56.3 | 0.0 | 0.0 | 0.10 | 0.20 | 0.25 | 0.22 | 0.50 | 0.50 | 0.50 | 0.13 | Jog in Left and Right Alignment |
| 0.0 | 56.1 | 0.0 | 0.0 | 0.20 | 0.40 | 0.50 | 0.45 | 0.50 | 0.50 | 0.50 | 0.13 | Two Jogs in Left and Right Alignment |
| 1.5 | 56.4 | 1.1 | -1.4 | 0.15 | 0.32 | 0.32 | 0.32 | 0.50 | 0.50 | 0.50 | 0.13 | Spiral Exit |
| 2.0 | 56.5 | 2.5 | -0.8 | 0.10 | 0.45 | 0.40 | 0.45 | 0.25 | 0.25 | 0.25 | 0.02 | Spiral Entry |
| 2.0 | 56.5 | 1.5 | -1.8 | 0.20 | 0.30 | 0.35 | 0.30 | 0.63 | 0.50 | 0.63 | 0.13 | Spiral Exit |
| 2.0 | 56.5 | 1.5 | -1.8 | 0.20 | 0.35 | 0.40 | 0.35 | 0.50 | 0.50 | 0.50 | 0.13 | Spiral Exit |

F-12

TABLE F-9 (CONT)
 AVERAGE RMS VALUES OF ISOLATED GAGE AND ALIGNMENT
 VARIATIONS FOR CLASS 3 BOLTED TRACK

| Curvature | Gage | Crosslevel | E - e | a_g | a_λ | a_h | a_m | a_g/a_λ | a_g/a_h | a_g/a_m | $a_g^2/a_\lambda^2 + a_h^2$ | Remarks |
|-----------|------|------------|-------|-------|-------------|-------|-------|-----------------|-----------|-----------|-----------------------------|---|
| 2.0 | 56.5 | 2.0 | -1.3 | 0.10 | 0.35 | 0.35 | 0.35 | 0.63 | 0.63 | 0.63 | 0.25 | Spiral Entry |
| 2.0 | 56.6 | 3.0 | -0.3 | 0.10 | 0.35 | 0.35 | 0.35 | 0.38 | 0.38 | 0.38 | 0.05 | Spiral Exit |
| 2.0 | 57.3 | 3.8 | 0.5 | 0.12 | 0.50 | 0.50 | 0.50 | 0.38 | 0.38 | 0.38 | 0.05 | Bumps |
| 2.5 | 57.4 | 2.5 | 0.1 | 0.20 | 0.25 | 0.30 | 0.28 | 0.63 | 0.50 | 0.63 | 0.13 | Spiral Exit |
| 2.5 | 56.7 | 2.0 | -2.1 | 0.15 | 0.35 | 0.35 | 0.35 | 0.50 | 0.50 | 0.50 | 0.05 | Spiral Entry |
| 2.8 | 56.7 | 2.3 | -2.3 | 0.10 | 0.40 | 0.45 | 0.45 | 0.25 | 0.25 | 0.25 | 0.01 | Bump in Left and Right Alignment |
| 3.0 | 57.5 | 3.0 | -2.0 | 0.20 | 0.40 | 0.35 | 0.35 | 0.50 | 0.50 | 0.50 | 0.05 | Bump in Left Alignment, Cusp in Right Alignment |
| 3.0 | 56.3 | 3.8 | -1.2 | 0.25 | 0.40 | 0.52 | 0.45 | 0.63 | 0.50 | 0.50 | 0.13 | Jog in Left and Right Alignment |
| 3.5 | 57.5 | 5.5 | -0.3 | 0.12 | 0.50 | 0.50 | 0.50 | 0.25 | 0.25 | 0.25 | 0.01 | Series of Bumps in Left and Right Alignment |
| 3.5 | 57.4 | 3.8 | -2.0 | 0.15 | 0.40 | 0.35 | 0.35 | 0.30 | 0.50 | 0.35 | 0.02 | Spiral Entry |
| 3.8 | 57.5 | 4.3 | -1.9 | 0.20 | 0.35 | 0.35 | 0.35 | 0.10 | 0.10 | 0.10 | 0.38 | Gage With Series of Cusps |

F-13

TABLE F-9 (CONT)
 AVERAGE RMS VALUES OF ISOLATED GAGE AND ALIGNMENT
 VARIATIONS FOR CLASS 3 BOLTED TRACK

| Curvature | Gage | Crosslevel | E - e | a_g | a_l | a_h | a_m | a_g/a_l | a_g/a_h | a_g/a_m | $a_g^2/a_l^2 + a_h^2$ | Remarks |
|-----------|------|------------|-------|-------|-------|-------|-------|-----------|-----------|-----------|-----------------------|---|
| 4.5 | 56.7 | 4.3 | -0.5 | 0.10 | 0.40 | 0.40 | 0.40 | 0.30 | 0.30 | 0.30 | 0.10 | Spiral Entry |
| 4.5 | 57.4 | 4.3 | -0.5 | 0.20 | 0.65 | 0.60 | 0.65 | 0.25 | 0.25 | 0.25 | 0.05 | Spiral Exit |
| 5.0 | 57.7 | 4.0 | -1.3 | 0.25 | 0.50 | 0.50 | 0.50 | 0.38 | 0.38 | 0.38 | 0.05 | Cusp in Left Alignment, Dip in Right Alignment, Gage With Cusps |
| 5.0 | 58.0 | 3.8 | -1.53 | 0.35 | 0.20 | 0.30 | 0.20 | 2.00 | 1.25 | 2.00 | 1.25 | Abnormal Gage |
| 5.5 | 56.6 | 5.0 | -0.8 | 0.10 | 0.45 | 0.45 | 0.45 | 0.25 | 0.25 | 0.25 | 0.01 | Spiral Exit |

F-14

TABLE F-10

AVERAGE RMS VALUES OF ISOLATED GAGE AND
ALIGNMENT VARIATIONS FOR CLASS 3 WELDED TRACK

| Curvature | Gage | Crosslevel | E - e | a_g | a_ℓ | a_h | a_m | a_g/a_ℓ | a_g/a_h | a_g/a_m | $a_g^2/a_\ell^2+a_h^2$ | Remarks |
|-----------|------|------------|-------|-------|----------|-------|-------|--------------|-----------|-----------|------------------------|----------------------------------|
| 0.0 | 56.5 | 0.0 | 0.0 | 0.10 | 0.40 | 0.40 | 0.40 | 0.25 | 0.25 | 0.25 | 0.01 | Jog in Left and Right Alignment |
| 0.0 | 56.0 | 0.0 | 0.0 | 0.12 | 0.20 | 0.15 | 0.20 | 0.38 | 1.00 | 0.75 | 0.25 | Bump in Right Alignment |
| 0.8 | 56.4 | 0.5 | -0.7 | 0.10 | 0.20 | 0.20 | 0.20 | 0.25 | 0.25 | 0.25 | 0.01 | Bump in Left and Right Alignment |
| 1.0 | 56.1 | 0.1 | -1.6 | 0.10 | 0.30 | 0.30 | 0.30 | 0.27 | 0.25 | 0.25 | 0.05 | Spiral Entry |
| 1.6 | 56.2 | 1.3 | -1.3 | 0.20 | 0.40 | 0.50 | 0.50 | 0.50 | 0.40 | 0.50 | 0.10 | Jog in Left and Right Alignment |
| 2.0 | 56.0 | 1.3 | -2.1 | 0.15 | 0.45 | 0.45 | 0.45 | 0.25 | 0.30 | 0.30 | 0.05 | Jog in Left and Right Alignment |
| 2.3 | 56.2 | 2.0 | -1.7 | 0.10 | 0.35 | 0.35 | 0.35 | 1.00 | 1.00 | 1.25 | 0.05 | Spiral Entry |
| 2.3 | 56.2 | 2.0 | -1.7 | 0.10 | 0.30 | 0.25 | 0.30 | 0.30 | 0.30 | 0.30 | 0.05 | Spiral Exit |
| 2.3 | 56.5 | 1.3 | -1.2 | 0.10 | 0.40 | 0.35 | 0.40 | 0.25 | 0.25 | 0.25 | 0.01 | Spiral Entry |
| 2.5 | 56.5 | 3.0 | -1.1 | 0.10 | 0.35 | 0.35 | 0.35 | 0.35 | 0.35 | 0.35 | 0.05 | Spiral Exit |
| 2.5 | 56.4 | 3.0 | -1.1 | 0.10 | 0.35 | 0.35 | 0.35 | 0.27 | 0.27 | 0.27 | 0.05 | Spiral Exit |
| 3.0 | 56.5 | 3.0 | -2.0 | 0.15 | 0.35 | 0.30 | 0.30 | 0.38 | 0.50 | 0.38 | 0.10 | Bump in Left and Right Alignment |

TABLE F-10 (CONT)
 AVERAGE RMS VALUES OF ISOLATED GAGE AND
 ALIGNMENT VARIATIONS FOR CLASS 3 WELDED TRACK

| Curvature | Gage | Crosslevel | E - e | a_g | a_ℓ | a_h | a_m | a_g/a_ℓ | a_g/a_h | a_g/a_m | $a_g^2/a_\ell^2 + a_h^2$ | Remarks |
|-----------|------|------------|-------|-------|----------|-------|-------|--------------|-----------|-----------|--------------------------|---|
| 3.0 | 56.5 | 3.5 | -1.5 | 0.10 | 0.30 | 0.30 | 0.30 | 0.32 | 0.32 | 0.32 | 0.05 | Bump in Left and Right Alignment |
| 3.0 | 56.3 | 3.0 | -1.1 | 0.10 | 0.35 | 0.35 | 0.35 | 0.27 | 0.27 | 0.27 | 0.05 | Spiral Exit |
| 3.8 | 57.3 | 2.5 | -1.5 | 0.20 | 0.70 | 0.70 | 0.70 | 0.25 | 0.25 | 0.25 | 0.02 | Jog in Left and Right Alignment |
| 3.8 | 57.2 | 2.5 | -1.5 | 0.10 | 0.80 | 0.80 | 0.80 | 0.25 | 0.30 | 0.23 | 0.02 | Bump in Left Alignment |
| 4.0 | 56.7 | 4.0 | -0.2 | 0.15 | 0.40 | 0.40 | 0.40 | 0.30 | 0.30 | 0.30 | 0.02 | Spiral Entry |
| 4.0 | 56.5 | 4.0 | -0.2 | 0.08 | 0.35 | 0.40 | 0.35 | 0.25 | 0.25 | 0.25 | 0.01 | Spiral Exit; Bump in Left and Right Alignment |
| 5.0 | 56.6 | 3.8 | -1.5 | 0.30 | 0.35 | 0.45 | 0.40 | 0.75 | 0.72 | 0.75 | 0.25 | Spiral Entry |
| 6.0 | 57.5 | 3.5 | -2.8 | 0.10 | 1.00 | 1.00 | 1.00 | 0.13 | 0.13 | 0.13 | 0.01 | Jog in Left and Right Alignment |
| 6.5 | 57.2 | 3.5 | -3.4 | 0.20 | 1.00 | 1.00 | 1.00 | 0.22 | 0.22 | 0.22 | 0.01 | Jog in Left and Right Alignment |

F-16

of Transportation
**Research and
Special Programs
Administration**

Kendall Square
Cambridge, Massachusetts 02142

Postage and Fees Paid
Research and Special
Programs Administration
DOT 513



Official Business
Penalty for Private Use \$300

PROPERTY OF FRA
RESEARCH & DEVELOPMENT
LIBRARY